Technische Universität München

Fakultät für Medizin

Non-invasive transcranial magnetic language mapping complemented by fiber tracking

Antonia Angela Dorothea Kubitscheck-Sutter

Vollständiger Abdruck der von der Fakultät für Medizin der Technischen Universität München zur Erlangung des akademischen Grades eines Doktors der Medizin genehmigten Dissertation.

Vorsitzende/-r: Prof. Dr. Gabriele Multhoff

Prüfende/-r der Dissertation:

1. apl. Prof. Dr. Sandro M. Krieg

2. Prof. Dr. Jürgen Schlegel

Die Dissertation wurde am 23.03.2021 bei der Technischen Universität München eingereicht und durch die Fakultät für Medizin am 13.07.2021 angenommen.

Für alle unermüdlichen Motivatoren und Unterstützer, insbesondere Claudio und Emilia

TABLE OF CONTENTS

1. INTRODUCTION

1.1. Inducement for investigation

Gliomas make up for a majority of intracranial tumors in adult patients. Of these, 14.6% can histologically be identified as glioblastoma, the most malignant entity (Ostrom et al., 2019). Despite promising research in the field of both non-surgical and surgical oncologic therapy, only a minority of glioma patients can be cured to date (De Angelis, 2001; Wen et al., 2008; Ottenhausen et al., 2013). However, early surgical intervention and maximum resection have repeatedly been shown to decisively improve overall survival time (Ammirati et al., 1987; Berger et al., 1994; Keles et al., 2001; Sanai et al., 2008b; Jakola et al., 2012; Capelle et al., 2013). Aside of general risk factors present in any surgical setting, neurosurgical procedures always pose the risk of iatrogenous neurological deficits. Cortical areas in which tissue damage correlates with neurological deficits are referred to as eloquent. Sparing these eloquent areas often limits the extent of resection (EOR) in glioma surgery. Yet, maximizing the EOR without damaging eloquent tissue in the process is among the main factors determining the overall survival time in glioma patients (Chang et al., 2011; Jakola et al., 2012).

Optimizing the methods at hand for the identification of eloquent cortical tissue therefore marks an important goal of neurosurgical research. On the one hand, this requires improvement of macroanatomical diagnostic imaging techniques such as magnetic resonance imaging (MRI) and diffusion tensor imaging fiber tracking (DTI FT) as well as refinement of the ways of inclusion of said techniques for guidance of the operator prior and during the procedure (Claus et al., 2005; Barone et al., 2014). On the other hand, functional diagnostic methods were developed to allow for the spatial localization of cortical functions. Combining both structural and functional information about a certain structure allows for the identification of eloquent areas that need to be handled with care during the procedure to improve the patients quality of life in a process called mapping (Ottenhausen et al., 2015). Utilizing multiple preoperative as well as intraoperative techniques, e.g. cortical language mapping was shown to lead to a significant reduction of post-operative language disorders (Sanai et al., 2008c).

Functional diagnostic techniques that can be used in language mapping include measurements of metabolic surrogate parameters, such as functional magnetic resonance imaging (fMRI) and positron emission tomography (PET). Both techniques measure brain activity by detecting changes of the spatial blood flow (Price, 2012). While fMRI identifies the change in the blood oxygen level dependent (BOLD) signal (Logothetis et al., 2004), PET detects the spatial increase of radiation derived from a radiopharmaceutical that was injected to the blood stream prior to the examination (Petersen et al., 1988). Further, changes in neural activity can be detected by measuring changes in the brain's electric field. Electroencephalography (EEG) measures voltage fluctuations on the cranial surface, while magnetoencephalographic imaging (MEG) uses dipole analysis to quantify the magnetic brain activation (Findlay et al., 2012; Tarapore et al., 2012). Both electrical and metabolic measurements can represent underlying neurophysiologic pathways. Yet, both methods lack information about the exact function a cortical area partakes in that pathway (Rutten et al., 2010).

To do so, direct electrophysiological functional testing methods directly influence neural activity via electrical stimulation, allowing for the observance of changes in a certain neural function – e.g. language – following an increase or decrease of electrical activity of a certain cortical region. Preoperatively, this is conducted using transcranial magnetic stimulation (TMS) while the gold standard of intraoperative stimulation mapping (ISM) utilizes direct electrical stimulation (DES).

As the german philosopher Immanuel Kant (*1724 - †1804) already aptly put it: language is the manifestation of thoughts and the greatest means of understanding oneself and others (Kant, 1798). Fittingly, language function is among the most important factors that determine quality of life in glioma patients. It is hence of outmost importance to securely identify and preserve

language-eloquent cortical areas during neurosurgery while at the same time safely maximizing the EOR to enable the longest possible progression-free survival with maintained high quality of life.

1.2. Essentials of language

1.2.1. Basics of neuroanatomy and brain tumors

Figure 1 *Frontal slice of the human brain showing the white matter (= substantia alba) and the grey matter (= substantia grisea). Inter alia the grey matter forms the cortex (= cortex cerebri) with its ridges (= gyri; singular gyrus) and valleys (= sulci; singular sulcus). Localization regarding the midline: lateral = sideward, medial = inward. (Source: Gillroy, Atlas of Anatomy, 1st ed., Abb 39.4 A, Illustrator: Markus Voll © 2019 Thieme Medical Puplishers, Inc. All Rights Reserved).*

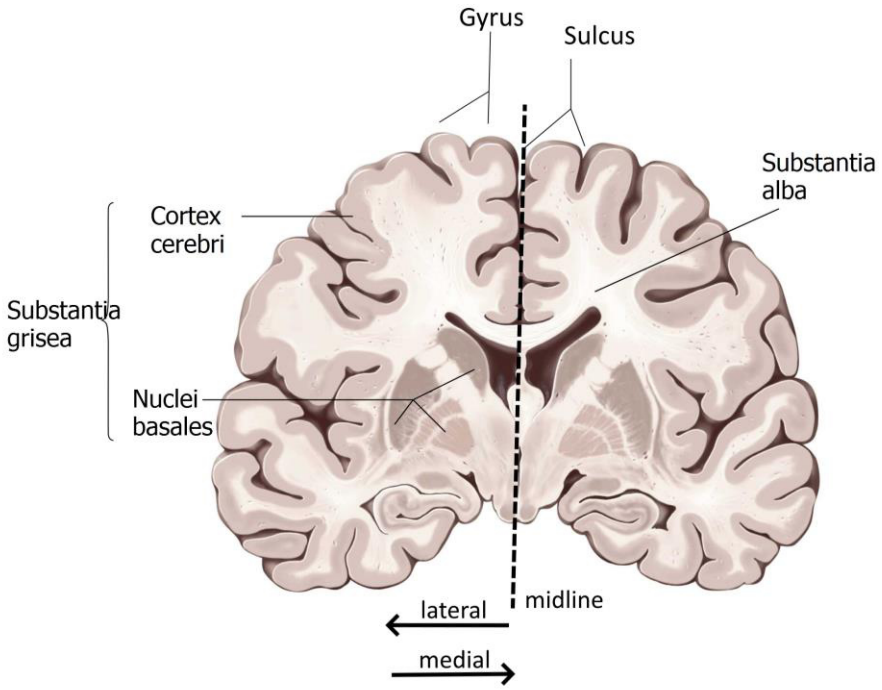

Covered by different layers (the scalp, the scull, the meninges) and floating in cerebrospinal fluid (CSF), the brain can be segmented into two layers, the white and grey matter (Figure 1) (Benninghoff et al., 2011; Trepel, 2017). The functionally most relevant cell of the brain is the neuron, consisting of the soma and the axon (Figure 2). Myelinated axons – referred to as nerve fibers - merge to form nerve cell bundles. These bundles mark the foundation of the white matter. The grey matter, forming inter alia (i.a.) the cortex, consists of neuron somata (Speckmann et al., 2009). The shape of the cortex is determined by gyri, meaning cortical ridges, and sulci, meaning cortical valleys (Figure 1). Further, the cortex is divided into different macroscopic lobes (frontal, temporal, occipital, parietal, insular) which are separated from another by characteristic sulci (Figure 3) (Paulsen et al., 2010; Trepel, 2017). Nerve cells interconnect via axons, building so-called neuronal synapses. Here, information is transmitted via chemical messengers, referred to as neurotransmitters (Speckmann et al., 2009; Rassow, 2012). When leaving the brain en route to their respective target organ, most nerve fibers switch to the opposite body half. Hence, motor function of the right body is represented by the left hemispheric cortex (Pinto, 2012).

The brain further consists of different types of supporting cells, mostly glial cells (Speckmann et al., 2009). These glial cells are the origin of gliomas (Pinto, 2012; Trepel, 2017). The World Health Organisation (WHO) classifies gliomas into four grades of malignancy. The higher the grade, the more aggressive and destructive is their growth.This grading system is based on the glial tumor's original cell type (astrocytoma, oligodendroglioma, ependymoma), the grade of differentiation (e.g. pilocytic, low-malignant or anaplastic) as well as further histologic and

Figure 2 *Nerve cell bodies (= 1) with their connecting axons (= 2) and surrounding myelin shields (= 3). The stamp-like contact points between the axons correspond to synapses (Source: Gillroy, Atlas of Anatomy, 1st ed., Abb 39.2, Illustrator: Markus Voll © 2019 Thieme Medical Puplishers, Inc. All Rights Reserved).*

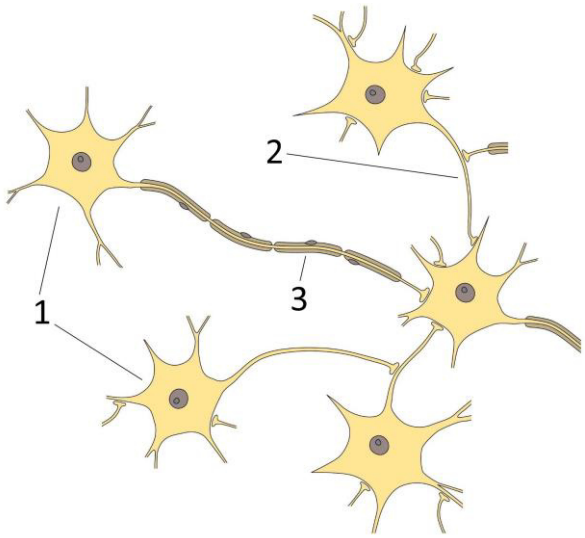

molecular characteristics (Pinto, 2012; Komori, 2017; Kristensen et al., 2019). WHO grade I contains i.a. the pilocytic astrocytoma, while the most malignant glioblastoma multiforme corresponds to WHO grade IV (Pinto, 2012; Louis et al., 2016; Gupta et al., 2017). This grading system is also used for other types of primary intracranial tumors, such as meningiomas. Metastases on the other hand are to be distinguished from primary intracranial tumors (Pinto, 2012; Gupta et al., 2017). Other anatomic structures can also give rise to neoplastic effects. An example is the arteriovenous malformation (AVM). Unlike the above-mentioned tumors that originate from pathological cell proliferation, the AVM originates from a congenital anomaly of the blood vessels, a direct connection between artery and veins without a braking capillary bed in between. Due to the unhindered blood flow, AVMs can grow significantly in size, have an increased risk of causing intracerebral bleeding and can further lead to neurological failures due to blood bypasses (Henkes et al., 2006).

Figure 3 *Division of the brain in its four cortical represented lobes. Frontal lobe (= green), temporal lobe (= blue), parietal lobe (= yellow) and occipital lobe (= red). The two big sulci, which separate the frontal, the temporal and the parietal lobe from each other are further displayed (sulcus centralis, sulcus lateralis) as well as the two sulci involved in working memory (sulcus frontalis inferior, sulcus intraparietalis) (Source: Gillroy, Atlas of Anatomy, 1st ed., Abb 39.12 A, Illustrator: Markus Voll © 2019 Thieme Medical Puplishers, Inc. All Rights Reserved).*

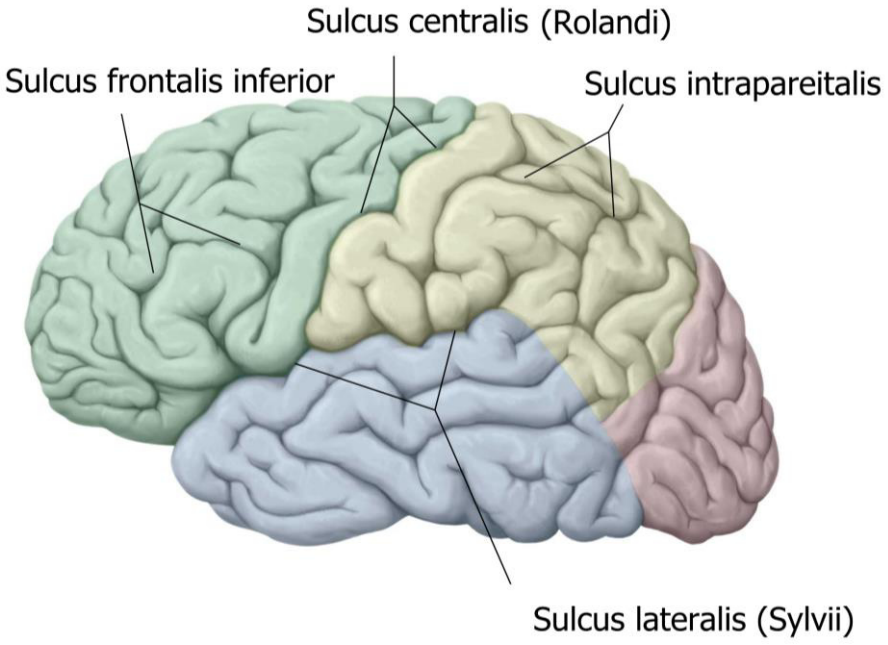

1.2.2. Neurophysiological processing of language

Unlike motor activity, the cortical basis of language and speech production is still not fully understood (Duffau, 2008; Price, 2012; Cattaneo, 2013). The complexity of language and speech processing is retrieved in the wide field of linguistics. First, the terms “speech” and “language” have to be kept apart. Language refers to the entirety of processes included in the act of communication between different individuals except for the act of communicating itself, which is referred to as speech. Language hence involves both verbal- and non-verbal means of communication. This communication has to be planned, shaped, conveyed, understood and processed. Language therefore involves multiple cortical networks, such as the auditory and the visual network. Speech on the other hand comprimises of the active act of communicating without regard to the mean of communication. Factors of speech include articulation and pronunciation, fluency of talking and voice skills. In this context, it should be noted that prearrangig processes preceding articulation and pronunciation of communication are regarded as part of language and not speech (Schwarz-Friesel, 2008). This doctoral thesis focuses on language production by the human brain while explicitly excluding the motor-dominated field of speech.
Language is a complex framework of meaning and structure. It is further divided into receptive, expressive and non-verbal domains. The term Semantics refers to the concept of the meaning of linguistic units. Semantics encompasses the meaning of single words, phrases and full sentences both expressed and recepted. Language further includes i.a. sentence structure, as well as grammatical and syntactical rules. The connection between language and speech is established, i.a. by the field of Phonology. The term Phonology refers to the knowledge of the correct pronunciation of certain parts of e.g. words both receptively and expressively while the actual act of pronunciation itself is part of speech. During receptive language processing, an extrinsic acoustic piece of information is transformed into an invariant internal representation of the verbal material and further analysed for correct understanding (Cattaneo, 2013). Language further consists of a multitude of characteristics that need to be considered and put in contex by the human brain to enable for proper communication (Schwarz-Friesel, 2008).

1.2.3. Cortical organisation of language

The term Aphasia refers to language errors due to an illness with consecutive impairment of brain function. As stated above, language consists of a multitude of separate processes and factors. Hence, the clinical manifestation of Aphasia significantly varies depending on the defected cortical area. Observing these defects allows to establish connections between

Figure 4 *Representation of the cortical parcellation system with its 37 parcels based on Corina et al. (2005). The respective designations for the CPS abbreviations can be found on page 101 in section 8.2.*

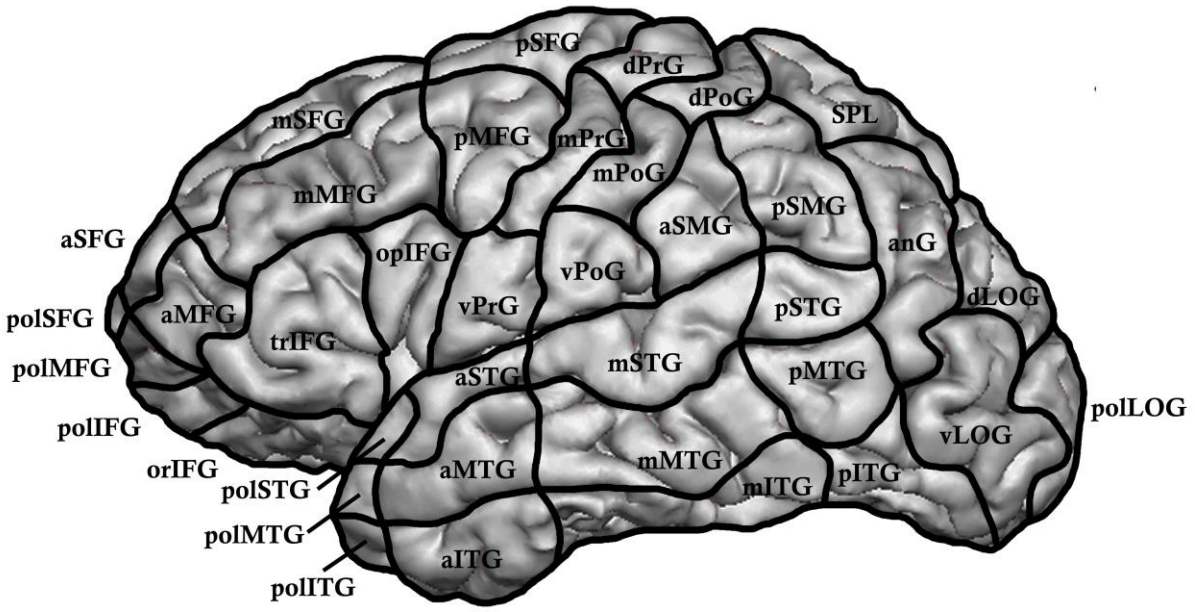

certain cortical areas and certain language functions. Hence, Aphasias led to a first understanding of language processing in the human brain (Naeser et al., 1978; Dronkers, 1996). Modern studies using either fMRI (McGraw et al., 2001; Indefrey, 2011; Schuhmann et al., 2012; Wheat et al., 2013), or stimulation techniques such as TMS and DES (Ojemann et al., 1989; Haglund et al., 1994; Tarapore et al., 2013) have led to new insights into these connections and have established more detailed anatomical models of language processing (Cattaneo, 2013). To do so, Corina et al. introduced the cortical parcellation system (CPS). The CPS divides the cortex of each hemisphere into 37 parcels. Each parcel is identifiable based on given anatomical landmarks (Figure 4) (Corina et al., 2005; Corina et al., 2010).
Based on prior findings from Aphasia studies, language processing is roughly segmented into an anterior (= frontal) and a posterior (= temporoparietal) part. The anterior part consists of the triangular (trIFG) and opercular inferior frontal gyrus (opIFG), the ventral pre-central gyrus (vPrG) and the middle middle frontal gyrus (mMFG). It includes the Broca's area (trIFG, opIFG) with its known focus on expressive language (Figure 5) (Broca, 1861; Brodmann, 1925). The posterior (= temporoparietal) part includes the anterior (aMTG), middle (mMTG) and posterior middle temporal gyrus (pMTG) as well as the receptive Wernicke's area consisting of the anterior (aSTG), middle (mSTG) and posterior superior temporal gyrus (pSTG) (Figure 5) (Wernicke, 1874; Brodmann, 1925; Cattaneo, 2013; Tarapore et al., 2013).
Yet, based on recent findings, a simple division into anterior and posterior regions seems unfit to adequately describe cortical depiction of language. Instead, a complex language architecture involving multiple separate cerebral areas and networks should be assumed (Chang et al., 2011; Indefrey, 2011; Cattaneo, 2013). Broca's area was repeatedly found to host expressive language. It manages phonation, syntax and preparation for speech production (Penfield et al., 1950; Poeppel, 1996; Tarapore et al., 2013). Broca's area is directly and indirectly connected to supplemental areas of motor speech processing, i.e. the posterior middle frontal gyrus (pMFG), the middle (mPoG) and ventral post-central gyrus (vPoG), as well

Figure 5 *Representation of the four cerebral main directions (anterior, superior, posterior, inferior), the anterior (= frontal, rostral) part (red) with its Broca's area (orange), the posterior part (dark blue) with its Wernicke's area (light blue), areas of motor speech processing (yellow) and the Geschwind's area (green). Inferior = ventral. Superior = dorsal. The respective designations for the CPS abbreviations can be found on page 101 in section 8.2.*

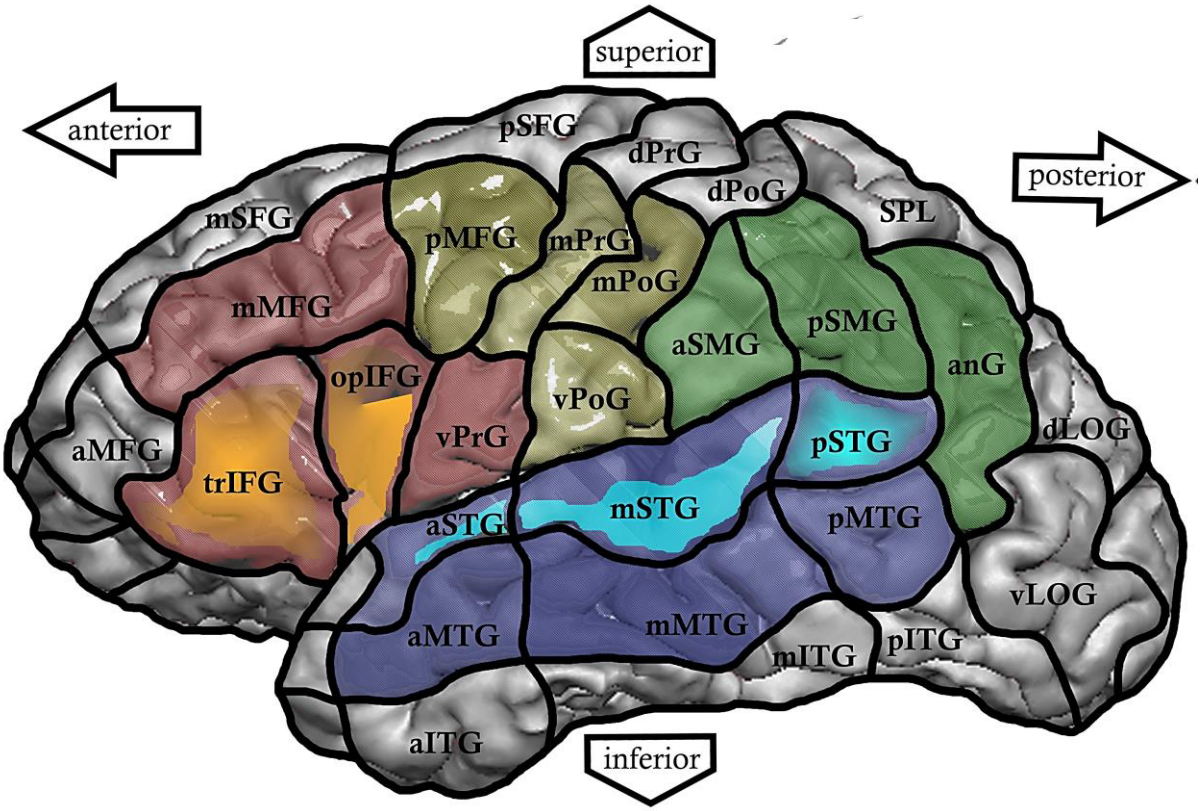

Figure 6 *Brodmann areas with its functional assignment (Brodmann, 1925). E.g. somatosensory cortex (= 1 - 3), primary motor cortex (= 4), primary (= 17) and secondary visual cortex (= 18 - 19), Wernicke's area (= 22), primary auditory cortex (= 41), secondary auditory cortex (= 42) and Broca's area (= 44 - 45). The primary auditory cortex is located mainly inside of the lateral sulcus on the gyri temporales transversi (Source: Gillroy, Atlas of Anatomy, 1st ed., Abb 39.11 A, Illustrator: Markus Voll © 2019 Thieme Medical Publishers, Inc. All Rights).*

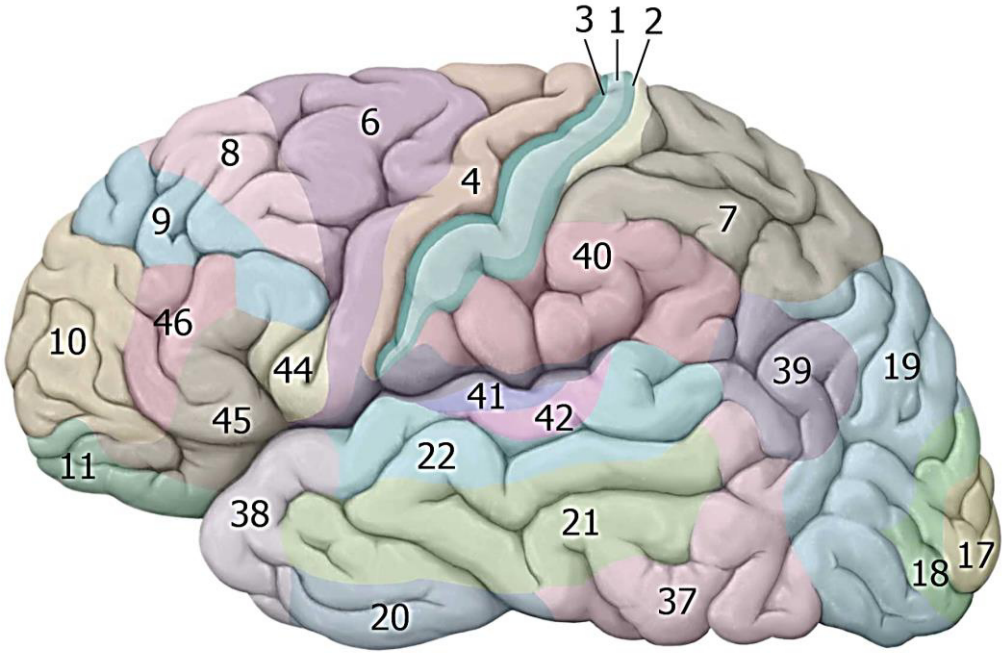

as the middle pre-central gyrus (mPrG) (Figure 5) (Sanai et al., 2008c; Bohland et al., 2010; Rauschecker, 2012; Tarapore et al., 2013; Sollmann, 2015). The mPrG, as well as the dorsal (dPrG) and ventral pre-central gyrus (vPrG) form the pre-central gyrus (PrG). The PrG is located anterior to the sulcus centralis, is the main seat of the primary motor cortex and the main site of peripheral motor control (Figure 3 on page 3 and Figure 6). For example hand motor function is located inside the macroscopically distinguishable omega- or epsilon-shaped hand knob in the area of dPrG or mPrG (Yousry et al., 1997; Boroojerdi et al., 1999; Caulo et al., 2007; Ahdab et al., 2016). Further, muscles that are related to speech are controlled by neurons inside the vPrG (Edwards et al., 2010; Houde et al., 2011; Price et al., 2011; Hickok, 2012; Tarapore et al., 2013).

One of the most relevant efferences onto Broca's area stems from Wernicke's area, which is in turn part of the secondary auditory cortex (Wernicke, 1874; Brodmann, 1925). Wernicke's area is the sensoric language centre and interpretates incoming visual (e.g. reading, facial expression, gestures) and auditory information. Wernicke's area neurons transform heard or read information into an internal representation of verbal material. This process is called phonological processing (Boatman, 2004; Cattaneo, 2013). To do so, Wernicke's area is directly connected to the primary auditory cortex (= gyri temporales transversi) and indirectly connected to the visual cortex via the angular gyrus (anG) (Figure 6) (Roux et al., 2004; Graves et al., 2010; Cattaneo, 2013; Sollmann, 2015). Aside of projecting visual information to Wernicke's area, anG itself is part of Geschwind's area (Figure 5). Further including the anterior (aSMG) and posterior supramarginal gyrus (pSMG), Geschwind's area hosts semantic processing of language reception and expression. I.a. somatosensoric information is incorporated to internal representations of verbal material based on context (e.g. "cold/hot" or "painful/pleasant") (Catani et al., 2005).

Broca's, Wernicke's and Geschwind's areas each are connected to several supplemental association fields. These fields elaborate the process of semantic interpretation. E.g., sourrounding smells, tastes, emotions or gained individual experiences are associated to the verbal material. Most language-eloquent areas are located bordering the lateral sulcus, also called Sylvian fissure. Aphasia is therefore a possible pathology in patients suffering from perisylvan brain tumors. Yet, also non-perisylvian regions, such as the middle superior frontal gyrus (mSFG) give input for semantic comprehension of language (Scott et al., 2003; Catani

et al., 2005). The verbal working memory, which serves as a storage for the processed syntactic information during language production, can be located based on two other sulci, the inferior frontal sulcus and the sulcus intraparietalis (Figure 3 on page 3) (Makuuchi et al., 2013). The phonological working memory is mostly located in aSMG and pSTG. Further, caudal parts of Broca's area as well as the posterior superior frontal gyrus (pSFG) have been found to save language-relevant information (Simos et al., 2002; Du Boisgueheneuc et al., 2006; Jacquemot et al., 2006; Graves et al., 2008).
Expressive word production is triggered in the temporal areas mMTG and pMTG. Information is then forwarded to anterior temporal regions such as the aMTG, aSTG, polar middle (polMTG) and polar superior temporal gyrus (polSTG). There, information is further processed and projected onto anterior frontal expressive areas including Broca's area (trIFG, mMFG, pMFG) (Binder et al., 2009; Indefrey, 2011; Gow, 2012; Price, 2012; Henseler et al., 2014; Hauck et al., 2015). The process of syllabification, meaning articulatory planning with phonological coding, is sited in opIFG (Poldrack et al., 1999). Ultimately, motor efferences are produced by vPrG, the orofacial domain of the primary motor cortex (Indefrey, 2011; Hauck et al., 2015). Based on clinical findings of Aphasias, as well as fMRI and PET studies, a possible separation between production of verbs and nouns is being discussed (Damasio et al., 1993; Daniele et al., 1994). While noun processing appears to happen mainly in the temporal regions of expressive word production, processing of verbs seems to include more frontal areas as well as the anterior cingulate cortex and the nucleus dentatus of the cerebellum (Buckner et al., 1995; Papathanassiou et al., 2000; Kircher et al., 2001; Thurling et al., 2011). Yet, other studies findings oppose that theory (Soros et al., 2003; Siri et al., 2008).

1.2.4. Subcortical organisation of language

Every exchange of information between two cortical areas bases on reciprocal connected nerve fibers (Axer et al., 2013). According to the hodotopical model of Duffau et al., language processing represents a widely branched and dynamic interaction of cortex and connecting fibers (Duffau et al., 2014). Damage to one cortical region or subcortical tract may affect the functional integrity of further connected parts of the directly or indirectly appending language network (Axer et al., 2013; Bajada et al., 2015). Hence, occurring symptoms (e.g. Aphasias) or provoked language errors may not simply reflect the inherit function of the injured or disturbed anatomical site itself (Rubinov et al., 2010; Sporns, 2013; Bajada et al., 2015), but reflect that the fiber tracts running through that cortical area may be part of a network involved in said function. Thus, fiber tracts do not have an exclusive function on their own (Axer et al., 2013). This is an explanation for in part contradictory conclusions regarding the functional role of language fiber tracts (Axer et al., 2013). Furthermore, also the exact terminology and findings about the course of the tracts show discrepancies (Bajada et al., 2015).
Still, an anatomic and in part functional division of fiber tracts into a dual-stream model consisting of a predominantly semantic ventral (= inferior) and a phonological dorsal (= superior) language fiber stream can be postulated (Hickok et al., 2004; Duffau, 2008; Saur et al., 2008; Axer et al., 2013; Ueno et al., 2013; Bajada et al., 2015). Both streams represent tracts that interconnect Broca's, Wernicke's and Geschwind's areas among each another and with other language-relevant regions (Matsumoto et al., 2004; Catani et al., 2005; Duffau, 2008; Cattaneo, 2013; Sollmann, 2015). The ventral stream is associated with Semantics, understanding the meaning of heard or read as well as self-formulated content. The dorsal stream is involved in phonological processing, proofing and refining i.a. the pronunciation or articulation of received and newly produced content (Hickok et al., 2004; Saur et al., 2008; Hickok, 2009). The dorsal stream is hence also required for verbal repetition as well as internal feedback (Saur et al., 2008; Edwards et al., 2010; Houde et al., 2011; Price et al., 2011; Hickok, 2012). Reflecting the different aspects of communication, the ventral stream is also part of visual and emotional processing, e.g. during reading as well as the integration of emotional context (Williamson et al., 2013; Bajada et al., 2015). A relevant degree of interaction between both streams is suggested (Cloutman, 2013; Bajada et al., 2015). E.g. both streams are required to allow for correct syntax and morphology, meaning the structure of words (Rolheiser et al., 2011; Axer et al., 2013). Driven by DES studies, the dual-stream model has been

extended by two complementary pathways, the speech perception pathway and the articulatory loop (Duffau, 2008; Axer et al., 2013).
Bajada et al. postulated a division of the ventral stream into 4 key tracts of the temporal lobe (Bajada et al., 2015), the uncinate fasciculus (UF), the inferior fronto-occipital fasciculus (IFOF), the middle longitudinal fasciculus (MdLF) and the inferior longitudinal fasciculus (ILF) (Figure 7). Axer et al. further discussed, whether fibers of the external capsule (ExC) and extreme capsule (EmC) are also part of the ventral system (Figure 8 A) (Axer et al., 2013). The dorsal stream contains the arcuate fasciculus (AF) and the superior longitudinal fasciculus (SLF) (Figure 7) (Cattaneo, 2013; Sollmann, 2015). Each language tract can be further divided into smaller subsections inheriting different functional language skills (Duffau et al., 2002).
Findings about the validity of the two-stream model are inconsistent. An electrical inhibition of the lateral portion of the SLF was found to cause a phonemic paraphasia (Maldonado et al., 2011), while inhibition of the IFOF lead to semantic paraphasias (Duffau et al., 2008). In phonemic (= phonological) paraphasia, a non-word is expressed that still resembles the intended word in e.g. half of the syllables. In semantic paraphasia, the expressed word is of correct structure, yet the meaning of the word deviates from the intended word, albeit in semantic paraphasias, the meaning is still close to the intended word. The UF has been found to be essential in lexical and semantic storage and retrieval (Cattaneo, 2013), enabling semantic control of the ventral stream (Harvey et al., 2013). These findings would fit the above

Figure 7 *Schematic illustration of the different language-related tracts of the ventral and dorsal stream. Typical lesions provoked by stimulation according to Chang et al. (2015) are shown. EmC and EC are not depicted. (Source: Chang et al. (2015) - Contemporary model of language organisation. Figure 4. DOI: https://doi.org/10.3171/2014.10.JNS132647. Online Publication Date: Feb 2015. © Edward F. Chang.)*

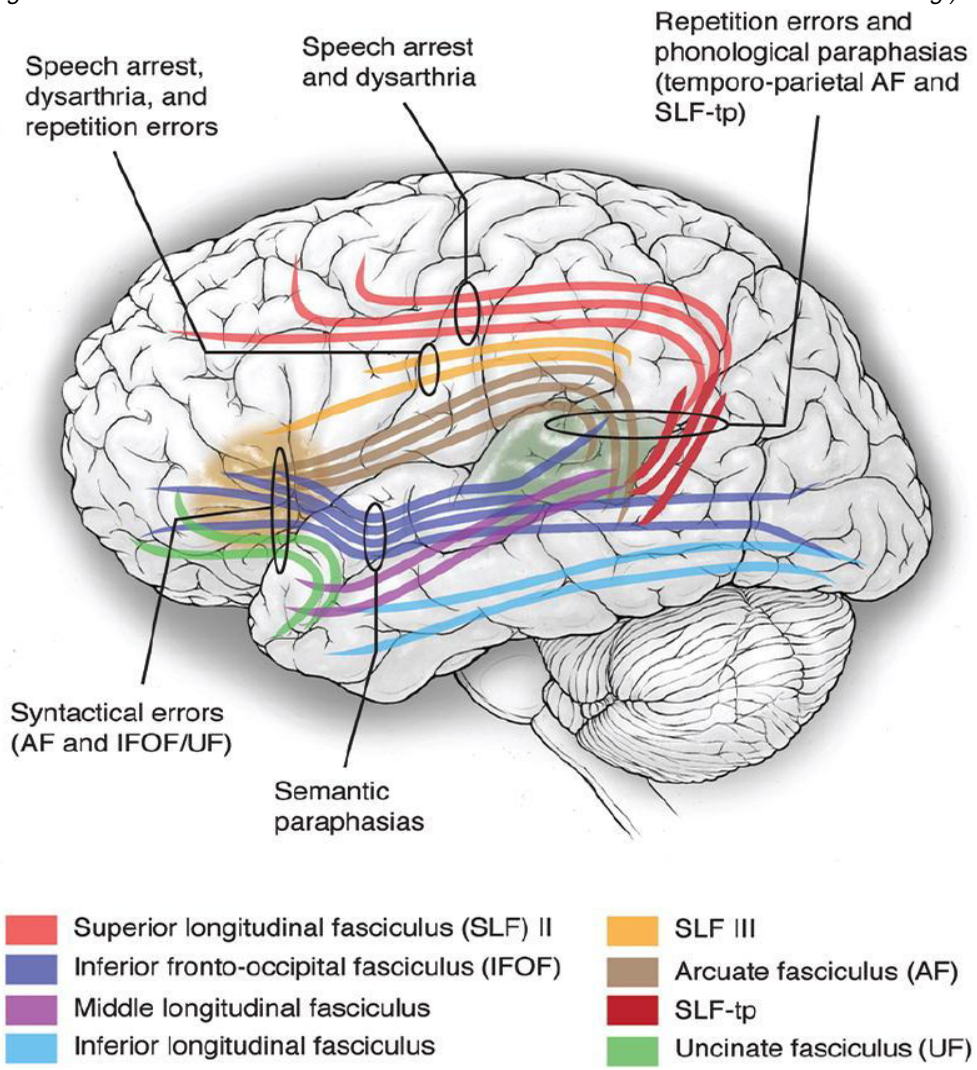

described model. Inhibition of the AF was found to be associated to anomia, the disability of naming (Duffau et al., 2002), as well as to phonological paraphasias (Duffau et al., 2008). Again, these findings fit the attribution of the AF as part of the dorsal stream. Yet, inhibition of the AF was also found to lead to semantic paraphasias, a feature attributed to the ventral stream (Duffau, 2006; Bello et al., 2007). Catani et al. and Axer et al. have both challenged the existence of an isolated MdFL and postulated it to be included in the posterior segment of the AF (Catani et al., 2005; Axer et al., 2013). Yet, both tracts are assigned to different parts of the two-stream model. Again, data availability is heterogenous as others have contradicted this assumption (Makris et al., 2009). Similarly, the EmC and ExC have been postulated to be included in the IFOF due to their similarity in fiber course (Axer et al., 2013).
The speech perception pathway and the articulatory loop run lateral to the AF (Duffau, 2008; Nishida et al., 2017). In 2017 Nishida et al. developed a model of the articulatory loop (Figure 8 B) (Nishida et al., 2017), which connects the supramarginal gyrus with the inferior frontal cortex (Duffau, 2008). These two areas are located next to the two sulci assumed for verbal working memory (Makuuchi et al., 2013). It is suggested that the articulatory loop stores the language content temporary until its reproduction (Duffau, 2008; Nishida et al., 2017). The suggested functions of the articulatory loop and the speech perception pathway overlap with the tasks previously assigned to the ventral and dorsal stream (Bajada et al., 2015).
As already depicted in Ille et al. (2015b), although the amount of gained informations continually rises, language distribution and processing is still not fully understood and more investigation is needed.

Figure 8 ***A*** *Anatomic position of the external capsule (= EC = ExC in this doctoral thesis) and the extreme capsule (= EmC). The claustrum (= green) is the dividing structure. Both are located on a level with the putamen (= blue) and the insular cortex (= red) (Source: Bajada et al. (2015) - Transport for language south of the Sylvian fissure. Figure 2. DOI: https://doi.org/10.1016/j.cortex.2015.05.011. Online publication date: May 2015. © 2015 The Authors. Published by Elsevier Ltd. All rights reserved.* **B** *Proposed model of the articulatory loop system (Source: Nishida et al. (2017) - Brain network dynamics in the human articulatory loop. Figure 9. DOI: https://doi.org/10.1016/j.clinph.2017.05.002. Online publication date: May 2017. © 2017 International Federation of Clinical Neurophysiology. Published by Elsevier Ireland Ltd. All rights reserved.)*

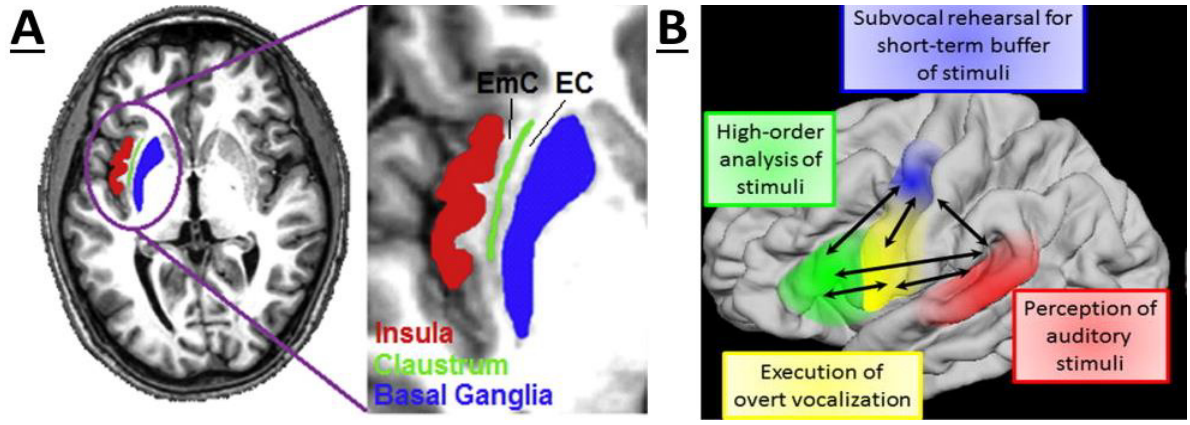

1.3. The relevance of individuality in the context of neurosurgery

Human anatomy varies interindividually, not only referring to general factors such as skull shape and size, but also regarding e.g. the assembly of gyri and sulci (Ruohonen et al., 2010). Further, the spatial distribution of langauge-eloquent cortical areas significantly varies as well (Ojemann et al., 1978; Giussani et al., 2010). E.g., partly language dominance is influenced by a patient's sex and handedness (Witelson, 1989; Steinmetz et al., 1992; Kulynych et al., 1994; Binder et al., 1996; Jancke et al., 1997; Kansaku et al., 2001; Hirnstein et al., 2013). Aside of interindividual variances, language distribution also varies intraindividually, especially in the presence of neoplasia-related processes such as pressure and tissue damage due to invasive and destructive growth, space-occupying edema, as well as necrosis (Suess et al., 2001; Hastreiter et al., 2004; Suess et al., 2007; Robles et al., 2008; Gil-Robles et al., 2010; De Witt Hamer et al., 2012; Potgieser et al., 2014; Shahar et al., 2014). Aside of possible hindering

macroscopic identification of anatomic conditions (Pouratian et al., 2010), these processes can also induce a functional reorganisation due to neuroplasticity (Duffau, 2005, 2006; Desmurget et al., 2007; Krieg et al., 2013b; Duffau, 2014c; Rosler et al., 2014; Southwell et al., 2016). Neuroplasticity is the rearrangement of synaptic interconnection based on modulated cell activity patterns (Abraham et al., 1996; Todd et al., 2009). As these factors cannot be addressed based on structural information, functional diagnostics are required to correctly identify language-eloquent tissue.
The first functional testing method, ISM, was introduced as early as 1950 (Penfield et al., 1950). Since then, language-eloquent cortical and also subcortical tissue can be identified and allow for safe maximization of the EOR (Duffau, 2005; Benzagmout et al., 2007; Sarubbo et al., 2012). In 1985 TMS was firstly used for cortical stimulation of the human brain (Barker et al., 1985). TMS allows to temporarily and non-invasively modulate cortical activity, e.g. in a preoperative setting (Hallett, 2000; Ruohonen et al., 2010). Further, the addition of neuronavigation to ISM and TMS allows for the exact localization of the stimulated areas. Adding these assets to the diagnostic process significantly reduces the number of iatrogenous severe neurological deficits and permanent neurological restrictions during tumor surgery of language- or motor-eloquent areas to less than 3.5% and 2%, respectively, while at the same time allowing for an increase in EOR (Ojemann et al., 1989; Haglund et al., 1994; Duffau et al., 2008; Sanai et al., 2008c; De Witt Hamer et al., 2012).
Both, repetitive transcranial magnetic stimulation (rTMS) and DES electrically disturbe nerve cell activity in the targeted brain region, thereby setting a virtual lesion that leads to clinically identifiable language errors (Ojemann et al., 1989; Pascual-Leone et al., 1991; Haglund et al., 1994; Wassermann et al., 1999; Corina et al., 2005; Corina et al., 2010; Lioumis et al., 2012). Underlying this effect is the induction of an inhibitory postsynaptic potential by a long-lasting repetitive electrical stimulation of a certain frequency and intensity (Pascual-Leone et al., 1999; Amassian et al., 2006). To correctly identify language errors, patients complete language tasks with different emphasis on the linguistic domains. Different emphases include expressive versus receptive tasks as well as phonologic or semantic tasks. To date of the study, the standard for language testing during rTMS and DES was an object-naming task (Duffau, 2008).

1.4. Intraoperative stimulation mapping

1.4.1. Direct electrical stimulation via DCS and SCS

DES currently marks the gold standard for language mapping (Duffau et al., 2005; Szelenyi et al., 2010; Chang et al., 2011; De Witt Hamer et al., 2012; Duffau et al., 2014; Ottenhausen et al., 2015). Depending on intended stimulation site, it can be conducted either as direct cortical stimulation (DCS) or as subcortical stimulation (SCS).
Unlike intraoperative motor mapping, which can be performed under general anaesthesia, language mapping requires an alert and cooperative patient (Sanai et al., 2008c; Ottenhausen et al., 2015). Different anaesthesiological approaches are in use to allow for this, most commonly performed as a so-called “asleep-awake-asleep” sequence (Duffau, 2013). In this case, general anaesthesia is only performed during craniotomy and closure. This minimizes the waking phase with minimal loss of patient concentration. In addition, potentially painful or frightening as well as time-consuming surgical phases can be overslept by the patient (Duffau, 2013). Specific complications such as aspiration, epileptic seizures or swelling are rare (Duffau et al., 2008; Deras et al., 2012). Awake surgery is well tolerated and rarely has to be interrupted or stopped (Nossek et al., 2011; Beez et al., 2013). The degree of sedation is monitored using the EEG-based bispectral index (BIS). Semantic tasks require a BIS of above 90, while other parts can be conductet at BIS values of 80-90 (Tamura et al., 2016; Saito et al., 2018). Absolute contraindications for awake surgery are uncontrollable coughing, incooperation e.g. due to severe cognitive impairment, persistent focal neurologic deficit despite a therapy trial with dexamethason and mannitol as well as significant mass effects. In the last case, a separate awake resurgery can be performed following debulking (Hervey-Jumper et al., 2015).
Various language mapping protocols have been published (Ottenhausen et al., 2015). DES utilizes both monopolar and bipolar flow, with amplitudes of up to 20 mA, the general DES

maximum stimulation intensity. When using a bipolar flow, the probe tip distance is standardly 5 - 10 mm and the induced charge is twice as high compared to monophasic flow using the same current (Szelenyi et al., 2010; Saito et al., 2018). In case of awake language mapping, the biphasic flow intensity is limited to 6 - 8 mA (12 - 16 mA for monophasic flow) due to a higher risk of induced seizures due to the lack of anti-epileptic drug effects of the sedatives e.g. propofol (Sanai et al., 2008c; Szelenyi et al., 2010; Hervey-Jumper et al., 2015; Spena et al., 2017; Saito et al., 2018). Language mapping utilizes stimulation frequencies of 50 - 60 Hz with a stimulation duration of 1 to 4 sec (Ottenhausen et al., 2015; Saito et al., 2018). An area is never directly stimulated several times in succession to avoid epileptic seizures. Pauses must be observed between each stimulation (Duffau, 2008). Language impairments caused by epileptic potentials are distinguished from intended errors via an EEG derived from electrodes directly placed on the cortex, referred to as electrocorticography (ECoG) (Ottenhausen et al., 2015). Further the applied stimulation intensity is limited to a level lower than a positive ECoG (Hervey-Jumper et al., 2015). Prior to mapping, the individually required stimulation intensity is tested sensomotorically or via a counting test with 1 mA steps up to a maximum of 6 - 8 mA (Duffau, 2004, 2005). To distinguish between eloquent and non-eloquent tissue, each cortical area usually is mapped three times (Ojemann et al., 1989).
DCS-based language mapping yields a high degree of reliability when conducted under similar conditions (Ojemann et al., 1989; Haglund et al., 1994; Sanai et al., 2008c; Corina et al., 2010; Chang et al., 2011). SCS is performed parallel to tumor resection to define the boundaries of the surgical cavity (Duffau et al., 2005). Damage to connecting fibers leads to more severe and persistent language disorders compared to cortical erroneous resection. Hence, a positive stimulation by SCS leads to an immediate stop of resection (Bello et al., 2007; Duffau et al., 2008; Trinh et al., 2013). A simultaneous stimulation of cortical and subcortical structures can lead to erroneus results and should be avoided (Szelenyi et al., 2010).

1.4.2. Supporting techniques of ISM

In tumor surgery, the balance between maximum EOR, which is associated with prolonged survival, and a sufficient safety margin to avoid iatrogenous neurological deficits must be maintained. Thereby, the individual prognosis of the patient and the tumor entity must always be addressed.
Different forms of DES-based intraoperative neurophysiological monitoring are used to monitor motor, somatosensory, visual and brainstem auditory evoked potentials (Barbosa et al., 2015; Saito et al., 2018). A loss of evoked potential amplitudes can warn against impending or of already caused damage (Kombos et al., 2001; Krieg et al., 2012c; Seidel et al., 2013). Another well suited screening parameter is the patient's ability to speak. This not only applies to the timespan of language mapping but is continued throughout all phases that include tissue irritation. The monitoring is enabled by a continuous conversation between the patient and an especially trained team member (Muragaki et al., 2005; Szelenyi et al., 2010; Saito et al., 2018). Knowledge gained by neurophysiological monitoring can be used to define a safety margin for tumor resection. The greater the safety margin, the faster patients with already reduced prognosis can recover from transient deficits stemming from postoperative edema formation and hypoperfusion (Gil-Robles et al., 2010). Permanent deficits mostly stem from postresection ischemia following unintentional damage to supplying vessels (De Witt Hamer et al., 2012). Fluorescence guided surgery is another promising resection tool (Stummer et al., 2006; Tonn et al., 2008). The fluorescent dye 5-aminolevulinic acid accumulates in epithelia while preferring brain tumors. However, this method is limited by a lower or missing accumulation in necrotic or less malignant tissue (Barbosa et al., 2015). Further, findings by Stummer et al. indicate an increase in morbidity following more radical resections when using this technique (Stummer, 2014).
Preoperative MRI validity is often compromised by tumor progression in the timespan between the MRI and the surgery as well as brain shift following craniotomy, swelling and the spatial impact of the resection itself (Hastreiter et al., 2004; Suess et al., 2007; Barbosa et al., 2015; Sastry et al., 2017). Due to these insecurities, surgeon experience is decisive for the successive use of neuronavigation (Willems et al., 2006). The introduction of an intraoperative

ultrasonic device and intraoperative neuronavigation using intraoperative MRI (iMRI) of the brain have softened these hindrances. Yet, in particular iMRI is time-consuming and cost-intensive (Barbosa et al., 2015; Sastry et al., 2017). The postoperative outcome is further influenced by the use of corticosteroids, which reduces the induced inflammatory response and thus the extent of edema formation. This results in faster regeneration and a better functional outcome (De Witt Hamer et al., 2012).

1.5. Fundamentals of rTMS for language mapping

1.5.1. Basic technical TMS setup

TMS is based on electromagnetic induction as described by Faraday's law. In short, the varying electric current flowing through the TMS coil induces an electric field (e-field) on the targeted brain surface conveyed by a magnetic field. The TMS coil is placed tangentially on the skull to align the magnetic field axis with the cortex (Barker et al., 1985; Ruohonen et al., 1999; Hallett, 2000; Rossi et al., 2009; Klooster et al., 2016; Sollmann et al., 2016a). Characteristics of the e-field correlate to the magnetic field. Since hair, skin and bone consist no noteworthy electric conductivity, they do not influence the electromagnetic field (Klooster et al., 2016). Once the field hits the brain, field strength declines exponentially with increasing distance to the coil (Figure 9) (Barker et al., 1987; Barker, 1991; Roth et al., 1991). The only significantly affected structure between coil and cortex is muscle tissue (Barker et al., 1987). Besides tissue conductivity, the intensity of the magnetic field and the type of coil construction influences penetration depth, as well as e-field shape and strength (Ravazzani et al., 1996; Ruohonen et al., 1999; Wagner et al., 2007; Ruohonen et al., 2010). In general, higher stimulation intensities enable stimulation of deeper tissue. Yet, higher stimulation intensities also widen the e-field, leading to losses of focality (Levy et al., 1991; Brasil-Neto et al., 1992; Deng et al., 2013; Klooster et al., 2016). Hence, stimulation intensity is to be set as low as possible, without loss of effect.

TMS head coils usually consist of tightly wound, insulated copper wires. Ring shaped coils lead to a ring-shaped, evenly distributed e-field (Figure 9) (Hallett, 2000; Wagner et al., 2007). Superior focality is achieved by the introduction of the figure-of-eight coil, which is most widely used for language mapping (Klooster et al., 2016). These coils consist of two adjacent and overlapping circular coils through which the two circling currents of each ring flow in opposite directions. The maximum electric current hence happens at the point of overlap. This leads to a conical shaped magnetic and hence e-field with a clear local maximum in field strength at the tip. Again, this focality is lost when using higher stimulation intensities (Levy et al., 1991; Brasil-Neto et al., 1992; Hallett, 2000; Liu et al., 2003; Deng et al., 2013).

Roughly $\frac{1}{10^6}$ of the electromagnetic energy emitted by the coil ultimately reaches the actual targeted nerve cells. On a cellular level, the field leads to a voltage reversal over the cell membrane, triggering depolarisation (Ravazzani et al., 2002; Speckmann et al., 2009). When exceeding a specific depolarisation threshold, the nerve cell produces a so-called action

Figure 9 *Electric current in the magnetic coil and the targeted brain illustrated by Hallett (2000) (Source: Hallett (2007) - Transcranial Magnetic Stimulation: A Primer. Figure 1. DOI: https://doi.org/10.1016/j.neuron.2007.06.026. Online publication date: July 2017. © 2007 Elsevier Inc. All rights reserved.)*

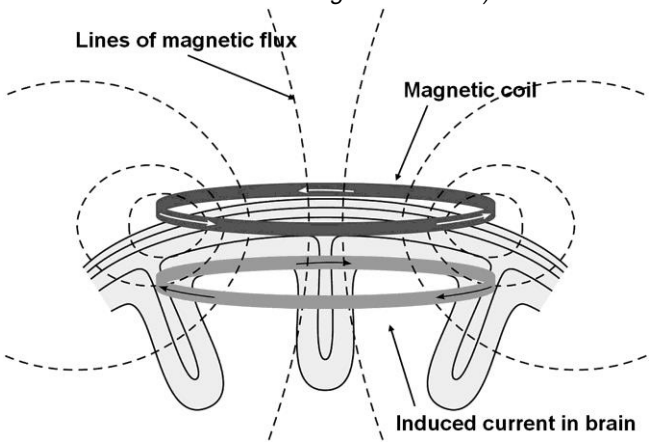

potential along the axon where ultimately stimulation is passed on to other nerve cells (Speckmann et al., 2009; Ruohonen et al., 2010). Again, the distribution and dimension of depolarisation depend on the spread and strength of the induced e-field (Ravazzani et al., 2002).

1.5.2. Further technical development of TMS

1.5.2.1. nTMS - neuronavigation for TMS

Until the turn of the millenium, TMS was classically oriented towards external landmarks on the skull's surface. Yet, stimulation intensity and coil position need to be adjusted to the actual cerebral anatomy (Steinmetz et al., 1990; Cykowski et al., 2008). Therefore, information regarding patient-specific anatomy as well as the spatial position of the coil in relation to the subject's head must be merged. To do so, a stereotactic camera registers the exact position of the coil as well as of the head and forwards this information to a stereotactic navigation system. This system contains prior MRI scans providing the exact anatomy of the brain and head structures. In this manner, navigated TMS (nTMS) enables a real-time three-dimensional (3D) tracking of the coil via neuronavigation and a pinpoint cortical stimulation (Ruohonen et al., 2010; Lioumis et al., 2012). Further, the exact site of stimulation paired with the documented clinical response can be stored. Using these assets, the reasonable implementation of preoperative nTMS in surgical planning and a precise comparison to other mapping tools such as DCS are possible (Krings et al., 2001; Picht et al., 2009; Tarapore et al., 2013). Hence, nTMS reliability has been improved (Gugino et al., 2001).
To date, two different procedures are in use, line-navigated (Ln-TMS) and electric-field-navigated TMS (En-TMS). While En-TMS calculates the produced e-field based on i.a. influencing factors such as the coil-cortex distance and coil tilting, Ln-TMS visualizes the geometric centre of the coil using a surface normal vector (Ruohonen et al., 1999; Ruohonen et al., 2010; Sollmann et al., 2016a). Recent findings imply a superior stimulation efficiency when using En-TMS rather than Ln-TMS, addressing the duration of stimulation and the mere mapping as well as the rate of positive responses. Yet, these findings were solely observed based on motor mapping and were lacking a comparison to the gold standard of DCS (Sollmann et al., 2016a). A comparison between Ln-TMS and En-TMS for language mapping is still pending.

1.5.2.2. Depiction of the induced electric field and its alignment

Aside of nTMS coil localization, coil alignment also influences the resultant depolarisation of the cerebral nerve cells (Kaneko et al., 1996; Thielscher et al., 2011; Tarapore et al., 2013; Klooster et al., 2016). Tarapore et al. (2013) found even slight rotations of just 10° to 15° to significantly influence the amplitude of muscle evoked potentials (MEP) or the positivity of a language site. Opitz et al. (2013) further found the rotative component to be more influential than coil angulation. In motor mapping, highest electromyography (EMG) values or MEP are found when stimulating perpendicularly rotated to the neighbouring brain sulcus (Day et al., 1987; Mills, 1991; Brasil-Neto et al., 1992; Kaneko et al., 1996; Sakai et al., 1997; Werhahn et al., 1999). The same applies further when the coil is aligned perpendicular angled (= tangential) to the targeted gyrus (Thielscher et al., 2011; Klooster et al., 2016).
In En-TMS, the assumed resultant e-field is illustrated and serves as a real-time visual tool for controlling coil alignment (Tarapore et al., 2013; Laakso et al., 2014; Klooster et al., 2016). Because visualizing the spread of the factual e-field or measuring its strength in situ could not be enabled so far, mathematic calculations based on complex head models were developed to draw a real-time theoretical field strength. These models pay respect to i.a. the diverse conductivity of brain tissue types, the individual anatomy, the applied coil geometry and alignment as well as current stimulation parameters (Tarkiainen et al., 2003; Salinas et al., 2007; Tarapore et al., 2013; Klooster et al., 2016). Due to charge accumulation at the cortical surface, a secondary inversely oriented e-field appears (Salinas et al., 2009). By including these considerations, EnTMS allows the examiner to adjust the proposed stimulation before it is conducted. A deeper understanding of current distribution may further elucidate the

correlation between the applied stimulation parameters and the triggered physiological effects (Klooster et al., 2016).

1.5.2.3. The development of single-pulse TMS to rTMS

Single-pulse nTMS can induce single instantaneous depolarisations of neurons without long-lasting effects. These stimuli can lead to involuntary motor reactions or visual sensations (Klooster et al., 2016). Paired-pulse or multiple-pulse nTMS concepts aim to influence cortical excitability and were initially used as priming conditioning stimuli before the proper (single) test stimulus (Pascual-Leone et al., 2002; Hamada et al., 2007; Sacco et al., 2009; Klooster et al., 2016). Underlying this effect is the model of induced plasticity by cumulative TMS stimulations (Siebner et al., 2003; Hamada et al., 2007). This model also encourages the use of repetitive TMS for therapeutic purposes in clinical and scientifical settings (Hoogendam et al., 2010), e.g. depression (Berlim et al., 2013), migraine (Barker et al., 2017) and tinnitus (Kim et al., 2014). Klooster et al. (2016) define rTMS as trains of stimuli of a specific frequency and intensity, i.e. regularly repeated single navigated or non-navigated TMS pulses (Rossi et al., 2009). Similar to single-pulse TMS, rTMS also induces an instantaneous effect by eliciting a virtual cortical lesion aiming at changes in the examined cognitive function, e.g. language (Pascual-Leone et al., 2000; Devlin et al., 2007; Tarapore et al., 2013). Since the first report by Pascual-Leone et al. (1991), several stimulating protocols for rTMS were introduced. These protocols provoke varying degrees of language interruption using different stimulation frequencies (Hz) and intensities as well as language tasks (Epstein et al., 1996; Wassermann et al., 1999; Sparing et al., 2001; Devlin et al., 2007; Lioumis et al., 2012; Tarapore et al., 2013; Wheat et al., 2013; Hauck et al., 2015).
Compared to DCS, rTMS causes significantly lower electrical currents in different frequencies. Therefore, single-trial rTMS stimulations so far do not provide the same powerful blocking stimulus as DCS per sé. Hence, it is recommended to search for clusters of language errors in certain cortical areas by means of stimulation trains in several passes (Krieg et al., 2017).

1.6. Diffusion tensor fiber tracking

Figure 10 *T1-weighted MRI of the brain with DTI of the AF & SLF lying close to a brain tumor.* ***A*** *= axial cut,* ***B*** *= sagittal cut,* ***C*** *= coronal cut. (Source: Henning Stieglitz et al. (2012) - Localization of primary language areas by arcuate fascicle fiber tracking. Figure 3. DOI: https://doi-org.eaccess.ub.tum.de/10.1227/NEU.0b013e31822cb882. Online publication date: July 2011. Copyright © 2011, Oxford University Press.)*

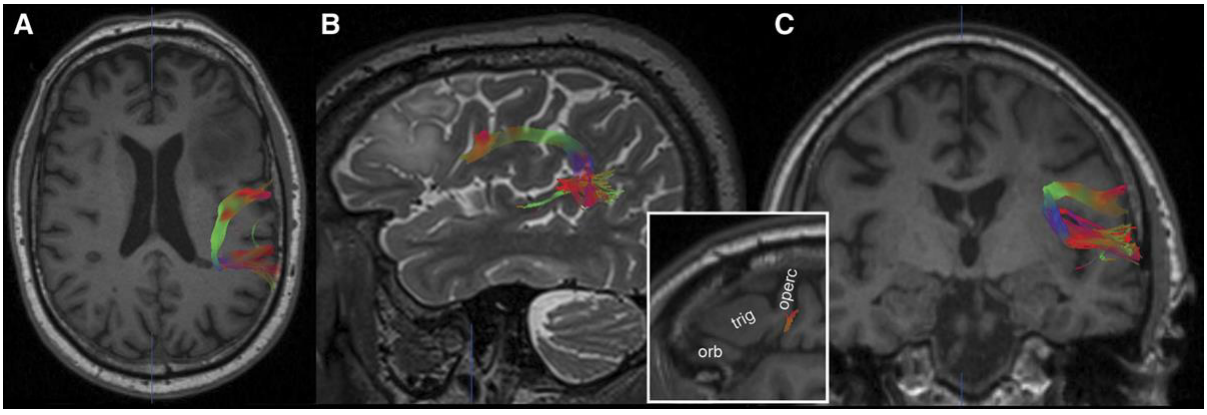

1.6.1. Basic technical principles

nTMS-based mapping targets the outer layer of the human brain, the cortex. Yet, traditional MRI sequences used for cortical language mapping do not suffice at depicting subcortical fiber tracts. To do so, a special MRI technique referred to as diffusion tensor imaging (DTI) is used. DTI is a subset of the special MRI technique diffusion-weighted imaging (DWI) (Figure 10). In short, DWI is based on the quantification of diffusion of water (dihydrogen oxide) molecules in the human brain introduced in 1986 (Le Bihan et al., 1986). Diffusion depicts the random proper motion of e.g. water molecules resultant of the Brownian motion described as a function of

temperature by Einstein in 1905 (Potgieser et al., 2014; Grover et al., 2015). In an open space, these molecules would spread randomly in all directions. This would be referred to as isotropic diffusion. In tissues, the possible range of motion is limited and hence diffusion does not happen evenly spread. A vectored diffusion is referred to as anisotropic (Chenevert et al., 1990; Le Bihan et al., 2012).
In the human brain, diffusion is facilitated in and along white matter nerve cell fibers (Chenevert et al., 1990; Moseley et al., 1990; Le Bihan et al., 1993; Conturo et al., 1999; Basser et al., 2000b). This effect in part relies upon the surrounding myelin sheaths that act as diffusion barrier. The higher the degree of myelinisation, the higher the extend of anisotropy (Toft et al., 1996; Vorisek et al., 1997; Neil et al., 1998). Yet, a high level of anisotropy does also exist along non-myelinated fiber tracts indicating further underlying mechanisms than just myelinisation (Rutherford et al., 1991; Beaulieu, 2002). Diffusion happens both outside and inside of a nerve cell while cell membranes restrict diffusion. Yet, cell membranes do not fully subdue diffusion pathways (Le Bihan et al., 1993; Alexander et al., 2007). Therefore, grey matter is more isotropic compared to white matter due to the increased presence of myelinisation in the white matter. CSF contains nearly no diffusion barrier. A demarcation of white matter areas is hence possible (Alexander et al., 2007).
To evaluate diffusion, DWI applies magnetic field gradients along different axes of a voxel. The higher the applied magnetic power, the faster the magnetic nuclear spin axis of a hydrogen core inside a water molecule rotates. In a magnetic gradient, the spin phases, i.e. rotation speed, hence starts to spread along the specific gradient axis in a process called dephasing. Following dephasing, the magnetic field gradient is inversed and held for the exact same duration as during dephasing. Thereby, spin phase changes were leveled out in a process called rephasing. With restricted diffusion, i.e. no changed hydrogen molecule position, the original state would be reinstated. Rephasing can be recorded as a strong electromagnetic signal. In presence of diffusion, it is not possible to rephase the hydrogene core which have changed position. Hence, the electromagnetic signal declines correlating with the amount of diffusion (De Figueiredo et al., 2011). Diffusion thresholds can be set by changing the so-called b-value, a function of magnetic field gradient strength and the time between the gradient shifts (Basser et al., 2002; O'Donnell et al., 2011).

1.6.2. Fiber assignment by a continuous tracking

The mathematical model of a diffusion tensor describes the diffusion directions in a 3D voxel as ellipsoids build by eigenvectors and eigenvalues (Basser et al., 1994b; Conturo et al., 1999; Mori et al., 1999b; Basser et al., 2002; Grover et al., 2015). Different movement axes for water molecules are weighted to determine the primary diffusion direction, the principal eigenvector (PEV). Moreover, the degree of anisotropy depicting the alignement of diffusion (= fractional anisotropy) as well as the mean diffusivity (= quantity of water motion) are calculated (Farrell et al., 2007; Grover et al., 2015). Calculation of the diffusion tensor includes diffusion data from at least six non-collinear directions to assure independency of rotational errors (Basser et al., 2002; Grover et al., 2015).
The calculation of the PEV is supplied for each voxel (Stejskal et al., 1965; Basser et al., 1994a, 1994b). Using these values and starting from a seeding point or region of interest (ROI), fiber tracts can be built following stringed diffusion pathways (Catani et al., 2002; Mori et al., 2002a). This approach is referred to as fiber assignment by a continuous tracking (FACT) and to date marks the most commonly used deterministic approach of DTI FT (Mori et al., 1999b; Mori et al., 2002b; Hana et al., 2014). The seeding points can base on anatomical landmarks or e.g. nTMS points derived from a beforehand taken mapping. The latter would be referred to as nTMS-based DTI FT (Bello et al., 2008; Leclercq et al., 2011; Frey et al., 2012; Krieg et al., 2012a; Conti et al., 2014; Sollmann et al., 2015a). Tracked fiber pathways are commonly depicted direction-coded by colour and matched with the anatomic MRI images (Figure 10) (Basser et al., 2000b; Pajevic et al., 2000; Witwer et al., 2002; Leclercq et al., 2011).

1.7. Objective of this thesis

Navigated rTMS was repeatedly found to exceed other preoperative language mapping procedures (Picht et al., 2013; Tarapore et al., 2013; Ille et al., 2015b). Yet, the method's comparability to DCS has not met expectations yet. Navigated rTMS language mapping suffers from low specificity and limited positive predictive values (PPV), while it achieves high sensitivity results and negative predictive values (NPV) (sensitivity of 90.2% and specificity of 23.8% in Picht et al. (2013)). So far, this receiver operating characteristic (ROC) constellation only allows for negative language mapping by navigated rTMS, meaning that negative tested cortical areas have to be confirmed or discarded by DCS (Indefrey, 2011; Picht et al., 2013; Tarapore et al., 2013; Krieg et al., 2014a; Ille et al., 2015b). Yet, albeit these setbacks, negative language mapping using navigated rTMS already resulted in more tailored and smaller craniotomies (Tarapore et al., 2013; Sollmann et al., 2015b). However, during the data collecting process of this study in 2013, the rate of permanent neurologic morbidity after surgery of language-eloquent tumors still ranged between 3.2% and 20% (Tarapore et al., 2013).
In 2015, the combination of preoperative fMRI and navigated rTMS enabled a moderate improvement in the comparison to DCS (sensitivity 98%; NPV 95%; specificity 83%; PPV 51%) (Ille et al., 2015b). This thesis combines rTMS-based DTI FT with navigated rTMS as preoperative language mapping tools to achieve a higher comparability of cortical language mapping by navigated rTMS to DCS. To improve specificity, this study aims to screen out language-involved from truly language-eloquent brain areas. Underlying this method is the assumption that truly eloquent areas should cross-linked more intensely which may correlate with higher numbers of nerve fibers depicted via DTI FT (Duffau et al., 2014; Sollmann et al., 2016b). Exploiting the functional connection between cortical regions and subcortical fibers also reflects the hodotopical model by Duffau et al. (2014).
DTI FT has already been successfully deployed for depicting subcortical language-related fiber bundles in the past (Henry et al., 2004; Nimsky et al., 2007; Bello et al., 2008). Further, the approach of using nTMS-based seed regions instead of user-dependent anatomic seed regions for DTI FT was already implemented for preoperative language mapping (Bello et al., 2008; Leclercq et al., 2011; Sollmann et al., 2015a). One case report in 2015 further established a connection between loss of language function and rTMS-based language DTI FT results (Sollmann et al., 2015a).
In this study, the further information of functional connectivity gained by rTMS-based DTI FT was used to confirm or disprove navigated rTMS language mapping results, examining several different analysing parameters in the process. Aim of this investigation was to evaluate whether the combination of data from navigated rTMS and rTMS-based DTI FT was suited to improve the preoperative ROC in comparison to intraoperative DCS. Thereby, the following hypotheses were formulated and reviewed:

- The number of fibers coming from one rTMS language-positive CPS region reflects the underlying connectivity and hence correlates with its language eloquence. Non-eloquent regions can be filtered out and thereby the number of by rTMS false-positive detected regions can be reduced.
- The usage of different fiber tracking parameters can be used to adapt the depiction of this connectivity in order to improve ROC.
- The implementation of different language error thresholds for the determination of rTMS language positivity or negativity influences the comparability to DCS and can be used to improve ROC.
- The differing error types are not equally well detectable by rTMS as well as DCS. Evaluating single error types can influence the comparability to DCS and hence ROC.
- The differences in language processing regarding the classical segregation in anterior and posterior cortical regions is reflected in a different comparability to DCS. A segregated analysis can uncover these differences in ROC regarding the spatial distribution of stimulation.

2. MATERIALS AND METHODS

2.1. Study design

Data collection took place between June 2011 and November 2014. During this time span 20 patients were recruited. Patients had to fulfil the following study inclusion criteria:

- Left-hemispheric perisylvian brain tumor with medical indication for tumor surgery
- Age over 18 years
- Ability of speaking German fluently
- Given informed consent by signature

Exclusion criteria were defined as following:

- Prevailing rTMS and MRI exclusion criteria containing unsafe ferromagnetic or conductive objects and devices i.a. cardiac pacemaker, cochlea implant and deep brain stimulator (Rossi et al., 2009; Cross et al., 2018)
- Exclusion criteria for a conclusive language testing (i.a. distinct Aphasia)
- Absolute contradiction for awake surgery (i.a. uncontrolled coughing, significant mass effect, severe cognitive impairment)

Each patient underwent a precise neuropsychological testing as well as an assessment of handedness via the Edinburgh Handedness Inventory (Oldfield, 1971). Cranial MRI along with DTI provided the basis for all subsequent steps. If not otherwise specified, rTMS always refers to navigated rTMS in this thesis. The different employed rTMS language mapping parameters reflect the retrospective analysis of this prospectively collected cohort of patients who underwent language mapping by rTMS congruent with the standards of practice. Language-positive or -negative CPS regions were identified by rTMS (= rTMS**+**/**-**), rTMS-based DTI FT (= DTI FT**+**/**-**) as well as DCS (= DCS**+**/**-**). ROC calculation was conducted as based on the following combinations: DCS versus rTMS (= rTMS vs. DCS), DCS versus rTMS-based DTI FT (= DTI FT vs. DCS) and DCS versus rTMS-positive sites affirmed by rTMS-based DTI FT (= (rTMS + DTI FT) vs. DCS).

2.2. Safety and ethical considerations

Above stated inclusion and exclusion criteria were implemented to reduce the probability of following possible hazardous side effects (Wassermann, 1998; Rossi et al., 2009; Hervey-Jumper et al., 2015; Panych et al., 2018):

- Burn injuries of tissue by heating up conductive material (e.g. silver, gold)
- Activation or malfunction of electronic devices (e.g. deep brain stimulator)
- Demagnetisation of magnets (e.g. in cochlea implants)
- Displacing of ferromagnetic objects (i.a. risk of flying objects)
- Damage on the auditory system (e.g. tinnitus)
- Increased surgical risk due to a non-cooperative patient

In addition, the following rules were established:

- Removal of all ferromagnetic or conductive objects - if possible - during nTMS and MRI (e.g. glasses, jewellery)
- Reconciliation of non-removable objects with the listed safe devices by the MRI Safety Committee
- In case of uncertainty regarding ferromagnetic or conductive characteristics of not removable objects, further proof ex-vivo or exclusion of the investigation

- Necessity of hearing protection during MRI

The study design was reviewed by the ethics committee of the Klinikum rechts der Isar and was approved by the local institutional review board in accordance with the ethical standards stated in the 1964 Declaration of Helsinki and its addenda (Registration Number: 2793/10). Hence, the potential benefit was found to outweigh the risks. Patients were informed in detail about the course of the study, the potential risks or discomfort, the use of the collected data and their rights. This took place in an individual consultation with the investigator and with the help of a standardized information sheet. Patient gave their informed consent to their inclusion in this study and the use of their data for academic purposes by signing the information sheet.

2.3. Neuroradiologic imaging

Imaging studies were performed on a 3-Tesla MRI scanner (Achieva 3T, Philips Medical System, The Netherlands B.V.) equipped with an eight-channel phased-array head coil. This study's imaging was part of a standardized imaging protocol for patients with brain tumors. This protocol included a fluid-attenuated-inversion-recovery (FLAIR) (repetition time (TR)/echo time (TE): 12.000/140 ms, voxel size: 0.9 × 0.9 × 4 mm^3, acquisition time: 3 min), a 3D T1-weighted gradient echo sequence (TR/TE: 9/4 ms, 1 mm^3 isovoxel covering the whole head, acquisition time: 6 min 58 s) and a DTI with six orthogonal diffusion directions (single-shot spin echo EPI, TR/TE 7.571/55 ms, spatial resolution of 2 × 2 × 2 mm^3, b-values of 0 and 800, acquisition time: 2 min 15 s). Motion image artefacts of DTI data were adapted and eddy currents emerging during MRI corrected. 3D T1-weighted gradient echo sequence were conducted at a slice thickness of 1 mm. Images were produced both natively and with the use of 0.1 mmol/kg intravenous contrast agent (gadopentetate dimeglumine, Magnograf, Marotrast GmbH).

2.4. Language mapping by repetitive navigated TMS

2.4.1. Setup and preparation

Figure 11 *Basic setup for a language mapping using navigated rTMS. The examiner steers the nTMS coil pinpointed over the patient's head while using real-time neuronavigation using the 3D MRI head image and the stereotactic tracking system (stereotactic camera, head tracker and nTMS coil each with reflective sphere markers). A screen and a video camera serves for the application and analysis of the language task. The EMG connected to the APB of the right hand is needed for the determination of the RMT.*

Patients were again informed about the possible side effects of the rTMS procedure and general exclusion criteria were again checked before the beginning of each rTMS procedure (Rossi et al., 2009). Navigated rTMS studies were performed on an EnTMS-based eXimia

Figure 12 *Co-Registration for neuronavigation. In total 12 reference points were presented with the digitizing pen.*

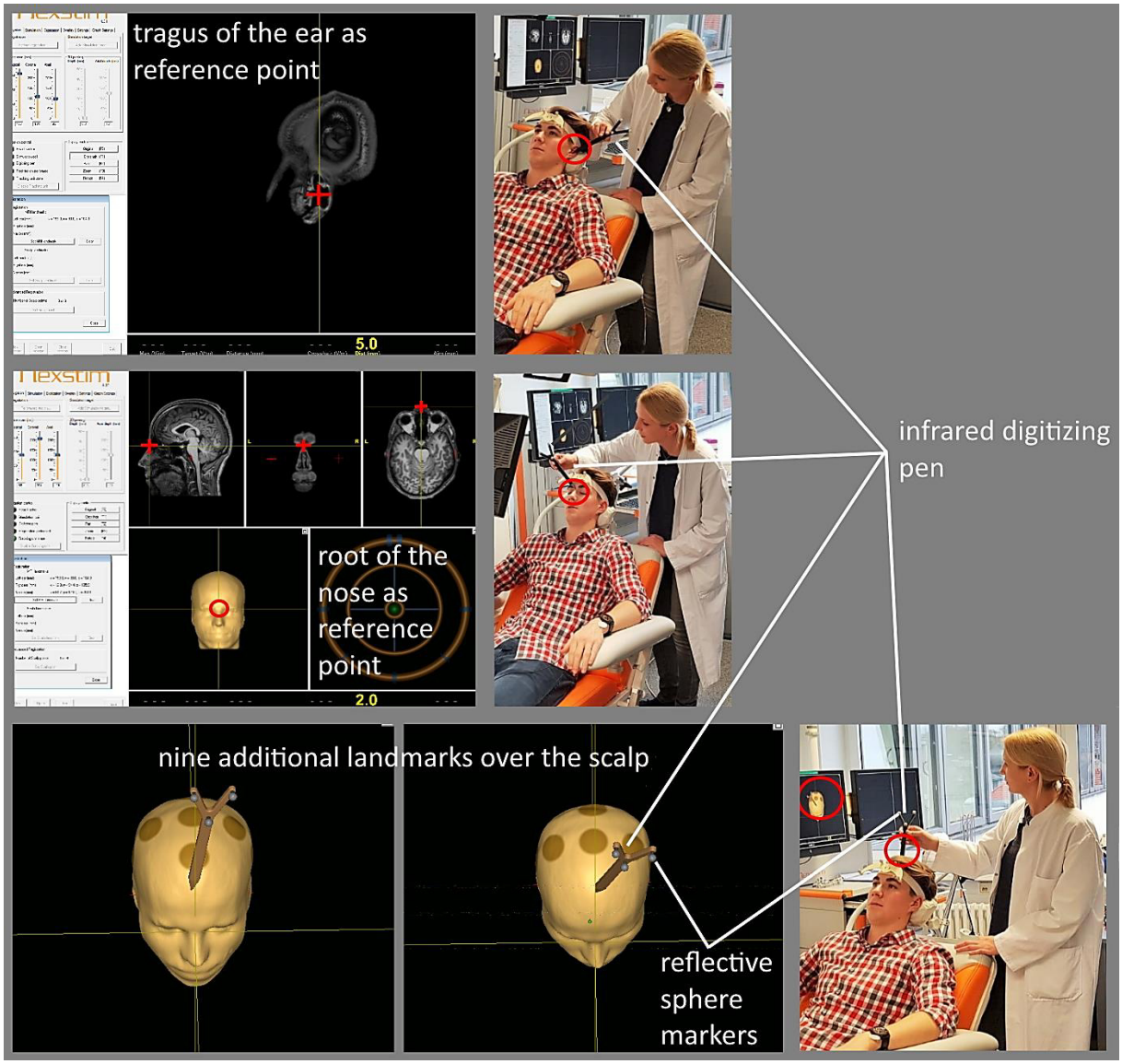

navigated brain stimulation (NBS) system with a figure-of-eight coil (eXimia NBS version 3.2.2 or 4.3, Nextim Oy, Helsinki, Finland). This system to date marks the only device approved for preoperative cortical mapping by the U.S. Food and Drug Administration (FDA) (Eldaief et al., 2013; Mäkelä, 2015). The system includes an electromyography device for simultaneous recording of muscle responses and was complemented by a NexSpeech® module to enable for language mapping. Worldwide this setup is in use in more than 40 neurosurgical centres and has been employed in several clinical trials (Figure 11) (Picht et al., 2013; Sollmann et al., 2013c; Tarapore et al., 2013; Ille et al., 2015b; Mäkelä, 2015).

Patients were positioned in an examination chair in the most comfortable position to reduce EMG-interference due to increased muscle tension, especially in the upper extremities. An stable and interference-free upper extremity EMG is essential for resting motor threshold (RMT) determination later on (Rossini et al., 1994; Auriat et al., 2015; Rossini et al., 2015; Ahdab et al., 2016). A fitting head position reduces possible headache and neck pain during the examination (Machii et al., 2006; Rossi et al., 2009). Following positioning of the patient, a tracker containing reflective sphere markers for the stereotactic camera of the infrared tracking system for real-time neuronavigation was mounted on the patient's head (Polaris Spectra, Waterloo, Ontario, Canada) (Figure 11) (Picht et al., 2013; Ille et al., 2015b).

Contrast-enhanced 3D T1-weighted gradient echo sequence images of the brain that serve as imaging part for real-time neuronavigation were then uploaded to the NBS system (Figure 11) (Ruohonen et al., 2010; Lioumis et al., 2012). Following import of the MRI data, pre-defined

reference points on the patient's head were marked on the 3D image. These reference points were then spatially presented to the stereotactic camera using an infrared digitizing pen equipped with reflective spheres. MRI and spatial coordinates were then aligned by combining each reference point's spatial coordinates registered by the stereotactic camera with its coordinates in the MRI. This was done adhering to the commonly used protocol outlined in Karhu et al. (2014). At first, rough alignment was achieved by marking each tragus of the ear and the root of the nose. To refine alignment, nine additional landmarks, disseminated over the 3D subject's scalp, were presented by the NBS system and again presented in vivo using the infrared digitizing pen (Figure 12). This alignment of coordinate systems, also referred to as MRI to head co-registration allows for an accurate coil navigation during rTMS unaffected by head movement (Karhu et al., 2014). To ensure correct alignment, the head tracker must not be moved on the patient's head after co-registration as it's spatial coordinates represent the head's position to the NBS system. Should the tracker be moved by accident, co-registration had to be redone.

2.4.2. RMT determination

Figure 13 *3D MRI head image with the sulcus centralis (= orange line), the precentral gyrus (= blue shading) and the area of the hand knob (= red encircling).*

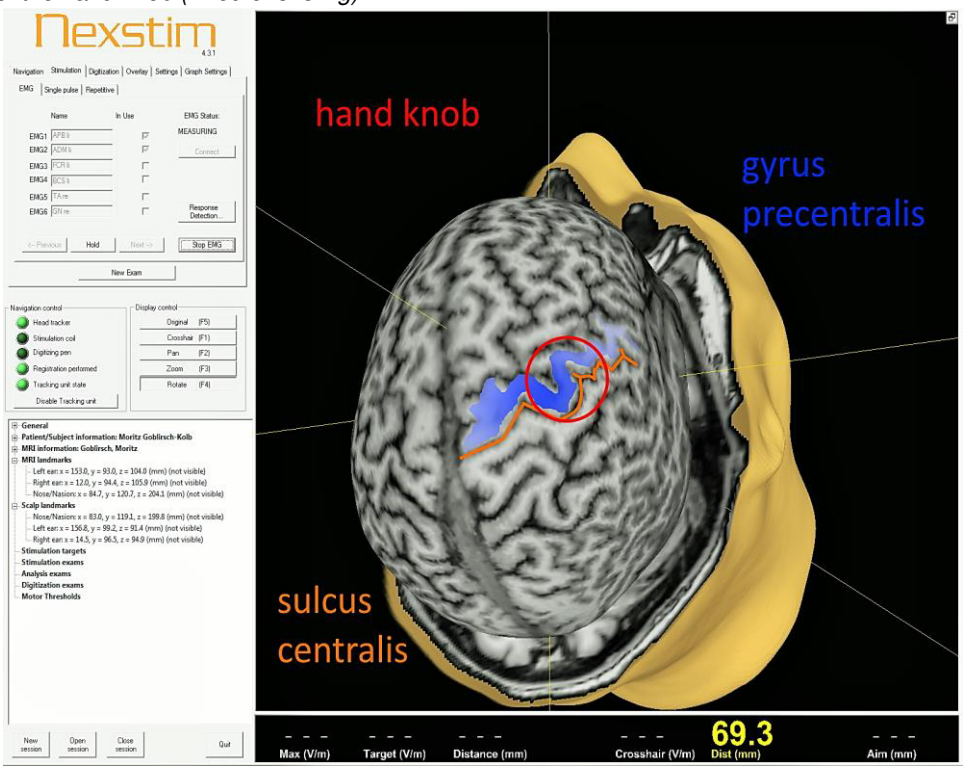

The RMT of the examined left hemisphere was determined to adapt stimulation intensity to the individual level of cortical motor excitability (Klooster et al., 2016). It is defined as the minimal stimulus intensity that produces MEP > 50 µV in peak to peak amplitude in at least five out of ten trials with MEP recorded from the same, fully relaxed muscle (Rossini et al., 1994; Auriat et al., 2015; Rossini et al., 2015; Ahdab et al., 2016). Muscle tension leads to a decrease of the stimulus threshold and hence to higher MEP amplitudes. Moreover, spontaneous activity may superimpose muscle contraction provoked by the magnetic stimulus (Picht, 2015). Active pregelled surface electrodes (Neuroline 720, Ambu, Ballerup, Denmark) were linked to the right abductor pollicis brevis (APB) muscle and complemented by a reference electrode to the bone transition area. Joint position was modified until the resting activity (spontaneous EMG amplitudes) was always below the threshold for positive MEP responses (0.05 mV) (Krieg et al., 2012b; Picht, 2015).
The systems depiction of the patient's MRI reconstruction was adjusted to centre the left hemisphere's hand knob, which is typically located in a depth of around 20 - 25 mm below the

Figure 14 *In* ***no. 1*** *the neuronavigation surface during the rough motor mapping for the detection of the hotspot is depicted. The further recorded EMG is displayed in real-time as well as every MEP of every nTMS stimulation. In* ***no. 2*** *an upward, as originally directed, and green, so correctly angulated, arrow is shown during the recheck of the hotspot. In* ***no. 3*** *the same stimulation point is rechecked 45° anticlockwise. The visual tool in* ***no. 2*** *and* ***3*** *is also used for the determination of the RMT.*

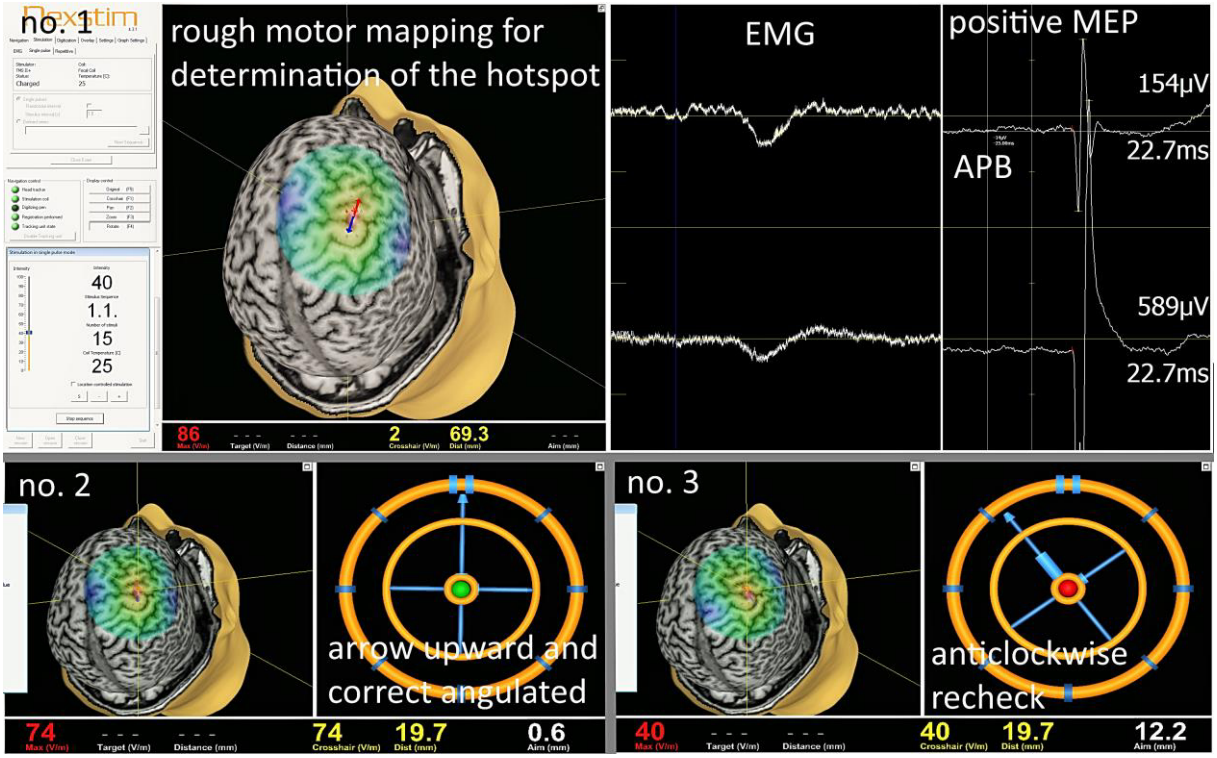

scalp tissue (Figure 13). Starting there, a rough motor mapping was started to find the spot with the highest evoked amplitude in EMG, the hotspot (Yousry et al., 1997; Park et al., 2007). Mapping procedure followed common mapping protocols (Rothwell et al., 1991; Rossini et al., 1994). Stimulation was started with an intensity of around 40% of the systems maximum output aiming at EMG amplitudes between 0.1 and 0.5 mV. Using the visualized induced e-field, the coil was positioned tangentially to aim the e-field maximum to the targeted spot. The cortex was then stimulated in rectangular (= perpendicular) direction to the closest cerebral sulcus, the sulcus centralis (Day et al., 1987; Mills, 1991; Brasil-Neto et al., 1992; Kaneko et al., 1996; Sakai et al., 1997; Werhahn et al., 1999; Thielscher et al., 2011; Klooster et al., 2016).
Stimulation intensity was manually adjusted until MEP amplitudes were between 0.1 and 0.5 mV (Figure 14 no. 1) (Krieg et al., 2017). Once the assumed hotspot was narrowed down and marked, optimal stimulation orientation and coil angulation were rechecked. This was done using a visual software tool with an arrow corresponding to the coil's alignment. Coil orientation was tested in the original direction (= 0° deviation), as well as rotated by 45 degrees both clockwise and counterclockwise. For each trial, correct angulation was depicted by the arrow's green colour (Figure 14 no. 2 and no. 3). Each alignment was tested 10 times using the original stimulation intensity. For affirmation of the optimal coil alignment, highest MEP had to be evoked in at least 5 out 10 stimuli.
RMT determination was then done using the optimal alignment. If this procedure resulted in another than the original 0° orientation, hotspot detection had to be done anew. The actual determination of the RMT was done machine aided with the NBS automatically applying stimuli every 2 seconds (Sollmann et al., 2017b), utilizing a maximum-likelihood-threshold-hunting algorithm to narrow down the stimulation intensities until reaching the RMT as defined above (Rossini et al., 1994; Picht, 2015). Again, using the above outlined visual tool, the examiner ensured optimal stimulation orientation, angulation and location during automated RMT determination. Inaccurate coil position was detected by the system and stimulation was automatically stopped until coil position was corrected. The RMT is stated as the resultant stimulation intensity, declared as percentage of the maximum output of the system (Ruohonen

et al., 2010; Picht et al., 2011; Auriat et al., 2015; Picht, 2015). The later applied stimulation intensity for language mapping is based on the individual RMT (Ruohonen et al., 2010; Auriat et al., 2015).

2.4.3. Language task and baseline performance

Figure 15 *Baseline object naming. Pictures are presented on the screen. The patient's voice and face are video recorded for later analysis of language errors.*

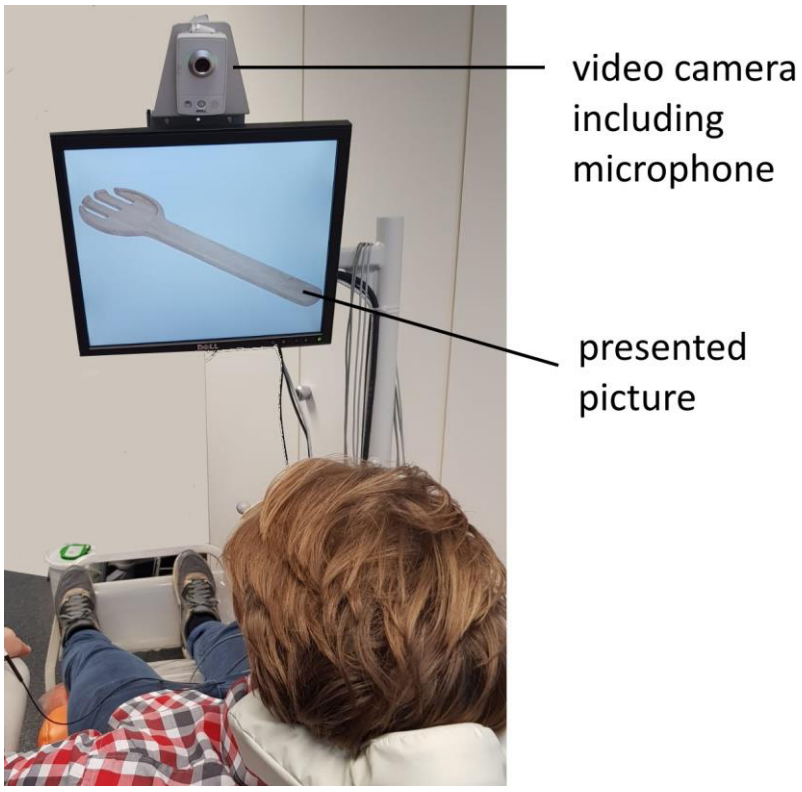

This thesis utilizes the current standard of an object-naming task (Lioumis et al., 2012; Picht et al., 2013; Krieg et al., 2014b; Krieg et al., 2016). Before starting rTMS language mapping, patients had to perform baseline object naming with the NexSpeech® module, in which 131 coloured pictures of common objects and creatures based on the Snodgrass and Vanderwart picture set were presented on a computer screen (Snodgrass et al., 1980; Lioumis et al., 2012; Picht et al., 2013; Tarapore et al., 2013). The patient was asked to name the pictures in German as fast and clearly as possible without using an article (“house” instead of “the or a house”) (Figure 15). All pictures, which were pronounced unclearly or faltering or which were entitled incorrectly were separated out. This was done based on the database of the German version of the "International Picture Naming Project" (Szekely et al., 2004). This procedure was then repeated using only pictures named correctly during the first session. In this manner, an individually adjusted object-naming batch containing familiar and identifiable pictures could be created for each patient. The number of pictures in this individual batch was noted. The applied period between two shown pictures, the interpicture interval (IPI), and the duration of picture presentation, the picture presentation time (PPT) are outlined in Table 1.

2.4.4. Stimulation

Video and audio of the baseline performance and the actual language mapping procedure were recorded by the NexSpeech® module. Pictures were presented as infinite loop in randomized order to avoid possible learning effects. During stimulation, the interval between the beginning of picture presentation and the onset of the rTMS burst, also referred to as picture-to-trigger interval (PTI) was set individually (Ille et al., 2015b). PTI was either set to 0 ms, meaning that stimulation and picture presentation happen simultaneous, also referred to as time-locked stimulation, or to 300 ms (Table 1). The applicability of both PTI variants was

Table 1 *Different applied language mapping parameters regarding PPT, IPI, PTI, stimulation intensity as well as frequency and pulse count per study subject and further the usage of a CPS template for stimulation is listed. ID = identification number of each patient.*

ID	PPT (ms)	IPI (ms)	PTI (ms)	int. (%)	freq. (Hz)/ pulse count	CPS template
1	700	2500	0	100	7/5	No
2	700	2500	0	100	5/5	No
3	700	2500	0	106	7/7	No
4	700	2500	0	113	7/5	No
5	700	2500	0	120	5/5	No
6	700	2500	0	100	7/5	No
7	700	2500	0	100	5/5	No
8	700	2500	300	100	5/5	No
9	700	2500	300	100	5/5	No
10	700	2500	300	100	5/5	No
11	2000	4500	300	100	5/5	No
12	700	2500	300	122	7/7	No
13	700	2500	300	121	5/5	No
14	700	2500	300	121	5/5	No
15	1000	3000	300	100	7/7	No
16	700	2500	300	100	7/7	No
17	700	2500	300	80	5/5	No
18	1000	2500	0	100	7/5	No
19	700	2500	0	100	5/5	Yes
20	700	2500	0	100	5/5	Yes

demonstrated in earlier studies (Indefrey et al., 2004; Indefrey, 2011; Brennan et al., 2012; Picht et al., 2013; Krieg et al., 2014b; Sollmann et al., 2017a).
During IPI, the coil was moved manually to the next stimulation point with regard to perpendicular angulation (Ruohonen et al., 1999; Ruohonen et al., 2010; Lioumis et al., 2012). Unlike motor mapping and RMT determination, the electromagnetic field was directed strictly anterior-posterior for the entire language mapping procedure (Epstein et al., 1996; Wassermann et al., 1999; Lioumis et al., 2012). E-field strength varied between 55 and 80 V/m. Patient-specific stimulation frequency and intensity were determined adhering to the prevailing standard protocol (Table 1) (Pascual-Leone et al., 1991; Sollmann et al., 2013a; Sollmann et al., 2013c; Ille et al., 2015b). Stimulation intensity was at first set to 100% of the ipsilateral RMT while stimulation frequency and pulse count was evaluated using three possible combinations (a: 5 Hz, 5 pulses; b: 5 Hz, 7 pulses; c: 7 Hz, 7 pulses). Using these settings, the most comfortable and effective combination was chosen based on both the patient's and investigator's impression. In ambiguous situations the decision was made with the help of video analysis. If there was still a lack of language errors, the stimulation intensity was gradually increased, up to a maximum of 122% whereas stimulation intensity was decreased if result-interfering pain or discomfort occurred (Epstein et al., 1996). The resultant mapping intensity calculates as follows:

$$|RMT| \times \frac{intensity\ (\%)}{100} = mapping\ intensity \times 100 = mapping\ intensity\ (\%)$$

18 out of 20 subjects were stimulated without fixation points, meaning that mapping was aimed to cover all presumably language-eloquent CPS regions as best as possible. Areas important for surgery were mapped with greater accuracy, meaning a reduced distance between the stimuli of about 10 mm and at least triply repeated stimulation of each point (Lioumis et al., 2012; Picht et al., 2013; Tarapore et al., 2013; Hernandez-Pavon et al., 2014; Ille et al., 2015b). Due to a change in protocol that happened during the observation period of this study, the last

Figure 16 *CPS stimulation template with orientation dots added. Each dot was identified and marked in the 3D MRI head model of the respective subject prior to the actual mapping. Each point was stimulated 6 times.*

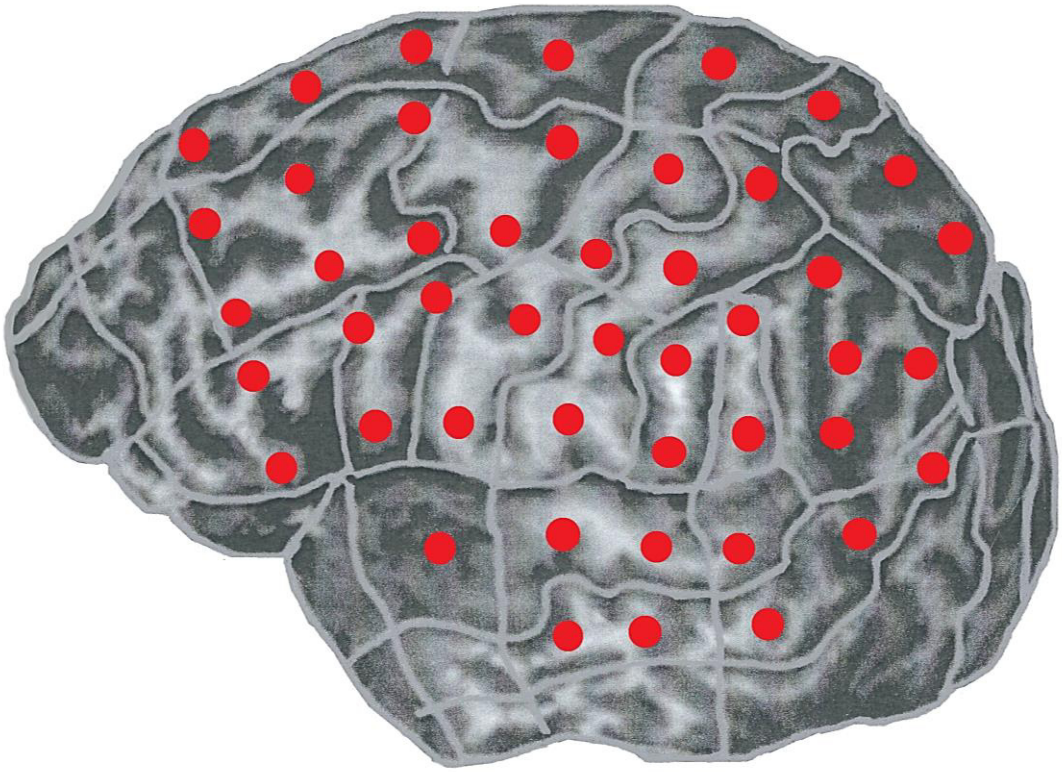

two patients (identification numbers #19 and #20) were stimulated using a predefined schematic (Figure 16). This schematic bases on 46 orientation dots on the left hemisphere that are set before starting the language mapping. Each orientation dot is then stimulated 6 times. Doing so simplifies correct allocation of stimuli to each CPS parcel and further standardizes the count of stimulations set to each CPS parcel. Irrespective of protocol used, stimulation was never successively applied to the same cortical region to prevent summation effects or focal seizure-type phenomena (Krieg et al., 2017).
Following language mapping, patients were asked about their subjective intraprocedural pain sensation. Pain was assessed separately for the left temporal region and the remaining areas of the left hemisphere. Using the visual analogue scale (VAS), both $VAS_{temporal}$ and $VAS_{convexity}$ could be obtained per each subject. VAS intensity score ranges from 0 to 10, referring to no pain (0) to the highest imaginable distress (10).

2.4.5. Offline analysis

Language mapping data was stored as NBS session file, containing the stimulation sites marked on the 3D head model and as speech session file, containing the video and audio recordings of the examination. Both files were then combined using the NexSpeech® analyser tool. From here on, each stimulation was connected to the resultant clinical finding documented in video and audio. Yet, to avoid possible bias, the software did not display the site of stimulation during evaluation of audio and video files (Lioumis et al., 2012; Picht et al., 2013; Krieg et al., 2014a). To asses each event with respect to the patient's individual pronunciation and reaction latency as well as to detect sublime language errors, each rTMS stimulus video was compared to the baseline performance video for the same picture (Corina et al., 2010; Picht et al., 2013). Incorrect rTMS stimulations due to i.a. interrupted stimuli as well as errors evoked by pain, muscle contraction or non-compliance were discarded. The remaining language errors were ascribed to the stimulation. To do so, the examiner was properly and specifically trained. These errors were classified to the following, standardized scientific error types (Corina et al., 2010; Sollmann et al., 2013a):

- No response errors: complete malfunction during stimulation. No verbal reaction in respect to a shown object during the object-naming task.
- Performance errors: every change in language performance during stimulation e.g. stuttering, slurred speech or uncommon emphasis, including dysarthria (difficult or unclear articulation of speech) and apraxia (inability to perform purposive actions e.g. opening the mouth).
- Hesitation errors: delayed verbal reaction to a shown picture compared to baseline output.
- Neologism: new word creation to a shown picture ("tremy" instead of "tree").
- Semantic paraphasias: erronous naming of a semantically similar object ("bush" instead of "tree").
- Phonological paraphasias: unspecific phonemic alteration of the proper original word ("bree" instead of "tree").
- Circumlocution: paraphrasing the shown object ("apples grow on it" instead of "tree").

Following review of all rTMS stimulation sites, language-positive (= rTMS**+**) denoted spots were automatically listed in a report file that included the assigned language error type.

2.4.6. Further processing of raw data

Language errors were further categorized into five different error categories (EC). These categories were *all errors* (AE), an overview of the total error number, *all errors without hesitation* (AEWH), *no response errors* (NRE), *performance errors* (PE) and *hesitation errors* (HE). Error types *neologism, circumlocution, phonological paraphasias* and *semantic paraphasias* were not specifically categorized. They are included in AE and AEWH.
rTMS**+** stimulation sites and their coordinates in the corresponding MRI's coordinate plane were exported as a *digital imaging and communications in medicine* (DICOM) file. Using this file, the stimulation site coordinates could be integrated in the clinic's *picture archiving and communication system* (PACS) to allow for later use in rTMS-based DTI FT. Export was conducted separately for each EC resulting in one file for each EC containing the data of all sites in which stimulation leads to an error of the corresponding EC. Further, information about rTMS**+** and rTMS**-** sites was separately integrated in PACS to allow for intraoperative neuronavigation (Dellani et al., 2007). Language error sites were further assigned to the corresponding CPS regions. CPS regions were identified using the respective MRI of the study subject and a template based on Corina et al. (Corina et al., 2005). Doing so allowed to calculate CPS-specific error counts and enables for statistical analysis of error frequency and distribution. For the preoperative surgical planning and preoperative DTI FT, a CPS region was regarded rTMS**+** if at least one error of any error type could be provoked in this region. All other regions were deemed rTMS language-negative (rTMS**-**). As was done with single errors, rTMS**+** areas were again categorized to the above described EC. Doing so, the assignment of language positivity was only done exclusively based on language errors of a specific EC. Regarding the comparison to DCS (= rTMS vs. DCS), positivity of a CPS region was designated based on 12 different threshold categories (TC) taken from prior studies (Haglund et al., 1994; Sanai et al., 2008a; Krieg et al., 2013b; Picht et al., 2013; Ille et al., 2015b). Of these 12 TC, eleven are based on different error rates. Error rates are defined as the number of triggered errors in a single CPS region divided by the total number of rTMS stimulation trials in said CPS region (Krieg et al., 2013b; Picht et al., 2013; Ille et al., 2015b).

$$error\ rate = \frac{number\ of\ errors}{number\ of\ stimulations}$$

This study utilizes eleven different error rate thresholds (ERT) as lower limits for the decision of rTMS positivity for each CPS region. ERT values start at 0% and increment in 5% steps up to an ERT of 50%. rTMS positivity was assigned when the error rate was greater or equal (≥) to the specific ERT, with the exception of the 0% ERT. In this case, the error rate had to be greater than (>) the ERT, an error rate of 0 resulted in a designation as rTMS**-**.

These eleven ERT based TC were complemented by a final TC based on the 2-out-of-3 rule (Haglund et al., 1994; Sanai et al., 2008a). Adhering to this rule, at least 2 out of 3 rTMS stimulations on the same spot within a single CPS region must lead to provoked language errors to designate said region as rTMS**+**.

2.5. rTMS-based DTI FT

2.5.1. Setup and preparation

To allow for rTMS-based DTI FT, the above mentioned DICOM file containing rTMS**+** stimulation sites, as well as the patient's DTI and contrast-enhanced 3D gradient echo sequence were uploaded into the *Image Fusion Software BrainLAB iPlanNet server®* (iPlan Cranial 3.0.1, BrainLab AG, Feldkirchen, Germany). Making use of this frequently used neurosurgical tractography software, these files could be fused and their coordinate planes aligned (Nimsky et al., 2007; Frey et al., 2012; Krieg et al., 2012a; Sollmann et al., 2015a; Weiss et al., 2015). Fusion is carried out semiautomatic and offline on a PC workstation following a rough alignment based on the investigator's visual impression of certain anatomical landmarks (nose and ears). Following this first step, a "rigid registration algorithm applying an intensity-based pyramidal approach using mutual information" completes data fusion (Studholme et al., 1996; Thevenaz et al., 1998; Nimsky et al., 2007). This algorithm results in a 3D head model that contains information about the anatomic head and brain structure, nerve fiber pathways derived from the deterministic diffusion tensor model with its PEV and FACT approach, and the rTMS**+** spots of each patient. This procedure was separately done for each EC to allow for a differentiated analysis of each EC's influence on fiber tracking parameters as well as their comparability to intraoperative DCS.

2.5.2. ROI definition

Figure 17 *3D head model with rTMS language-positive spots marked as objects (= yellow coloured balls) supplemented by an additional rim (5 mm) (= transparent yellow shells) to form a ROI. Further, tracked fibers are displayed. Colour coding was done as follows: blue = superior/inferior; red = left/right; green = anterior/posterior) (Pajevic et al., 2000; Witwer et al., 2002).*

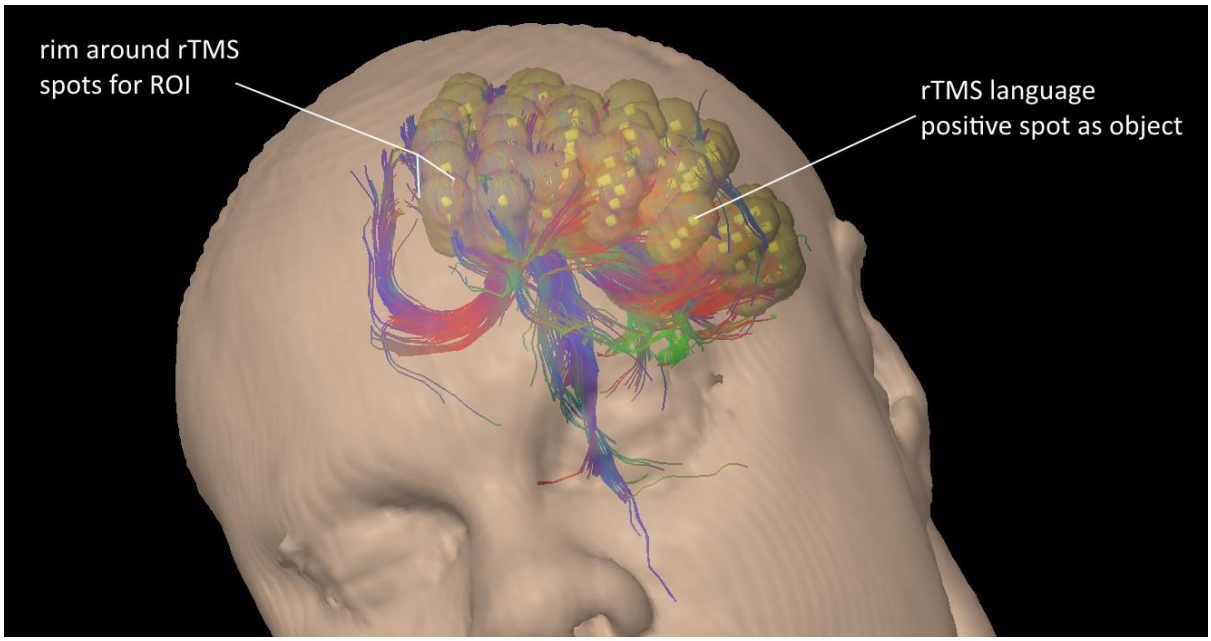

ROIs mark the starting points for fiber tracking. EC-specific rTMS**+** spots were transformed into ROIs using the auto-segmentation tool of the software. First, rTMS**+** spots were transferred into trackable objects and then enlarged by an added rim of 5mm. The area covered by the resultant spheres was then used as a ROI (Figure 17) (Frey et al., 2012; Krieg et al., 2012a; Conti et al., 2014; Sollmann et al., 2015a; Negwer et al., 2017). Following surgery, cortically directly stimulated CPS regions (DCS**+** and DCS**-**) were manually marked as objects and

formed into ROIs on the same model (Figure 18). These CPS ROIs were used to assign tracked fibers to specific CPS regions as well as for the definition of language positivity or negativity by means of rTMS-based DTI FT (= DTI FT**+**/**-**).

Figure 18 *Illustration of fiber deletion:* ***no. 1*** *shows tracked fibers passing through the concerned CPS ROI. In* ***no. 2*** *these fibers are excluded. For a better illustration the fibers were not presented in the standard colour-code.*

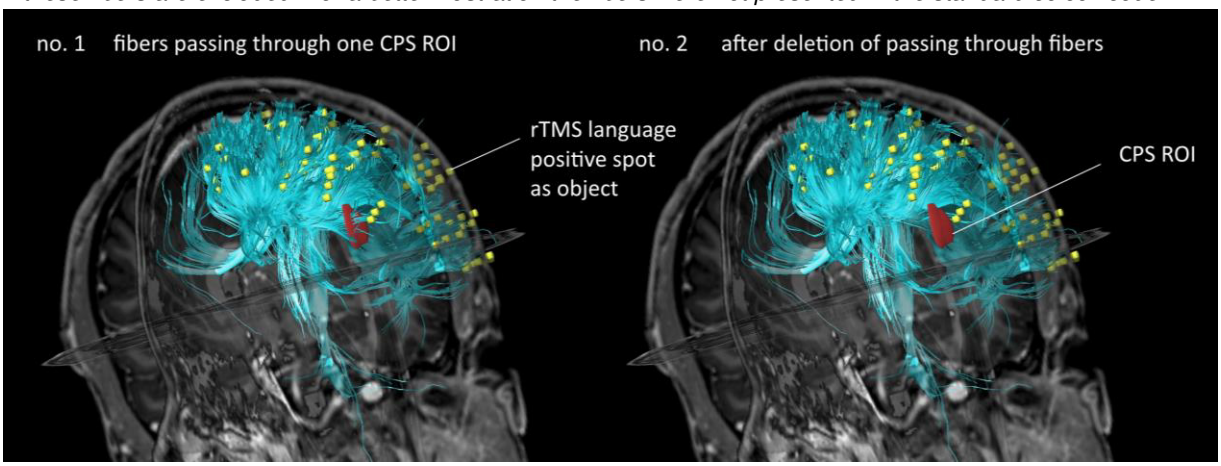

2.5.3. Tracking parameters and fiber tracking

Displayed fibers are color-coded dependent on their route of passage: anterior-posterior direction in green, left-right in red and superior-inferior in blue (Pajevic et al., 2000; Witwer et al., 2002). Adjustable tracking parameters, e.g. the minimum fractional anisotropy (FA) and the minimum fiber length (MFL) serve as filters for the FACT-based fiber tractography and influence the delineation of fibers (Mori et al., 2002a; Mori et al., 2002b). Patient- and EC-specific tracking parameter combinations were therefore assessed prior to the comparison of DTI FT to DCS (DTI FT vs. DCS). The individual fractional anisotropy threshold (FAT) was determined as outlined by Frey et al. in 2012. To do so, fiber tracking was conducted with a MFL of 110 mm using the rTMS ROI of each EC as starting point. FA was adapted in 0.01 (1%) steps until first fibers could be visualized. The maximal FA value at which fibers could still be depicted defines the specific FAT for each patient and EC (Frey et al., 2012). DTI FT was then conducted using four different percentages of the FAT (100%, 75%, 50% and 25%). E.g. with a determined FAT of 0.35 the four applied FA values were 0.35 (= 100%), 0.26 (= 75%), 0.18 (= 50%) and 0.09 (= 25%), each rounded to two decimal places. Each of these FA values was then combined with three different MFLs (100 mm, 70 mm, 40 mm), resulting in twelve different tracking parameter combinations (Table 2) for each of the five EC. In total 60 fiber trackings were conducted per patient.

Table 2 *12 different rTMS-based DTI FT parameter combinations regarding one EC.*

	100% FAT	75% FAT	50% FAT	25% FAT
MFL 100	1	4	7	10
MFL 70	2	5	8	11
MFL 40	3	6	9	12

2.5.4. Definition of language positivity and negativity by rTMS-based DTI FT

Aside of fiber tracking, ROIs can also be used to exclude certain fibers from the analysis. Doing so, CPS regions were defined as DTI FT**+** or DTI FT**-** for each EC. Following fiber tracking with one of the 12 above described sets of parameters, the resultant total number of fibers (NoF) was noted. In a next step, the CPS ROI of concern was activated. Fibers that passed through this area were excluded from the analysis. The difference in NoF before and after this analysis yielded the count of fibers passing through the CPS ROI. If at least one fiber bundle was found to be passing through - respectively originating from - the CPS ROI of concern, this CPS region

was defined as DTI FT**+** (Figure 18). If no fiber was passing through, the CPS region was tagged as DTI FT**-**. This approach assumes language eloquence of a CPS region to correlate with language-related fiber connectivity. Fibers were regarded language-related as they were generated using rTMS**+** spot-based ROIs. This procedure was repeated for each CPS ROI and for each of the 12 tracking parameter combinations per EC. This wide spread was done to ensure that the appropriate combination of parameters will be used to identify language-relevant fiber tracts and corresponding CPS regions. At the same time, the fibers wrongly assumed to be language-relevant should be faded out.

2.6. Direct cortical stimulation

2.6.1. Setup and preparation

Results gathered during language mapping by rTMS as well as the patient's MRI images were uploaded to the neuronavigation system (BrainLAB iPlan Net®, iPlan Cranial 3.0.1, and BrainLAB Curve, BrainLab AG, Feldkirchen, Germany) and used both during presurgical planning as well as the actual procedure (Krieg et al., 2012b; Krieg et al., 2013a). During DCS and SCS, neuronavigation was again established. Surgical tools and a navigation pointer were again marked with reflective spheres and tracked by a stereotactic camera as well as a tracker fixed on the patient's head. To ensure immobility, the patient's head was fixed in a Mayfield clamp and co-registration of a presurgical cranial MRI and actual anatomy was performed. The asleep-awake-asleep approach was chosen. Anaesthesia was applied by continuous infusion of remifentanil and propofol (Hervey-Jumper et al., 2015; Spena et al., 2017). Vigilance during DCS and SCS was monitored by BIS and held at a Ramsay score of 2, defined as the patient being awake, calm and cooperative (Picht et al., 2006; Ille et al., 2015b). Thereby optimal surgical conditions could be maintained. This was achieved by terminating general anaesthesia at least ten to fifteen minutes before ISM. A mixture of local anaesthesia and epinephrine was further injected into the head fixation pin sites, as well as the galea and dura to avoid local pain (Picht et al., 2006; Ille et al., 2015b; Saito et al., 2018). Body temperature was monitored and kept in the optimal range for ISM between 36° C and 37° C (Hervey-Jumper et al., 2015).

2.6.2. Language assessment and definition of language positivity and negativity

DCS was performed using a bipolar electrode with a tip distance of 5 mm (Inomed Medizintechnik GmbH). Stimulation intensities were between 1 and 10 mA, stimulation frequency was 50 Hz with 5 pulses applied to provoke virtual language lesions. The stimulation took place at intervals of 5 to 10 mm. Monitoring via electroencephalography (bandpass filter of 10 Hz to 1.5 kHz) was attached to detect epileptic potentials and afterdischarges (Szelenyi et al., 2010; Saito et al., 2018). Optimal stimulation intensity was assessed under EcOG monitoring with regard to the functional outcome of the language task. Using an intraoperative examination monitor for awake surgery (IEMAS), surgeons were able to track the current language task as well as the patient's face and hence performance, the depth of anaesthesia and the neuronavigation-monitoring in real-time (Muragaki et al., 2011; Saito et al., 2018). Language errors were registered using the same object-naming task as employed by rTMS language mapping. Yet, unlike rTMS mapping, naming of the object was intraoperatively opened with the German phrase "This is a …" (Kohn et al., 1985).
Information from preoperative rTMS mapping was used for negative cortical mapping, meaning the confirmation of rTMS**-** sites via DCS. If rTMS**-** sites were confirmed as DCS**-**, they were deemed safe for resection. Craniotomy was planned in regard to rTMS results with a focus on rTMS**-** sites. Unlike in positive mapping, rTMS**+** sites were not necessarily encompassed by the craniotomy. This approach bases on results by Sanai et al. in 2008. To account for inconsistencies in the trigger-response correlation of language-eloquent areas (Ojemann et al., 1989), each site was tested three times without directly successive stimulation of one site. If stimulation of a certain site resulted in at least two language errors, it was deemed language-positive and tagged with a marker for later integration into the navigation system using the navigation pointer (Picht et al., 2006; Sanai et al., 2008c; Picht et al., 2013). This approach

mimics the 2-out-of-3 rule described above. DCS language errors were not further categorized, all errors were counted.
The comparison of DCS to rTMS and rTMS-based DTI FT (= rTMS vs. DCS and DTI FT vs. DCS) hence included all surgically exposed language-positive or -negative CPS regions that were stimulated by DCS (= DCS**+**/**-**). If a region contained at least one stimulation site that fulfilled the 2-out-of-3 rule, or an ERT of 66%, it was deemed DCS**+**. The remaining areas were tagged as DCS**-**. Following DCS, resection could be started. Resection was monitored by SCS and stopped immediately when SCS of a certain direction yielded language errors. This approach was continued in every direction to allow for a maximized safe extent of resection. SCS results were not further recorded.

Figure 19 *Flow chart of data analysis. 2/3 rule = 2-out-of-3 rule.*

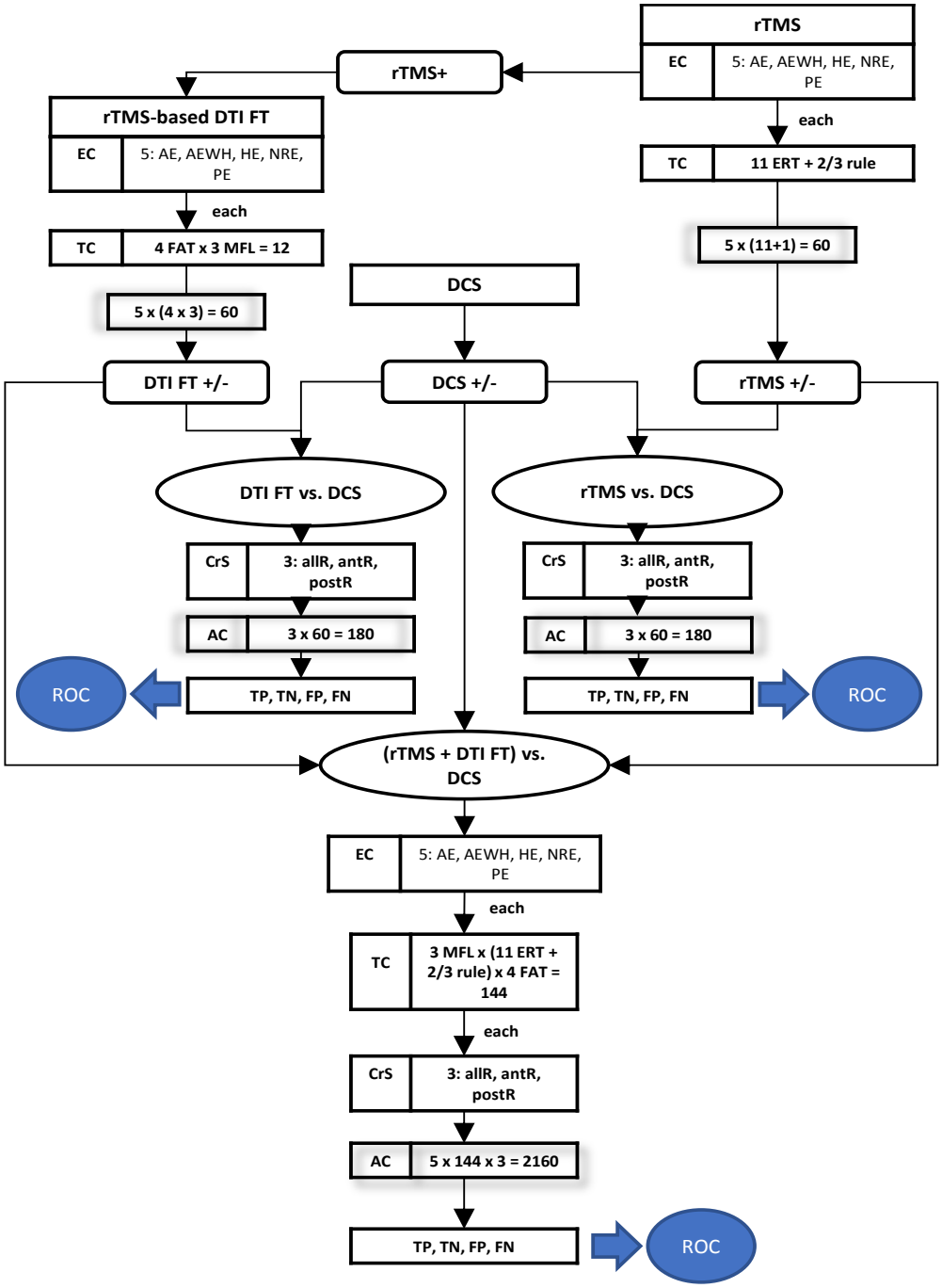

2.7. Data analysis

Language-positive and -negative areas were identified and assigned to the CPS system as outlined in the respective sections: rTMS**+/-** (section 2.4.5 and 2.4.6), DTI FT**+/-** (section 2.5.4) and DCS**+/-** (section 2.6.2). DCS-based results were used as reference for language eloquence for the analysis of rTMS and rTMS-based DTI FT results (rTMS vs. DCS and DTI FT vs. DCS), as DCS currently marks the gold standard for this examination (Duffau et al., 2005; Szelenyi et al., 2010; Chang et al., 2011; De Witt Hamer et al., 2012; Duffau et al., 2014; Ottenhausen et al., 2015). Hence, DCS**+** and DCS**-** areas could have been confirmed by rTMS as well as rTMS-based DTI FT or otherwise objected to. Whereby only CPS regions exposed by surgery could be used and therefore compared.
Figure 19 depicts the process of data analysis. Language rTMS**+/-** as well as DTI FT**+/-** areas were assessed separately for each EC (AE, AEWH, HE, NRE and PE) and different threshold categories. TC are created using either the 12 DTI FT parameter combinations, namely three different MFLs combined with four different FATs, or the 11 ERTs as well as the 2-out-of-3 rule for the analysis of the rTMS results. Following earlier studies, the CPS system was categorized in three CPS region subdivisions (CrS) for the DCS-based analysis (Picht et al., 2013; Sollmann et al., 2013a; Krieg et al., 2014a; Krieg et al., 2014b; Krieg et al., 2016). The CrS *all regions* (allR) includes all CPS regions. The CrS *anterior regions* (antR) encompasses trIFG, opIFG as well as vPrG, while the CrS *posterior regions* (postR) includes anG, aSMG, pSMG, mSTG and pSTG (Figure 20).

Figure 20 *Anterior (= green area) and posterior (= blue area) CrS. The respective designations for the CPS abbreviations can be found on page 101 in section 8.2 (Abbreviation - Cortical parcellation system).*

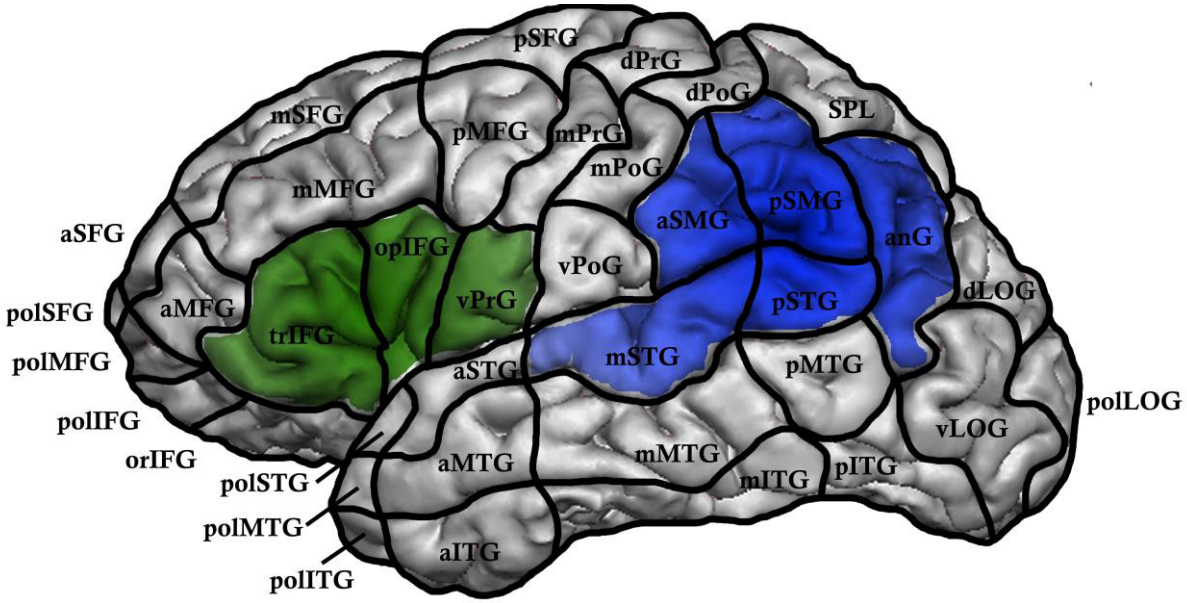

Regarding the three mapping comparisons (rTMS vs. DCS, DTI FT vs. DCS and (rTMS + DTI FT) vs. DCS), each combination of EC, TC and CrS resulted in a specific number of analysis combination (AC), applied separately for each patient (Figure 19).

2.8. Statistics

Statistical data analysis was performed using GraphPad Prism (GraphPad Prism 6.04, La Jolla, CA, USA). Results regarding patient characteristics, language mapping and fiber tracking parameters, technical setup details as well as rTMS and DTI FT are presented as mean value (MV) ± standard deviation (SD) with the range between the minimum value (MIN) and the maximum value (MAX) in parenthesis: MV ± SD (MIN - MAX). The median value (MEDIAN) was calculated as well. The Wilcoxon-test was used for significance testing. A p-value of < 0.05 was considered significant.

2.8.1. Calculating the ROC

Four fractions of CPS regions were determined based on the comparison of rTMS**+/-** and DTI FT**+/-** CPS regions to DCS**+/-** regions (rTMS vs. DCS and DTI FT vs. DCS). This was done separately for each AC:

1) true positive (TP) [= language positivity correctly identified]
2) true negative (TN) [= language negativity correctly identified]
3) false positive (FP) [= language positivity incorrectly identified]
4) false negative (FN) [= language negativity incorrectly identified]

The comparison of DCS to the combined results of rTMS and rTMS-based DTI FT also referred to as (rTMS + DTI FT) vs. DCS was conducted as depicted in Table 3. Language positivity or negativity was only regarded as such when rTMS and rTMS-based DTI FT results were in accordance to each other. Conflictive results were deemed false by definition. Thereby, the further information of functional connectivity gained by rTMS-based DTI FT confirmed or disproved rTMS language mapping results. The count of regions assigned to each fraction was used to calculate the ROC *sensitivity*, *specificity*, *PPV* and the *NPV*:

$$\text{sensitivity} = \frac{\text{TP}}{\text{TP} + \text{FN}} = true\ positive\ rate$$

$$\text{specificity} = \frac{\text{TN}}{\text{TN} + \text{FP}} = true\ neagtive\ rate$$

$$\text{PPV} = \frac{\text{TP}}{\text{TP} + \text{FP}}$$

$$\text{NPV} = \frac{\text{TN}}{\text{TN} + \text{FN}}$$

The analysis of rTMS vs. DCS and DTI FT vs. DCS resulted in 180 ACs and hence sets of ROC per patient, while (rTMS + DTI FT) vs. DCS yielded 2160 ACs and hence sets of ROC per patient. Data was further analysed without distinction for patient identity.

Table 3 *Definition of the four fractions (TP, TN, FP, FN) for each comparison group.*

Definition	rTMS +/-	DTI FT +/-	DCS +/-
rTMS vs. DCS			
TP	+		+
TN	-		-
FP	+		-
FN	-		+
rTMS-based DTI FT vs. DCS			
TP		+	+
TN		-	-
FP		+	-
FN		-	+
(rTMS and rTMS-based DTI FT) vs. DCS			
TP	+	+	+
TN	-	-	-
FP	+	+	-
	-	+	-
	+	-	-
FN	-	-	+
	-	+	+
	+	-	+

2.8.2. Graphic representation and statistic comparison of ROC

2.8.2.1. ROC plot

Figure 21 *Exemplary presentation of a ROC plot. A comparison based on a perfect match (= orange), caused by chance (= green) is displayed. The grey course is an example for a possible ROC outcome with good comparability.*

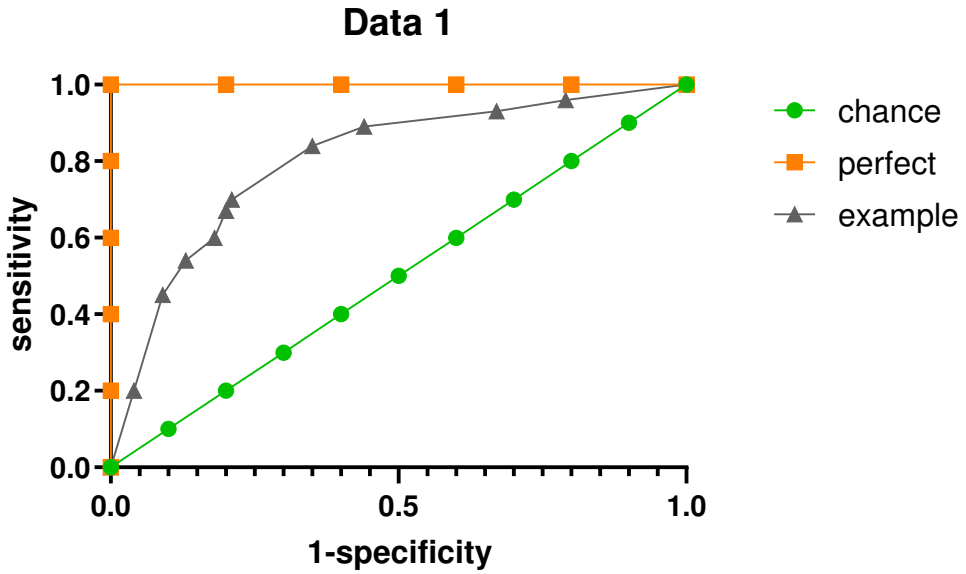

ROC values based on EC, CrS and TC variations were plotted as illustrated in Figure 21. Sensitivity is plotted on the y axis against 1-specificity on the x axis. This plot style is commonly used to visualize ROC feasibility (Akobeng, 2007). As shown in Figure 21, the orange curve depicts a perfectly matched comparison, while the green curve (= diagonal line) shows ROC parameters created by chance with equally shared true- and false-positive results (Akobeng, 2007). Curves tending to the bottom right side comprise a majority of false-positive results. The grey line exemplifies realistic ROC results with good comparability.

2.8.2.2. Youden's index and best-balanced result

Objective measures were further implemented to enhance ROC analysis. These measures were the Youden's index (YI) (Youden, 1950) and the self-implemented balance index (BI), which both process the each specific ROC pair of sensitivity and specificity. YI and BI were calculated for each AC and each of the three comparison groups (rTMS vs. DCS, DTI FT vs. DCS, (rTMS + DTI FT) vs. DCS) as follows:

$$BI = (sensitivity + specificity) - |(sensitivity - specificity)|$$
$$YI = sensitivity + specificity - 1$$

The self-implemented BI was developed following fixed assumptions. A BI value of 2.00 indicates 100% sensitivity and 100% specificity. A BI value equal 0.00 stands for sensitivity or specificity of 0%. BI values equal to 1.00 represent a sensitivity and specificity of 50%. A BI between 1.00 and 2.00 reflects sensitivity and specificity values each above 50%. A BI less than (<) 1.00 indicates that either sensitivity or specificity or both are lower than 50%. Higher BI values indicate higher ROC pair values and/or better balance while lower BI values indicate the opposite. The best balance index (BBI) is used to indicate the most reasonable sensitivity and specificity pairing regarding its single values as well as their balance in this doctoral thesis. Unlike the self-implemented BI, the YI has been in scientifical usage for curve-based ROC optimization since its introduction in 1950 by Youden (Zweig et al., 1993; Schisterman et al., 2005; Akobeng, 2007; Lai et al., 2012). In this study, the YI is employed to investigate the feasibility of the preoperative tests rTMS, DTI FT and their combination compared to DCS. In general, higher cut-off values correlate with lower sensitivity and higher specificity and vice versa (Greiner et al., 2000; Akobeng, 2007). Akobeng (2007) states that the best YI "is defined as the maximum vertical distance between the ROC curve and the diagonal or chance line

[…]", meaning that the best YI "corresponds to the point on the curve farthest from chance". The best YI can therefore be used as a "global measure of overall […] accuracy" (Lai et al., 2012). YI values range from −1.00 to +1.00. A YI equal to 1.00 represents a perfectly accurate comparison with no FN or FP (sensitivity and specificity each 100%). A value equal or less to (≤) 0.00 indicates incongruent matches in the concerned comparison.

2.8.2.3. ROC sums for positive or negative mapping

Analysis of rTMS feasibility has to differentiate between the applicability of rTMS for positive or negative intraoperative mapping. Negative mapping requires high specificity in combination with a high NPV, whereas positive mapping requires high sensitivity and a high PPV (Ille et al., 2015b). The respective sums required to identify the best suited AC for both negative and positive mapping were calculated as follows:

$$sum\ for\ a\ positive\ mapping = sensitivity + PPV$$
$$sum\ for\ a\ negative\ mapping = specificity + NPV$$

2.8.3. Pearson's correlation coefficient

Figure 22 *Area under the musculus temporalis. The respective designations for the CPS abbreviations can be found on page 101 in section 8.2 (Abbreviation - Cortical parcellation system) (Source head model in the upper left corner: Gillroy, Atlas of Anatomy, 1st ed., Abb 30.12 B, Illustrator: Karl Wesker © 2020 Thieme Medical Puplishers, Inc. All Rights Reserved).*

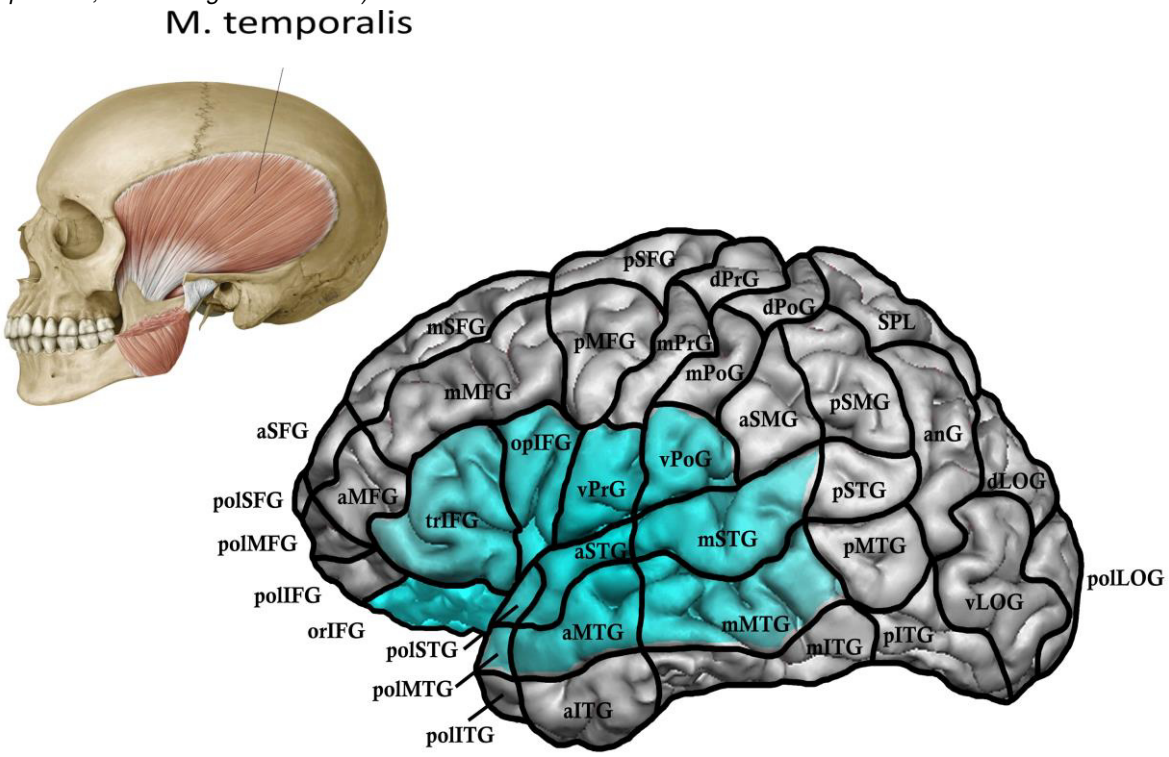

Pearson's correlation coefficient (r) including the respective p-value was utilized to evaluate the possibility of increased provoked errors due to an increase in number of rTMS trials (Zou et al., 2003). The analysis was done with distinction for study subject as well as for CPS region. Results were presented as r = x, p = y. The coefficient's algebraic sign indicates the positivity or negativity of the correlation. The coefficient's value indicates the strength of correlation. Values ≤ 0.10 indicate weak correlation, values ≤ 0.30 moderate and values > 0.50 strong correlation. The value of p indicates the correlation's significance (Cohen, 2013). In addition, this study utilized r to explore a possible impact of rTMS stimulation intensities on the temporal and convexity pain levels regarding each patient. Further, r was used to assess whether the temporal pain level influenced AE count of the CPS regions under the temporal muscle and whether the applied rTMS intensities are connected to the AE count of each patient. The area

under the temporalis muscle includes aSTG, mSTG, polSTG, aMTG, mMTG, polMTG, the orbital part of the inferior frontal gyrus (orIFG), trIFG, opIFG, vPrG and vPoG (Figure 22). This area slightly exceeds the area encompassed by the definition of anterior temporal CPS regions by Brennan et al. (2012). The twelve threshold categories in DTI FT, consisting of four different FAT values and three different MFLs (Table 2 on page 27), influence the resultant NoF. The number of provoked rTMS errors ultimately influences the size of the ROI used for DTI FT. This could confound the individual determined FAT value and NoF of each study subject. This possibility is again assessed using r.

3. RESULTS

Table 4 *Patient characteristics per study subject. Characteristics consist of age, sex, handedness and the intake of antiepileptic medication. The underlying tumor entity and its location in relation to essential language sites is further listed. ID = identification number of each patient.*

ID	Age	Sex	Tumor entity	Relation to essential language sites	Handedness	antiepileptic medication
1	27	M	IV	-	R	Yes
2	24	M	II	Within	R	Yes
3	31	M	I	-	R	Yes
4	38	M	III	Remote	R	Yes
5	47	M	IV	Adjacent	R	-
6	49	M	II	Adjacent	R	Yes
7	27	F	AVM	Adjacent	R	-
8	43	M	II	Within	R	-
9	53	M	IV	Within	R	No
10	33	M	IV	Within	R	-
11	47	F	IV	Adjacent	R	No
12	63	F	II	Within	R	-
13	34	M	AVM	Adjacent	R	-
14	40	M	IV	Within	R	-
15	52	F	IV	Within	R	Yes
16	51	M	IV	Within	R	Yes
17	43	M	IV	Adjacent	L	Yes
18	43	F	II	Adjacent	R	Yes
19	28	M	II	Remote	R	Yes
20	34	F	III	Within	L	Yes

3.1. Patient cohort

Subject count was 20. Age average was 40 ± 11 (24 - 63) years. 70% were male while 30% were female. Only 10% were left-handed based on the Edinburgh Handedness Inventory. Table 4 further lists the intake of antiepileptic medication, the underlying tumor entity and its location in each study subject.

3.2. rTMS language mapping results

3.2.1. Technical setup data, pain level and its potential systematic bias

During baseline performance, 83 ± 20 (31 - 104) out of 131 presented coloured objects could be named immediately and correctly. The RMT averaged to 0.35 ± 0.09 (0.21 - 0.58). RMT values as well as the finally applied mapping intensities per patient are listed in Table 5. Four study subjects were mapped at a frequency of 7 Hz/7 pulses or 7 Hz/5 pulses, while the remaining 12 patients underwent a 5 Hz/5 pulses stimulation (Table 1 on page 27). Figure 23 further lists the maximum provoked pain intensity for each patient. With an average $VAS_{temporal}$ of 5 ± 2 (2 - 9) compared to $VAS_{convexity}$ of 2 ± 2 (0 - 7), rTMS stimulation of the temporal head area was significantly more dolorous ($p < 0.0001$) (Figure 23). Based on Pearson's correlation coefficient, there was no significant correlation between pain level and the applied mapping intensity ($VAS_{convexity}$: $r = 0.00$, $p = 0.994$; $VAS_{temporal}$: $r = 0.07$, $p = 0.762$). $VAS_{temporal}$ level and AE count in the area under the temporal muscle correlate moderately, but not significantly ($r = -0.24$; $p = 0.153$).

Table 5 *Overview of the technical setup data (baseline number of objects, RMT in %, mapping intensity in %) and the collected data regarding temporal and convexity VAS per subject. The respective mean value (= MV), standard deviation (= SD), minimum value (= MIN), maximum value (= MAX) and the median value (= MEDIAN) were further calculated. ID = identification number of each patient.*

ID	Baseline number of objects	RMT (%)	mapping intensity (%)	VAS *convexity*	VAS *temporal*
1	78	35	35	3	2
2	61	33	35	4	8
3	96	29	31	5	7
4	-	23	26	3	7
5	82	25	30	3	6
6	102	46	46	4	9
7	102	36	36	1	3
8	71	21	21	0	5
9	101	41	41	1	3
10	82	37	37	2	4
11	31	30	30	1	3
12	90	36	44	1	4
13	104	43	52	2	5
14	87	39	47	2	3
15	98	33	33	7	7
16	72	25	25	1	2
17	95	58	46	2	8
18	68	34	34	2	6
19	100	42	42	1	4
20	52	35	35	0	5
MV	**83**	**35**	**37**	**2**	**5**
SD	**20**	**9**	**8**	**2**	**2**
MIN	**31**	**21**	**21**	**0**	**2**
MAX	**104**	**58**	**52**	**7**	**9**
MEDIAN	**87**	**35**	**35**	**2**	**5**

Figure 23 *Box plots for $VAS_{temporal}$ and $VAS_{convexity}$ with their median value (= MEDIAN), maximum value (= MAX), minimum value (= MIN), first (= q1) and third quartile (= q3). A significantly higher pain level over temporal areas is shown. The mean value (= MV) is depicted as cross sign (= +). **** indicates p < 0.0001.*

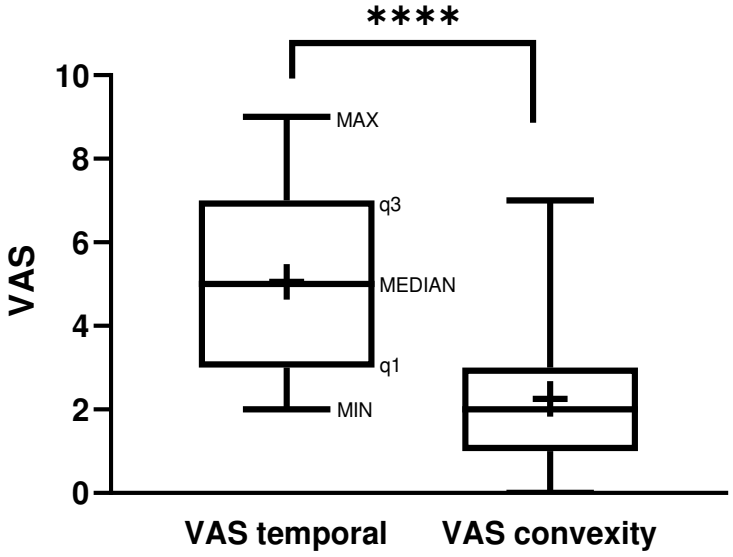

3.2.2. Number of rTMS stimulation trials and error counts

All patients underwent rTMS, but the number of stimulations applied on the left hemisphere of each patient differs. The stimulation count averaged to 378.8 ± 135.3 (223 - 665) applied rTMS stimulations. Language errors could be induced by means of rTMS in each case, although error counts varied. MV ± SD of each EC's error counts is illustrated in Figure 24. PE could not be produced in three cases, one case produced no NRE. HE marks the most common error type, without significant difference to NRE ($p = 0.1201$), while PE was significantly less prevalent. A significant association of mapping intensities to the AE count could not be proven, besides a moderate positive correlation ($r = 0.25$, $p = 0.290$).

Figure 24 *Box plots for the error counts of each EC with their median value (= MEDIAN), maximum value (= MAX), minimum value (= MIN), first (= q1) and third quartile (= q3). The mean value (= MV) is depicted as cross sign (= +) and in small boxes above each box plot the respective MV ± SD of each EC is shown. **** indicates a significant p-value < 0.0001. Further ** stands for a p-value of 0.0028, * for p = 0.0410. The Abbreviation ns means "non-significant".*

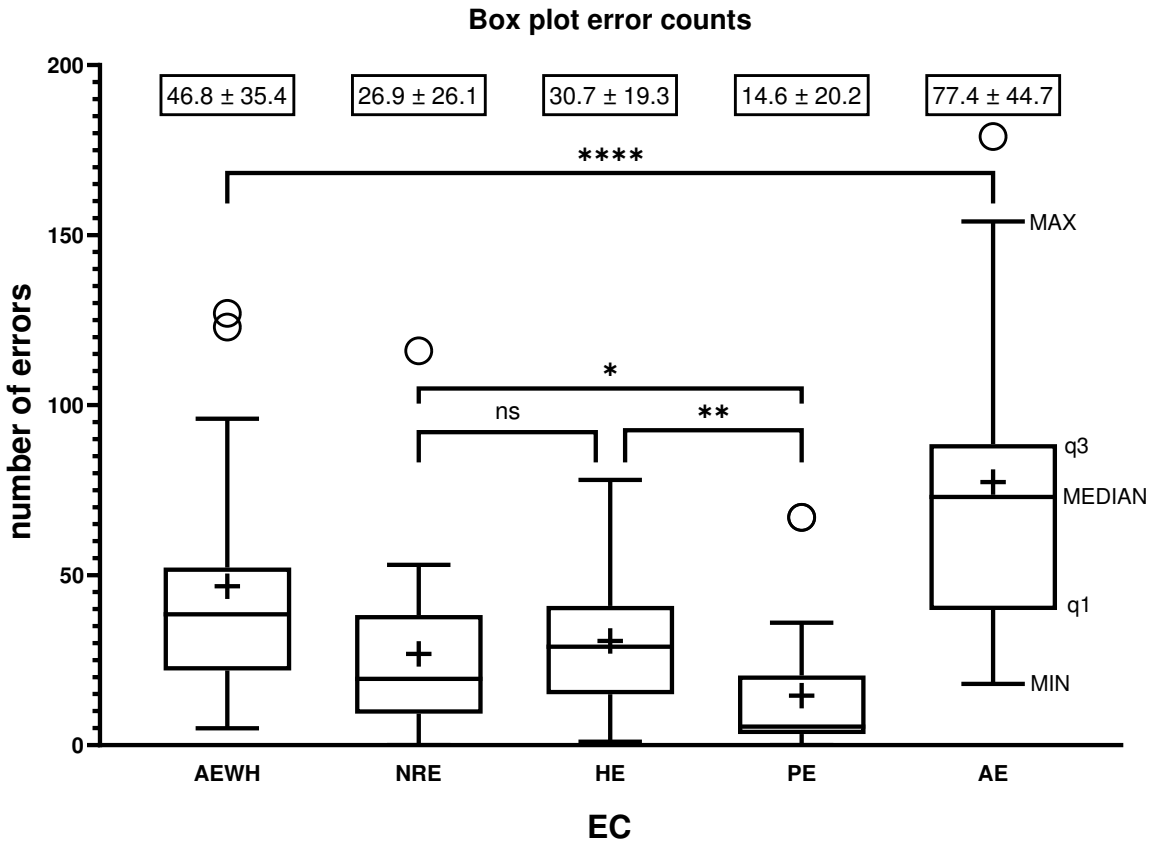

3.2.3. Cortical distribution of error counts and stimulation trials

Figure 25 indicates varying counts of rTMS stimuli between different CPS regions. rTMS mean stimulation counts coincide with each EC's mean error counts. Pearson's correlation coefficient of the count of rTMS trials and the AE count of each subject is $r = 0.46$ ($p = 0.021$), indicating a significant positive correlation. Moreover, the number of rTMS trials applied on each CPS region and the mean number of provoked AE per CPS region significantly correlate as well ($r = 0.96$, $p < 0.001$). Thus, higher error counts of certain CPS regions can be influenced by higher number of rTMS trials, e.g. in antR.

Figure 25 *Colour-coded illustration of the mean number of applied rTMS trials per CPS region (**no. 1**) and error counts per EC (**no. 2** = AE; **no. 3** = AEWH; **no. 4** = HE; **no. 5** = NRE; **no. 6** = PE). The respective designations for the CPS abbreviations can be found on page 101 in section 8.2 (Abbreviation - Cortical parcellation system).*

mean number of provoked errors	0	0.01	1	2	3	4	5	7	9	11	13
mean number of stimulation trials	0	0.01	0.5	2.5	5	10	15	20	30	40	50

no. 1 mean stimulation trials

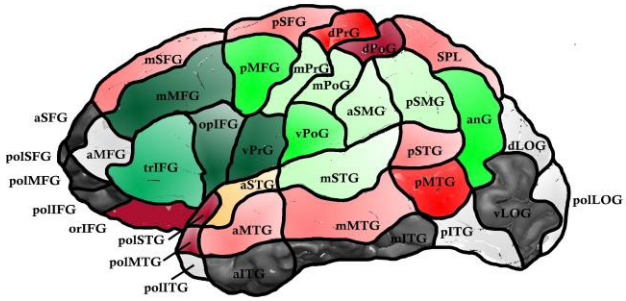

no. 2 mean number of AE

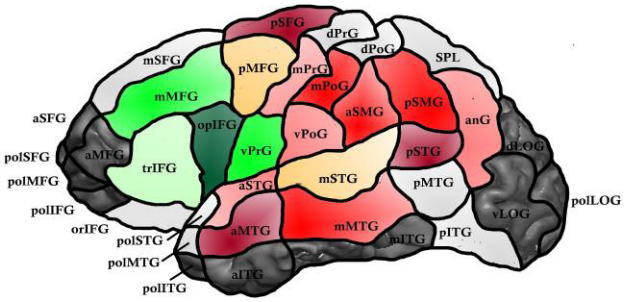

no. 3 mean number of AEWH

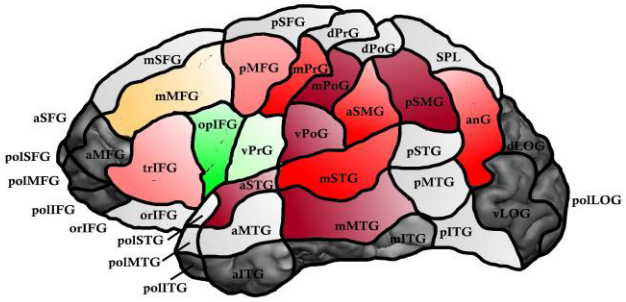

no. 4 mean number of HE

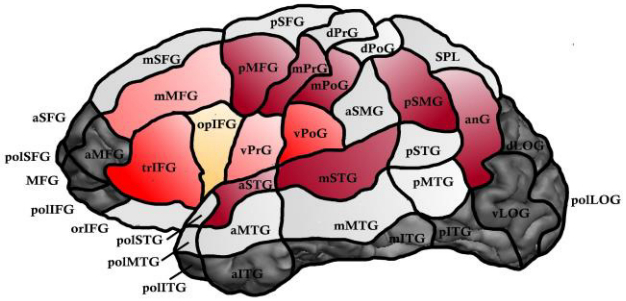

no. 5 mean number of NRE

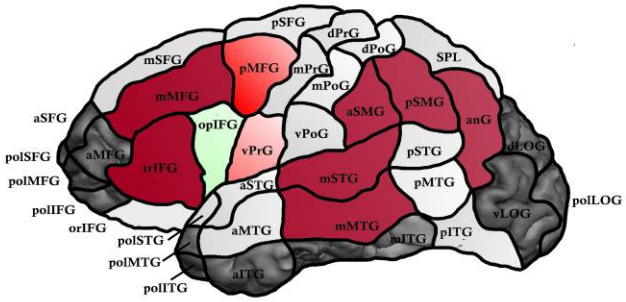

no. 6 mean number of PE

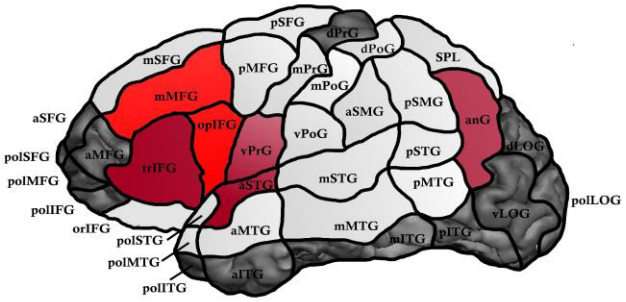

3.3. rTMS-based DTI FT results

3.3.1. FAT values in the context of each EC

Figure 26 depicts the FAT values of all study subject with distinction to the EC. Values listed are MEDIAN, MIN, MAX, first and third quartile. The median and mean FAT values of AE, AEWH, NRE and HE lie close to each other. A significantly higher FAT was found for AE versus HE ($p = 0.0026$). PE median FAT amounts to 0.24, significantly below all other EC values (p-values listed in Figure 26). AE counts produced by rTMS of each study subject and its respective FAT value in rTMS-based DTI FT do not significantly correlate ($r = -0.04$; $p = 0.439$). When including all 96 FAT without distinction for EC, again no significant interrelationship was found ($r = 0.13$; $p = 0.100$).

Figure 26 *Box plots for the mean FAT value for each EC with their median value (= MEDIAN), maximum value (= MAX), minimum value (= MIN), first (= q1) and third quartile (= q3). The mean value (= MV) is depicted as cross sign (= +) and in small boxes below each box plot the respective MV ± SD of each EC is shown. * - *** indicates a significant p-value (AE to PE: p = 0.0001; AEWH to PE: p = 0.0004; AE to HE: p = 0.0026; HE to PE: p = 0.0050; NRE to PE: p = 0.0062). The remaining mean FAT values do not differ significantly.*

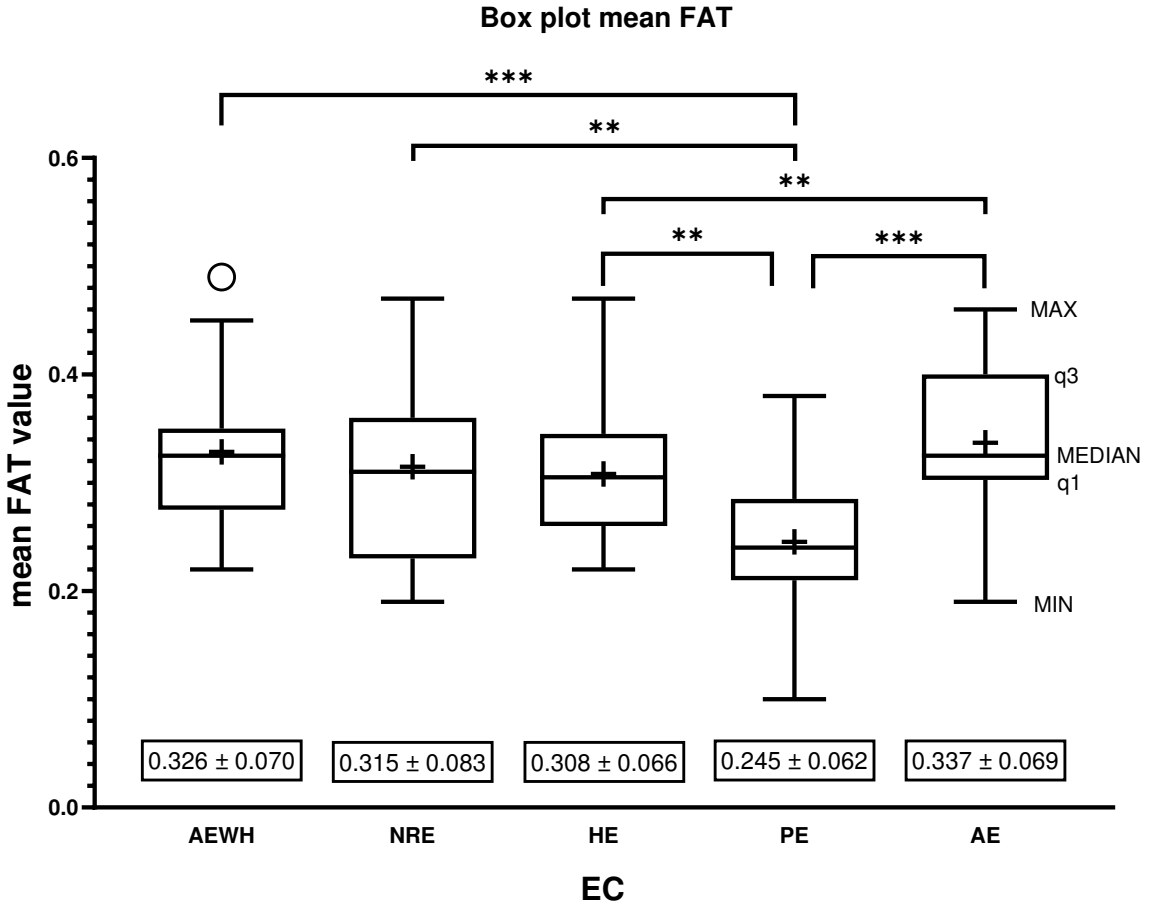

3.3.2. Progression pattern for the number of fibers

Table 6 illustrates the 60 different DTI FT parameter combinations used in this study. NoF rises with lower MFL and FAT values. Highest NoF levels were produced at an MFL of 40 mm and 25% FAT without distinction for EC. Further, error categories PE and AE present the highest mean NoF values. As stated above, PE is associated with the lowest mean FAT value while AE is associated with the highest mean FAT value (Figure 26), which underlines that the FAT level alone is not mainly predefining the NoF. Further, there is no significant correlation between the mean NoF per subject and the error count regarding all ECs ($r = 0.02$; $p = 0.8304$). The contingent of fibers passing through at least one of the CPS regions, which were exposed to DCS averages to 35.5%. This is mainly explained by the limited amount of DCS**+** and DCS**-** CPS regions to compare with.

3.4. DCS results: surgical exposure and DCS positivity considering CPS regions

On average, 9.15 ± 3.13 (5 - 19) CPS regions were exposed and underwent DCS during surgery. Of these CPS regions on average 2.15 ± 1.66 (0 - 6) were identified as language-positive. The boxplots in Figure 27 on page 41 visualize the inter-individual distribution of the count of exposed and language-positive DCS CPS regions. Figure 28 no. 1 on page 41 depicts each CPS region's counts of exposure in relation to the twenty study participants. E.g. opIFG was disclosed seventeen times while the dorsal post-central gyrus (dPoG) was only disclosed

Table 6 *Progression of mean NoF in rTMS-based DTI FT dependent on EC and TC. The shade-code and the arrows illustrate rising NoF. The single parameter combinations are numbered as follows: one alphabetic letter for each EC (AE: A; AEWH: B; NRE: C; HE: D; PE: F; each in respective parenthesis behind) combined with a number ranging from 1 to 12 regarding the TC combination (see upper box).*

	100% FAT	75% FAT	50% FAT	25% FAT
MFL 100	1	4	7	10
MFL 70	2	5	8	11
MFL 40	3	6	9	12

AE (A)	**100% FAT**	**75% FAT**	**50% FAT**	**25% FAT**
MFL 100	9	83	353	1877
MFL 70	60	383	1466	5149
MFL 40	359	1466	4084	10919
AEWH (B)	**100% FAT**	**75% FAT**	**50% FAT**	**25% FAT**
MFL 100	11	76	318	1456
MFL 70	72	304	1161	4071
MFL 40	350	1149	3249	8874
NRE (C)	**100% FAT**	**75% FAT**	**50% FAT**	**25% FAT**
MFL 100	12	80	323	1279
MFL 70	85	379	1199	3820
MFL 40	448	1396	3388	8248
HE (D)	**100% FAT**	**75% FAT**	**50% FAT**	**25% FAT**
MFL 100	10	109	432	1724
MFL 70	88	445	1391	4295
MFL 40	516	1660	3956	9144
PE (E)	**100% FAT**	**75% FAT**	**50% FAT**	**25% FAT**
MFL 100	15	122	631	2248
MFL 70	304	897	2369	5750
MFL 40	826	2124	5122	10950

three times. Figure 28 no. 2 illustrates the rate at which each CPS region was identified as language DCS**+**, proportional to the amount of surgical exposure. The two CPS regions with the highest proportion of DCS**+** in relation to exposure by surgery are opIFG (approx. 65% [11/17]) and vPrG (approx. 53% [9/17]).
Language errors could not be provoked by means of DCS in 2 out of 20 patients. Figure 28 no. 2 labels the surgically exposed and stimulated CPS regions of these two patients (identification numbers #1 and #3) with yellow and blue dots.

3.5. Report of adverse events

Beside the above-mentioned pain sensation, no adverse events or technical difficulties were reported during the language mapping procedures of either modality (DCS, rTMS and rTMS-based DTI FT). In particular, no patient suffered a seizure regardless of the intake of antiepileptic medication (Table 4 on page 35).

Figure 27 *Box plots for the number of CPS regions exposed by surgery and DCS language positivity. Further illustrated is their median value (= MEDIAN), maximum value (= MAX), minimum value (= MIN), first (= q1) and third quartile (= q3). The mean value (= MV) is depicted as cross sign (= +). **** indicates a significant p-value < 0.0001.*

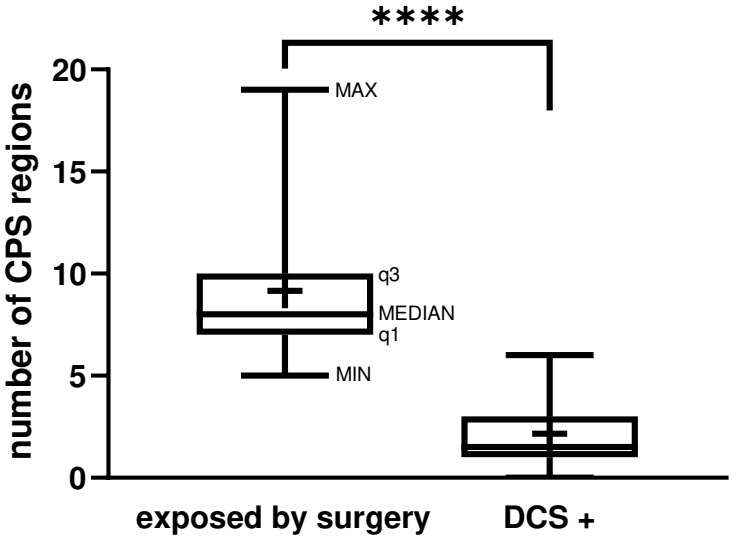

Figure 28 *Colour-coded illustration of the count of surgical exposures per CPS region (= **no. 1**) and the corresponding counts of DCS language positivity (= **no. 2**). Explicit numbers are partially added. The blue dots refer to the surgical exposed CPS regions of patient with the ID 1 and the yellow dots to patient with the ID 3. ID 1 and 3 had no DCS**+** results. ID = identification number of each patient. The respective designations for the CPS abbreviations can be found on page 101 in section 8.2 (Abbreviation - Cortical parcellation system).*

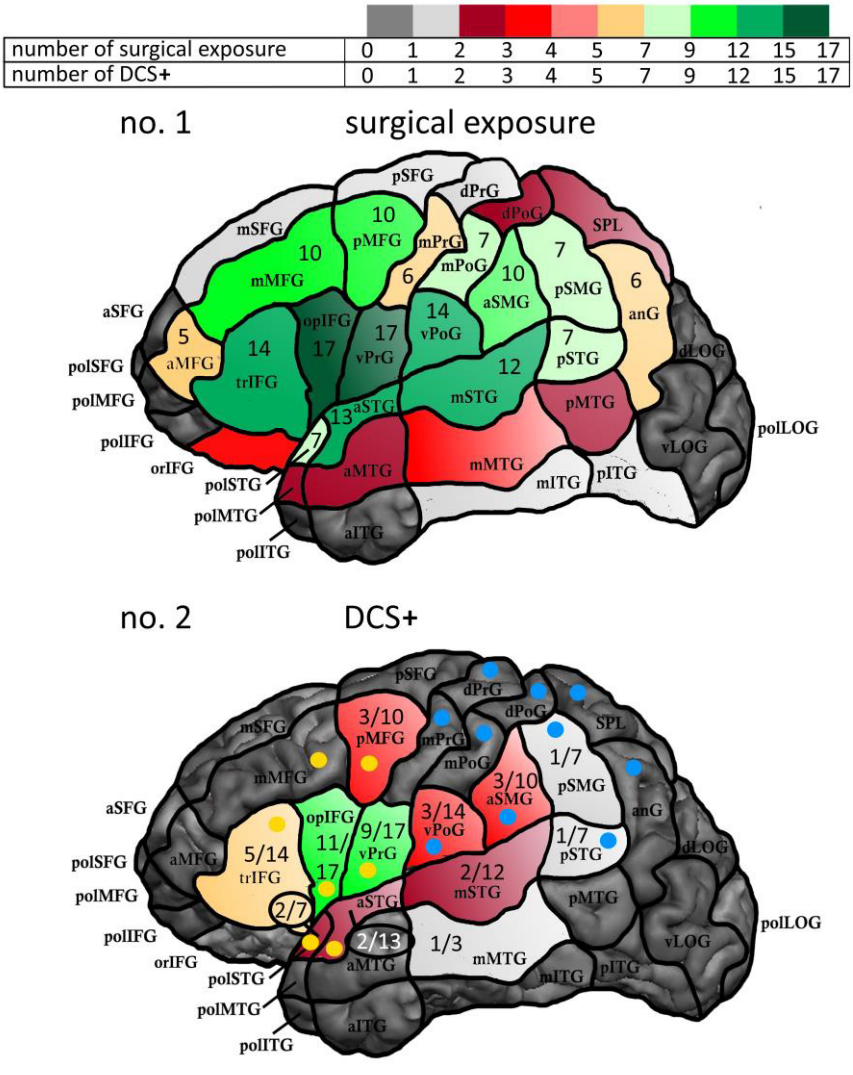

3.6. Results of the comparison rTMS vs. DCS

3.6.1. Results regarding the different ERTs

Figure 29 *ROC plot rTMS vs. DCS allR for all ERTs distincted for EC. The green line represents ROC results created by chance.*

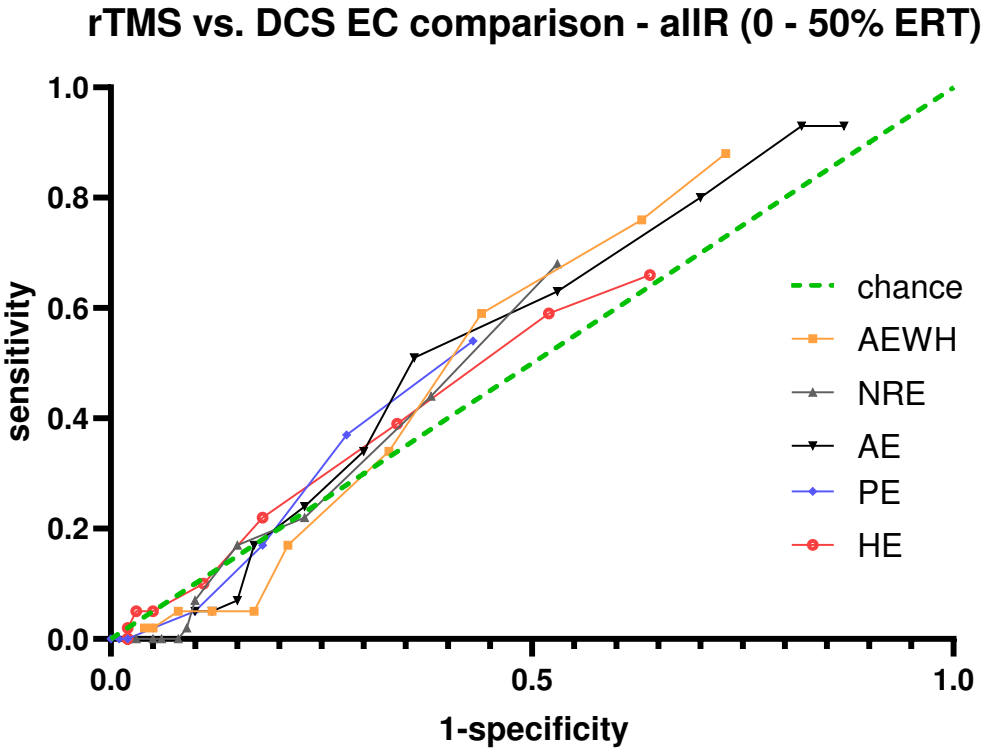

Figure 30 *ROC plot rTMS vs. DCS AE for all ERTs regarding CrS. Further are the corresponding %ERT illustrated, exemplary for the course of the postR. The green line represents ROC results created by chance.*

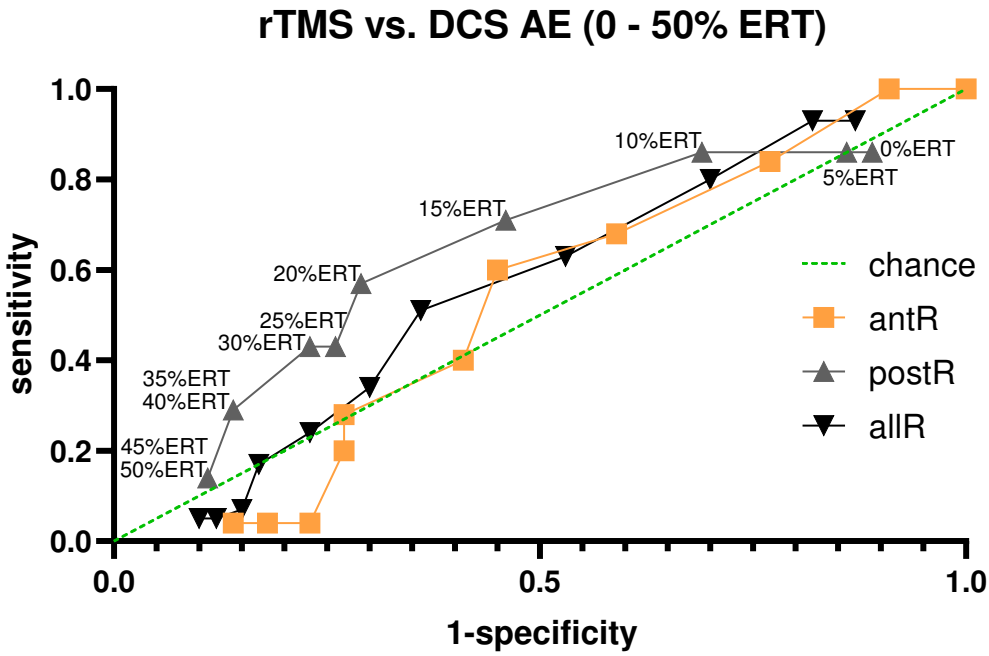

Figure 29 and Figure 30 depict different ERT's ROC curves spread around the 45-degree diagonal (= green line) of the ROC space. The spread is similar, regardless of the EC or CrS, as supplementary illustrated for CrS allR and each EC in Figure 29. This indicates a low accuracy of language mapping by rTMS compared to DCS. Lower ERT lead to rising sensitivity with decreasing specificity, as shown by the posterior CrS ROC curve and its corresponding

ERT in Figure 30. Again, this finding was consistent throughout all EC and CrS in the comparison rTMS vs. DCS. Hence, the TC ERT is a possible tool for reacting to the high sensitivity of rTMS. Regarding the EC AE, best results compared to DCS could be achieved including only postR (Figure 30). Again, this finding was persistent across all ERT.

3.6.2. Results regarding the 2-out-of-3 rule

Figure 31 *ROC plot rTMS vs. DCS 2-out-of-3 rule for all ECs regarding CrS. Further are the corresponding EC illustrated, exemplary for the course of the antR. The green line represents ROC results created by chance.*

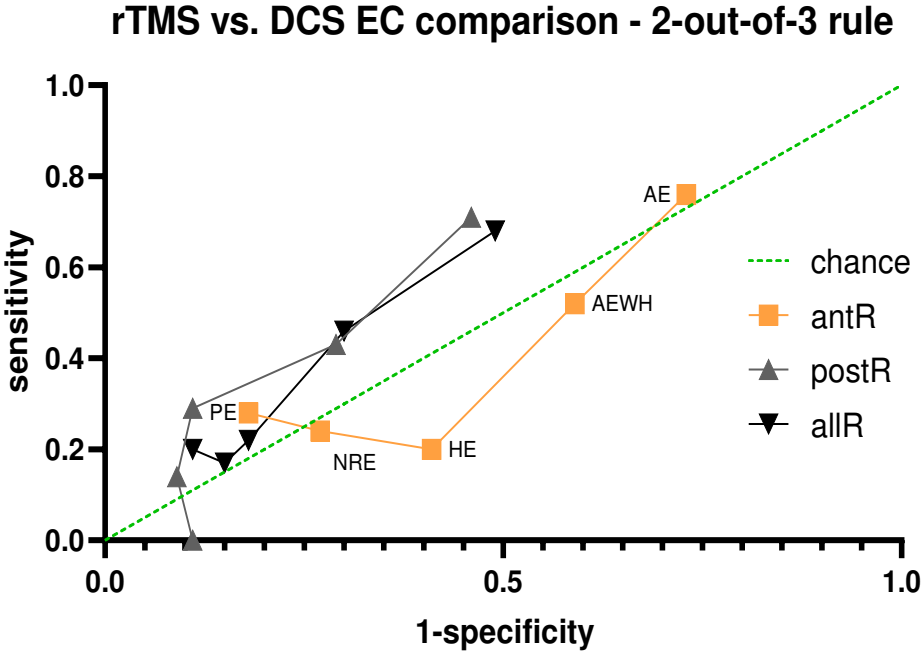

ROC based on the TC 2-out-of-3 rule are illustrated in Figure 31. The CrS postR and allR dominate over antR. Best YI was achieved by analysing AE in postR (sensitivity/specificity: 71%/54%; YI = 0.26). Worst comparability based on the 2-out-of-3 rule lead from analysis HE in antR (sensitivity/specificity: 20%/59%; YI = −0.21). This YI is the lowest achieved YI in the whole comparison rTMS vs. DCS.

3.6.3. BI and YI with the corresponding AC

Table 7 *rTMS vs. DCS addressing the different ACs: BBI and best YI, including corresponding sensitivity (sv) and specificity (sc). 2/3 rule = 2-out-of-3 rule.*

rTMS vs. DCS						
EC	**BBI (sv[%]/sc[%])**	**TC of BBI**	**CrS of BBI**	**Best YI (sv[%]/sc[%])**	**TC of best YI**	**CrS of best YI**
AE	1.11 (57%/71%)	20% ERT	postR	0.29 (57%/71%)	20% ERT	postR
AEWH	1.12 (59%/56%)	10% ERT	allR	0.20 (86%/34%)	5% ERT	postR
HE	0.97 (59%/48%)	5% ERT	allR	0.29 (43%/86%)	15% ERT	postR
NRE	0.93 (68%/47%)	0% ERT	allR	0.15 (68%/47%)	0% ERT	allR
PE	1.14 (57%/69%)	0% ERT	postR	0.26 (57%/69%)	0% ERT	postR

Table 7 lists the BBI and best YI for each EC and their corresponding TC, CrS and ROC. Highest BBI values (0.93 - 1.14) as well as highest best YI (0.15 - 0.29) were found when analysing postR, followed by allR. Employed TC for BBI ranged from 0% ERT to 20% ERT not

including the 2-out-of-3 rule. Hence, to achieve BBI no favouring TC suitable for all EC can be stated.TC + CrS combinations yielding the best YI often coincide with BBI. Yet, this is not mandatory, as can be seen in AEWH and HE (Table 7).

Table 8 depicts the YI comparing language mapping by rTMS vs. DCS for all ACs (EC + TC + CrS). Lower ERT and the 2-out-of-3 rule appear to yield higher YI, while higher ERT mostly lead to decreased YI. While this assumption holds true for the most part, this trend did not show consistency across the entire dataset. Seven YI > 0.17, including one of the two best YI belonged to the EC AE. The highest two best YI (each 0.29) both belong to postR and to the error categories HE and AE. Regarding the EC AE, this YI was achieved using an ERT of 20%. AE also included three of the five highest YI when combined with the CrS postR. Fittingly, AE/postR also yielded the highest $YI_{mean\ CrS}$ (AE + postR: 0.14).

Regarding YI_{mean} per EC, highest values were resultant applying AE for all CrS combined ($YI_{mean\ EC}$ = 0.06). As for YI_{mean} per TC, an ERT of 20% combined with the EC AE yielded the highest value ($YI_{mean\ TC}$ = 0.20), followed by the 2-out-of-3 rule again combined with the EC AE ($YI_{mean\ TC}$ = 0.16) and AE plus 15% ERT ($YI_{mean\ TC}$ = 0.15). Lowest $YI_{mean\ EC}$ were generated using the EC NRE (−0.03), while lowest $YI_{mean\ TC}$ resulted from combining AEWH with 25% ERT (-0.11). YI > 0.14 were almost exclusively found in the CrS postR. Sporadic outliers were mostly found for allR (AE, 20% ERT + 2/3 rule; AEWH, 0% ERT + 2/3 rule; NRE, 0% ERT), while antR only once yielded YI > 0.14 (AE, 20% ERT, YI = 0.15).

The CrS antR in general yielded low YI values across all EC. All YI < −0.12 including the minimal YI (HE, antR, 2-out-of-3 rule) are found in this CrS. The combination of antR and AEWH leads further to the minimal $YI_{mean\ CrS}$ (-0.05), followed by postR when combined with NRE ($YI_{mean\ CrS}$ = −0.04). Yet, only AE, AEWH and HE resulted in higher $YI_{mean\ CrS}$ over postR (AE: 0.14; AEWH: 0.06; HE: 0.12) compared to antR (AE: -0.01; AEWH: -0.05; HE: -0.03), whereas $YI_{mean\ CrS}$ values were almost on par for PE and NRE. YI ranges from -0.21 to 0.29.

Table 8 *Overview rTMS vs. DCS for all AC. Corresponding YI and calculated YI_{mean} (blue shadowed boxes). YI values above 0.00 were tagged and shadowed yellow, the highest YI values green and the lowest red. Highest and lowest YI_{mean} values are emphasised by coloured and bold digits (green = highest; red = lowest). 2/3 rule = 2-out-of-3 rule.*

rTMS vs. DCS

Youden's indices

		TC													
EC	**CrS**	ERT											2/3 rule	*Mean values*	
		0%	5%	10%	15%	20%	25%	30%	35%	40%	45%	50%			
AE	allR	0.06	0.11	0.10	0.11	0.15	0.04	0.01	0.00	-0.08	-0.07	-0.05	0.19	0.05	**0.06**
	antR	0.00	0.09	0.07	0.09	0.15	-0.01	0.01	-0.07	-0.19	-0.14	-0.10	0.03	-0.01	
	postR	-0.03	0.00	0.17	0.26	0.29	0.17	0.20	0.14	0.14	0.03	0.03	0.26	**0.14**	
Mean values		0.01	0.07	0.11	**0.15**	**0.20**	0.07	0.07	0.02	-0.04	-0.06	-0.04	**0.16**		
AEWH	allR	0.15	0.12	0.14	0.02	-0.04	-0.12	-0.07	-0.03	-0.03	-0.02	-0.02	0.16	0.02	0.01
	antR	0.01	0.03	0.04	-0.06	0.01	-0.19	-0.14	-0.05	-0.05	-0.05	-0.05	-0.07	**-0.05**	
	postR	0.17	0.20	0.06	-0.11	-0.06	-0.03	0.03	0.03	0.09	0.09	0.09	0.14	0.06	
Mean values		0.11	**0.12**	0.08	-0.05	-0.03	**-0.11**	-0.06	-0.02	0.00	0.01	0.01	**0.08**		
NRE	allR	0.15	0.06	-0.01	0.02	-0.03	-0.07	-0.08	-0.06	-0.05	-0.03	-0.03	0.02	-0.01	**-0.03**
	antR	0.03	-0.16	-0.08	-0.03	-0.01	-0.05	-0.05	-0.05	-0.05	0.00	0.00	-0.03	-0.04	
	postR	-0.11	-0.06	-0.06	-0.03	0.03	0.03	-0.09	-0.09	-0.06	-0.06	-0.06	0.06	**-0.04**	
Mean values		0.02	-0.05	-0.05	-0.01	0.00	-0.03	**-0.07**	**-0.06**	-0.05	-0.03	-0.03	**0.02**		
PE	allR	0.10	0.09	0.00	-0.05	-0.03	-0.02	-0.01	-0.01	0.00	0.00	0.00	0.09	0.01	0.01
	antR	-0.18	0.08	0.02	-0.06	-0.01	-0.05	0.00	0.00	0.00	0.00	0.00	0.10	-0.01	
	postR	0.26	0.17	0.03	-0.06	-0.03	-0.03	-0.03	-0.03	0.00	0.00	0.00	-0.11	0.01	
Mean values		0.06	0.11	0.01	-0.05	-0.02	-0.03	-0.01	-0.01	0.00	0.00	0.00	**0.02**		
HE	allR	0.02	0.07	0.05	0.04	-0.01	0.00	0.02	0.01	-0.02	-0.02	-0.02	0.04	0.01	0.03
	antR	-0.10	0.09	-0.01	0.02	-0.14	-0.01	-0.01	0.00	0.00	0.00	0.00	-0.21	-0.03	
	postR	0.06	0.17	0.14	0.29	0.20	0.11	0.14	0.14	0.00	0.00	0.00	0.17	**0.12**	
Mean values		-0.01	0.11	0.06	0.11	0.02	0.04	0.05	0.05	-0.01	-0.01	-0.01	**0.00**		
Total mean values for each single TC		0.04	**0.07**	0.04	0.03	0.03	-0.01	0.00	0.00	**-0.02**	-0.02	-0.01	**0.06**		

3.6.4. Results regarding a positive or a negative mapping

Table 9 *rTMS vs. DCS, highest sums for positive or negative mapping. Respective AC and corresponding ROC values are listed. Sensitivity = sv; specificity = sc.*

rTMS vs. DCS						
EC	Highest PPV + Sensitivity for positive mapping			Highest NPV + Specificity for negative mapping		
	Highest sum [%] (PPV[%]/sv[%])	TC of highest sum	CrS of highest sum	Highest sum [%] (NPV[%]/sc[%])	TC of highest sum	CrS of highest sum
AE	156% (56%/100%)	5% ERT	antR	173% (84%/89%)	45-50% ERT	postR
AEWH	149% (53%/96%)	0% ERT	antR	179% (85%/94%)	40-50 % ERT	postR
HE	126% 50%/76%	0% ERT	antR	185% (85%/100%)	30-35% ERT	postR
NRE	134% (54%/80%)	0% ERT	antR	177% (83%/94%)	40-50% ERT	postR
PE	111% (47%/64%)	0% ERT	antR	183% (83%/100%)	40-50% ERT	postR

Table 9 lists the highest sums for a positive or negative mapping subdivided per AC. Comparing rTMS to DCS, maximum achieved NPV + specificity sums ranged from 173% to 185%. The maximum sums for PPV + sensitivity were comparatively lower and spread wider (111% to 156%). Best negative mapping sums could be achieved applying high ERTs over postR (HE: 30 - 35% ERT; remaining ECs: 40 - 50% ERT), while positive mapping benefitted from lower ERTs over antR. PostR in general worsened PPV + sensitivity sums compared to higher sums achieved over antR. Best positive mapping results were achieved for AE and 5% ERT over antR. Regarding positive mapping characteristics, all EC achieved PPV around 50%, yet only AE and AEWH also yield high sensitivities up to 100%. Highest sums for negative mapping are comparatively on the same level across all EC, with NPV and specificities both exceeding 80%. The highest sum of specificity and NPV belongs to the analysis of postR in combination with HE (185%).
Combining allR and 0% ERT, i.e. analysis without error count and spatial limitation, yielded the following results: there was no EC with a PPV exceeding 30% (NRE and PE), the maximum sensitivity was 93% (AE), the maximum NPV was 87% (AEWH) and the maximum specificity was 57% (PE). Best sum for a positive mapping was 119% (AE) outperformed by 135% for a negative mapping (PE).

3.7. Results of the comparison DTI FT vs. DCS

3.7.1. Influence of TC and CrS for the EC AE

Figure 32 illustrates ROC curves for all TC combining AE and allR. The curve depicting 100 mm MFL nearly parallels the 45-degree diagonal (= green line) of the ROC space, indicating mediocre fit of results, while the curve depicting 40 mm MFL shows a better fitted course oriented towards the top left. Fittingly, the highest YI (0.27) for AE + allR, is achieved by tracking with 40 mm MFL and 100% FAT. Further, this TC results in the best-balanced result for AE based on the BBI (1.26). Using 25% FAT increases sensitivity to close to 100% at the cost of vastly reduced specificity (40 mm MFL [sensitivity/specificity]: 100%/2%; 70 mm MFL [sensitivity/specificity]: 98%/2%; 100 mm MFL [sensitivity/specificity]: 98%/4%).
The remaining EC's (AEWH, HE, NRE, PE) ROC plots for allR show a similar curve shape as Figure 32 while running even closer to the 45-degree diagonal of the ROC space.

Figure 32 *ROC plot of rTMS-based DTI FT vs. DCS combining AE and allR per TC. Corresponding %FAT are exemplary illustrated for 40 mm MFL. The green line represents ROC results created by chance.*

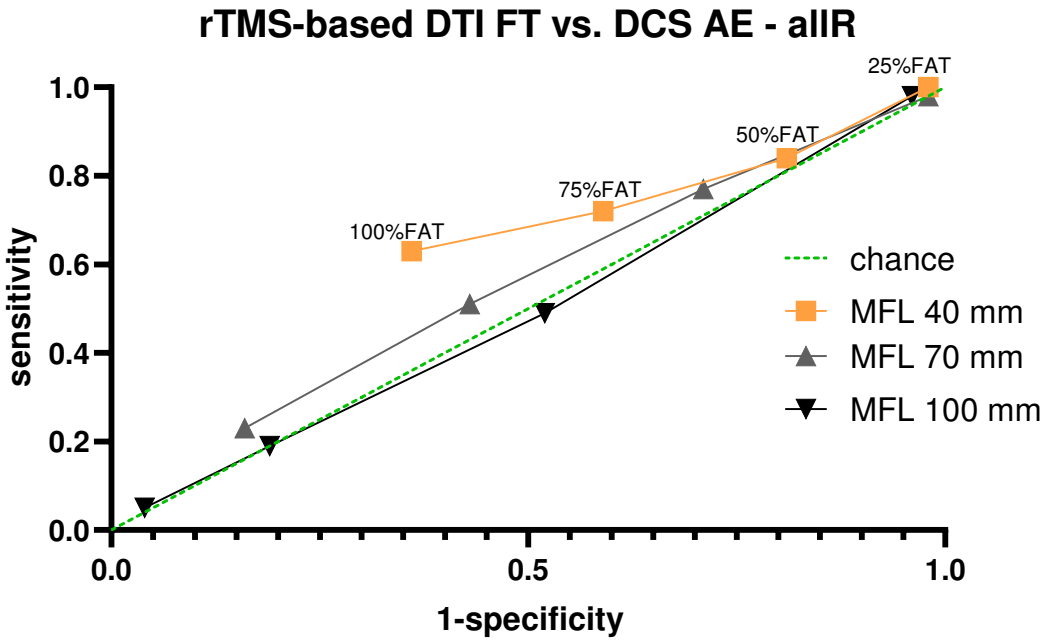

In comparison, Figure 33 shows the ROC curves regarding only postR with AE. Observing postR, graphs run more distant to the green line. Again, 40 mm MFL leads to best results including the topmost YI (0.29) for the category AE, again tracked with 100% FAT. AntR yields the lowest agreement to DCS for the EC AE. This is further outlined in Figure 34, comparing YI achieved with 40 mm MFL for each CrS. Independet of CrS, tracking with 40 mm MFL and 100% FAT results in highest YI (postR: 0.29; allR: 0.27; antR: 0.25).

Figure 33 *ROC plot of rTMS-based DTI FT vs. DCS combining AE and postR per TC. Corresponding %FAT are exemplary illustrated for 40 mm MFL. The green line represents ROC results created by chance.*

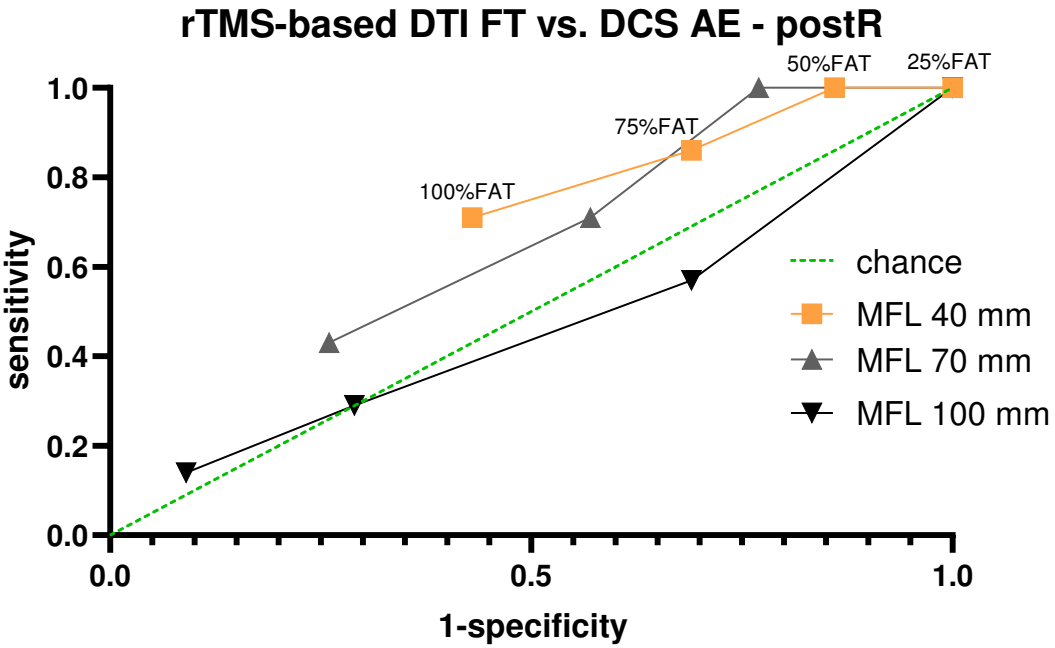

Figure 34 *rTMS-based DTI FT vs. DCS - progression of YI for all FAT and CrS underlying the fixed EC AE and tracked with 40 mm MFL*

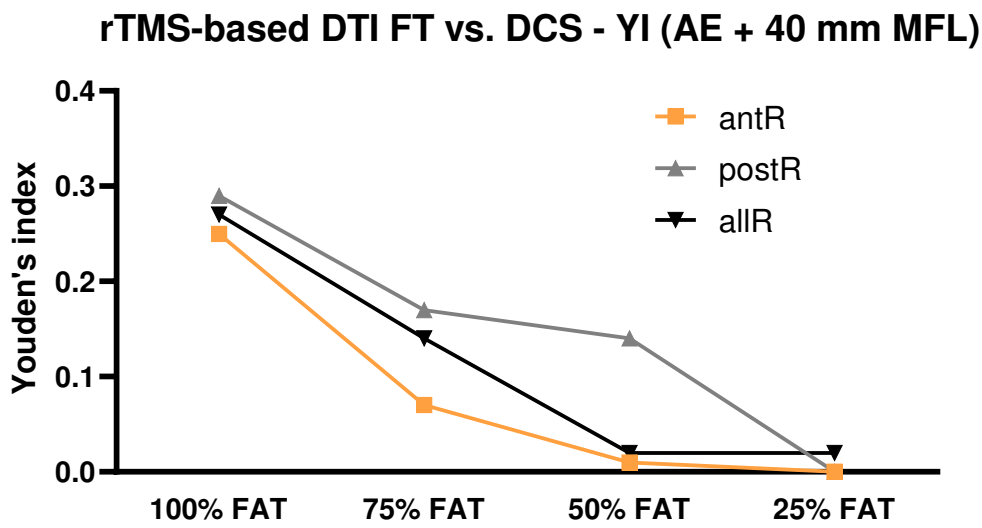

3.7.2. BI and YI with the corresponding AC

Table 10 *DTI FT vs. DCS indices per AC: BBI and best YI, including corresponding sensitivity (sv) and specificity (sc).*

DTI FT vs. DCS						
EC	**BBI (sv[%]/sc[%])**	**TC of BBI**	**CrS of BBI**	**Best YI (sv[%]/sc[%])**	**TC of best YI**	**CrS of best YI**
AE	1.26 (63%/64%)	MFL 40 100 % FAT	allR	0.29 (71%/57%)	MFL 40 100% FAT	postR
AEWH	1.22 (64%/61%)	MFL 100 50% FAT	antR	0.30 (56%/74%)	MFL 40 100% FAT	antR
HE	1.37 (71%/69%)	MFL 100 75% FAT	postR	0.40 (71%/69%)	MFL 100 75% FAT	postR
NRE	1.20 (67%/60%)	MFL 40 100% FAT	postR	0.36 (36%/100%)	MFL 70 100% FAT	antR
PE	0.97 (49%/60%)	MFL 40 100% FAT	allR	0.44 (100%/44%)	MFL 40 75% FAT	postR

The highest best YI (0.44) for the comparison DTI FT vs. DCS was achieved by analyzing PE only over postR with an MFL of 40 mm and 75% FAT (Table 10). Yet, the high YI results from widely imbalanced ROC values (sensitivity/specificity: 100%/44%). As illustrated in Table 10, a clear dominance of one CrS for all five EC could not be found based on the YI.
Throughout all five EC, there was a tendency towards higher BI values for either lower FAT levels combined with higher MFL or higher FAT levels combined with lower MFL. The highest BI was found for 40 mm MFL + 100% FAT and 100 mm MFL + 50% FAT. As illustrated in Table 11, this trend does not apply to YI. For YI no clear rule or trend is deducible instead. BI values ranged from 0.00 to 1.37 (Table 10).
Table 11 further illustrates that even though DTI FT vs. DCS yielded more positive YI and higher mean YI values than rTMS vs. DCS, total mean YI levels remained low. Highest $YI_{mean\ CrS}$ was 0.16 (PE, postR). Highest $YI_{mean\ TC}$ was 0.28 (NRE, 40 mm MFL, 100% FAT). Combining 40 mm MFL and 100% FATalso yielded a comparatively high $YI_{mean\ TC}$ for AE (0.27). In general, YI leveled close to zero with single positive and negative peaks. YI ranged from -0.30 to 0.44, exceeding the range of rTMS vs. DCS YI (-0.21 to 0.29). Lowest YI belonged to PE over antR (MFL 40 mm, 75% FAT) and NRE over postR (MFL 100 mm, 25% FAT). Lowest $YI_{mean\ TC}$ was -0.11 (NRE, 100 mm MFL, 25% FAT), lowest $YI_{mean\ CrS}$ was -0.12 (PE, antR).

Unlike rTMS vs. DCS, all single EC subelements (NRE, PE, HE) demonstrated a clear CrS dominance: PE and HE yield higher $YI_{mean\ CrS}$ over postR (PE: 0.16 vs. -0.12; HE: 0.15 vs. 0.03), while NRE yields higher $YI_{mean\ CrS}$ over antR (0.14 vs. 0.00) (Table 11). $YI_{mean\ CrS}$ values were almost on par for AE and less divergent for AEWH.

Table 11 *rTMS-based DTI FT vs. DCS per AC. Corresponding YI and YI_{mean} (blue shadowed boxes). YI values above 0.00 were tagged and shadowed yellow, the highest YI values green and the lowest red. Highest and lowest YI_{mean} values are emphasised by coloured and bold digits (green = highest; red = lowest).*

DTI FT vs. DCS

Youden's indices

		TC													
EC	CrS	MFL												Mean values	
		40 mm				70 mm				100 mm					
		FAT				FAT				FAT					
		100%	75%	50%	25%	100%	75%	50%	25%	100%	75%	50%	25%		
AE	allR	0.27	0.14	0.02	0.02	0.08	0.08	0.05	0.00	0.00	0.00	-0.03	0.02	0.05	
	antR	0.25	0.07	0.01	0.00	0.19	0.13	0.02	-0.04	0.04	0.15	0.12	0.00	0.08	0.07
	postR	0.29	0.17	0.14	0.00	0.17	0.14	0.23	0.00	0.06	0.00	-0.11	0.00	0.09	
Mean values		**0.27**	0.13	0.06	0.01	0.15	0.12	0.10	-0.01	0.03	0.05	-0.01	0.01		
AEWH	allR	0.21	0.10	0.11	0.03	0.08	0.10	0.07	0.01	0.01	0.03	0.06	-0.04	0.06	
	antR	0.30	-0.01	0.09	0.00	0.28	0.17	0.06	0.00	0.04	0.19	0.25	0.00	0.11	**0.08**
	postR	-0.03	0.23	0.17	0.00	0.11	-0.06	0.26	0.00	0.09	0.00	0.06	-0.11	0.06	
Mean values		0.16	0.11	0.13	0.01	0.16	0.07	0.13	0.00	0.05	0.07	0.12	**-0.05**		
NRE	allR	0.29	0.18	0.09	0.03	0.16	0.19	0.06	-0.01	0.05	0.10	-0.01	-0.03	0.09	
	antR	0.29	0.20	0.04	0.00	0.36	0.24	0.07	-0.09	0.09	0.32	0.15	0.00	0.14	0.08
	postR	0.27	0.12	-0.02	0.00	0.02	0.12	0.12	0.00	-0.09	-0.15	-0.13	-0.30	0.00	
Mean values		**0.28**	0.17	0.04	0.01	0.18	0.18	0.08	-0.03	0.02	0.09	0.00	**-0.11**		
PE	allR	0.08	-0.01	0.01	-0.02	0.02	-0.04	0.00	-0.06	0.03	-0.10	-0.07	-0.10	**-0.02**	
	antR	-0.11	-0.30	-0.17	-0.09	-0.02	-0.11	-0.12	-0.13	-0.05	-0.15	-0.07	-0.13	**-0.12**	**0.01**
	postR	-0.07	0.44	0.22	0.07	0.00	0.15	0.30	0.07	0.22	0.04	0.37	0.11	**0.16**	
Mean values		-0.03	0.04	0.02	-0.01	0.00	0.00	0.06	-0.04	0.07	**-0.07**	0.08	-0.04		
HE	allR	0.10	0.07	-0.03	0.03	0.18	0.13	0.01	0.04	-0.02	0.08	-0.03	0.02	0.05	
	antR	0.09	0.12	-0.15	-0.04	0.31	0.09	-0.06	-0.04	-0.04	0.07	0.00	-0.03	0.03	0.08
	postR	0.09	0.09	0.17	0.09	0.17	0.26	0.17	0.09	0.06	0.40	0.17	0.11	**0.15**	
Mean values		0.09	0.09	0.00	0.03	**0.22**	0.16	0.04	0.03	0.00	0.18	0.05	0.03		
Total mean values		**0.15**	0.11	0.05	0.01	0.14	0.10	0.08	-0.01	0.03	0.07	0.05	**-0.03**		
for each single TC		0.08				**0.08**				**0.03**					

3.7.3. Results regarding a positive or a negative mapping

For the EC AE and AEWH, the highest sums regarding positive or negative mapping are on par to rTMS vs. DCS (Table 12), while differences can be detected for the remaining EC. Superior sums for a positive mapping were achieved using 40 mm MFL and 25% FAT. Hence, highest sums ranged from 140% to 152%. Compared to rTMS vs. DCS, this mainly resulted of higher sensitivities, the maximum PPV still was 52%.
Sums regarding a negative mapping again exceeded those for a positive mapping. Negative mapping sums ranged from 175% to 179%, resulting from high NPVs (79% - 86%) and specificities (89% - 97%). Best results were attained for 100 mm MFL and 100% FAT and no significant difference between the single EC was found. Compared to the results of rTMS vs. DCS there is a slightly impairing tendency for HE and PE.

Table 12 *Highest sums achieved for positive or negative mapping. Respective AC and corresponding ROC values are listed (sensitivity = sv; specificity = sc).*

	Highest PPV + Sensitivity for positive mapping			Highest NPV + Specificity for negative mapping	
AC	rTMS vs. DCS	DTI FT vs. DCS	AC	rTMS vs. DCS	DTI FT vs. DCS
All errors					
	156%	152%		173%	175%
CrS	antR	antR	CrS	postR	postR
	5% ERT	-		45-50% ERT	-
TC	-	MFL 40	TC	-	MFL 100
	-	25% FAT		-	100% FAT
PPV[%]/sv[%]	56%/100%	52%/100%	NPV[%]/sc[%]	84%/89%	84%/91%
All errors without hesitation					
	149%	152%		179%	179%
CrS	antR	antR	CrS	postR	postR
	0% ERT	-		40-50 % ERT	-
TC	-	MFL 40&70	TC	-	MFL 100
	-	25% FAT		-	100% FAT
PPV[%]/sv[%]	53%/96%	52%/100%	NPV[%]/sc[%]	85%/94%	85%/94%
Hesitation errors					
	126%	147%		185%	175%
CrS	antR	antR	CrS	postR	postR
	0% ERT	-		30-35% ERT	-
TC	-	MFL 40&70	TC	-	MFL 100
	-	25% FAT		-	100% FAT
PPV[%]/sv[%]	50%/76%	51%/96%	NPV[%]/sc[%]	85%/100%	84%/91%
No response errors					
	134%	149%		177%	176%
CrS	antR	antR	CrS	postR	allR
	0% ERT	-		40-50% ERT	-
TC	-	MFL 40	TC	-	MFL 100
	-	25% FAT		-	100% FAT
PPV[%]/sv[%]	54%/80%	49%/100%	NPV[%]/sc[%]	83%/94%	79%/97%
Performance errors					
	111%	140%		183%	175%
CrS	antR	antR	CrS	postR	postR
	0% ERT	-		40-50% ERT	-
TC	-	MFL 40	TC	-	MFL 100
	-	25% FAT		-	100% FAT
PPV[%]/sv[%]	47%/64%	49%/91%	NPV[%]/sc[%]	83%/100%	86%/89%

3.8. Results of the comparison (rTMS + DTI FT) vs. DCS

Combining rTMS results with rTMS-based DTI FT does not improve ROC values compared to DCS. On the contrary, BBI and best YI decreased for all EC, as illustrated in Table 13.
Highest BBI was 1.00, highest best YI was 0.06. Both values were achieved using the same analysis combination (HE + postR + 15% ERT + MFL 100 mm + 100% FAT). YI values generally were equal or less to zero, while the major share (93 - 98%) of BI values did not overcome a value of 0.50. A high percentage share (AE: 40%; AEWH: 60%; HE: 40%; NRE: 72%; PE: 72%) each yielded the lowest possible BI value of 0.00.
Regarding the overall comparison (rTMS + DTI FT) vs. DCS, no clear dominance in the applied analysis combinations and CrS can be stated (Table 13). While the highest sums for a positive mapping (109% - 155%) are comparable to results in rTMS vs. DCS, the sums for a negative mapping were lower (165% - 175%).

Table 13 *All mapping comparisons addressing the different AC: BBI and best YI, including corresponding sensitivity (sv) and specificity (sc). 2/3 rule = 2-out-of-3 rule.*

AC	BBI			Best YI		
	rTMS vs. DCS	DTI FT vs. DCS	(rTMS + DTI FT) vs. DCS	rTMS vs. DCS	DTI FT vs. DCS	(rTMS + DTI FT) vs. DCS
All errors						
	1.11	1.26	0.71	0.29	0.29	0.00
CrS	postR	allR	postR	postR	postR	antR
	20% ERT	-	2/3 rule	20% ERT	-	0 & 5% ERT
TC	-	MFL 40	MFL 40	-	MFL 40	MFL 40
	-	100% FAT	100% FAT	-	100% FAT	25% FAT
sv[%]/sc[%]	57%/71%	63%/64%	50%/35%	57%/71%	71%/57%	100%/0%
All errors without hesitation						
	1.12	1.22	0.63	0.20	0.30	0.00
CrS	allR	antR	antR	postR	antR	antR
	10% ERT	-	10% ERT	5% ERT	-	40-50% ERT
TC	-	MFL 100	MFL 40	-	MFL 40	MFL 100
	-	50% FAT	100% FAT	-	100% FAT	100% FAT
sv[%]/sc[%]	59%/56%	64%/61%	35%/32%	86%/34%	56%/74%	0%/100%
Hesitation errors						
	0.97	1.37	1.00	0.29	0.40	0.06
CrS	allR	postR	postR	postR	postR	postR
	5% ERT	-	15% ERT	15% ERT	-	15% ERT
TC	-	MFL 100	MFL 100	-	MFL 100	MFL 100
	-	75% FAT	75% FAT	-	75% FAT	75% FAT
sv[%]/sc[%]	59%/48%	71%/69%	50%/56%	43%/86%	71%/69%	50%/56%
No response errors						
	0.93	1.20	0.63	0.15	0.36	0.00
CrS	allR	postR	antR	allR	antR	antR
	0% ERT	-	5% ERT	0% ERT	-	20-50% ERT
TC	-	MFL 40	MFL 40	-	MFL 70	MFL 70 & 100
	-	100% FAT	100% FAT	-	100% FAT	100% FAT
sv[%]/sc[%]	68%/47%	67%/60%	33%/32%	68%/47%	36%/100%	0%/100%
Performance errors						
	1.14	0.97	0.74	0.26	0.44	0.00
CrS	postR	allR	postR	postR	postR	postR
	0% ERT	-	0 & 5% ERT	0% ERT	-	0% ERT
TC	-	MFL 40	MFL 70	-	MFL 40	MFL 40
	-	100% FAT	75% FAT	-	75% FAT	75% FAT
sv[%]/sc[%]	57%/69%	49%/60%	50%/37%	57%/69%	100%/44%	67%/33%

4. DISCUSSION

4.1. Overview of results

One aim of this study was to assess and possibly improve the accordance of rTMS-based language mapping to DCS-based language mapping using rTMS-based fiber tracking. Ideally, increased sensitivity and PPV would allow for positive mapping. Further, negative mapping would have been improved given increased specificity and NPV. This study also aimed to evaluate possible differences in ROC based on different EC as well as CrS and TC.
At first, rTMS-based results were compared to DCS-based results, differentiated per EC, TC and CrS. This examination found anterior regions to be better suited for positive mapping, although still suffering from low PPV values with posterior regions better suited for negative mapping. ROC sums were superior for negative mapping. In negative mapping, no significant deviation of ROC sums was found between different EC, while higher ERT (30 - 50% ERT) consistently yielded better results. In contrast, positive mapping ROC values were more distinctively spread. Best results were achieved for the EC AE while PE yielded the lowest positive ROC sums (AE: 156%; PE: 111%). Further, positive mapping contributed from lower ERT (0 - 5% ERT). AE and AEWH are the most favourable ECs for a positive mapping, whereas positive mapping was least accurate based on PE. Among the three EC in focus of this study, namely HE, PE and NRE - NRE (sum 134%) followed by HE (sum 126%) outperformed PE. These findings indicate that TC and EC should be adapted based on the goal of either a positive or negative mapping, based on this study.
This analysis was complemented by ROC curves and the statistical factors YI and BI to evaluate the method's ROC without distinction for positive or negative mapping. Combined, these measures identified the CrS postR, the EC AE and the TC 20% ERT as ideal combination. When only regarding the BI, postR again yielded best results, paired with a low ERT (0% ERT) and based on the EC PE (1.14). This combination's YI was 0.26, the third highest YI only surpassed by the first mentioned combination of AE, postR and 20% ERT as well as HE, postR and 15% ERT (both YI = 29). Fittingly, posterior regions outperformed anterior regions in the comparison rTMS vs. DCS based on YI and BI. Worst results were attained using antR and NRE. Overall, the accordance of rTMS-based language mapping to DCS-based language mapping was low. YI ranged from −0.21 to 0.29, the BI ranged from 0.00 and 1.14.
The second part of the analysis compared language mapping results derived from rTMS-based DTI FT to DCS-based language mapping. Intriguingly, the incorporation of DTI FT lead to a slight improvement of the ROC. The analysis yielded more YI values above zero, higher mean YI and higher BBI and best YI. Further, BI (0.00 - 1.37) and YI (-0.30 - 0.44) ranged towards higher values. Yet, accordance to DCS is still afflicted by the occurrence of values far below the possible maximum. The addition of DTI FT further increased sensitivity for the EC HE, NRE and PE. Interestingly, this did not influence the results of AE and AEWH. Regarding negative mapping, no clear improvement of ROC was achieved. Aside of singular deviations, best results for positive mapping were again found for mapping of the anterior CPS regions combined with a FAT of 25% and an MFL of 40 mm. In the case of negative mapping, best results were again achieved by mapping of the posterior CPS regions using a 100 mm MFL and 100% FAT.
Again, regarding BI and YI values, using 40 mm MFL with 75% or 100% FAT obtained together seven BBIs and best YIs in the comparison DTI FT vs. DCS, albeit i.a. not including the highest BBI (HE). Across allR, irrespective of the EC, BI and YI favoured the usage of 40 mm MFL and 100% FAT. Tracking with this combination yielded further the highest YI for the EC AE independent of the analysed CrS. This combination of a high FAT and low MFL balances the above described ideal combinations for a positive (low FAT, low MFL) and negative (high FAT, high MFL) mapping. Due to a decrease in specificity, comparable, albeit slightly inferior results were achieved using low FAT and high MFL values. When comparing DTI FT vs. DCS per EC,

no clear distinction could be found for either CrS based on YI and BI for AE and AEWH. When regarding PE and HE, postR yielded higher $YI_{mean\ CrS}$. Opposingly, mapping for NRE yielded higher $YI_{mean\ CrS}$ over antR. Summing up, including DTI FT based on rTMS language mapping spots in the comparison to DCS slightly improved ROC characteristics.
Finally, the results of the aforementioned comparisons were checked against each other, including concurrent findings of language positivity or negativity (rTMS vs. DCS + DTI FT vs. DCS = (rTMS + DTI FT) vs. DCS). This combination lead to a clear impairment of the ROC across all AC. Possible underlying reasons and potential solutions are discussed in the following. Doing so, previously used standards are also being queried.

4.2. Favourites in respect of CrS in the comparison rTMS vs. DCS

The superiority of posterior regions for negative mapping as well as for BI and YI found in this study is particularly interesting, as previous studies found anterior regions more reliable and scoring better when compared to DCS (Picht et al., 2013; Sollmann et al., 2013a; Krieg et al., 2014a; Krieg et al., 2014b).
One difference to these studies is the PTI of 0 ms instead of 300 ms that was used in 50% of this study's patients. Other authors already outlined the superiority of a PTI of 0 ms (Krieg et al., 2014b; Ille et al., 2015b). Sollmann et al. stated in 2013 that due to the early activation of the posterior regions including the perceptive Wernicke's and Geschwind's area during language processing (Indefrey, 2011; Schuhmann et al., 2012), a PTI of 300 ms would be too late to properly interrupt the language process of those areas (Sollmann et al., 2013a). Fittingly, Krieg et al. found a PTI reduction to 0 ms to mainly improve NPV, PPV and specificity in the posterior regions, while the change in PTI only lead to an increase in specificity over anterior regions (Krieg et al., 2014b). Yet, Krieg et al. still found antR to outperform postR in their study. Hence, further underlying mechanisms can be assumed to underly the dominance of postR found in this doctoral thesis. It should be noted that the outperformance of postR was most distinct for the EC HE. HE also accounts for the largest single subelement of EC, only surpassed by the grouped EC AE and AEWH. HE's influence could be decisive. Yet, AEWH also found superior ROC for posterior regions, albeit less pronounced compared to AE. Another possible factor could be the higher number of surgical exposures of the anterior areas. This would also influence the findings for positive mapping.
Finally, it must be stated that the different results for posterior and anterior regions compared to other studies may also be influenced by different definitions of anterior and posterior CPS sectors.

4.3. Comparison of rTMS vs. DCS results to present findings

As initial efficiency in this doctoral thesis the comparison rTMS vs. DCS was carried out. This study extended the comparison of language mapping results gained by rTMS to DCS by several EC. This has not been done in the comparisons between rTMS and DCS to date (Picht et al., 2013; Tarapore et al., 2013; Krieg et al., 2014a; Krieg et al., 2014b; Ille et al., 2015a; Ille et al., 2015b; Babajani-Feremi et al., 2016; Sollmann et al., 2016b; Sollmann et al., 2017a; Lehtinen et al., 2018; Jung et al., 2019; Bahrend et al., 2020; Freigang et al., 2020; Motomura et al., 2020).
When not applying a TC (= ERT of 0%), the resultant ROC values make a positive mapping impractical. Only anterior regions showed a degree of applicability for positive mapping, especially when based on the EC AE and AEWH (NRE: PPV 54%, sensitivity 80%; AEWH: PPV 53%, sensitivity 96%; AE: PPV 53%, sensitivity 100%). Despite good NPV (maximum NPV for AEWH + postR: 92%), negative mapping appear infeasible as well due to low specificity (highest specificity for PE + postR: 69%; for AEWH + postR: 31%). This combination of high NPV and high sensitivity paired with a loss of PPV and specificity resultant from 0% ERT, hence no error threshold, is in line with prior findings (Picht et al., 2013; Tarapore et al., 2013; Krieg et al., 2014a; Ille et al., 2015b; Sollmann et al., 2017a).
Research done by Ille et al. found high ERT to enable for negative language mapping for AE + allR with a high NPV and specificity, but with a loss of PPV and sensitivity. Again, this doctoral

thesis was able to repeat these findings. Fittingly, Ille et al. also used PTI of 0 and 300ms, generating almost identical ROC values (50% ERT, AE, allR for both studies: this doctoral thesis - NPV 74%, specificity 90%; Ille et al. - NPV 73%, specificity 96%). Further, this thesis, in line with Ille et al. found no satisfying increase in sensitivity and PPV through the addition of TC. Ille et al. achieved best ROC values for positive mapping and 0 ms PTI by applying the following TC: ERT of 15%, 20%, 25% or the 2-out-of-3 rule. These combinations were identified based on the greater ROC balance and a maximum PPV. Conversion of these results into BI and YI yield the following values (Ille et al., 2015b):

- 2-out-of-3 rule: BI 1.12 & YI 0.47
- 15% ERT: BI 0.84 & YI 0.33
- 20% ERT: BI 1.26 & YI 0.36
- 25% ERT: BI 1.10 & YI 0.24

Ille et al.'s results exceed comparative results of this thesis (AE + allR, listed below in parentheses alongside). Yet, ROC values gained in this thesis include both PTI (0 and 300 ms). As stated above, the inclusion of 300 ms PTI has been found to reduce ROC especially for negative mapping. The following lists YI and BI values gained from Ille et al.'s dataset including both PTI (300 ms + 0 ms) with this thesis' findings added in parenthesis alongside:

- 2-out-of-3 rule: BI 0.98 & YI 0.16 (BI 1.02 & YI 0.19)
- 15% ERT: BI 0.86 & YI 0.06 (BI 0.95 & YI 0.11)
- 20% ERT: BI 0.94 & YI 0.05 (BI 1.02 & YI 0.15)
- 25% ERT: BI 0.80 & YI 0.07 (BI 0.68 & YI 0.04)

Mimicking Ille et al.'s results, who reached a maximum PPV of 30%, this study achieved a PPV of 33% as a maximum for those four TC, allR + AE. A subdivision into EC and CrS was not carried out by Ille et al.
Krieg et al. also applied a PTI of 0 ms instead of 300 ms in 2014 (Krieg et al., 2014b). Further, this group was stimulated with a pulse train of 10 instead of 5, at a reduced IPI of 2.5 instead of 3.0 seconds and with an introductory sentence in the naming of the objects ("This is…"). Compared to the 300 ms control group, this group performed significantly better regarding the PPV (allR: 53% to 39%) and NPV (allR: 97% to 81%). Furthermore, specificity was significantly increased both anterior and posterior (allR: 79% to 26%). Krieg et al.'s results surpass this thesis' ROC even when combining Krieg et al.'s control and intervention group (0% ERT + AE + allR, 0 + 300 ms PTI, Krieg et al.'s findings – specificity 41%, PPV 41%) (Krieg et al., 2014b). This difference might stem from modification of the other 3 parameters. Moreover, Tarapore et al. could achieve significantly better ROC (sensitivity 90%, PPV 69%, specificity 98%, NPV 99%). This difference is mainly seen in the context of a different cortical subdivision system as the CPS and is further discussed in section 4.6.3 on page 61 (Tarapore et al., 2013).
Compared to DCS, rTMS-based language mapping could achieve ROC values comparable to prior findings (Picht et al., 2013; Ille et al., 2015b), while not surpassing other studies' outcomes that were achieved using further differing protocols (Tarapore et al., 2013; Krieg et al., 2014b). This dissertation could further confirm the feasibility of ERT and the 2-out-of-3 rule as a simple method to refine mapping for a positive or negative mapping (Sollmann et al., 2016b; Sollmann et al., 2017a). Moreover, this doctoral thesis extended pre-existing analyses by subdividing results for several EC, which so far has not been done. Doing so, a significant influence of different EC on the ROC of language mapping could be demonstrated for the first time.
In Table 14 best ROC achieved by already published comparative studies on language rTMS to DCS were listed and further transferred into YI, BI as well as positive and negative sums. Krieg et al. and Tarapore et al. clearly surpassed this thesis' findings even including the superior DTI FT vs. DCS results. This holds particularly true for superior sensitivity and NPV. Further, comparatively high specificity and PPV could be achieved. This is reflected by the corresponding superior BI and YI values as well as high positive and negative sums (Tarapore et al., 2013; Krieg et al., 2014b). Still, positive sums published never exceeded 160% (Motomura et al., 2020).

Table 14 Publications' best ROC *comparing rTMS with DCS (extended representation based on a review by Jeltema et al. (2020)): Highest results were shadowed green, lowest red. Corresponding BI, YI, positive and negative sums were further calculated, values tagged and underlined green if exceeding this dissertation's findings including DTI FT vs. DCS (BI > 1.37; YI > 0.44; positive sum > 156%, negative sum > 185%).*

Publication	sensitivity [%]	specificity [%]	PPV [%]	NPV [%]	BI	YI	positive sum [%]	negative sum [%]
Picht et al., 2013								
allR	90%	24%	36%	84%	0.48	0.14	126%	108%
antR (Broca's area)	100%	13%	57%	100%	0.26	0.13	157%	113%
Tarapore et al., 2013	90%	98%	69%	99%	1.80	0.88	159%	197%
Krieg et al., 2014a	10%	89%	17%	82%	0.20	-0.01	27%	171%
Krieg et al., 2014b								
allR, PTI 0 ms	90%	79%	53%	97%	1.58	0.69	143%	176%
antR, PTI 0 ms	100%	67%	55%	100%	1.34	0.67	155%	167%
postR, PTI 0 ms	75%	92%	75%	92%	1.50	0.67	150%	184%
Ille et al., 2015a	67%	49%	34%	79%	0.98	0.16	101%	128%
Ille et al., 2015b	97%	15%	34%	91%	0.30	0.12	131%	106%
Babajani-Feremi et al., 2016	67%	66%	24%	95%	1.32	0.33	91%	161%
Sollmann et al., 2017b								
no ERT	93%	13%	27%	84%	0.27	0.06	120%	98%
2-out-of-3 rule	68%	51%	32%	82%	1.02	0.19	101%	133%
≥ 20% ERT	51%	64%	33%	79%	1.02	0.15	84%	144%
Jung et al., 2018	63%	67%	55%	74%	1.26	0.30	118%	141%
Lehtinen et al., 2018	68%	76%	27%	95%	1.36	0.44	95%	171%
Motomura et al., 2020	82%	60%	79%	64%	1.19	0.41	160%	124%
Bahrend et al., 2020	35%	90%	16%	96%	0.70	0.25	51%	186%

4.4. Methodical explanations for the impairment of ROC by (rTMS + DTI FT) vs. DCS

One possible reason for the inferior results of the final analysis might lie in fiber tracking being conducted only with rTMS**+** stimulation sites, rendering this analysis much more vulnerable to false-positive or false-negative results. Yet, a fiber tracking based on rTMS**-** points, i.e. non-language-eloquent areas, does not depict language-related fibers and hence would not fit the underlying research question.

Anatomical-based fiber tracking could constitute an alternative. However, anatomical ROIs did not show satisfactory results in the context of preoperative planning, due to distorted anatomy (Nimsky et al., 2006; Schonberg et al., 2006; Robles et al., 2008) and a high degree of examiner dependency (Wakana et al., 2007; Catani et al., 2008). Further, anatomic measure lack adaptation to the hodotopical model and neuroplasticity (Robles et al., 2008; Duffau, 2014c; Southwell et al., 2016). Yet, as the comparison (rTMS + DTI FT) vs. DCS is a new approach introduced in this dissertation, DTI FT vs. DCS based on anatomical ROIs has not been performed so far.

Another possible explanation for the findings regarding (rTMS + DTI FT) vs. DCS could base on the strict definition of the four fractions TP, TN, FP and FN. Instead of exploiting the strengths of each method to compensate for the other method's respective weaknesses, each method's positive and negative results were treated to be equivalent. A future refinement of this method should pay respect to the specific advantages and shortcomings of either technique, as well as their specific ROC. Doing so, Ille et al. successfully combined the high specificity of fMRI with the high NPV and sensitivity of rTMS (Ille et al., 2015b). To ensure a similar experimental setup, the advantages of nTMS-based DTI FT need to be further investigated.

4.5. Evaluation of results regarding certain aspects of the respective methods

4.5.1. Possible reasons for the low number of and missing DCS+ results

4.5.1.1. Regarding the methodical approach

Using rTMS, language-positive areas were found in every subject. Yet, two subjects did not show DCS**+** sites despite exposure and stimulation of the traditionally language-related areas (Figure 28 on page 41). Further, in spite of the known wide cortical spread of language function, only few DCS**+** areas could be identified in the other patients. Again, these findings mirror prior studies (Krieg et al., 2014b). One possible underlying reason might lie in restricted stimulation intensities due to early EcOG signalling not achieving sufficient intensities to provoke language impairment. Fittingly, especially tumor infiltration of cortical areas as well as pre-existing neurologic deficits were found to lead to higher stimulation intensities required for language mapping (Szelenyi et al., 2010; Saito et al., 2018). DCS stimulation intensities per patient were not recorded in this study. Further, stimulation intensity depended on the surgeon's subjective assessment of language performance and can therefore be assumed to vary between different surgeons. These uncertainties could be addressed via the assessment of language function by an independent language specialist or neuropsychologist, as it is meanwhile recommended for rTMS (Krieg et al., 2017).
This doctoral thesis was based on a negative intraoperative mapping. This common technique reduces craniotomy size, as craniotomy is done based on the site and size of the tumor mass and not on the possible localization of language-positive areas (Sanai et al., 2008c; Sollmann et al., 2015b; Saito et al., 2018). The tailored craniotomy leads to less associated tissue damage and time saving during ISM (Sanai et al., 2008c; Hervey-Jumper et al., 2015; Sollmann et al., 2015b; Hendrix et al., 2017; Saito et al., 2018). Further, the reduced craniotomy size might reduce postoperative morbidity due to reduced e.g. pain, bleeding, scarring area, wound complications and post-craniotomy headache (Hardavella et al., 2005; Arjipour et al., 2015; Rocha-Filho, 2015). This is reflected by the shorter surgery time and inpatient stay as well as improved short-term language performance (Hendrix et al., 2017). Yet, the smaller craniotomy could have reduced exposure of individual language-positive areas to DCS. For scientific purposes, a positive language mapping might be more informative. Yet, this method was found to increase the risk of postoperative early neurologic disorders while no difference in the long-term follow up was found (Kim et al., 2009; Chacko et al., 2013; Trinh et al., 2013). In theory, perisylvian tumors could also have impaired language function to a degree, where no more function could be deduced. Yet, this is highly unlikely, as normal language function was an inclusion criterion. Rather, plasticity might have relocated DCS**+** areas outside the craniotomy border, leaving less rTMS**+** sites in the surgical exposed areas (Duffau, 2006; Robles et al., 2008; Krieg et al., 2013b; Duffau, 2014c; Rosler et al., 2014; Southwell et al., 2016).

4.5.1.2. Questioning the ground truth

Insufficiency of the gold standard of DCS states another possibility to explain this and further studies' results. This would fit the assumption of an increased sensitivity in rTMS-based language mapping, detecting additional at least language-involved areas.
The current status of DCS as gold standard is supported by long-time data of intraoperative mapping (Ojemann et al., 1978; Ojemann et al., 1989; Haglund et al., 1994; Sanai et al., 2008a; Corina et al., 2010), meta studies, albeit randomised studies are lacking, (De Witt Hamer et al., 2012) and recurring findings of at least temporary language deficits after removal of DCS**+** regions in the majority of cases (Duffau, 2006; Robles et al., 2008; Gil-Robles et al., 2010; Martino et al., 2011). Yet, two reports found the existence of multiple DCS**+** regions to reduce the likeliness of long-term deficits following resection of one of these regions (Duffau, 2006; Robles et al., 2008). Yet, similar observations were made regarding the resection of rTMS**+** but DCS**-** sites, again showing transient but not persistent deficits (Krieg et al., 2014a). In both

cases, the induced plasticity could have regained lost language function. Furthermore, postoperative oedema and hypoperfusion must be discussed as possible alternative reasons for transient deficits (Duffau, 2006; Robles et al., 2008; Gil-Robles et al., 2010; Martino et al., 2011; Picht et al., 2013). The fact that in 2013, amid the data collecting process of this study, the rate of permanent neurologic morbidity after surgery of language-eloquent tumors still ranged between 3.2% and 20% indicates that DCS is not infallible (Tarapore et al., 2013). Yet, these deficits might also be due to other perioperative complications such as ischemia or injury to subcortical structures (Petrovich Brennan et al., 2007). Still, as already stated by Sollmann et al., DCS doesn't provide absolute reproducibility, which is reflected by the defined cut-off of 66% needed for DCS positivity (Sollmann et al., 2013a). Moreover, Gonen et al. (2017) found simultaneously applied multi-sided DCS stimulations to yield additional DCS**+** sites in 73% of the patients. This might reflect a more detailed insight of language processing.
Further, the higher language error detection rate in rTMS could be due to the video recording and its consecutive more precise offline analysis of language errors. In 2016, resection based on a negative language mapping by rTMS and rTMS-based DTI FT was carried out on four patients who couldn't undergo awake surgery with DCS. In these cases, an optimal functional outcome and EOR could be achieved (Ille et al., 2016). A further advantage of rTMS is the less stressful setting for the patient, reducing the occurrence of errors due to a lack of concentration (Ille et al., 2015b). Further, the influence of perioperatively applied sedative drugs on the patient's performance should be considered as possible confounder. Yet a lack of concentration during DCS would rather lead to false DCS**+** results, which does not fit to the overall low number of DCS**+** regions.
Summing up, DCS still holds the status of a gold standard for cortical language mapping, but several upcoming findings demonstrate specific advantages of rTMS that need to be further examined systematically to establish e.g. a superior degree of sensitivity in rTMS-based language mapping.

4.5.2. Possible biased detection of language errors by rTMS

4.5.2.1. Possible confounders on error counts

The high standard deviation of number of errors by rTMS for each EC (Figure 24 on page 37) could well be explained by the high variance of interindividual language distribution even across the two hemispheres (Sanai et al., 2008c). This analysis further found the number of errors per patient and per CPS region to correlate to the amount of applied rTMS trials per CPS region. Adhering to the non-standardized protocol at that time (see 4.5.2.2), not all CPS regions were stimulated equally often, illustrated by the high variability of rTMS stimuli (378.8 ± 135.3). This confounder likely impacts ROC results, especially regarding the used TC, i.e. ERT and 2-out-of-3 rule. Interestingly, the individual pain level, commonly thought to cause misinterpretations or language errors due to deceasing patient concentration, especially in the regions below the temporal muscle was found irrelevant to this issue in this study (Tarapore et al., 2013; Krieg et al., 2017). Also, this study found no correlation between mapping intensity and patient's pain level, differing from prior findings showing a subjective decline in pain level by reduced rTMS intensities (Rossi et al., 2009; Tarapore et al., 2013; Sollmann et al., 2015c). Mapping intensity itself did not correlate to error count either. Prior findings by Hauck et al. (2015) further found no correlation between the number of rTMS errors and a patient's general language performance depicted by the quality of the baseline performance.

4.5.2.2. User-dependent lack of standardization

As this study was done in the course of clinical practice, language mappings were performed by different investigators. This leads to the question whether inter-observer variance significantly influences the results of rTMS language mapping. A study by Sollmann et al. (2013a) published during the time of data collection found both inter- and intra-observer variability to significantly decrease this diagnostic method's reliability. This study included three sequential mappings of healthy subjects. A possible confounder of said study could consist of changes in language function distribution due to neuroplasticity which was shown to occur

even over short timespans (Pascual-Leone et al., 1995; Ungerleider et al., 2002; Draganski et al., 2006; Sollmann et al., 2013a). Yet, this effect was not done during sequential mapping of the motor area using single-pulse nTMS (Sollmann et al., 2013b; Forster et al., 2014).
To improve rTMS reliability for language mapping, a standard protocol introduced in 2017 by Krieg et al. recommends a random rTMS stimulation pattern, covering the perisylvian cortex at approximately 10 mm intervals (Krieg et al., 2017). A similar strategy was used for 90% of the patients in this study. Still, some CPS regions were particularly high frequented, while others were neglected. As stated above, these differences in the number of applied stimulation trials are likely to influence the number of errors. 10% of study subjects were stimulated adhering to a newly introduced guiding template (Figure 16 on page 24). This template simplified allocation of stimulation sites to CPS regions and stipulated the number of stimulations in each CPS region. A standardization of stimulation patterns, which is especially important in comparison studies, is hence possible. However, this template may result in a fixed pattern regarding the order of stimulated CPS regions, the effect of which cannot yet be foreseen.
Furthermore, inter-observer variance can also influence the user-dependent offline analysis of the produced language errors and hence weaken the methods reliability, i.e. the number of errors as well as the assigned error categories. This is further outlined in section 4.7.5 on page 66.

4.5.2.3. Lack of standardization regarding stimulation parameters

Since this dissertation's data collection period was 3 years, new study results led to changes in the respective rTMS protocols during the course of data collection. Hence, a certain lack of standardization occurred.
In 2013 Tarapore et al. warned against fast and non-systematic changes of the rTMS parameters, e.g. stimulation frequency, number of pulses or PTI, recommending a more systematic approach (Tarapore et al., 2013). First, different stimulation intensities as used in this doctoral thesis (80% to 122% RMT) can influence the depth of neuronal activation. Activation can hence occur cortically, subcortically and even outside the neuronal structures. Stimulation intensity exceeded 120% in three cases. Stimulating at this intensity is considered to stimulate deeper than 2 cm beneath the scalp and hence more likely to influence subcortical nerve fibers (Roth et al., 2002; Rossi et al., 2009). Further, the moment of disturbance within language processing is crucial. While previously a PTI of 200 - 500 ms was considered promising, leading to the widespread usage of a PTI of 300 ms (Indefrey et al., 2004; Brennan et al., 2012; Krieg et al., 2013b; Sollmann et al., 2013a), recent studies found a PTI of 0 ms to reduce the rate of false-positive rTMS results, increasing the rate of true-negative results. Therefore, a PTI of 0 ms is currently recommended for a negative mapping (Indefrey, 2011; Picht et al., 2013; Krieg et al., 2014b; Sollmann et al., 2017a). Stimulation frequency and number of pulses further varied over the data acquisition timespan of this study, as can be seen in Table 1 on page 23.
Adhering to the standard protocol by Krieg et al. (2017), the following default parameters should to date be chosen: IPI 2500 ms, PPT 700 ms, PTI 0 ms, intensity 100% RMT, frequency and number of pulses 5 Hz/5 pulses.

4.5.3. Possible insufficiency of fiber displaying by rTMS-based DTI FT

4.5.3.1. TC combinations

Insufficient fiber depiction may underly the unsuccessful identification of language-eloquent CPS regions by means of linking the number of fibers originating from one rTMS**+** site to its functional relevance. Although the user-dependend process of individual FA definition was acounted for by the FAT (Frey et al., 2012; Abdullah et al., 2013), a possible influence of the number of rTMS**+** spots on the individual FAT, distorting both the functional representation of fibers and the utility of the FAT as a TC parameter, remained possible. Yet, this dissertation found no correlation to support this consideration.
As expected, main factors to influence fiber count were the TC MFL and FAT following a certain

pattern (Table 6 on page 40). As nTMS-based DTI FT is a relatively new concept, the correct combination of these parameters still needs to be assessed in detail. Different combinations of FAT and MFL might appear most effective for the representation of certain language fiber tracts. This could be due to each tract's different fiber length and amount of fibers. AF and SLF are considered to be particularly significant language fiber tracts. Fittingly, damage to those tracts has a high risk of postoperative loss of function (Duffau et al., 2002; Bernal et al., 2009). Intriguingly, these two fiber tracts could best be depicted combining high MFL and low FAT for nTMS-based DTI FT (Negwer et al., 2017). Another recent study found an inverted correlation between the number of errors during language mapping and the percentage of visualization of language-related fiber tracts (Negwer, 2017). While these findings couldn't be reproduced by this dissertation, it is important to note that the underlying protocol differed decisively. This dissertation was based on comparing DTI FT to DCS, while Negwer focussed on optimal fiber tract depiction.

4.5.3.2. Biological influences

Diffusion is influenced by cellular and microstructural modification of the brain tissue. Higher myelinisation and higher cell density both increase anisotropy. Hence, the natural process of aging already changes the cerebral diffusion process due to the loss of myelin sheaths and cell mass (Alexander et al., 2007).
To date, the second largest clinical application of DTI FT is the presurgical depiction of white matter in tumor patients (Witwer et al., 2002; Jellison et al., 2004; Lazar et al., 2006; Alexander et al., 2007). Necrosis, edema, brain shift and displacement as well as invasion of tracts are typical tumor-related brain tissue pathologies that influence tractography (Lu et al., 2004; Alexander et al., 2007; Duffau, 2014a). Necrosis results in a loss of cell mass. This declining cell density is accompanied by declining anisotropy (Alexander et al., 2007). Diffusion levels are further affected by tumor type due to different inherit tissue architectures (Guo et al., 2002; Beppu et al., 2003; Alexander et al., 2007).
Each of these factors can falsify fiber representation. This issue was already outlined in an earlier comparison between DTI FT, conducted with anatomical ROIs, and fMRI results. This comparison found functional fibers traversing through or near a tumor to be less detectable. This effect was particularly distinct for language-related fibers and less distinct for sensorimotor fibers (Leclercq et al., 2010; Spena et al., 2010). Interestingly, a subgroup analysis of study on language nTMS-based DTI FT by Negwer in 2017 found no significant difference in the NoF between low-grade and high-grade gliomas (Negwer, 2017).

4.5.3.3. Methodical approach

Another possible confounder for language fiber pathway depiction is the experimental introduction of rims around the rTMS**+** points in ROI generation (Negwer et al., 2017). This approach bases on the theory that rTMS**+** spots correspond to regions rather than points (Tarapore et al., 2013). This artificial extension of rTMS**+** sites might have hindered specificity in this study. Furthermore, the anatomically derived CPS ROIs introduced in this study can lead to an unavoidable subjective influence by the user. Further examination of these possible effects using adapted protocols is required.
A general limitation of rTMS itself seems to lie in the fact that cortical language positivity is often due to language-involved short-distance fibers, which are not considered to be eloquent in the strict sense. These fibers serve general cognitive processing of information. The high NoF by means of rTMS-based DTI FT may be stem from these short-range corticocortical fibers (Sollmann et al., 2016b). Other methods enabling for function-based DTI FT, include fMRI or MEG. While MEG is a comparatively rare and expensive technology, fMRI suffers from a decline in accuracy due to changed oxygen levels e.g. in peritumorous tissues (Kuchcinski et al., 2015). Thus, all methods of fiber depiction can be assumed to suffer from specific technical disadvantages. Further refinement and possible combination of those techniques might lead to an improvement of DTI FT quality.

4.5.3.4. Mechanical MRI DTI aspects

The quality of DTI depends on the quality of the diffusion data taken from DWI. Like all MRI techniques, DWI inherits possible technical biases including thermal and physiologic image noises or different artefacts (e.g. head motion, eddy currents, air-tissue-boundary etc.) (Pierpaoli et al., 1996; Basser et al., 2000a; Alexander et al., 2001; Skare et al., 2001). In this thesis, DWI was conducted using a 3-Tesla MRI scanner. Ideally, the signal-to-noise ratio as well as the contrast-to-noise ratio could have been improved using a higher field strength, e.g. 7-Tesla (Laader et al., 2017). However this would have increased the susceptibility for motion artefacts, occurrence of eddy currents as well as the resulting degree of image distortion (Norris, 2001), which would have to be corrected using parallel imaging techniques and field strength maps (Jezzard et al., 1995; Alexander et al., 2006; Lee et al., 2009).
B-values commonly range between 700 and 1300 s/mm² (Alexander et al., 2007). As recommended, this thesis employed more than one b-value to improve data quality. In this case, 0 and 800 s/mm² were chosen (Jones, 2004; Correia et al., 2009; Lee et al., 2009). Grover et al. suggest utilizing more than two b-values, if compatible with the scanning time (Grover et al., 2015). Yet, longer scanning time may lead to an increase of motion artefacts due to a higher risk of patient discomfort (Jones et al., 2011).
Seeing as data collection was begun in 2011, a technical limitation of this study is the low count of initially only six encoding DTI directions (Basser et al., 2002; Grover et al., 2015). In general, higher numbers of non-collinear directions lower the variability of DTI parameters and hence improve imaging. Yet, scanning time increases as well (Basser et al., 1994a, 1994b; Jones, 2004; Correia et al., 2009; Lee et al., 2009; Potgieser et al., 2014). Although still not standardized, neurosurgical routine diagnostics to date include 15 or 32 directions by default. Grover et al. (2015) recommended a minimum of 20 directions to counteract image noise and thereby achieve more reliable DTI data, whereas Alexander et al. (2007) even recommended 64 directions. Moreover, excessively large voxel sizes lead to misinterpretation in overlapping areas, especially at tissue borders (e.g. white matter and CSF). Downsizing could be achieved using either higher field strengths or a more sensitive receiving radiofrequency MRI coil (Alexander et al., 2001; Alexander et al., 2007).
As long as fiber tractography bases on a deterministic approach with a diffusion tensor, even these adjustments cannot eliminate the unavoidable distorted display of crossing or kissing fibers (Berman et al., 2007). Even a one millimetre-sized voxel contains thousands of axons, each with a specific possible inherent orientation (Potgieser et al., 2014). Yet, only one PEV is determined. Further, these crossing or kissing fibers lower fractional anisotropy values and are thought to be the main reason for the large and in part confounding fractional anisotropy scale of 0.1 to 1.0 in white matter tissue (Alexander et al., 2001; Frank, 2001; Alexander et al., 2007). Also, the mathematical construct underlying the diffusion tensor itself is not entirely exact, as it contains various statistical methods (Burgel et al., 2009). Alternative algorithms including deterministic and probabilistic fiber tracking approaches exist and may lead to a future improvement of DTI FT quality (Staempfli et al., 2006; Farquharson et al., 2013; Kuhnt et al., 2013). Probabilistic concepts use stochastic models to estimate the distribution of fiber orientations in one voxel. This would enable for the depiction of more than just one fiber direction and reduce uncertainty in data or halts (Hess et al., 2006; Behrens et al., 2007; Berman et al., 2008; Farquharson et al., 2013; Sarwar et al., 2019). Yet, probabilistic fiber tracking is computationally expensive and very time-consuming, while the outcome is still not necessarily congruent to real anatomy (Alexander et al., 2007; Potgieser et al., 2014). Moreover, it was not possible to use other models than the diffusion tensor model to support intraoperative neuronavigation at the beginning of this study (Potgieser et al., 2014; Sarwar et al., 2019). Also DTI FT based on the diffusion tensor model was found to show good congruency to real-tissue dissection of white matter tract atlases (Lawes et al., 2008; Verhoeven et al., 2010; Thiebaut de Schotten et al., 2011) and to be able to depict anatomical tracts such as the AF or IFOF (Catani et al., 2002; Mori et al., 2002a; Jellison et al., 2004; Wakana et al., 2004; Alexander et al., 2007).

4.6. Limited comparability to ISM

4.6.1. Anatomic changes and technical aspects

One possible reason for inaccuracies in the comparison of rTMS results to DCS relates brain shift induced by durotomy and surgical resection (Hastreiter et al., 2004; Suess et al., 2007). Brain shift is particularly striking in malignant tumors, where it can lead to a shift exceeding 5 mm (Suess et al., 2001; Shahar et al., 2014). Further, depending on the growth rate of the tumor and time period between preoperative mapping and surgery, the underlying anatomic conditions can change. Surgery and preoperative planning should therefore be timed as closely together as possible. Yet, these are general limitations affecting the comparison to all preoperative mapping methods. These limitations can further be counteracted by additional macroscopic anatomical correction by the surgeon itself, e.g. via orientation on the pial veins and photographic documentation during ISM for correct CPS region assignment (Krieg et al., 2013a; Tarapore et al., 2013). Intraoperative technical orientation aids, such as ultrasound or iMRI with or without intraoperative DTI are further helpful at reducing these hindrances (Kuhnt et al., 2012). Still, corrective iMRI imaging is not yet part of clinical routine (Barbosa et al., 2015; Sastry et al., 2017).
Despite the general technical progress, avoidable and unavoidable inaccuracies in the underlying technologies can still lead to a significant distortion of the results. Co-registration during nTMS alone has a tolerance limit of 2 - 3 mm. Adding the tolerance limit of the intraoperative co-registration (again 2 - 3 mm) yields a technical possible variance of about 5 mm, not including perioperative brain shifts (Hastreiter et al., 2004; Suess et al., 2007; Tarapore et al., 2013). Such inaccuracies could already impair e.g. assignment of certain stimuli to different CPS regions in the comparison of rTMS to DCS.
While both mapping methods evaluate language function based on similar electrophysiologic considerations, it has not yet been conclusively clarified whether or not rTMS unlike DCS also stimulates subcortical structures, i.e. fibers (Szelenyi et al., 2010; Tarapore et al., 2013; Duffau et al., 2014). Yet, nTMS has already been found to stimulate deeper cortical areas such as those located in the sulci (Klooster et al., 2016). nTMS stimulation can reach as deep as 4 cm. Yet, a targeted excitation of subcortical structures is not possible due to a significant loss of focus with increasing depth (Deng et al., 2013). Hence, if subcortical structures, i.e. nerve fibers, were to be stimulated by nTMS, this stimulation would be distributed over a larger area with less focus. Common stimulation depth is 1.5 - 3.0 cm depending on the applied stimulation intensity (Roth et al., 2002; Roth et al., 2007; Rossi et al., 2009).

4.6.2. Variable number of CPS regions to compare with

One of the main advantages of preoperative planning is the decrease in craniotomy size in tumor surgery (Picht et al., 2013). However, the smaller surgical access site may further aggravate a pre-existing methodological problem that is innate in all comparative studies to DCS. Due to invasiveness and time management, only the areas exposed during surgery can be mapped and therefore compared. Craniotomy size and location is mainly influenced by tumor location and spatial extent. In this thesis 9 ± 3 of total 37 CPS regions were uncovered on average, with some areas being compared less or more often. This proportion corresponds to the contingent of fibers originating from a CPS region in relation to all tracked fibers during the comparison of DTI FT vs. DCS (about 25%).
The count of DCS**+** regions were even lower, namely 2 ± 1. Therefore, only one individual set of CPS regions per patient could be compared. This reduces a certain CPS region's significance for the overall evaluation. This especially shows the division of the evaluation into anterior and posterior areas. Anterior regions [trIFG, opIFG, vPrG], including Broca's area [trIFG, opIFG] (Broca, 1861; Brodmann, 1925), were exposed more frequently than the posterior regions [anG, aSMG, pSMG, mSTG, pSTG], containing Wernicke`s area [pSTG, mSTG, aSTG] and Geschwind's area [anG, pSMG, aSMG] (Figure 28 on page 41) (Wernicke, 1874; Brodmann, 1925; Catani et al., 2005). At the same time, more DCS**+** spots were found in the anterior regions. Interestingly, anterior areas tended to perform worse based on YI and BI values, but better when only regarding ROC sums for a positive mapping. Still, most of the

traditional language-relevant areas were tested at least twice regarding all patients. However, considering that an object-naming task was used, the underrepresentation of the MTG as a functionally relevant part of word production is critical (Binder et al., 2009; Indefrey, 2011; Gow, 2012; Price, 2012; Henseler et al., 2014; Hauck et al., 2015). Further, CPS regions relevant for working memory or semantic comprehension such as mSFG and pSFG are underrepresented as well (Simos et al., 2002; Scott et al., 2003; Catani et al., 2005; Du Boisgueheneuc et al., 2006; Jacquemot et al., 2006; Graves et al., 2008). It remains to be seen whether rTMS and hence rTMS-based DTI FT perform better when compared to DCS of all CPS regions. Ideally such an analysis would be subdivided for different EC and TC combinations.
Also, some areas were not or only rarely mapped during rTMS. This occurs due to certain CPS regions' difficult accessibility during the procedure, e.g. because the stimulation there seems to be particularly unpleasant or painful. These regions include orIFG or the polar CPS regions of the temporal [polSTG, polMTG] and frontal brain [polar inferior (polIFG), polar middle (polMFG) and polar superior frontal gyrus (polSFG)] (Hauck et al., 2015).

4.6.3. Questioning the CPS for comparison

It is currently recommended to search for clusters of language errors in several passes during the process of rTMS-based language mapping due to the significantly lower electrical charge and the different stimulation frequencies compared to DCS (Krieg et al., 2017). Further, both rTMS and DCS do not actually stimulate isolated points but larger areas. Also, adjacent areas are likely to belong to a coherent cortical region (Tarapore et al., 2013). These were among the main reasons for the introduction of the CPS system as a cluster template, allowing for the comparison of results gained by different methods. However, the CPS system has its disadvantages. Although a guidance template exists (Corina et al., 2005), the borders between the individual CPS regions must be adjusted individually for each subject, leading to user dependency. The application of the template is further hindered in case of an altered anatomy, e.g. in case of brain tumors.
In this dissertation, the CPS regions were assigned twice per subject, once by the rTMS investigator and another time by the surgeon. This setting was found to lead to an error margin greater than 10 mm for the CPS borders, while the spatial resolution of DCS is lower (Gil-Robles et al., 2010). Hence, rTMS- and DCS-positive stimulation points may not end up in the same parcel, despite of their actual spatial overlap, leading to a false tagging of the CPS parcel. This problem was already identified by Tarapore et al. (2013). The significantly better results in the comparison of rTMS vs. DCS by Tarapore et al. (2013) despite the use of a PTI of 300 ms (section 4.3 on page 52), could be due to their resultant application of the alternative Montreal Neurological Institute (MNI) atlas template. The MNI template is based on a parcel size of 10 mm. It is further spatially normalised and adjusted to the individual MRI using reference points. Using this template, the geometrical distance between two points to be compared from rTMS and DCS is decisive.
As for the CPS, a further subdividing of certain CPS regions can be considered. This would support a detailed analysis of different functions within a certain CPS region. E.g., the anG can be subdivided into the language-relevant ventrolateral and dorsomedial parts, added by an uninvolved middle part (Roux et al., 2004; Graves et al., 2010; Seghier et al., 2010). aSMG also shows higher ventral/perisylvian language response compared to other parts (Sliwinska et al., 2012; Tarapore et al., 2013).
Yet, CPS is still underlying most topographic studies and is therefore useful for mapping analysis. Nevertheless, a retrospective assignment to the traditional CPS is still possible following application of a different parcellation system for the comparison of the respective methods.

4.6.4. Lack of comparison to SCS

Regarding the technical basis of each technique, a comparison of the results of DTI FT to SCS would have seemed more useful than to DCS. Yet, this study based on increasing the coverage of rTMS and DCS mappings and not to conduct a comparison based on fiber depiction. DTI

FT was indicated to assess the degree of subcortical connectivity to distinguish between language-involved areas and -eloquent ones.
Nevertheless, a comparison with SCS could have assessed interesting aspects regarding the eloquence and quality of the tracts identified by DTI FT. At this point, it is important to emphasise that DTI FT itself is an anatomical diagnostic measure without information about the actual function of the identified fibers, whereas SCS like DCS and nTMS actually depicts causality and functional activity. Even though this disadvantage of DTI FT is softened by the combination to the functional diagnostic measure of rTMS, the simple fact that a fiber connects to a certain functionally active region does not guarantee that this fiber also holds exactly that function at the time of the examination. Especially the context of space-occupying processes such as tumors, the induced plasticity could cause known anatomical fiber tracts to change their original language eloquence. These rudimentary tracts were then hence resectable and would not support the eloquence of rTMS**+** regions, despite still being identifiable by rTMS-based DTI FT (Duffau, 2005; Benzagmout et al., 2007; Sarubbo et al., 2012).
Further revaluations of DTI FT by means of SCS are required. This holds true especially since the validation of the procedure was not yet completed during the timeframe of this study. The usage of DTI FT-based information for surgical planning was therefore also limited (Mori et al., 2002a; Tournier et al., 2002; Nimsky et al., 2006; Vassal et al., 2013; Duffau, 2014a, 2014b). This applied to both motor and language DTI FT.
In general, a high accordance of DTI FT and ISM could be shown for motor as well as for language tractography. Motor depiction reached a sensitivity of 92.6% and a specificity of 93.2% in a study conducted by Zhu et al., 2012. Language tractography reached a sensitivity of up to 97% and a specificity up to 100% in a study conducted by Bello et al., 2008 (Berman et al., 2004; Bello et al., 2008; Ohue et al., 2012; Zhu et al., 2012). Yet, the negative depiction of fiber tract was insufficiently valid, especially in tumor patients (Leclercq et al., 2010; Spena et al., 2010). The uncertainties at that time were mainly related to anatomical ROIs.
Despite studies showing a high accordance of nTMS-based DTI FT of language-relevant tracts with SCS (Bello et al., 2008; Leclercq et al., 2010), as well as the successful nTMS-based DTI FT of the corticospinal tract confirmed by SCS (Conti et al., 2014) and the promising case report of Ille et al. (2016) using only preoperative rTMS and nTMS-based DTI FT for surgery, the overall feasibility of nTMS-based DTI FT for language mapping remains a current research topic and has not been established in the standard clinical course yet (Sollmann et al., 2015a; Negwer et al., 2017).

4.7. Prospects and perspectives regarding rTMS

4.7.1. The optimal stimulation pattern

Despite various applications of rTMS for language interruption (Tarapore et al., 2013; Hauck et al., 2015), certain questions may arise regarding the validity of the underlying lesion model due to the comparison of rTMS language mapping results to DCS. The inhibition of cortical processing by repetitive nTMS is still an assumption. Language defects following rTMS in theory could also occur due to stimulation of the speech-relevant muscles, discomfort and lack of concentration. Furthermore, repetitive nTMS was found to cause so-called "over-callings". Over-callings seem to appear due to the activation of already established neuronal circuits, which then influence the function of distant instead of the targeted regions (Paus et al., 1997; Valero-Cabre et al., 2005; Bestmann, 2008; Tarapore et al., 2013).
The virtual lesion model was first demonstrated in a study by Kosslyn et al. (1999), further outlined by Pascual-Leone et al. (1999). Both were able to induce an inhibitory effect on the visual cortex. As the visual cortex is not influenced by e.g. muscle twitches, inhibitory effects could be clearly depicted. Additional studies supporting the thesis of virtual lesion of non-language-relevant tasks followed. In 2015, rTMS was first used for the localization of brain regions relevant for calculating. Based on the virtual lesion model, subjects were stimulated with 5 Hz/10 pulses to interrupt calculating tasks. The resulting calculation errors were in good agreement with the known spread of relevant brain regions obtained from previous findings. However, an intraoperative comparison is still pending and a clear distinction between

language, calculation and visual errors was not possible (Maurer et al., 2016). In 2017, it could successfully be shown that visual neglects can be triggered by rTMS again using 5 Hz/10 pulses (Giglhuber et al., 2017). Unlike language and calculation errors, triggering a neglect can hardly be deducted to a lack of concentration. Thus, the interruption of cortical processing by navigated repetitive nTMS seems possible. Due to the complexity of the cortical and subcortical interconnection, no unanimously ideal protocol for the localization of language-eloquent areas has been found yet (Krieg et al., 2017). This could be due to the higher sensitivity of rTMS-based language mapping compared to DCS, i.e. by detecting all language-involved and not only -eloquent areas (Ille et al., 2015b). Interestingly, Maurer et al. and Giglhuber et al. both stimulated with 5 Hz/10 pulses. Fitting, the intervention group in the study by Krieg et al. was also stimulated with 5 Hz/10 pulses, outlined in section 4.3 on page 52 (Krieg et al., 2014b). A change in the stimulation parameters for cortical language mapping by rTMS towards 5 Hz/10 pulses seems worth evaluating in further studies. Yet, it should be noted that this Hz/pulses combination causes unpleasant muscle contractions with consecutive jaw rattling when stimulating the area of the temporalis muscle (Tarapore et al., 2013). Picht et al. found a range of 5 - 7 Hz to be better tolerated than 10 Hz (Picht et al., 2013). However, Sollmann et al. found higher frequencies up to 20 Hz to be most effective for eliciting clear NRE over Broca's and Wernicke's area in five healthy volunteers, albeit the optimal frequency differed between those two areas (Sollmann et al., 2015c). The effectiveness of higher frequencies is further underlined by other studies (Jennum et al., 1994; Michelucci et al., 1994; Rogic et al., 2014). Fitting, also during intraoperative DCS and extraoperative ECoG higher frequencies found to be advantageous (Lesser et al., 1987; Ottenhausen et al., 2015; Saito et al., 2018).
Ille et al. (2015b) used the same three stimulation frequencies as this doctoral thesis (a: 5 Hz/ 5 pulses; b: 5 Hz/7 pulses; c: 7 Hz/7 pulses), individually choosing the most effective and best tolerated one per patient. While Ille et al. found no dominating combination of frequency and pulse count, this study found 5 Hz/5 pulse stimulation to be chosen the most. Intriguingly, this combination is also recommended in the standard protocol introduced by Krieg et al. (2017).
The distinction between speech errors and language disturbances by means of nTMS is still challenging. Rogic et al. tried to avoid spatial overlaps by including a previous motor mapping of the hand and laryngeal muscles and further tested a new stimulation concept for language interruption. Using the new stimulation protocol, language disturbances could be induced in each of the 11 patients (8 - 16 bursts per spot, each with 4 stimulations and an interstimulus interval of 4 ms; burst repetition rate of 12 Hz). In addition, the stimulated regions were found several mm away from the determined motor areas (Rogic et al., 2014).
Despite possible alternative language interrupting protocols by navigated rTMS, identifying the ideal set of parameters remains challenging, especially due to the relative scarcity of subjects in neurosurgery (Tarapore et al., 2013).

4.7.2. Adapted coil alignment

Axons of the pyramidal cells are arranged perpendicular to the surface of the gyrus. They are assumedly best depolarised by a parallel running current, i.e. a coil positioned tangentially to the surface of the brain and perpendicularly rotated to the bordering sulcus (Lioumis et al., 2012; Picht, 2015). This rule applies well to motor mapping, in which the alignment is guided by the sulcus centralis. In language mapping, a tangential and strict anterior-posterior coil alignment is in use (Epstein et al., 1996; Wassermann et al., 1999; Lioumis et al., 2012; Hauck et al., 2015). This alignment has the advantage that the e-field runs perpendicular to anterior parts of the temporalis muscle, reducing muscle activation (Tarapore et al., 2013; Krieg et al., 2017).
However, adhering to Tarapore et al. (2013), stimulation is always to be applied perpendicular to the nearest sulcus and the fiber course of the posterior temporalis muscle. Coil alignment would hence have to be adjusted per targeted region, abandoning the strictly anterior-posterior alignment rule. Applying this rule to e.g. temporal lobe areas bordering the sylvian fissure would result in a superior-inferior alignment perpendicular to the horizontally running sulci. The rotational component's influence on stimulation efficiency has been further found to outscale

the effect of coil tilting. Even rotations of 10° - 15° were found decisive (Opitz et al., 2013; Tarapore et al., 2013). A recent study found the strongest and most easily reproducible e-field to be induced in the somatosensory and motor cortex using interindividual coil alignment. Over other cortical areas, a more individual coil rotation also resulted in superior e-field strength, albeit mean field strength remained to be lower (Gomez-Tames et al., 2018). Regarding stimulation near the vertex, posterior areas were stimulated best with the coil oriented perpendicular to the longitudinal sulcus (= vertical e-field), while a parallel alignment (= horizontal e-field) was found advantageous in the medial portion of the vertex, bordering the sulcus centralis (Lee et al., 2018). Hauck et al. further showed that the e-field strength in the area of the inferior temporal gyrus fell below 50 V/m during language mapping, stimulating in a strictly anterior-posterior orientation. By Sollmann et al. in none of the five healthy volunteers an anterior-posterior orientation over Broca's and Wernicke's area was optimal for eliciting clear NRE. Further, the optimal coil rotation differed interindividually and over the two areas. Unlike as stated before, no link between coil orientation, thus the stimulation direction of the musculus temporalis, and pain level could be found (Sollmann et al., 2015c).
A separate evaluation of the areas located temporally or close to the sylvian fissure is missing in this dissertation. It is hence indicated to further assess the effect of anterior-posterior versus individualised coil rotation on stimulation efficiency. Except Sollmann's study of eliciting NRE in five healthy volunteers (Sollmann et al., 2015c), a link of coil alignment to the functional outcome of language mapping is also pending.

4.7.3. Customized stimulation intensity

Required stimulation intensities vary both inter- as well as intra-individually. Factors contributing to intra-individual variance include i.a. the thickness of the surrounding structures, the amount of CSF and microscopic anatomical conditions (Barker et al., 1987; Roth et al., 1991; Klooster et al., 2016; Lee et al., 2018). Stimulation in the area of synapses or sharp axon bends is assumed to require lower stimulation intensities. Interestingly, longer and thicker axons were also found to respond to lower stimulation intensities (Rossi et al., 2009). This supports the different stimulation intensities required for individual cortical regions with differing subcortical microscopic structures, i.e. differences in connectivity. In this context, a deeper knowledge of the subcortical fiber courses and axon characteristics could enrich nTMS-based mapping. An individual adjustment of stimulation intensity to the requirements of the respective mapping is hence necessary.
As done in this study, this variance of required stimulation intensity is usually addressed for using the RMT. Yet, the RMT is merely specified as percentage of the device's maximum output. Maximum output varies between different devices and can therefore not be used for comparison between devices (Danner et al., 2012). This hinders the comparison of different studies among each other, except for the small part of studies performed using the same device in the same setting. Picht recommended future studies to depict the RMT based on e-field strength (V/m) instead of the percentage share of the maximum output of the nTMS device (Ruohonen et al., 2010; Picht et al., 2011; Auriat et al., 2015; Picht, 2015).
Another hinderance of RMT-based standardization of stimulation intensities is the lacking evidence for the applicability of the transfer of motor-based measures of cortical excitability on to other than motor regions (Rossi et al., 2009; Klooster et al., 2016). An alternative approach is the determination of the phosphene threshold (PT), used to stimulate visual regions (Rossi et al., 2009). PT is defined as the minimum stimulation intensity needed to provoke a phosphene, a light sensation produced by an irritation of the visual system and not by light (Marg et al., 1994). Interestingly, the levels of PT and RMT do not correlate. This further strengthens the assumption of differing levels of cortical excitability between different cortical regions. However, the determination of PT to date is only possible in about half of the subjects (Rossi et al., 2009). Nevertheless, this is an example of a function specific threshold value being adapted to the examined function instead of motor function. Since both MEP and phosphenes represent increases in cortical activity due to nTMS, a reference value for inhibitory nTMS effects is still missing. Thereby, logically a high reproducibility of the virtual lesion seems to be crucial.

In addition to the application of a function-based stimulation intensity, changes in the respective anatomy should also be considered. Since language mapping covers a wide range of cortical areas, relevant factors such as tissue conductivity and permittivity, as well as coil-to-cortex distance significantly vary throughout the course of the mapping procedure (Rossi et al., 2009). Unlike scalp-to-cortex distance, coil-to-cortex distance significantly correlates with the magnitude of the RMT or e-field (Danner et al., 2012). Changes in thickness of non-brain structures and the amount of CSF influence both e-field strength and focality (Lee et al., 2018). Yet, simply increasing stimulation intensity to increase e-field strength would further decrease focality (Deng et al., 2013).
Defining the appropriate stimulation intensity for language mapping remains complex. Yet, these influential factors need to be investigated into as well as coil alignment for language mapping - individually for the respective macro- and microscopically similar structured brain areas. In this context, DES consists the advantage of shortening out several influential factors such as stimulator-to-cortex distance and CSF overlay. Further, DES was found less dependent on the structure and orientation of the targeted nerve cells compared to nTMS (Tarapore et al., 2013).

4.7.4. Appropriate choice of language task

The chosen object-naming task is a well-proven test, covering all presumably language-eloquent regions and encompassing the main functions of language formation (meaning, form, articulation). This task - like all picture-naming or picture-word matching tasks - captures the whole process of word production and amongst others phonologic, semantic as well as lexical skills (Price et al., 2005; De Leon et al., 2007; Siri et al., 2008; Corina et al., 2010; Indefrey, 2011; Lioumis et al., 2012; Cattaneo, 2013; Picht et al., 2013; Duffau et al., 2014; Sollmann, 2015). Object naming is the most discriminative test to date (Hauck et al., 2015). It is further well tolerated by the patient and fits within the time requirements of intraoperative DES (Krieg et al., 2017).
At the timepoint of this thesis, this task was the commonly used language task for rTMS and DCS, and well established in clinical usage in this institution (Price et al., 2005; De Leon et al., 2007; Indefrey, 2011; Lioumis et al., 2012; Cattaneo, 2013; Picht et al., 2013; Duffau et al., 2014). However, due to the longer intraoperative stimulation time (4 s), the naming of the picture during DES was initiated by the German phrase “This is a…”. To what extent this difference in the naming procedure affects the comparability to rTMS is questionable. However, if a technical bias due to this difference in the naming task were to be presumed, it would more likely be directed towards an increase in DES-based language errors due to the longer stimulation and articulation time. Interestingly, the two studies comparing rTMS- to DCS-based language mapping by Tarapore et al. (2013) and Krieg et al. (2014b) were also based on an object-naming tasks taken from Snodgrass et al. (1980). Both studies employed the introductory sentence during rTMS mapping as well, achieving better accordance of rTMS-based results to DCS. This could be due to an improved distinction of anomia (i.e. term slipped the mind) and speech arrests (i.e. being not able to speak) due to the usage of the introductory sentence (Tarapore et al., 2013).
It is known that the choice of the task has an influence on the incidence, the localization and the type of the language errors provoked by rTMS (Hauck et al., 2015; Krieg et al., 2017). Several language tasks have been examined since the beginning of cortical language mapping by rTMS in 1996 (Epstein et al., 1996; Wassermann et al., 1999). So far, the object-naming task was found best suited for this application (Hernandez-Pavon et al., 2014; Hauck et al., 2015). Yet, these comparisons might be in part biased as the commonly used error types and categories were explicitly developed for object-naming tasks (Hauck et al., 2015). Object-naming task further focus on word production, underrepresenting language comprehension (De Leon et al., 2007; Siri et al., 2008; Corina et al., 2010; Indefrey, 2011; Lioumis et al., 2012; Duffau et al., 2014). This might influence prior findings about decreased accuracy for rTMS applied to posterior CPS regions (Picht et al., 2013; Sollmann et al., 2013a; Krieg et al., 2014a; Krieg et al., 2014b). In contrast, verb generation was found rather suited to cover posteriorly processed language comprehension phase albeit also being a language production task

(Herholz et al., 1997; Thiel et al., 1998; Thompson-Schill et al., 1998; Ojemann et al., 2002; Edwards et al., 2010; Tarapore et al., 2013). Underlying this observation might be the addition of an auditory stimulus, namely the auditory presented noun that serves as basis for the generated verb. Hence, verb generation tasks might test language comprehension more specifically (Tarapore et al., 2013). Tarapore et al. (2013) further mention possible alternative tasks better focused on posterior areas due to e.g. a primarily semantic focus. These tasks include e.g. identification of famous faces or the categorization of objects (Gorno-Tempini et al., 2001; Peelen et al., 2012).
Hauck et al. (2015) further compared the language tasks object-naming, action-naming, verb generation and (pseudo-) word reading. Errors assignment was done identically as in this doctoral thesis. They found object-naming tasks, to provoke the largest error counts, presumably because of the tailored error types. NRE occurred with similar frequency in all tasks except (pseudo-) word reading. Interestingly, action-naming was even superior to verb generation regarding the posterior areas (Hauck et al., 2015). Here the verbs are not derived from auditory presented nouns, but from visually presented objects. Unlike verb generation, action-naming images daily activities such as sleeping or eating. Interestingly and in line with prior findings about the cortical distribution of different parts of language production, the location of language-eloquent sites of the anterior regions varied for picture-naming tasks, namely object-naming and action-naming, suggesting differences in the production of verbs and nouns (Daniele et al., 1994; Corina et al., 2005; Hauck et al., 2015). It should be mentioned that the division into anterior and posterior regions done by Hauck et al. (2015) was not identical to the division applied in this dissertation. In Hauck et al. more CPS regions were assigned to the respective categories. In total, Hauck et al. found no task to clearly outperform the other tasks. Yet, the weakest performance was shown for (pseudo-) word reading, mainly producing phonological errors, albeit a left-hemispheric widespread activation was previously described (Taylor et al., 2013). (Pseudo-) word reading as well as number counting with their reproductive, automated character are probably not challenging enough to provoke errors (Petrovich Brennan et al., 2007; Hauck et al., 2015).
Since different cortical regions are responsible for different parts of language processing, it seems difficult to develop a single language task equally fitting. Regarding DES, current studies recommend choosing an appropriate language task individually per patient, depending on the results of neuropsychological assessments and the location of the intracerebral lesion (Duffau et al., 2015; Hervey-Jumper et al., 2015). In 2015 Hervey-Jumper has tried to assign the tasks to the respective brain lobes for the intraoperative use (Hervey-Jumper et al., 2015). Based on these findings, this approach might also be reasonable for rTMS-based language mapping. Yet, patient concentration is limited and the applied number of different tasks needs to be restricted to a certain number (Hauck et al., 2015), e.g. depending on tumor location and affected region. Further, these new developed task types would have to be suitable for awake craniotomy as well. New error categories tailored to these new tasks should be developed as well, as the existing error categories were designed for the object-naming task.

4.7.5. Validity of error types

Error types can be divided into audible responses (performance errors, neologism, circumlocution, semantic or phonological paraphasias) and non-audible responses (no response, hesitation) (Sollmann, 2015). The comparison of the individual EC to DCS done in this thesis was thought to evaluate, whether either category and hence error type is represented more anteriorly or posteriorly. Further, this allowed for testing of a possible improvement of the ROC following exclusion of a certain category. However, this analysis is limited due to the missing subdivision of errors during DCS. rTMS-based language errors of a certain EC had to be compared to all errors produced by DCS, hindering a comparison of DCS-based error category spread. A post-hoc offline analysis of the intraoperative results would improve the allocation and analysis of the match and should be conducted in future studies.
Sollmann et al. (2013a) evaluated the stability of different error types within the same patient. Interestingly, they found reproducible to significantly vary for different EC. In particular, phonological paraphasias, performance errors and neologism showed greater inter- and intra-

observer fluctuation, while semantic paraphasias, NRE and hesitation errors were more stable. These findings contrast earlier studies. Speech arrests, such as NRE, used to be ascribed a significant inter-subject variability (Amunts et al., 1999). Yet, these studies were based on non-navigated instead of navigated rTMS. Further, hesitation errors have the reputation of being an unsafe error type and were therefore often excluded in other studies (Corina et al., 2010; Lioumis et al., 2012; Picht et al., 2013; Hernandez-Pavon et al., 2014). Interestingly, this dissertation's comparison of AE and AEWH found no significant difference concerning ROC sums for positive or negative mapping as well as BI and YI. Further, although all ROC curves regardless the EC indicate a rather random performance, HE outperformed PE for a positive mapping, while no significant difference was found for a negative mapping. HE occurred more often in anterior regions but achieved better YI and BI in posterior regions. Underlying this observation may be a reduced ability of comprehension resulting in a delay in response. As pointed out by Indefrey (2011) HE can represent a general disturbance in language processing. Further, a rTMS study measured the latency of language output to assess this general language deterioration (Schuhmann et al., 2012). An objectified definition of hesitation error by determining the latency was not performed in this thesis and should be further examined in future studies.
To improve validity of language errors it is generally recommended that the evaluation of language errors should be performed by a language specialist/neuropsychologist, regardless of the task used and unlike done in this doctoral thesis (Krieg et al., 2017).

4.8. Benefit-risk assessment of nTMS

4.8.1. Discomfort and pain

Due to its invasive character and the limited area exposed by craniotomy (Corina et al., 2010), ISM for investigative purposes can only be conducted with a strict medical indication. Therefore, ISM needs a non-invasive alternative that can be applied to e.g. healthy volunteers (Knecht et al., 2000; Rosler et al., 2014; Sollmann et al., 2014). Yet, nTMS also posesses potential side effects and risks.
Single-pulse nTMS to motor brain areas nearly doesn't provoke any side effects and is mostly described as painless including brain tumor patients (Kandler, 1990; Suess et al., 2001; Anand et al., 2002; Picht, 2015). rTMS on the other hand has an increased potential of discomfort or pain, especially headache (Bae et al., 2007; Loo et al., 2008; Rossi et al., 2009). In 1996, pain levels could effectively be diminished via a reduction of the stimulation frequency from 15 - 30 Hz to 4 Hz with unchanged stimulation efficiency (Epstein et al., 1996; Wassermann et al., 1999; Tarapore et al., 2013), yet opposing studies regarding the effectiveness exist (Jennum et al., 1994; Rogic et al., 2014; Sollmann et al., 2015c). Still, 100% of this study's subjects suffered from discomfort or pain while beeing stimulated over the temporal region. It is presumed that trigeminal and head muscle stimulation during rTMS are the underlying reasons. Increased pain during assessment of the regions below the temporalis muscle was again confirmed by this study ($VAS_{temporal}$ of 5 ± 2 compared to $VAS_{convexity}$ of 2 ± 2).
Moreover, uncomfortable head positioning, especially during a long-lasting mapping can induce neck pain (Mori et al., 1999a; Machii et al., 2006; Rossi et al., 2009; Tarapore et al., 2013).

4.8.2. Seizures

The most drastic, luckily today only occasionally occuring adverse event is the induction of seizures through rTMS. Most of the seizures were recorded before the introduction of the safety guidelines by Wassermann (1998), including the reduction of stimulation frequencies and the prolongation of the interval periods between the stimulation trains. Most though not all of the occasional seizures were since then either linked to pro-epileptogenic medication and pre-existing neurological disorders, to incompliance with the guidelines or couldn't be allocated to non-epileptic events for certain (Loo et al., 2008; Rossi et al., 2009; Klooster et al., 2016). These guidelines refer to single-pulse and repetitive TMS of only motor brain areas. Yet, the threshold of seizure induction is lowest over motor-inductive brain regions. It therefore seems

appropriate to transfer these guidelines to other cortical areas (Penfield et al., 1954; Rossi et al., 2009).
Stimulation with low frequencies (equal or less to 1 Hz) seems to result in no rTMS induced seizure, even in epileptic patients (Theodore et al., 2002; Fregni et al., 2006; Santiago-Rodriguez et al., 2008; Rossi et al., 2009). In 2004 the risk to suffer from an epileptic seizure induced by single-pulse was stated 0.0 - 2.8% for epilepsy patients, respectively 0.01 - 0.1% for all patients. In the case of rTMS, the risk for epilepsy patients was stated 1.4% in 2007. Yet, a clear link between nTMS and the induction of seizures could never be found (Schrader et al., 2004; Bae et al., 2007; Krishnan et al., 2015; Picht, 2015; Klooster et al., 2016). This is further suggested by an unsuccessful attempt to provoke epileptogenic foci through high frequency and high intensity rTMS (Tassinari et al., 2003). Data regarding a possible beneficial effect of non-epileptic drugs on the possible epileptogenic TMS side effect is insufficient (Rossi et al., 2009; Tarapore et al., 2013). Further, all documented seizures ended spontaneously and none caused late sequelae (Klooster et al., 2016).
More often than epileptic seizures, but still rarely, vasodepressive syncopes can occure, due to mental factors as for example anxiety (Wassermann, 1998; Rossi et al., 2009).

4.8.3. The risks of the magnetic field

Both TMS and MRI produce magnetic fields, reaching 3-Tesla via TMS coil and up to 7-Tesla via MRI (Laader et al., 2017). The magnitude of the field directly correlates to the time rate of change of the magnetic field (Rossi et al., 2009). The magnetic power itself and the induced currents are the main reason for possible severe side effects and adverse events. They therefore dominate the exclusion criteria for TMS and MRI as outlined in section 2.1 and 2.2 on page 17.
Unlike in MRI, the distance of e.g. ferromagnetic objects to the coil influences the decision of exclusion according to the TMS guidelines by Wassermann (1998) and Rossi et al. (2009). Some ferromagnetic objects, such as cardiac pace makers and aneurysma clips are therfore merely relative exclusion criteria (Chokroverty et al., 1995). Yet, future devices with higher magnetic field strengths will require a reevaluation of the risk to these objects due to rising conductive and ferromagnetic forces. E.g., rising eddy currents and their property of heating up conductive material inherit a higher risk for skin burns or irreversible damage of surrounding brain tissue, when temperature exceeds 43°C (Roth et al., 1992; Matsumi et al., 1994; Rotenberg et al., 2007). Aside of magnetic field strength, local rises in temperature also depend on the duration of stimulation, as well as on the geometry and conductivity of the conductive material, the surrounding tissue properties and in case of nTMS also the applied stimulation parameters (Roth et al., 1992). While gold and silver exhibit high conductivity properties, this applies less to common clinical materials such as titanium and plastic (Roth et al., 1992; Rotenberg et al., 2007). Titanium is among other appliances used for artificial joints and exhibits further low ferromagnetic characteristics. Even lover ferromagnetic characteristics are exhibited by stainless steel aneurysma clips (Barker, 1991; Rotenberg et al., 2007).
Some TMS systems may exceed the Occupational Safety and Health Administration (OSHA) sound pressure safety limit of 140 dB, indicating for appropriate hearing protection. Lower limits are required when examining children. For this reason, MRI for investigative purposes should be avoided in pregnant women (Counter et al., 1992; Rossi et al., 2009).
Summing up, the occurance of nTMS side effects highly depends on the applied protocol and TMS form. It could already be shown that navigated rTMS for language mapping can be conducted without safety concerns or serious side effects (Tarapore et al., 2013; Klooster et al., 2016). Fittingly, no severe adverse events occurred during the course of this dissertation.

4.9. Limited analysis of patient characteristics

Language processing was primarily assigned strictly to the left cerebral hemisphere (Broca, 1861; Wernicke, 1874). Over time, this model was challenged by findings of individuals with varying degrees of right-sided language eloquence, including cases with right-sided language dominance**.** Comparing left- and bi-handers to right-handers, language function was more

common executed by the right hemisphere. Right hemispherical involvement differed, up to balanced or switched language dominance. Left-handers were found to show right-sided language dominance in about 22% of the cases (Knecht et al., 2000; Szaflarski et al., 2002). Interestingly, a dominance shift can also occur in right- and bi-handers, while bi-handers more often tend to balanced dominance (Medina et al., 2007). Still, the majority of people shows left-sided dominated language processing independent of their handedness (Knecht et al., 2000; Medina et al., 2007). Further, essential left hemispherical language sites exist irrespective of handedness (Pujol et al., 1999; Sanai et al., 2008c; Matsuda et al., 2014; Tussis et al., 2016). This study also included two left-handers with left-sided perisylvian brain tumors. An influence of differences in handedness on the results e.g. due to right hemispherical language dominance in these two patients cannot be eliminated entirely. Yet, exclusion of these patients would have further restricted the already limited patient count of 20, despite the long period of data collection.
Sub-analyses of the patients' characteristics, such as tumor type, sex differences and handedness were not carried out due to the low statistical significance. Regarding sex differences, a possible influence on the results of language mapping are inconclusive. On the one hand, the lobus temporalis contains many language-involved areas and is statistical bigger in men (Kulynych et al., 1994; Binder et al., 1996; Binder et al., 2009), while the isthmus of the corpus callosum with its connecting commissures is larger in women, supporting more bilaterally dominated language processing for the female sex (Witelson, 1989; Steinmetz et al., 1992; Jancke et al., 1997). Further findings underline a more pronounced language lateralisation in male subjects (Kansaku et al., 2000; Kansaku et al., 2001; Hirnstein et al., 2013). On the other hand, separate examinations found no sex-specific divergences. The actual impact of sex on language processing hence still remains uncertain (Buckner et al., 1995; Frost et al., 1999).

4.10. BI, YI and ROC sums as surrogate for classic ROC

The large number of ROC produced by the different AC in this thesis required an objective measure for comparison. Future analysis of different TC or mapping parameter combinations will result in even larger amounts of data.
The Youden's index as well as the ROC plot are proven tools for the analysis of ROC values (Youden, 1950; Zweig et al., 1993; Schisterman et al., 2005; Akobeng, 2007; Lai et al., 2012). The additional introduction of BI was an attempt to objectify analysis for the best-balanced ROC pair and has been utilized as terminology in the published paper corresponding to this study (Ille et al., 2015b; Sollmann et al., 2016b).
Interestingly, the YI has not yet been used in studies comparing nTMS to DCS (Picht et al., 2013; Tarapore et al., 2013; Krieg et al., 2014a; Krieg et al., 2014b; Ille et al., 2015a; Ille et al., 2015b; Babajani-Feremi et al., 2016; Sollmann et al., 2016b; Sollmann et al., 2017a; Lehtinen et al., 2018; Jung et al., 2019; Bahrend et al., 2020; Freigang et al., 2020; Motomura et al., 2020). The Youden's index marks the optimal point of a ROC curve, indicating the least coincidental ROC pair. It further serves as a measure of overall accuracy in a test and is therefore used for comparison of methods in this dissertation (Lai et al., 2012). It was found to be easily appliable and to facilitate data comparability both within a single study, as well as with other studies (see 4.3 on page 52).
Intriguingly, high YI values do not coincide with high BI values necessarily. This can be explained by the fact that ROC imbalance and ROC magnitude were weighted equally against each other calculating the BI. Therefore, as exemplified in Table 15, the BI seems only partially suited as surrogate parameter for a good result. Comparing the BBI values of AE, AEWH and PE in Table 15, one would expect AE to achieve the highest BI due to its specificity of 71%. However, it is placed 3rd due to the higher imbalance of the individual values. Fitting, ROC values for AEWH and PE are well balanced, leading to a higher BBI despite reduced ROC magnitude. The respective YI better reflect the intuitive order (AE = 0.29; PE = 0.26; AEWH = 0.14).

Table 15 *BBI with corresponding sensitivity (= sv) and specificity (= sc), TC and CrS.*

EC	BBI (sv[%]/sc[%])	TC of BBI	CrS of BBI
AE	1.11 (57%/71%)	20% ERT	postR
AEWH	1.12 (59%/56%)	10% ERT	allR
HE	0.97 (59%/48%)	5% ERT	allR
NRE	0.93 (68%/47%)	0% ERT	allR
PE	1.14 (57%/69%)	0% ERT	postR

This leads to the question of the importance of ROC balance. In theory, it would be desirable if all ROC values achieved highest possible results, indicating an ideal agreement between both mapping methods. Regarding the overview table of the best YI (Table 13 on page 50), highest YI values could be achieved in the comparison group DTI FT vs. DCS, albeit showing in part high imbalances (e.g. PE: YI = 0.44 [sensitivity 100%/specificity 44%]; NRE: YI = 0.36 [sensitivity 36%/specificity 100%]). Instead of determining best-balanced results based on subjective standards, an alternative method for different weighting of the two components should be considered. This study was only the first attempt to do so.
The calculation of specific ROC sums regarding only a positive or negative mapping was also performed during this study as outlined in section 2.8.2.3 on page 33. This method again proved useful and can be used as a possible tool for future comparative studies.

5. CONCLUSION

A correlation of NoF gained by rTMS-based DTI FT of a certain CPS region to said region's language eloquence could not be found to reduce the number of false-positive rTMS stimulations in the comparison (rTMS + DTI FT) vs. DCS.
Yet, it could be shown that FAT level and MFL influence NoF in the expected pattern. These factors can be used to optimize language fiber depiction. The resulting ROC can further be improved by applying different language error thresholds for rTMS. In this context, favourable TC differed regarding their aim for either BBI, best YI or highest ROC sum. Prior findings regarding the comparison rTMS vs. DCS could be confirmed in this study. Further, DTI FT vs. DCS improved ROC. Still, ROC values derived from both comparisons remained comparatively low and better results, in particular sensitivity and NPV, have already been achieved in earlier and subsequent studies. Interestingly both comparisons yielded similar findings regarding error types and CrS. Better results belonged to the CrS postR and the EC AE or AEWH. Further, positive mapping performed better in antR, while negative mapping excelled in postR.
Mapping intensity and pain level did not bias the number of rTMS errors. Yet, the number of rTMS trials could be identified as a confounder, albeit the number of rTMS errors was found to not influence the NoF.
Possible underlying reasons for the findings regarding the comparison to DCS are seen in the inconsistency of applied rTMS mapping parameters, a user-dependency regarding the language error analysis, a limited comparability to ISM due to a variable and restricted exposure of CPS regions, preferring antR, a low number of DCS**+** results, as well as the strict definition of the four fractions (TP, TN, FP, FN) not considering the possible respective advantages of rTMS and DTI FT.
Nonetheless, this study marks the first systematic analysis of different EC in combination with various TC for rTMS and DTI FT. This allowed for valuable insights into said parameters' influence on mapping validity, identifying further potential for mapping parameter optimization. Further, the analysing tools YI and ROC sums, supplemented by the newly introduced BI, were implemented not only for rTMS vs. DCS, but also for the evaluation of the new methodological approaches rTMS-based DTI FT vs. DCS and (rTMS + DTI FT) vs. DCS.

6. SUMMARY

6.1. English

A safe maximization of the degree of resection of intracranial brain tumors is still the therapeutic approach with the best overall survival. However, in order to maintain quality of life, it must be ensured that functionally relevant brain areas are preserved. The invasive gold standard of intraoperative direct cortical stimulation (DCS) as well as the preoperative, non-invasive repetitive transcranial magnetic stimulation (rTMS) are suitable for the detection of language-eloquent regions. Previous studies have not been able to achieve a satisfactory comparability of rTMS to DCS. rTMS-based cortical language mapping is characterized by false-positive results and therefore mainly be used for negative cortical mapping. The aim of this study was to reduce false-positive results by including additional information about a region's subcortical nerve fiber connection, ideally resulting in a better overall comparability to DCS. This was evaluated comparing the results of the relatively new method of rTMS-based diffusion tensor imaging fiber tracking (DTI FT) to DCS for the first time. The resulting information about the cortical distribution of the language-positive areas was then evaluated against the results of the comparison between rTMS and DCS.

Data of 20 patients suffering from left-sided perisylvian tumors between the years 2011 and 2014 was collected for this purpose. Each patient underwent language mapping by navigated rTMS and DCS following an MRI examination including six DTI directions. rTMS results were assigned to five different language error categories. Further, 12 different thresholds for the definition of language-positive areas were evaluated followed by a comparison with the intraoperative DCS results. Furthermore, language-positive rTMS stimulation points were used as starting points for the rTMS-based DTI FT. This analysis was done separately with respect to each language error category. DTI FT in turn was further analyzed using 12 different tracking parameter combinations. Cortical areas of fiber origin depicted by this method were then compared to DCS results. Finally, language-positive areas determined in the two comparisons (rTMS versus DCS and rTMS-based DTI FT versus DCS) were cross-checked in the final comparison (DCS versus rTMS-positive sites affirmed by rTMS-based DTI FT). For all three comparisons, receiver operating characteristic (ROC) were determined and evaluated using the Youden's index (YI), a newly introduced balance index (BI) and calculated ROC sums regarding a positive or negative mapping.

The comparison of rTMS-based DTI FT versus DCS slightly outperformed rTMS versus DCS (rTMS vs. DCS: highest best BI = 1.14 [sensitivity 57%/specificity 69%], highest best YI = 0.29 [sensitivity 43%/specificity 86% and sensitivity 57%/specificity 71%] / DTI FT vs. DCS: highest best BI = 1.37 [sensitivity 71%/specificity 69%], highest best YI = 0.44 [sensitivity

100%/specificity 44%]). The final comparison ((rTMS + DTI FT) versus DCS) led to a deterioration in ROC (highest best BI = 1.00 [sensitivity 50%/specificity 56%], highest best YI = 0.06 [sensitivity 50%/specificity 56%]).

Reasons for this could be seen in the strict definition of the fractions underlying the ROC (true positive (TP), true negative (TN), false positive (FP), false negative (FN)), a limited comparability to intraoperative DCS, the lack of standardization of rTMS and methodological as well as technical preconditions for DTI FT that allow for future improvement. Although many factors remain to be optimized in order to improve preoperative rTMS-based language mapping, valuable insights could be gained. Further, the limited amount of pre-existing data could be illuminated or substantiated. A systematic analysis by different language error categories in combination with different threshold categories both for DTI FT and rTMS has not been performed so far. Furthermore, this is the first scientific publication that applied YI, BI and the respective sums for a positive or negative mapping successfully to the analysis of a large amount of ROC. This will ease the analysis of similar amounts of data in the future. Finally, rTMS-based DTI FT versus DCS and the final comparison ((rTMS + DTI FT) versus DCS) represent new methodological approaches. Moreover, there are already promising new studies that could further improve the applicability of rTMS language mapping and DTI FT for everyday clinical practice in the future.

6.2. Deutsch

Die möglichst maximale chirurgische Resektion intrakranieller Tumore ist nach wie vor der therapeutische Ansatz mit der höchsten Gesamtüberlebensrate. Jedoch muss zur Aufrechterhaltung einer adäquaten Lebensqualität auf eine Schonung funktionell relevanter Areale geachtet werden. Zur Auffindung sprachеloquenter Bereiche eignet sich prinzipiell neben den invasiven Goldstandards der intraoperativen direkten kortikalen Stimulation (*englische Abkürzung*: DCS) auch die präoperativ durchzuführende, nicht invasive repetitive transkranielle magnetische Stimulation (*englische Abkürzung*: rTMS). In bisherigen Studien konnte noch keine zufriedenstellende Vergleichbarkeit zu DCS erreicht werden. rTMS zur Lokalisierung sprach-eloquenter Areale weist zu viele falsch positive kortikale Bereiche auf und kann bisher nur für eine negative kortikale Kartierung genutzt werden. Ziel dieser Studie war es durch zusätzlich generierte Information über die subkortikale Nervenfaserverbindung, diese falsch positiven Bereiche zu reduzieren und insgesamt eine bessere Vergleichbarkeit zu DCS zu erreichen.

Zu diesem Zweck wurde zum ersten Mal ein Vergleich zwischen den Ergebnissen der relativ neuen Methode der rTMS-basierten Diffusions-Tensor-Bildgebung-Traktografie (*englische Abkürzung*: DTI FT) und DCS hergestellt. Die daraus gewonnenen Informationen über die kortikale Verteilung der sprachpositiven Areale wurden mit den Ergebnissen aus einem Vergleich zwischen rTMS und DCS abgeglichen.

Dafür wurden die Daten von 20 Patienten mit linksseitigen perisylvischen Raumforderungen aus den Jahren 2011 bis 2014 zusammengetragen, an denen jeweils eine Sprachkartierung mittels navigierter rTMS und DCS durchgeführt wurde und die daher eine MRT Untersuchung inklusive sechs DTI Richtungen erhalten haben. Die Ergebnisse aus rTMS wurden zum einen in fünf unterschiedliche Sprachfehlerkategorien eingeteilt und zum anderen wurden 12 verschiedene Grenzwerte für die Definition sprachpositiver Bereiche ausgewertet, bevor ein Vergleich mit den intraoperativen DCS Ergebnissen erfolgte. Weiter wurden für jede Sprachfehlerkategorie einzeln die sprachpositiven rTMS Stimulationspunkte als Startpunkte für das rTMS-basierte DTI FT verwendet. Dieses wiederum wurde mit 12 verschiedenen Tracking-Parameter-Kombinationen weiter analysiert und direkt mit den Ergebnissen aus DCS verglichen, indem der kortikale Bereich des Faserbahnursprungs als Entscheidungsgrundlage für einen sprachpositiven Bereich definiert wurde. Zuletzt wurden die in den beiden Vergleichen (rTMS versus DCS und rTMS-basiertes DTI FT versus DCS) ermittelten sprachpositiven Areale in dem finalen Vergleich (rTMS kombiniert mit rTMS-basierter DTI FT versus DCS) gegeneinander abgeglichen. Für alle drei Vergleiche wurden die receiver operating characteristic (ROC) ermittelt und diese mittels des Youden's Index (YI), des neu eingeführten Balance Index (BI) sowie in Hinblick auf die Möglichkeit einer positiven und negativen Kartierung hin untersucht.

DTI FT versus DCS konnte eine leichte Verbesserung der Vergleichbarkeit erzielen (rTMS vs. DCS: höchster best BI = 1,14 [Sensitivität 57%/Spezifität 69%], höchster best YI = 0,29 [Sensitivität 43%/Spezifität 86% und Sensitivität 57%/Spezifität 71%] / DTI FT vs. DCS: höchster best BI = 1,37 [Sensitivität 71%/Spezifität 69%], höchster best YI = 0,44 [Sensitivität 100%/Spezifität 44%]). Im Vergleich ((rTMS + DTI FT) versus DCS) kam es jedoch zu einer Verschlechterung der ROC (höchster best BI = 1,00 [Sensitivität 50%/Spezifität 56%], höchster best YI = 0,06 [Sensitivität 50%/Spezifität 56%]).

Gründe dafür konnten unter anderem in der strengen Definition der den ROC zugrundeliegenden Fraktionen (true positive (TP), true negative (TN), false positive (FP), false negative (FN)), einer eingeschränkten Vergleichbarkeit zum intraoperativen DCS, dem Mangel an Standardisierung des rTMS und bis dato noch ausbaufähigen methodischen und technischen Voraussetzungen für DTI FT gesehen werden. Obwohl noch viele Faktoren optimiert werden können, um das präoperative rTMS zur Sprachkartierung zu verbessern, konnten wertvolle Einsichten gewonnen sowie bereits vorhandene Daten neu beleuchtet oder untermauert werden. Eine Analyse nach verschiedener Sprachfehlerkategorien in Kombination mit unterschiedlichen Schwellenwerten sowohl für DTI FT als auch für rTMS ist bisher nicht erfolgt. Des Weiteren ist dies die erste wissenschaftliche Arbeit die YI, BI und die jeweiligen für eine positive oder negative Sprachkartierung berechneten Summen zur Auswertung einer großen Datenmenge an ROC in diesem Kontext erfolgreich angewendet hat, wodurch auch in Zukunft die Analyse großer Datenmengen erleichtert werden kann. Zuletzt stellen rTMS-basiertes DTI FT versus DCS, sowie der finale Vergleich ((rTMS + DTI FT) versus DCS) einen neuen methodischen Ansatz dar. Schon jetzt gibt es vielversprechende neue Studien, die die Anwendbarkeit einer rTMS Sprachkartierung und eines DTI FT für die alltägliche klinische Praxis in Zukunft verbessern könnten.

7. REFERENCES

Abdullah, K.G., Lubelski, D., Nucifora, P.G., & Brem, S. (2013). Use of diffusion tensor imaging in glioma resection. *Neurosurg Focus, 34*(4), E1. doi:10.3171/2013.1.FOCUS12412

Abraham, W.C., & Bear, M.F. (1996). Metaplasticity: the plasticity of synaptic plasticity. *Trends Neurosci, 19*(4), 126-130.

Ahdab, R., Ayache, S.S., Brugieres, P., Farhat, W.H., & Lefaucheur, J.P. (2016). The Hand Motor Hotspot is not Always Located in the Hand Knob: A Neuronavigated Transcranial Magnetic Stimulation Study. *Brain Topogr, 29*(4), 590-597. doi:10.1007/s10548-016-0486-2

Akobeng, A.K. (2007). Understanding diagnostic tests 3: Receiver operating characteristic curves. *Acta Paediatr, 96*(5), 644-647. doi:10.1111/j.1651-2227.2006.00178.x

Alexander, A.L., Hasan, K.M., Lazar, M., Tsuruda, J.S., & Parker, D.L. (2001). Analysis of partial volume effects in diffusion-tensor MRI. *Magn Reson Med, 45*(5), 770-780.

Alexander, A.L., Lee, J.E., Wu, Y.C., & Field, A.S. (2006). Comparison of diffusion tensor imaging measurements at 3.0 T versus 1.5 T with and without parallel imaging. *Neuroimaging Clin N Am, 16*(2), 299-309, xi. doi:10.1016/j.nic.2006.02.006

Alexander, A.L., Lee, J.E., Lazar, M., & Field, A.S. (2007). Diffusion tensor imaging of the brain. *Neurotherapeutics, 4*(3), 316-329. doi:10.1016/j.nurt.2007.05.011

Amassian, V.E., & Maccabee, P.J. (2006). Transcranial magnetic stimulation. *Conf Proc IEEE Eng Med Biol Soc, 2006*, 1620-1623. doi:10.1109/IEMBS.2006.259398

Ammirati, M., Vick, N., Liao, Y.L., Ciric, I., & Mikhael, M. (1987). Effect of the extent of surgical resection on survival and quality of life in patients with supratentorial glioblastomas and anaplastic astrocytomas. *Neurosurgery, 21*(2), 201-206.

Amunts, K., Schleicher, A., Burgel, U., Mohlberg, H., Uylings, H.B., & Zilles, K. (1999). Broca's region revisited: cytoarchitecture and intersubject variability. *J Comp Neurol, 412*(2), 319-341.

Anand, S., & Hotson, J. (2002). Transcranial magnetic stimulation: neurophysiological applications and safety. *Brain Cogn, 50*(3), 366-386.

Arjipour, M., Hanaei, S., Habibi, Z., Esmaeili, A., Nejat, F., & El Khashab, M. (2015). Small size craniotomy in endoscopic procedures: Technique and advantages. *J Pediatr Neurosci, 10*(1), 1-4. doi:10.4103/1817-1745.154309

Auriat, A.M., Neva, J.L., Peters, S., Ferris, J.K., & Boyd, L.A. (2015). A Review of Transcranial Magnetic Stimulation and Multimodal Neuroimaging to Characterize Post-Stroke Neuroplasticity. *Front Neurol, 6*, 226. doi:10.3389/fneur.2015.00226

Axer, H., Klingner, C.M., & Prescher, A. (2013). Fiber anatomy of dorsal and ventral language streams. *Brain Lang, 127*(2), 192-204. doi:10.1016/j.bandl.2012.04.015

Babajani-Feremi, A., Narayana, S., Rezaie, R., Choudhri, A.F., Fulton, S.P., Boop, F.A., Wheless, J.W., & Papanicolaou, A.C. (2016). Language mapping using high gamma electrocorticography, fMRI, and TMS versus electrocortical stimulation. *Clin Neurophysiol, 127*(3), 1822-1836. doi:10.1016/j.clinph.2015.11.017

Bae, E.H., Schrader, L.M., Machii, K., Alonso-Alonso, M., Riviello, J.J., Jr., Pascual-Leone, A., & Rotenberg, A. (2007). Safety and tolerability of repetitive transcranial magnetic stimulation in patients with epilepsy: a review of the literature. *Epilepsy Behav, 10*(4), 521-528. doi:10.1016/j.yebeh.2007.03.004

Bahrend, I., Muench, M.R., Schneider, H., Moshourab, R., Dreyer, F.R., Vajkoczy, P., Picht, T., & Faust, K. (2020). Incidence and linguistic quality of speech errors: a comparison of preoperative transcranial magnetic stimulation and intraoperative direct cortex stimulation. *J Neurosurg*, 1-10. doi:10.3171/2020.3.JNS193085

Bajada, C.J., Lambon Ralph, M.A., & Cloutman, L.L. (2015). Transport for language south of the Sylvian fissure: The routes and history of the main tracts and stations in the ventral language network. *Cortex, 69*, 141-151. doi:10.1016/j.cortex.2015.05.011

Barbosa, B.J., Mariano, E.D., Batista, C.M., Marie, S.K., Teixeira, M.J., Pereira, C.U., Tatagiba, M.S., & Lepski, G.A. (2015). Intraoperative assistive technologies and extent of

resection in glioma surgery: a systematic review of prospective controlled studies. *Neurosurg Rev, 38*(2), 217-226; discussion 226-217. doi:10.1007/s10143-014-0592-0
Barker, A.T., Jalinous, R., & Freeston, I.L. (1985). Non-invasive magnetic stimulation of human motor cortex. *Lancet, 1*(8437), 1106-1107.
Barker, A.T., Freeston, I.L., Jalinous, R., & Jarratt, J.A. (1987). Magnetic stimulation of the human brain and peripheral nervous system: an introduction and the results of an initial clinical evaluation. *Neurosurgery, 20*(1), 100-109.
Barker, A.T. (1991). An introduction to the basic principles of magnetic nerve stimulation. *J Clin Neurophysiol, 8*(1), 26-37.
Barker, A.T., & Shields, K. (2017). Transcranial Magnetic Stimulation: Basic Principles and Clinical Applications in Migraine. *Headache, 57*(3), 517-524. doi:10.1111/head.13002
Barone, D.G., Lawrie, T.A., & Hart, M.G. (2014). Image guided surgery for the resection of brain tumours. *Cochrane Database Syst Rev*(1), CD009685. doi:10.1002/14651858.CD009685.pub2
Basser, P.J., Mattiello, J., & LeBihan, D. (1994a). Estimation of the effective self-diffusion tensor from the NMR spin echo. *J Magn Reson B, 103*(3), 247-254.
Basser, P.J., Mattiello, J., & LeBihan, D. (1994b). MR diffusion tensor spectroscopy and imaging. *Biophys J, 66*(1), 259-267. doi:10.1016/S0006-3495(94)80775-1
Basser, P.J., & Pajevic, S. (2000a). Statistical artifacts in diffusion tensor MRI (DT-MRI) caused by background noise. *Magn Reson Med, 44*(1), 41-50.
Basser, P.J., Pajevic, S., Pierpaoli, C., Duda, J., & Aldroubi, A. (2000b). In vivo fiber tractography using DT-MRI data. *Magn Reson Med, 44*(4), 625-632.
Basser, P.J., & Jones, D.K. (2002). Diffusion-tensor MRI: theory, experimental design and data analysis - a technical review. *NMR Biomed, 15*(7-8), 456-467. doi:10.1002/nbm.783
Beaulieu, C. (2002). The basis of anisotropic water diffusion in the nervous system - a technical review. *NMR Biomed, 15*(7-8), 435-455. doi:10.1002/nbm.782
Beez, T., Boge, K., Wager, M., Whittle, I., Fontaine, D., Spena, G., Braun, S., Szelenyi, A., Bello, L., Duffau, H., Sabel, M., & European Low Grade Glioma, N. (2013). Tolerance of awake surgery for glioma: a prospective European Low Grade Glioma Network multicenter study. *Acta Neurochir (Wien), 155*(7), 1301-1308. doi:10.1007/s00701-013-1759-0
Behrens, T.E., Berg, H.J., Jbabdi, S., Rushworth, M.F., & Woolrich, M.W. (2007). Probabilistic diffusion tractography with multiple fibre orientations: What can we gain? *Neuroimage, 34*(1), 144-155. doi:10.1016/j.neuroimage.2006.09.018
Bello, L., Gallucci, M., Fava, M., Carrabba, G., Giussani, C., Acerbi, F., Baratta, P., Songa, V., Conte, V., Branca, V., Stocchetti, N., Papagno, C., & Gaini, S.M. (2007). Intraoperative subcortical language tract mapping guides surgical removal of gliomas involving speech areas. *Neurosurgery, 60*(1), 67-80; discussion 80-62. doi:10.1227/01.NEU.0000249206.58601.DE
Bello, L., Gambini, A., Castellano, A., Carrabba, G., Acerbi, F., Fava, E., Giussani, C., Cadioli, M., Blasi, V., Casarotti, A., Papagno, C., Gupta, A.K., Gaini, S., Scotti, G., & Falini, A. (2008). Motor and language DTI Fiber Tracking combined with intraoperative subcortical mapping for surgical removal of gliomas. *Neuroimage, 39*(1), 369-382. doi:10.1016/j.neuroimage.2007.08.031
Benninghoff, A., Drenckhahn, D., Waschke, J., Asan, E., & Benninghoff-Drenckhahn. (2011). *Taschenbuch Anatomie* (Fischer, E.U. Ed. 1 ed.). Munich.
Benzagmout, M., Gatignol, P., & Duffau, H. (2007). Resection of World Health Organization Grade II gliomas involving Broca's area: methodological and functional considerations. *Neurosurgery, 61*(4), 741-752; discussion 752-743. doi:10.1227/01.NEU.0000298902.69473.77
Beppu, T., Inoue, T., Shibata, Y., Kurose, A., Arai, H., Ogasawara, K., Ogawa, A., Nakamura, S., & Kabasawa, H. (2003). Measurement of fractional anisotropy using diffusion tensor MRI in supratentorial astrocytic tumors. *J Neurooncol, 63*(2), 109-116.
Berger, M.S., Deliganis, A.V., Dobbins, J., & Keles, G.E. (1994). The effect of extent of resection on recurrence in patients with low grade cerebral hemisphere gliomas. *Cancer, 74*(6), 1784-1791. doi:10.1002/1097-0142(19940915)74:6<1784::aid-cncr2820740622>3.0.co;2-d

Berlim, M.T., Van den Eynde, F., & Daskalakis, Z.J. (2013). A systematic review and meta-analysis on the efficacy and acceptability of bilateral repetitive transcranial magnetic stimulation (rTMS) for treating major depression. *Psychol Med, 43*(11), 2245-2254. doi:10.1017/S0033291712002802

Berman, J.I., Berger, M.S., Mukherjee, P., & Henry, R.G. (2004). Diffusion-tensor imaging-guided tracking of fibers of the pyramidal tract combined with intraoperative cortical stimulation mapping in patients with gliomas. *J Neurosurg, 101*(1), 66-72. doi:10.3171/jns.2004.101.1.0066

Berman, J.I., Berger, M.S., Chung, S.W., Nagarajan, S.S., & Henry, R.G. (2007). Accuracy of diffusion tensor magnetic resonance imaging tractography assessed using intraoperative subcortical stimulation mapping and magnetic source imaging. *J Neurosurg, 107*(3), 488-494. doi:10.3171/JNS-07/09/0488

Berman, J.I., Chung, S., Mukherjee, P., Hess, C.P., Han, E.T., & Henry, R.G. (2008). Probabilistic streamline q-ball tractography using the residual bootstrap. *Neuroimage, 39*(1), 215-222. doi:10.1016/j.neuroimage.2007.08.021

Bernal, B., & Ardila, A. (2009). The role of the arcuate fasciculus in conduction aphasia. *Brain, 132*(Pt 9), 2309-2316. doi:10.1093/brain/awp206

Bestmann, S. (2008). The physiological basis of transcranial magnetic stimulation. *Trends Cogn Sci, 12*(3), 81-83. doi:10.1016/j.tics.2007.12.002

Binder, J.R., Swanson, S.J., Hammeke, T.A., Morris, G.L., Mueller, W.M., Fischer, M., Benbadis, S., Frost, J.A., Rao, S.M., & Haughton, V.M. (1996). Determination of language dominance using functional MRI: a comparison with the Wada test. *Neurology, 46*(4), 978-984.

Binder, J.R., Desai, R.H., Graves, W.W., & Conant, L.L. (2009). Where is the semantic system? A critical review and meta-analysis of 120 functional neuroimaging studies. *Cereb Cortex, 19*(12), 2767-2796. doi:10.1093/cercor/bhp055

Boatman, D. (2004). Cortical bases of speech perception: evidence from functional lesion studies. *Cognition, 92*(1-2), 47-65. doi:10.1016/j.cognition.2003.09.010

Bohland, J.W., Bullock, D., & Guenther, F.H. (2010). Neural representations and mechanisms for the performance of simple speech sequences. *J Cogn Neurosci, 22*(7), 1504-1529. doi:10.1162/jocn.2009.21306

Boroojerdi, B., Foltys, H., Krings, T., Spetzger, U., Thron, A., & Topper, R. (1999). Localization of the motor hand area using transcranial magnetic stimulation and functional magnetic resonance imaging. *Clin Neurophysiol, 110*(4), 699-704. doi:10.1016/s1388-2457(98)00027-3

Brasil-Neto, J.P., Cohen, L.G., Panizza, M., Nilsson, J., Roth, B.J., & Hallett, M. (1992). Optimal focal transcranial magnetic activation of the human motor cortex: effects of coil orientation, shape of the induced current pulse, and stimulus intensity. *J Clin Neurophysiol, 9*(1), 132-136.

Brennan, J., & Pylkkanen, L. (2012). The time-course and spatial distribution of brain activity associated with sentence processing. *Neuroimage, 60*(2), 1139-1148. doi:10.1016/j.neuroimage.2012.01.030

Broca, P.P. (1861). Text N°1. *Bulletin de la société française d'anthropologie., Bd. 2,* 235-238.

Brodmann, K. (1925). *Vergleichende Lokalisationslehre der Grosshirnrinde. In ihren Principien dargestellt auf Grund des Zellenbaues.* Leipzig: Johann Ambrosius Barth Verlag.

Buckner, R.L., Raichle, M.E., & Petersen, S.E. (1995). Dissociation of human prefrontal cortical areas across different speech production tasks and gender groups. *J Neurophysiol, 74*(5), 2163-2173. doi:10.1152/jn.1995.74.5.2163

Burgel, U., Madler, B., Honey, C.R., Thron, A., Gilsbach, J., & Coenen, V.A. (2009). Fiber tracking with distinct software tools results in a clear diversity in anatomical fiber tract portrayal. *Cent Eur Neurosurg, 70*(1), 27-35. doi:10.1055/s-0028-1087212

Capelle, L., Fontaine, D., Mandonnet, E., Taillandier, L., Golmard, J.L., Bauchet, L., Pallud, J., Peruzzi, P., Baron, M.H., Kujas, M., Guyotat, J., Guillevin, R., Frenay, M., Taillibert, S., Colin, P., Rigau, V., Vandenbos, F., Pinelli, C., Duffau, H., & French Reseau d'Etude des, G. (2013). Spontaneous and therapeutic prognostic factors in adult hemispheric World Health

Organization Grade II gliomas: a series of 1097 cases: clinical article. *J Neurosurg, 118*(6), 1157-1168. doi:10.3171/2013.1.JNS121
Catani, M., Howard, R.J., Pajevic, S., & Jones, D.K. (2002). Virtual in vivo interactive dissection of white matter fasciculi in the human brain. *Neuroimage, 17*(1), 77-94.
Catani, M., Jones, D.K., & ffytche, D.H. (2005). Perisylvian language networks of the human brain. *Ann Neurol, 57*(1), 8-16. doi:10.1002/ana.20319
Catani, M., & Thiebaut de Schotten, M. (2008). A diffusion tensor imaging tractography atlas for virtual in vivo dissections. *Cortex, 44*(8), 1105-1132. doi:10.1016/j.cortex.2008.05.004
Cattaneo, L. (2013). Language. *Handb Clin Neurol, 116*, 681-691. doi:10.1016/B978-0-444-53497-2.00054-1
Caulo, M., Briganti, C., Mattei, P.A., Perfetti, B., Ferretti, A., Romani, G.L., Tartaro, A., & Colosimo, C. (2007). New morphologic variants of the hand motor cortex as seen with MR imaging in a large study population. *AJNR Am J Neuroradiol, 28*(8), 1480-1485. doi:10.3174/ajnr.A0597
Chacko, A.G., Thomas, S.G., Babu, K.S., Daniel, R.T., Chacko, G., Prabhu, K., Cherian, V., & Korula, G. (2013). Awake craniotomy and electrophysiological mapping for eloquent area tumours. *Clin Neurol Neurosurg, 115*(3), 329-334. doi:10.1016/j.clineuro.2012.10.022
Chang, E.F., Clark, A., Smith, J.S., Polley, M.Y., Chang, S.M., Barbaro, N.M., Parsa, A.T., McDermott, M.W., & Berger, M.S. (2011). Functional mapping-guided resection of low-grade gliomas in eloquent areas of the brain: improvement of long-term survival. Clinical article. *J Neurosurg, 114*(3), 566-573. doi:10.3171/2010.6.JNS091246
Chang, E.F., Raygor, K.P., & Berger, M.S. (2015). Contemporary model of language organization: an overview for neurosurgeons. *J Neurosurg, 122*(2), 250-261. doi:10.3171/2014.10.JNS132647
Chenevert, T.L., Brunberg, J.A., & Pipe, J.G. (1990). Anisotropic diffusion in human white matter: demonstration with MR techniques in vivo. *Radiology, 177*(2), 401-405. doi:10.1148/radiology.177.2.2217776
Chokroverty, S., Hening, W., Wright, D., Walczak, T., Goldberg, J., Burger, R., Belsh, J., Patel, B., Flynn, D., Shah, S., & et al. (1995). Magnetic brain stimulation: safety studies. *Electroencephalogr Clin Neurophysiol, 97*(1), 36-42.
Claus, E.B., Horlacher, A., Hsu, L., Schwartz, R.B., Dello-Iacono, D., Talos, F., Jolesz, F.A., & Black, P.M. (2005). Survival rates in patients with low-grade glioma after intraoperative magnetic resonance image guidance. *Cancer, 103*(6), 1227-1233. doi:10.1002/cncr.20867
Cloutman, L.L. (2013). Interaction between dorsal and ventral processing streams: where, when and how? *Brain Lang, 127*(2), 251-263. doi:10.1016/j.bandl.2012.08.003
Cohen, J. (2013). *Statistical Power Analysis for the Behavioral Sciences* (2nd ed. ed.). Hoboken: Taylor and Francis.
Conti, A., Raffa, G., Granata, F., Rizzo, V., Germano, A., & Tomasello, F. (2014). Navigated transcranial magnetic stimulation for "somatotopic" tractography of the corticospinal tract. *Neurosurgery, 10 Suppl 4*, 542-554; discussion 554. doi:10.1227/NEU.0000000000000502
Conturo, T.E., Lori, N.F., Cull, T.S., Akbudak, E., Snyder, A.Z., Shimony, J.S., McKinstry, R.C., Burton, H., & Raichle, M.E. (1999). Tracking neuronal fiber pathways in the living human brain. *Proc Natl Acad Sci U S A, 96*(18), 10422-10427.
Corina, D.P., Gibson, E.K., Martin, R., Poliakov, A., Brinkley, J., & Ojemann, G.A. (2005). Dissociation of action and object naming: evidence from cortical stimulation mapping. *Hum Brain Mapp, 24*(1), 1-10. doi:10.1002/hbm.20063
Corina, D.P., Loudermilk, B.C., Detwiler, L., Martin, R.F., Brinkley, J.F., & Ojemann, G. (2010). Analysis of naming errors during cortical stimulation mapping: implications for models of language representation. *Brain Lang, 115*(2), 101-112. doi:10.1016/j.bandl.2010.04.001
Correia, M.M., Carpenter, T.A., & Williams, G.B. (2009). Looking for the optimal DTI acquisition scheme given a maximum scan time: are more b-values a waste of time? *Magn Reson Imaging, 27*(2), 163-175. doi:10.1016/j.mri.2008.06.011
Counter, S.A., & Borg, E. (1992). Analysis of the coil generated impulse noise in extracranial magnetic stimulation. *Electroencephalogr Clin Neurophysiol, 85*(4), 280-288.

Cross, N.M., Hoff, M.N., & Kanal, K.M. (2018). Avoiding MRI-Related Accidents: A Practical Approach to Implementing MR Safety. *J Am Coll Radiol, 15*(12), 1738-1744. doi:10.1016/j.jacr.2018.06.022

Cykowski, M.D., Coulon, O., Kochunov, P.V., Amunts, K., Lancaster, J.L., Laird, A.R., Glahn, D.C., & Fox, P.T. (2008). The central sulcus: an observer-independent characterization of sulcal landmarks and depth asymmetry. *Cereb Cortex, 18*(9), 1999-2009. doi:10.1093/cercor/bhm224

Damasio, A.R., & Tranel, D. (1993). Nouns and verbs are retrieved with differently distributed neural systems. *Proc Natl Acad Sci U S A, 90*(11), 4957-4960. doi:10.1073/pnas.90.11.4957

Daniele, A., Giustolisi, L., Silveri, M.C., Colosimo, C., & Gainotti, G. (1994). Evidence for a possible neuroanatomical basis for lexical processing of nouns and verbs. *Neuropsychologia, 32*(11), 1325-1341.

Danner, N., Kononen, M., Saisanen, L., Laitinen, R., Mervaala, E., & Julkunen, P. (2012). Effect of individual anatomy on resting motor threshold-computed electric field as a measure of cortical excitability. *J Neurosci Methods, 203*(2), 298-304. doi:10.1016/j.jneumeth.2011.10.004

Day, B.L., Thompson, P.D., Dick, J.P., Nakashima, K., & Marsden, C.D. (1987). Different sites of action of electrical and magnetic stimulation of the human brain. *Neurosci Lett, 75*(1), 101-106.

De Angelis, L.M. (2001). Brain tumors. *N Engl J Med, 344*(2), 114-123. doi:10.1056/NEJM200101113440207

De Figueiredo, E.H., Borgonovi, A.F., & Doring, T.M. (2011). Basic concepts of MR imaging, diffusion MR imaging, and diffusion tensor imaging. *Magn Reson Imaging Clin N Am, 19*(1), 1-22. doi:10.1016/j.mric.2010.10.005

De Leon, J., Gottesman, R.F., Kleinman, J.T., Newhart, M., Davis, C., Heidler-Gary, J., Lee, A., & Hillis, A.E. (2007). Neural regions essential for distinct cognitive processes underlying picture naming. *Brain, 130*(Pt 5), 1408-1422. doi:10.1093/brain/awm011

De Witt Hamer, P.C., Robles, S.G., Zwinderman, A.H., Duffau, H., & Berger, M.S. (2012). Impact of intraoperative stimulation brain mapping on glioma surgery outcome: a meta-analysis. *J Clin Oncol, 30*(20), 2559-2565. doi:10.1200/JCO.2011.38.4818

Dellani, P.R., Glaser, M., Wille, P.R., Vucurevic, G., Stadie, A., Bauermann, T., Tropine, A., Perneczky, A., von Wangenheim, A., & Stoeter, P. (2007). White matter fiber tracking computation based on diffusion tensor imaging for clinical applications. *J Digit Imaging, 20*(1), 88-97. doi:10.1007/s10278-006-0773-7

Deng, Z.D., Lisanby, S.H., & Peterchev, A.V. (2013). Electric field depth-focality tradeoff in transcranial magnetic stimulation: simulation comparison of 50 coil designs. *Brain Stimul, 6*(1), 1-13. doi:10.1016/j.brs.2012.02.005

Deras, P., Moulinie, G., Maldonado, I.L., Moritz-Gasser, S., Duffau, H., & Bertram, L. (2012). Intermittent general anesthesia with controlled ventilation for asleep-awake-asleep brain surgery: a prospective series of 140 gliomas in eloquent areas. *Neurosurgery, 71*(4), 764-771. doi:10.1227/NEU.0b013e3182647ab8

Desmurget, M., Bonnetblanc, F., & Duffau, H. (2007). Contrasting acute and slow-growing lesions: a new door to brain plasticity. *Brain, 130*(Pt 4), 898-914. doi:10.1093/brain/awl300

Devlin, J.T., & Watkins, K.E. (2007). Stimulating language: insights from TMS. *Brain, 130*(Pt 3), 610-622. doi:10.1093/brain/awl331

Draganski, B., Gaser, C., Kempermann, G., Kuhn, H.G., Winkler, J., Buchel, C., & May, A. (2006). Temporal and spatial dynamics of brain structure changes during extensive learning. *J Neurosci, 26*(23), 6314-6317. doi:10.1523/JNEUROSCI.4628-05.2006

Dronkers, N.F. (1996). A new brain region for coordinating speech articulation. *Nature, 384*(6605), 159-161. doi:10.1038/384159a0

Du Boisgueheneuc, F., Levy, R., Volle, E., Seassau, M., Duffau, H., Kinkingnehun, S., Samson, Y., Zhang, S., & Dubois, B. (2006). Functions of the left superior frontal gyrus in humans: a lesion study. *Brain, 129*(Pt 12), 3315-3328. doi:10.1093/brain/awl244

Duffau, H., Capelle, L., Sichez, N., Denvil, D., Lopes, M., Sichez, J.P., Bitar, A., & Fohanno, D. (2002). Intraoperative mapping of the subcortical language pathways using direct

stimulations. An anatomo-functional study. *Brain, 125*(Pt 1), 199-214. doi:10.1093/brain/awf016
Duffau, H. (2004). [Peroperative functional mapping using direct electrical stimulations. Methodological considerations]. *Neurochirurgie, 50*(4), 474-483. doi:10.1016/s0028-3770(04)98328-2
Duffau, H. (2005). Lessons from brain mapping in surgery for low-grade glioma: insights into associations between tumour and brain plasticity. *Lancet Neurol, 4*(8), 476-486. doi:10.1016/S1474-4422(05)70140-X
Duffau, H., Lopes, M., Arthuis, F., Bitar, A., Sichez, J.P., Van Effenterre, R., & Capelle, L. (2005). Contribution of intraoperative electrical stimulations in surgery of low grade gliomas: a comparative study between two series without (1985-96) and with (1996-2003) functional mapping in the same institution. *J Neurol Neurosurg Psychiatry, 76*(6), 845-851. doi:10.1136/jnnp.2004.048520
Duffau, H. (2006). New concepts in surgery of WHO grade II gliomas: functional brain mapping, connectionism and plasticity--a review. *J Neurooncol, 79*(1), 77-115. doi:10.1007/s11060-005-9109-6
Duffau, H. (2008). The anatomo-functional connectivity of language revisited. New insights provided by electrostimulation and tractography. *Neuropsychologia, 46*(4), 927-934. doi:10.1016/j.neuropsychologia.2007.10.025
Duffau, H., Peggy Gatignol, S.T., Mandonnet, E., Capelle, L., & Taillandier, L. (2008). Intraoperative subcortical stimulation mapping of language pathways in a consecutive series of 115 patients with Grade II glioma in the left dominant hemisphere. *J Neurosurg, 109*(3), 461-471. doi:10.3171/JNS/2008/109/9/0461
Duffau, H. (2013). The reliability of asleep-awake-asleep protocol for intraoperative functional mapping and cognitive monitoring in glioma surgery. *Acta Neurochir (Wien), 155*(10), 1803-1804. doi:10.1007/s00701-013-1807-9
Duffau, H. (2014a). The dangers of magnetic resonance imaging diffusion tensor tractography in brain surgery. *World Neurosurg, 81*(1), 56-58. doi:10.1016/j.wneu.2013.01.116
Duffau, H. (2014b). Diffusion tensor imaging is a research and educational tool, but not yet a clinical tool. *World Neurosurg, 82*(1-2), e43-45. doi:10.1016/j.wneu.2013.08.054
Duffau, H. (2014c). The huge plastic potential of adult brain and the role of connectomics: new insights provided by serial mappings in glioma surgery. *Cortex, 58*, 325-337. doi:10.1016/j.cortex.2013.08.005
Duffau, H., Moritz-Gasser, S., & Mandonnet, E. (2014). A re-examination of neural basis of language processing: proposal of a dynamic hodotopical model from data provided by brain stimulation mapping during picture naming. *Brain Lang, 131*, 1-10. doi:10.1016/j.bandl.2013.05.011
Duffau, H., & Taillandier, L. (2015). New concepts in the management of diffuse low-grade glioma: Proposal of a multistage and individualized therapeutic approach. *Neuro Oncol, 17*(3), 332-342. doi:10.1093/neuonc/nou153
Edwards, E., Nagarajan, S.S., Dalal, S.S., Canolty, R.T., Kirsch, H.E., Barbaro, N.M., & Knight, R.T. (2010). Spatiotemporal imaging of cortical activation during verb generation and picture naming. *Neuroimage, 50*(1), 291-301. doi:10.1016/j.neuroimage.2009.12.035
Eldaief, M.C., Press, D.Z., & Pascual-Leone, A. (2013). Transcranial magnetic stimulation in neurology: A review of established and prospective applications. *Neurol Clin Pract, 3*(6), 519-526. doi:10.1212/01.CPJ.0000436213.11132.8e
Epstein, C.M., Lah, J.J., Meador, K., Weissman, J.D., Gaitan, L.E., & Dihenia, B. (1996). Optimum stimulus parameters for lateralized suppression of speech with magnetic brain stimulation. *Neurology, 47*(6), 1590-1593.
Farquharson, S., Tournier, J.D., Calamante, F., Fabinyi, G., Schneider-Kolsky, M., Jackson, G.D., & Connelly, A. (2013). White matter fiber tractography: why we need to move beyond DTI. *J Neurosurg, 118*(6), 1367-1377. doi:10.3171/2013.2.JNS121294
Farrell, J.A., Landman, B.A., Jones, C.K., Smith, S.A., Prince, J.L., van Zijl, P.C., & Mori, S. (2007). Effects of signal-to-noise ratio on the accuracy and reproducibility of diffusion tensor imaging-derived fractional anisotropy, mean diffusivity, and principal eigenvector measurements at 1.5 T. *J Magn Reson Imaging, 26*(3), 756-767. doi:10.1002/jmri.21053

Findlay, A.M., Ambrose, J.B., Cahn-Weiner, D.A., Houde, J.F., Honma, S., Hinkley, L.B., Berger, M.S., Nagarajan, S.S., & Kirsch, H.E. (2012). Dynamics of hemispheric dominance for language assessed by magnetoencephalographic imaging. *Ann Neurol, 71*(5), 668-686. doi:10.1002/ana.23530

Forster, M.T., Limbart, M., Seifert, V., & Senft, C. (2014). Test-retest reliability of navigated transcranial magnetic stimulation of the motor cortex. *Neurosurgery, 10 Suppl 1*, 51-55; discussion 55-56. doi:10.1227/NEU.0000000000000075

Frank, L.R. (2001). Anisotropy in high angular resolution diffusion-weighted MRI. *Magn Reson Med, 45*(6), 935-939.

Fregni, F., Otachi, P.T., Do Valle, A., Boggio, P.S., Thut, G., Rigonatti, S.P., Pascual-Leone, A., & Valente, K.D. (2006). A randomized clinical trial of repetitive transcranial magnetic stimulation in patients with refractory epilepsy. *Ann Neurol, 60*(4), 447-455. doi:10.1002/ana.20950

Freigang, S., Fresnoza, S., Mahdy Ali, K., Zaar, K., Jehna, M., Reishofer, G., Rammel, K., Studencnik, F., Ischebeck, A., & von Campe, G. (2020). Impact of Priming on Effectiveness of TMS in Detecting Language-eloquent Brain Areas in Tumor Patients. *J Neurol Surg A Cent Eur Neurosurg, 81*(2), 111-129. doi:10.1055/s-0039-1698382

Frey, D., Strack, V., Wiener, E., Jussen, D., Vajkoczy, P., & Picht, T. (2012). A new approach for corticospinal tract reconstruction based on navigated transcranial stimulation and standardized fractional anisotropy values. *Neuroimage, 62*(3), 1600-1609. doi:10.1016/j.neuroimage.2012.05.059

Frost, J.A., Binder, J.R., Springer, J.A., Hammeke, T.A., Bellgowan, P.S., Rao, S.M., & Cox, R.W. (1999). Language processing is strongly left lateralized in both sexes. Evidence from functional MRI. *Brain, 122 (Pt 2)*, 199-208. doi:10.1093/brain/122.2.199

Giglhuber, K., Maurer, S., Zimmer, C., Meyer, B., & Krieg, S.M. (2017). Evoking visual neglect-like deficits in healthy volunteers - an investigation by repetitive navigated transcranial magnetic stimulation. *Brain Imaging Behav, 11*(1), 17-29. doi:10.1007/s11682-016-9506-9

Gil-Robles, S., & Duffau, H. (2010). Surgical management of World Health Organization Grade II gliomas in eloquent areas: the necessity of preserving a margin around functional structures. *Neurosurg Focus, 28*(2), E8. doi:10.3171/2009.12.FOCUS09236

Giussani, C., Roux, F.E., Ojemann, J., Sganzerla, E.P., Pirillo, D., & Papagno, C. (2010). Is preoperative functional magnetic resonance imaging reliable for language areas mapping in brain tumor surgery? Review of language functional magnetic resonance imaging and direct cortical stimulation correlation studies. *Neurosurgery, 66*(1), 113-120. doi:10.1227/01.NEU.0000360392.15450.C9

Gomez-Tames, J., Hamasaka, A., Laakso, I., Hirata, A., & Ugawa, Y. (2018). Atlas of optimal coil orientation and position for TMS: A computational study. *Brain Stimul, 11*(4), 839-848. doi:10.1016/j.brs.2018.04.011

Gonen, T., Gazit, T., Korn, A., Kirschner, A., Perry, D., Hendler, T., & Ram, Z. (2017). Intra-operative multi-site stimulation: Expanding methodology for cortical brain mapping of language functions. *PLoS One, 12*(7), e0180740. doi:10.1371/journal.pone.0180740

Gorno-Tempini, M.L., & Price, C.J. (2001). Identification of famous faces and buildings: a functional neuroimaging study of semantically unique items. *Brain, 124*(Pt 10), 2087-2097.

Gow, D.W., Jr. (2012). The cortical organization of lexical knowledge: a dual lexicon model of spoken language processing. *Brain Lang, 121*(3), 273-288. doi:10.1016/j.bandl.2012.03.005

Graves, W.W., Grabowski, T.J., Mehta, S., & Gupta, P. (2008). The left posterior superior temporal gyrus participates specifically in accessing lexical phonology. *J Cogn Neurosci, 20*(9), 1698-1710. doi:10.1162/jocn.2008.20113

Graves, W.W., Desai, R., Humphries, C., Seidenberg, M.S., & Binder, J.R. (2010). Neural systems for reading aloud: a multiparametric approach. *Cereb Cortex, 20*(8), 1799-1815. doi:10.1093/cercor/bhp245

Greiner, M., Pfeiffer, D., & Smith, R.D. (2000). Principles and practical application of the receiver-operating characteristic analysis for diagnostic tests. *Prev Vet Med, 45*(1-2), 23-41. doi:10.1016/s0167-5877(00)00115-x

Grover, V.P., Tognarelli, J.M., Crossey, M.M., Cox, I.J., Taylor-Robinson, S.D., & McPhail, M.J. (2015). Magnetic Resonance Imaging: Principles and Techniques: Lessons for Clinicians. *J Clin Exp Hepatol, 5*(3), 246-255. doi:10.1016/j.jceh.2015.08.001

Gugino, L.D., Romero, J.R., Aglio, L., Titone, D., Ramirez, M., Pascual-Leone, A., Grimson, E., Weisenfeld, N., Kikinis, R., & Shenton, M.E. (2001). Transcranial magnetic stimulation coregistered with MRI: a comparison of a guided versus blind stimulation technique and its effect on evoked compound muscle action potentials. *Clin Neurophysiol, 112*(10), 1781-1792.

Guo, A.C., Cummings, T.J., Dash, R.C., & Provenzale, J.M. (2002). Lymphomas and high-grade astrocytomas: comparison of water diffusibility and histologic characteristics. *Radiology, 224*(1), 177-183. doi:10.1148/radiol.2241010637

Gupta, A., & Dwivedi, T. (2017). A Simplified Overview of World Health Organization Classification Update of Central Nervous System Tumors 2016. *J Neurosci Rural Pract, 8*(4), 629-641. doi:10.4103/jnrp.jnrp_168_17

Haglund, M.M., Berger, M.S., Shamseldin, M., Lettich, E., & Ojemann, G.A. (1994). Cortical localization of temporal lobe language sites in patients with gliomas. *Neurosurgery, 34*(4), 567-576; discussion 576.

Hallett, M. (2000). Transcranial magnetic stimulation and the human brain. *Nature, 406*(6792), 147-150. doi:10.1038/35018000

Hallett, M. (2007). Transcranial magnetic stimulation: a primer. *Neuron, 55*(2), 187-199. doi:10.1016/j.neuron.2007.06.026

Hamada, M., Hanajima, R., Terao, Y., Arai, N., Furubayashi, T., Inomata-Terada, S., Yugeta, A., Matsumoto, H., Shirota, Y., & Ugawa, Y. (2007). Quadro-pulse stimulation is more effective than paired-pulse stimulation for plasticity induction of the human motor cortex. *Clin Neurophysiol, 118*(12), 2672-2682. doi:10.1016/j.clinph.2007.09.062

Hana, A., Husch, A., Gunness, V.R., Berthold, C., Hana, A., Dooms, G., Boecher Schwarz, H., & Hertel, F. (2014). DTI of the visual pathway - white matter tracts and cerebral lesions. *J Vis Exp*(90). doi:10.3791/51946

Hardavella, G., & Ianovici, N. (2005). Current trends in minimally invasive neurosurgery: neuro-endoscopy. *Rev Med Chir Soc Med Nat Iasi, 109*(3), 528-531.

Harvey, D.Y., Wei, T., Ellmore, T.M., Hamilton, A.C., & Schnur, T.T. (2013). Neuropsychological evidence for the functional role of the uncinate fasciculus in semantic control. *Neuropsychologia, 51*(5), 789-801. doi:10.1016/j.neuropsychologia.2013.01.028

Hastreiter, P., Rezk-Salama, C., Soza, G., Bauer, M., Greiner, G., Fahlbusch, R., Ganslandt, O., & Nimsky, C. (2004). Strategies for brain shift evaluation. *Med Image Anal, 8*(4), 447-464. doi:10.1016/j.media.2004.02.001

Hauck, T., Tanigawa, N., Probst, M., Wohlschlaeger, A., Ille, S., Sollmann, N., Maurer, S., Zimmer, C., Ringel, F., Meyer, B., & Krieg, S.M. (2015). Task type affects location of language-positive cortical regions by repetitive navigated transcranial magnetic stimulation mapping. *PLoS One, 10*(4), e0125298. doi:10.1371/journal.pone.0125298

Hendrix, P., Senger, S., Simgen, A., Griessenauer, C.J., & Oertel, J. (2017). Preoperative rTMS Language Mapping in Speech-Eloquent Brain Lesions Resected Under General Anesthesia: A Pair-Matched Cohort Study. *World Neurosurg, 100*, 425-433. doi:10.1016/j.wneu.2017.01.041

Henkes, H., Berg-Dammer, E., & Kühne, D. (2006). Arteriovenöse Malformationen. In Berlit, P. (Ed.), *Klinische Neurologie* (2. Auflage ed., pp. 1040 ff.). Heidelberg: Springer Medizin.

Henning Stieglitz, L., Seidel, K., Wiest, R., Beck, J., & Raabe, A. (2012). Localization of primary language areas by arcuate fascicle fiber tracking. *Neurosurgery, 70*(1), 56-64; discussion 64-55. doi:10.1227/NEU.0b013e31822cb882

Henry, R.G., Berman, J.I., Nagarajan, S.S., Mukherjee, P., & Berger, M.S. (2004). Subcortical pathways serving cortical language sites: initial experience with diffusion tensor imaging fiber tracking combined with intraoperative language mapping. *Neuroimage, 21*(2), 616-622. doi:10.1016/j.neuroimage.2003.09.047

Henseler, I., Madebach, A., Kotz, S.A., & Jescheniak, J.D. (2014). Modulating brain mechanisms resolving lexico-semantic Interference during word production: A transcranial

direct current stimulation study. *J Cogn Neurosci, 26*(7), 1403-1417. doi:10.1162/jocn_a_00572
Herholz, K., Reulen, H.J., von Stockhausen, H.M., Thiel, A., Ilmberger, J., Kessler, J., Eisner, W., Yousry, T.A., & Heiss, W.D. (1997). Preoperative activation and intraoperative stimulation of language-related areas in patients with glioma. *Neurosurgery, 41*(6), 1253-1260; discussion 1260-1252.
Hernandez-Pavon, J.C., Makela, N., Lehtinen, H., Lioumis, P., & Makela, J.P. (2014). Effects of navigated TMS on object and action naming. *Front Hum Neurosci, 8*, 660. doi:10.3389/fnhum.2014.00660
Hervey-Jumper, S.L., Li, J., Lau, D., Molinaro, A.M., Perry, D.W., Meng, L., & Berger, M.S. (2015). Awake craniotomy to maximize glioma resection: methods and technical nuances over a 27-year period. *J Neurosurg, 123*(2), 325-339. doi:10.3171/2014.10.JNS141520
Hess, C.P., Mukherjee, P., Han, E.T., Xu, D., & Vigneron, D.B. (2006). Q-ball reconstruction of multimodal fiber orientations using the spherical harmonic basis. *Magn Reson Med, 56*(1), 104-117. doi:10.1002/mrm.20931
Hickok, G., & Poeppel, D. (2004). Dorsal and ventral streams: a framework for understanding aspects of the functional anatomy of language. *Cognition, 92*(1-2), 67-99. doi:10.1016/j.cognition.2003.10.011
Hickok, G. (2009). The functional neuroanatomy of language. *Phys Life Rev, 6*(3), 121-143. doi:10.1016/j.plrev.2009.06.001
Hickok, G. (2012). Computational neuroanatomy of speech production. *Nat Rev Neurosci, 13*(2), 135-145. doi:10.1038/nrn3158
Hirnstein, M., Westerhausen, R., Korsnes, M.S., & Hugdahl, K. (2013). Sex differences in language asymmetry are age-dependent and small: a large-scale, consonant-vowel dichotic listening study with behavioral and fMRI data. *Cortex, 49*(7), 1910-1921. doi:10.1016/j.cortex.2012.08.002
Hoogendam, J.M., Ramakers, G.M., & Di Lazzaro, V. (2010). Physiology of repetitive transcranial magnetic stimulation of the human brain. *Brain Stimul, 3*(2), 95-118. doi:10.1016/j.brs.2009.10.005
Houde, J.F., & Nagarajan, S.S. (2011). Speech production as state feedback control. *Front Hum Neurosci, 5*, 82. doi:10.3389/fnhum.2011.00082
Ille, S., Sollmann, N., Hauck, T., Maurer, S., Tanigawa, N., Obermueller, T., Negwer, C., Droese, D., Boeckh-Behrens, T., Meyer, B., Ringel, F., & Krieg, S.M. (2015a). Impairment of preoperative language mapping by lesion location: a functional magnetic resonance imaging, navigated transcranial magnetic stimulation, and direct cortical stimulation study. *J Neurosurg, 123*(2), 314-324. doi:10.3171/2014.10.JNS141582
Ille, S., Sollmann, N., Hauck, T., Maurer, S., Tanigawa, N., Obermueller, T., Negwer, C., Droese, D., Zimmer, C., Meyer, B., Ringel, F., & Krieg, S.M. (2015b). Combined noninvasive language mapping by navigated transcranial magnetic stimulation and functional MRI and its comparison with direct cortical stimulation. *J Neurosurg, 123*(1), 212-225. doi:10.3171/2014.9.JNS14929
Ille, S., Sollmann, N., Butenschoen, V.M., Meyer, B., Ringel, F., & Krieg, S.M. (2016). Resection of highly language-eloquent brain lesions based purely on rTMS language mapping without awake surgery. *Acta Neurochir (Wien), 158*(12), 2265-2275. doi:10.1007/s00701-016-2968-0
Indefrey, P., & Levelt, W.J. (2004). The spatial and temporal signatures of word production components. *Cognition, 92*(1-2), 101-144. doi:10.1016/j.cognition.2002.06.001
Indefrey, P. (2011). The spatial and temporal signatures of word production components: a critical update. *Front Psychol, 2*, 255. doi:10.3389/fpsyg.2011.00255
Jacquemot, C., & Scott, S.K. (2006). What is the relationship between phonological short-term memory and speech processing? *Trends Cogn Sci, 10*(11), 480-486. doi:10.1016/j.tics.2006.09.002
Jakola, A.S., Unsgard, G., Myrmel, K.S., Kloster, R., Torp, S.H., Lindal, S., & Solheim, O. (2012). Low grade gliomas in eloquent locations - implications for surgical strategy, survival and long term quality of life. *PLoS One, 7*(12), e51450. doi:10.1371/journal.pone.0051450

Jancke, L., Staiger, J.F., Schlaug, G., Huang, Y., & Steinmetz, H. (1997). The relationship between corpus callosum size and forebrain volume. *Cereb Cortex, 7*(1), 48-56. doi:10.1093/cercor/7.1.48

Jellison, B.J., Field, A.S., Medow, J., Lazar, M., Salamat, M.S., & Alexander, A.L. (2004). Diffusion tensor imaging of cerebral white matter: a pictorial review of physics, fiber tract anatomy, and tumor imaging patterns. *AJNR Am J Neuroradiol, 25*(3), 356-369.

Jeltema, H.R., Ohlerth, A.K., de Wit, A., Wagemakers, M., Rofes, A., Bastiaanse, R., & Drost, G. (2020). Comparing navigated transcranial magnetic stimulation mapping and "gold standard" direct cortical stimulation mapping in neurosurgery: a systematic review. *Neurosurg Rev*. doi:10.1007/s10143-020-01397-x

Jennum, P., Friberg, L., Fuglsang-Frederiksen, A., & Dam, M. (1994). Speech localization using repetitive transcranial magnetic stimulation. *Neurology, 44*(2), 269-273. doi:10.1212/wnl.44.2.269

Jezzard, P., & Balaban, R.S. (1995). Correction for geometric distortion in echo planar images from B0 field variations. *Magn Reson Med, 34*(1), 65-73.

Jones, D.K. (2004). The effect of gradient sampling schemes on measures derived from diffusion tensor MRI: a Monte Carlo study. *Magn Reson Med, 51*(4), 807-815. doi:10.1002/mrm.20033

Jones, D.K., & Leemans, A. (2011). Diffusion tensor imaging. *Methods Mol Biol, 711*, 127-144. doi:10.1007/978-1-61737-992-5_6

Jung, J., Lavrador, J.P., Patel, S., Giamouriadis, A., Lam, J., Bhangoo, R., Ashkan, K., & Vergani, F. (2019). First United Kingdom Experience of Navigated Transcranial Magnetic Stimulation in Preoperative Mapping of Brain Tumors. *World Neurosurg, 122*, e1578-e1587. doi:10.1016/j.wneu.2018.11.114

Kandler, R. (1990). Safety of transcranial magnetic stimulation. *Lancet, 335*(8687), 469-470.

Kaneko, K., Kawai, S., Fuchigami, Y., Morita, H., & Ofuji, A. (1996). The effect of current direction induced by transcranial magnetic stimulation on the corticospinal excitability in human brain. *Electroencephalogr Clin Neurophysiol, 101*(6), 478-482.

Kansaku, K., Yamaura, A., & Kitazawa, S. (2000). Sex differences in lateralization revealed in the posterior language areas. *Cereb Cortex, 10*(9), 866-872. doi:10.1093/cercor/10.9.866

Kansaku, K., & Kitazawa, S. (2001). Imaging studies on sex differences in the lateralization of language. *Neurosci Res, 41*(4), 333-337.

Kant, I. (1798). *Anthropologie in pragmatischer Hinsicht. Erster Teil. Anthropologische Didaktik*: Fekix Meiner Verlag, Reclam.

Karhu, J., Hannula, H., Laine, J., & Ruohonen, J. (2014). Navigated Transcranial Magnetic Stimulation: Principles and Protocol for Mapping the Motor Cortex. *Rotenberg, Horvath et al. (Hg.) 2014 – Transcranial Magnetic Stimulation, 89*, 337-359. doi:10.1007/978-1-4939-0879-0_16

Keles, G.E., Lamborn, K.R., & Berger, M.S. (2001). Low-grade hemispheric gliomas in adults: a critical review of extent of resection as a factor influencing outcome. *J Neurosurg, 95*(5), 735-745. doi:10.3171/jns.2001.95.5.0735

Kim, B.G., Kim, D.Y., Kim, S.K., Kim, J.M., Baek, S.H., & Moon, I.S. (2014). Comparison of the outcomes of repetitive transcranial magnetic stimulation to the ipsilateral and contralateral auditory cortex in unilateral tinnitus. *Electromagn Biol Med, 33*(3), 211-215. doi:10.3109/15368378.2013.801353

Kim, S.S., McCutcheon, I.E., Suki, D., Weinberg, J.S., Sawaya, R., Lang, F.F., Ferson, D., Heimberger, A.B., DeMonte, F., & Prabhu, S.S. (2009). Awake craniotomy for brain tumors near eloquent cortex: correlation of intraoperative cortical mapping with neurological outcomes in 309 consecutive patients. *Neurosurgery, 64*(5), 836-845; discussion 345-836. doi:10.1227/01.NEU.0000342405.80881.81

Kircher, T.T., Brammer, M., Tous Andreu, N., Williams, S.C., & McGuire, P.K. (2001). Engagement of right temporal cortex during processing of linguistic context. *Neuropsychologia, 39*(8), 798-809.

Klooster, D.C., de Louw, A.J., Aldenkamp, A.P., Besseling, R.M., Mestrom, R.M., Carrette, S., Zinger, S., Bergmans, J.W., Mess, W.H., Vonck, K., Carrette, E., Breuer, L.E., Bernas, A., Tijhuis, A.G., & Boon, P. (2016). Technical aspects of neurostimulation: Focus on equipment,

electric field modeling, and stimulation protocols. *Neurosci Biobehav Rev, 65*, 113-141. doi:10.1016/j.neubiorev.2016.02.016
Knecht, S., Drager, B., Deppe, M., Bobe, L., Lohmann, H., Floel, A., Ringelstein, E.B., & Henningsen, H. (2000). Handedness and hemispheric language dominance in healthy humans. *Brain, 123 Pt 12*, 2512-2518.
Kohn, S.E., & Goodglass, H. (1985). Picture-naming in aphasia. *Brain Lang, 24*(2), 266-283.
Kombos, T., Suess, O., Ciklatekerlio, O., & Brock, M. (2001). Monitoring of intraoperative motor evoked potentials to increase the safety of surgery in and around the motor cortex. *J Neurosurg, 95*(4), 608-614. doi:10.3171/jns.2001.95.4.0608
Komori, T. (2017). The 2016 WHO Classification of Tumours of the Central Nervous System: The Major Points of Revision. *Neurol Med Chir (Tokyo), 57*(7), 301-311. doi:10.2176/nmc.ra.2017-0010
Kosslyn, S.M., Pascual-Leone, A., Felician, O., Camposano, S., Keenan, J.P., Thompson, W.L., Ganis, G., Sukel, K.E., & Alpert, N.M. (1999). The role of area 17 in visual imagery: convergent evidence from PET and rTMS. *Science, 284*(5411), 167-170. doi:10.1126/science.284.5411.167
Krieg, S.M., Buchmann, N.H., Gempt, J., Shiban, E., Meyer, B., & Ringel, F. (2012a). Diffusion tensor imaging fiber tracking using navigated brain stimulation--a feasibility study. *Acta Neurochir (Wien), 154*(3), 555-563. doi:10.1007/s00701-011-1255-3
Krieg, S.M., Shiban, E., Buchmann, N., Gempt, J., Foerschler, A., Meyer, B., & Ringel, F. (2012b). Utility of presurgical navigated transcranial magnetic brain stimulation for the resection of tumors in eloquent motor areas. *J Neurosurg, 116*(5), 994-1001. doi:10.3171/2011.12.JNS111524
Krieg, S.M., Shiban, E., Droese, D., Gempt, J., Buchmann, N., Pape, H., Ryang, Y.M., Meyer, B., & Ringel, F. (2012c). Predictive value and safety of intraoperative neurophysiological monitoring with motor evoked potentials in glioma surgery. *Neurosurgery, 70*(5), 1060-1070; discussion 1070-1061. doi:10.1227/NEU.0b013e31823f5ade
Krieg, S.M., Shiban, E., Buchmann, N., Meyer, B., & Ringel, F. (2013a). Presurgical navigated transcranial magnetic brain stimulation for recurrent gliomas in motor eloquent areas. *Clin Neurophysiol, 124*(3), 522-527. doi:10.1016/j.clinph.2012.08.011
Krieg, S.M., Sollmann, N., Hauck, T., Ille, S., Foerschler, A., Meyer, B., & Ringel, F. (2013b). Functional language shift to the right hemisphere in patients with language-eloquent brain tumors. *PLoS One, 8*(9), e75403. doi:10.1371/journal.pone.0075403
Krieg, S.M., Sollmann, N., Hauck, T., Ille, S., Meyer, B., & Ringel, F. (2014a). Repeated mapping of cortical language sites by preoperative navigated transcranial magnetic stimulation compared to repeated intraoperative DCS mapping in awake craniotomy. *BMC Neurosci, 15*, 20. doi:10.1186/1471-2202-15-20
Krieg, S.M., Tarapore, P.E., Picht, T., Tanigawa, N., Houde, J., Sollmann, N., Meyer, B., Vajkoczy, P., Berger, M.S., Ringel, F., & Nagarajan, S. (2014b). Optimal timing of pulse onset for language mapping with navigated repetitive transcranial magnetic stimulation. *Neuroimage, 100*, 219-236. doi:10.1016/j.neuroimage.2014.06.016
Krieg, S.M., Sollmann, N., Tanigawa, N., Foerschler, A., Meyer, B., & Ringel, F. (2016). Cortical distribution of speech and language errors investigated by visual object naming and navigated transcranial magnetic stimulation. *Brain Struct Funct, 221*(4), 2259-2286. doi:10.1007/s00429-015-1042-7
Krieg, S.M., Lioumis, P., Makela, J.P., Wilenius, J., Karhu, J., Hannula, H., Savolainen, P., Lucas, C.W., Seidel, K., Laakso, A., Islam, M., Vaalto, S., Lehtinen, H., Vitikainen, A.M., Tarapore, P.E., & Picht, T. (2017). Protocol for motor and language mapping by navigated TMS in patients and healthy volunteers; workshop report. *Acta Neurochir (Wien)*. doi:10.1007/s00701-017-3187-z
Krings, T., Chiappa, K.H., Foltys, H., Reinges, M.H., Cosgrove, G.R., & Thron, A. (2001). Introducing navigated transcranial magnetic stimulation as a refined brain mapping methodology. *Neurosurg Rev, 24*(4), 171-179.
Krishnan, C., Santos, L., Peterson, M.D., & Ehinger, M. (2015). Safety of noninvasive brain stimulation in children and adolescents. *Brain Stimul, 8*(1), 76-87. doi:10.1016/j.brs.2014.10.012

Kristensen, B.W., Priesterbach-Ackley, L.P., Petersen, J.K., & Wesseling, P. (2019). Molecular pathology of tumors of the central nervous system. *Ann Oncol, 30*(8), 1265-1278. doi:10.1093/annonc/mdz164

Kuchcinski, G., Mellerio, C., Pallud, J., Dezamis, E., Turc, G., Rigaux-Viode, O., Malherbe, C., Roca, P., Leclerc, X., Varlet, P., Chretien, F., Devaux, B., Meder, J.F., & Oppenheim, C. (2015). Three-tesla functional MR language mapping: comparison with direct cortical stimulation in gliomas. *Neurology, 84*(6), 560-568. doi:10.1212/WNL.0000000000001226

Kuhnt, D., Bauer, M.H., Becker, A., Merhof, D., Zolal, A., Richter, M., Grummich, P., Ganslandt, O., Buchfelder, M., & Nimsky, C. (2012). Intraoperative visualization of fiber tracking based reconstruction of language pathways in glioma surgery. *Neurosurgery, 70*(4), 911-919; discussion 919-920. doi:10.1227/NEU.0b013e318237a807

Kuhnt, D., Bauer, M.H., Sommer, J., Merhof, D., & Nimsky, C. (2013). Optic radiation fiber tractography in glioma patients based on high angular resolution diffusion imaging with compressed sensing compared with diffusion tensor imaging - initial experience. *PLoS One, 8*(7), e70973. doi:10.1371/journal.pone.0070973

Kulynych, J.J., Vladar, K., Jones, D.W., & Weinberger, D.R. (1994). Gender differences in the normal lateralization of the supratemporal cortex: MRI surface-rendering morphometry of Heschl's gyrus and the planum temporale. *Cereb Cortex, 4*(2), 107-118. doi:10.1093/cercor/4.2.107

Laader, A., Beiderwellen, K., Kraff, O., Maderwald, S., Wrede, K., Ladd, M.E., Lauenstein, T.C., Forsting, M., Quick, H.H., Nassenstein, K., & Umutlu, L. (2017). 1.5 versus 3 versus 7 Tesla in abdominal MRI: A comparative study. *PLoS One, 12*(11), e0187528. doi:10.1371/journal.pone.0187528

Laakso, I., Hirata, A., & Ugawa, Y. (2014). Effects of coil orientation on the electric field induced by TMS over the hand motor area. *Phys Med Biol, 59*(1), 203-218. doi:10.1088/0031-9155/59/1/203

Lai, C.Y., Tian, L., & Schisterman, E.F. (2012). Exact confidence interval estimation for the Youden index and its corresponding optimal cut-point. *Comput Stat Data Anal, 56*(5), 1103-1114. doi:10.1016/j.csda.2010.11.023

Lawes, I.N., Barrick, T.R., Murugam, V., Spierings, N., Evans, D.R., Song, M., & Clark, C.A. (2008). Atlas-based segmentation of white matter tracts of the human brain using diffusion tensor tractography and comparison with classical dissection. *Neuroimage, 39*(1), 62-79. doi:10.1016/j.neuroimage.2007.06.041

Lazar, M., Alexander, A.L., Thottakara, P.J., Badie, B., & Field, A.S. (2006). White matter reorganization after surgical resection of brain tumors and vascular malformations. *AJNR Am J Neuroradiol, 27*(6), 1258-1271.

Le Bihan, D., Breton, E., Lallemand, D., Grenier, P., Cabanis, E., & Laval-Jeantet, M. (1986). MR imaging of intravoxel incoherent motions: application to diffusion and perfusion in neurologic disorders. *Radiology, 161*(2), 401-407. doi:10.1148/radiology.161.2.3763909

Le Bihan, D., Turner, R., & Douek, P. (1993). Is water diffusion restricted in human brain white matter? An echo-planar NMR imaging study. *Neuroreport, 4*(7), 887-890.

Le Bihan, D., & Johansen-Berg, H. (2012). Diffusion MRI at 25: exploring brain tissue structure and function. *Neuroimage, 61*(2), 324-341. doi:10.1016/j.neuroimage.2011.11.006

Leclercq, D., Duffau, H., Delmaire, C., Capelle, L., Gatignol, P., Ducros, M., Chiras, J., & Lehericy, S. (2010). Comparison of diffusion tensor imaging tractography of language tracts and intraoperative subcortical stimulations. *J Neurosurg, 112*(3), 503-511. doi:10.3171/2009.8.JNS09558

Leclercq, D., Delmaire, C., de Champfleur, N.M., Chiras, J., & Lehericy, S. (2011). Diffusion tractography: methods, validation and applications in patients with neurosurgical lesions. *Neurosurg Clin N Am, 22*(2), 253-268, ix. doi:10.1016/j.nec.2010.11.004

Lee, C.E., Danielian, L.E., Thomasson, D., & Baker, E.H. (2009). Normal regional fractional anisotropy and apparent diffusion coefficient of the brain measured on a 3 T MR scanner. *Neuroradiology, 51*(1), 3-9. doi:10.1007/s00234-008-0441-3

Lee, E.G., Rastogi, P., Hadimani, R.L., Jiles, D.C., & Camprodon, J.A. (2018). Impact of non-brain anatomy and coil orientation on inter- and intra-subject variability in TMS at midline. *Clin Neurophysiol, 129*(9), 1873-1883. doi:10.1016/j.clinph.2018.04.749

Lehtinen, H., Makela, J.P., Makela, T., Lioumis, P., Metsahonkala, L., Hokkanen, L., Wilenius, J., & Gaily, E. (2018). Language mapping with navigated transcranial magnetic stimulation in pediatric and adult patients undergoing epilepsy surgery: Comparison with extraoperative direct cortical stimulation. *Epilepsia Open, 3*(2), 224-235. doi:10.1002/epi4.12110

Lesser, R.P., Luders, H., Klem, G., Dinner, D.S., Morris, H.H., Hahn, J.F., & Wyllie, E. (1987). Extraoperative cortical functional localization in patients with epilepsy. *J Clin Neurophysiol, 4*(1), 27-53. doi:10.1097/00004691-198701000-00003

Levy, W.J., Amassian, V.E., Schmid, U.D., & Jungreis, C. (1991). Mapping of motor cortex gyral sites non-invasively by transcranial magnetic stimulation in normal subjects and patients. *Electroencephalogr Clin Neurophysiol Suppl, 43*, 51-75.

Lioumis, P., Zhdanov, A., Makela, N., Lehtinen, H., Wilenius, J., Neuvonen, T., Hannula, H., Deletis, V., Picht, T., & Makela, J.P. (2012). A novel approach for documenting naming errors induced by navigated transcranial magnetic stimulation. *J Neurosci Methods, 204*(2), 349-354. doi:10.1016/j.jneumeth.2011.11.003

Liu, Z., Yin, T., & Guan, X. (2003). [A project of magnetic coils newly designed to restrain the negative value of the intensity of magnetic induced electric field]. *Sheng Wu Yi Xue Gong Cheng Xue Za Zhi, 20*(1), 45-48, 59.

Logothetis, N.K., & Wandell, B.A. (2004). Interpreting the BOLD signal. *Annu Rev Physiol, 66*, 735-769. doi:10.1146/annurev.physiol.66.082602.092845

Loo, C.K., McFarquhar, T.F., & Mitchell, P.B. (2008). A review of the safety of repetitive transcranial magnetic stimulation as a clinical treatment for depression. *Int J Neuropsychopharmacol, 11*(1), 131-147. doi:10.1017/S1461145707007717

Louis, D.N., Ohgaki, H., Wiestler, O.D., & Cavenee, W.K. (2016). *WHO Classification of Tumours of the Central Nervous System* (Revised 4th edition ed.). Lyon: International Agency for Research on Cancer.

Lu, S., Ahn, D., Johnson, G., Law, M., Zagzag, D., & Grossman, R.I. (2004). Diffusion-tensor MR imaging of intracranial neoplasia and associated peritumoral edema: introduction of the tumor infiltration index. *Radiology, 232*(1), 221-228. doi:10.1148/radiol.2321030653

Machii, K., Cohen, D., Ramos-Estebanez, C., & Pascual-Leone, A. (2006). Safety of rTMS to non-motor cortical areas in healthy participants and patients. *Clin Neurophysiol, 117*(2), 455-471. doi:10.1016/j.clinph.2005.10.014

Mäkelä, J.P. (2015). Navigated transcranial magnetic stimulation in clinical practice and research. *International Journal of Bioelectromagnetism*.

Makris, N., & Pandya, D.N. (2009). The extreme capsule in humans and rethinking of the language circuitry. *Brain Struct Funct, 213*(3), 343-358. doi:10.1007/s00429-008-0199-8

Makuuchi, M., & Friederici, A.D. (2013). Hierarchical functional connectivity between the core language system and the working memory system. *Cortex, 49*(9), 2416-2423. doi:10.1016/j.cortex.2013.01.007

Maldonado, I.L., Moritz-Gasser, S., de Champfleur, N.M., Bertram, L., Moulinie, G., & Duffau, H. (2011). Surgery for gliomas involving the left inferior parietal lobule: new insights into the functional anatomy provided by stimulation mapping in awake patients. *J Neurosurg, 115*(4), 770-779. doi:10.3171/2011.5.JNS112

Marg, E., & Rudiak, D. (1994). Phosphenes induced by magnetic stimulation over the occipital brain: description and probable site of stimulation. *Optom Vis Sci, 71*(5), 301-311. doi:10.1097/00006324-199405000-00001

Martino, J., Honma, S.M., Findlay, A.M., Guggisberg, A.G., Owen, J.P., Kirsch, H.E., Berger, M.S., & Nagarajan, S.S. (2011). Resting functional connectivity in patients with brain tumors in eloquent areas. *Ann Neurol, 69*(3), 521-532. doi:10.1002/ana.22167

Matsuda, R., Moritz-Gasser, S., Duvaux, S., Fernandez Coello, A., Martinoni, M., & Duffau, H. (2014). The persistent crucial role of the left hemisphere for language in left-handers with a left low grade glioma: a stimulation mapping study. *Acta Neurochir (Wien), 156*(4), 661-670; discussion 670. doi:10.1007/s00701-014-2003-2

Matsumi, N., Matsumoto, K., Mishima, N., Moriyama, E., Furuta, T., Nishimoto, A., & Taguchi, K. (1994). Thermal damage threshold of brain tissue--histological study of heated normal monkey brains. *Neurol Med Chir (Tokyo), 34*(4), 209-215.

Matsumoto, R., Nair, D.R., LaPresto, E., Najm, I., Bingaman, W., Shibasaki, H., & Luders, H.O. (2004). Functional connectivity in the human language system: a cortico-cortical evoked potential study. *Brain, 127*(Pt 10), 2316-2330. doi:10.1093/brain/awh246

Maurer, S., Tanigawa, N., Sollmann, N., Hauck, T., Ille, S., Boeckh-Behrens, T., Meyer, B., & Krieg, S.M. (2016). Non-invasive mapping of calculation function by repetitive navigated transcranial magnetic stimulation. *Brain Struct Funct, 221*(8), 3927-3947. doi:10.1007/s00429-015-1136-2

McGraw, P., Mathews, V.P., Wang, Y., & Phillips, M.D. (2001). Approach to functional magnetic resonance imaging of language based on models of language organization. *Neuroimaging Clin N Am, 11*(2), 343-353, x.

Medina, L.S., Bernal, B., & Ruiz, J. (2007). Role of functional MR in determining language dominance in epilepsy and nonepilepsy populations: a Bayesian analysis. *Radiology, 242*(1), 94-100. doi:10.1148/radiol.2421050677

Michelucci, R., Valzania, F., Passarelli, D., Santangelo, M., Rizzi, R., Buzzi, A.M., Tempestini, A., & Tassinari, C.A. (1994). Rapid-rate transcranial magnetic stimulation and hemispheric language dominance: usefulness and safety in epilepsy. *Neurology, 44*(9), 1697-1700. doi:10.1212/wnl.44.9.1697

Mills, K.R. (1991). Magnetic brain stimulation: a tool to explore the action of the motor cortex on single human spinal motoneurones. *Trends Neurosci, 14*(9), 401-405.

Mori, S., & Barker, P.B. (1999a). Diffusion magnetic resonance imaging: its principle and applications. *Anat Rec, 257*(3), 102-109. doi:10.1002/(SICI)1097-0185(19990615)257:3<102::AID-AR7>3.0.CO;2-6

Mori, S., Crain, B.J., Chacko, V.P., & van Zijl, P.C. (1999b). Three-dimensional tracking of axonal projections in the brain by magnetic resonance imaging. *Ann Neurol, 45*(2), 265-269.

Mori, S., Frederiksen, K., van Zijl, P.C., Stieltjes, B., Kraut, M.A., Solaiyappan, M., & Pomper, M.G. (2002a). Brain white matter anatomy of tumor patients evaluated with diffusion tensor imaging. *Ann Neurol, 51*(3), 377-380.

Mori, S., & van Zijl, P.C. (2002b). Fiber tracking: principles and strategies - a technical review. *NMR Biomed, 15*(7-8), 468-480. doi:10.1002/nbm.781

Moseley, M.E., Cohen, Y., Kucharczyk, J., Mintorovitch, J., Asgari, H.S., Wendland, M.F., Tsuruda, J., & Norman, D. (1990). Diffusion-weighted MR imaging of anisotropic water diffusion in cat central nervous system. *Radiology, 176*(2), 439-445. doi:10.1148/radiology.176.2.2367658

Motomura, K., Takeuchi, H., Nojima, I., Aoki, K., Chalise, L., Iijima, K., Wakabayashi, T., & Natsume, A. (2020). Navigated repetitive transcranial magnetic stimulation as preoperative assessment in patients with brain tumors. *Sci Rep, 10*(1), 9044. doi:10.1038/s41598-020-65944-8

Muragaki, Y., Iseki, H., Takakura, K., Maruyama, T., & Hori, T. (2005). [Awake craniotomy and functional mapping for surgery of brain tumors]. *Nihon Rinsho, 63 Suppl 9*, 330-340.

Muragaki, Y., Iseki, H., Maruyama, T., Tanaka, M., Shinohara, C., Suzuki, T., Yoshimitsu, K., Ikuta, S., Hayashi, M., Chernov, M., Hori, T., Okada, Y., & Takakura, K. (2011). Information-guided surgical management of gliomas using low-field-strength intraoperative MRI. *Acta Neurochir Suppl, 109*, 67-72. doi:10.1007/978-3-211-99651-5_11

Naeser, M.A., & Hayward, R.W. (1978). Lesion localization in aphasia with cranial computed tomography and the Boston Diagnostic Aphasia Exam. *Neurology, 28*(6), 545-551.

Negwer, C., Sollmann, N., Ille, S., Hauck, T., Maurer, S., Kirschke, J.S., Ringel, F., Meyer, B., & Krieg, S.M. (2017). Language pathway tracking: comparing nTMS-based DTI fiber tracking with a cubic ROIs-based protocol. *J Neurosurg, 126*(3), 1006-1014. doi:10.3171/2016.2.JNS152382

Negwer, C.N. (2017). *Sprachfaserbahndarstellung durch DTI Fiber Tracking basierend auf repetitiver transkranieller Magnetstimulation in Hirntumorpatienten: Umsetzung und Entwicklung einer neuen Technik.* (Dissertation), Technische Universität München.

Neil, J.J., Shiran, S.I., McKinstry, R.C., Schefft, G.L., Snyder, A.Z., Almli, C.R., Akbudak, E., Aronovitz, J.A., Miller, J.P., Lee, B.C., & Conturo, T.E. (1998). Normal brain in human newborns: apparent diffusion coefficient and diffusion anisotropy measured by using diffusion tensor MR imaging. *Radiology, 209*(1), 57-66. doi:10.1148/radiology.209.1.9769812

Nimsky, C., Ganslandt, O., Merhof, D., Sorensen, A.G., & Fahlbusch, R. (2006). Intraoperative visualization of the pyramidal tract by diffusion-tensor-imaging-based fiber tracking. *Neuroimage, 30*(4), 1219-1229. doi:10.1016/j.neuroimage.2005.11.001

Nimsky, C., Ganslandt, O., Hastreiter, P., Wang, R., Benner, T., Sorensen, A.G., & Fahlbusch, R. (2007). Preoperative and intraoperative diffusion tensor imaging-based fiber tracking in glioma surgery. *Neurosurgery, 61*(1 Suppl), 178-185; discussion 186. doi:10.1227/01.neu.0000279214.00139.3b

Nishida, M., Korzeniewska, A., Crone, N.E., Toyoda, G., Nakai, Y., Ofen, N., Brown, E.C., & Asano, E. (2017). Brain network dynamics in the human articulatory loop. *Clin Neurophysiol, 128*(8), 1473-1487. doi:10.1016/j.clinph.2017.05.002

Norris, D.G. (2001). Implications of bulk motion for diffusion-weighted imaging experiments: effects, mechanisms, and solutions. *J Magn Reson Imaging, 13*(4), 486-495.

Nossek, E., Korn, A., Shahar, T., Kanner, A.A., Yaffe, H., Marcovici, D., Ben-Harosh, C., Ben Ami, H., Weinstein, M., Shapira-Lichter, I., Constantini, S., Hendler, T., & Ram, Z. (2011). Intraoperative mapping and monitoring of the corticospinal tracts with neurophysiological assessment and 3-dimensional ultrasonography-based navigation. Clinical article. *J Neurosurg, 114*(3), 738-746. doi:10.3171/2010.8.JNS10639

O'Donnell, L.J., & Westin, C.F. (2011). An introduction to diffusion tensor image analysis. *Neurosurg Clin N Am, 22*(2), 185-196, viii. doi:10.1016/j.nec.2010.12.004

Ohue, S., Kohno, S., Inoue, A., Yamashita, D., Harada, H., Kumon, Y., Kikuchi, K., Miki, H., & Ohnishi, T. (2012). Accuracy of diffusion tensor magnetic resonance imaging-based tractography for surgery of gliomas near the pyramidal tract: a significant correlation between subcortical electrical stimulation and postoperative tractography. *Neurosurgery, 70*(2), 283-293; discussion 294. doi:10.1227/NEU.0b013e31823020e6

Ojemann, G., Ojemann, J., Lettich, E., & Berger, M. (1989). Cortical language localization in left, dominant hemisphere. An electrical stimulation mapping investigation in 117 patients. *J Neurosurg, 71*(3), 316-326. doi:10.3171/jns.1989.71.3.0316

Ojemann, G.A., & Whitaker, H.A. (1978). Language localization and variability. *Brain Lang, 6*(2), 239-260.

Ojemann, J.G., Ojemann, G.A., & Lettich, E. (2002). Cortical stimulation mapping of language cortex by using a verb generation task: effects of learning and comparison to mapping based on object naming. *J Neurosurg, 97*(1), 33-38. doi:10.3171/jns.2002.97.1.0033

Oldfield, R.C. (1971). The assessment and analysis of handedness: the Edinburgh inventory. *Neuropsychologia, 9*(1), 97-113.

Opitz, A., Legon, W., Rowlands, A., Bickel, W.K., Paulus, W., & Tyler, W.J. (2013). Physiological observations validate finite element models for estimating subject-specific electric field distributions induced by transcranial magnetic stimulation of the human motor cortex. *Neuroimage, 81*, 253-264. doi:10.1016/j.neuroimage.2013.04.067

Ostrom, Q.T., Cioffi, G., Gittleman, H., Patil, N., Waite, K., Kruchko, C., & Barnholtz-Sloan, J.S. (2019). CBTRUS Statistical Report: Primary Brain and Other Central Nervous System Tumors Diagnosed in the United States in 2012-2016. *Neuro Oncol, 21*(Supplement_5), v1-v100. doi:10.1093/neuonc/noz150

Ottenhausen, M., Bodhinayake, I., Banu, M., Kesavabhotla, K., Ray, A., & Boockvar, J.A. (2013). Industry progress report on neuro-oncology: Biotech update 2013. *J Neurooncol, 115*(2), 311-316. doi:10.1007/s11060-013-1222-3

Ottenhausen, M., Krieg, S.M., Meyer, B., & Ringel, F. (2015). Functional preoperative and intraoperative mapping and monitoring: increasing safety and efficacy in glioma surgery. *Neurosurg Focus, 38*(1), E3. doi:10.3171/2014.10.FOCUS14611

Pajevic, S., & Pierpaoli, C. (2000). Color schemes to represent the orientation of anisotropic tissues from diffusion tensor data: application to white matter fiber tract mapping in the human brain. *Magn Reson Med, 43*(6), 921.

Panych, L.P., & Madore, B. (2018). The physics of MRI safety. *J Magn Reson Imaging, 47*(1), 28-43. doi:10.1002/jmri.25761

Papathanassiou, D., Etard, O., Mellet, E., Zago, L., Mazoyer, B., & Tzourio-Mazoyer, N. (2000). A common language network for comprehension and production: a contribution to the

definition of language epicenters with PET. *Neuroimage, 11*(4), 347-357. doi:10.1006/nimg.2000.0546
Park, M.C., Goldman, M.A., Park, M.J., & Friehs, G.M. (2007). Neuroanatomical localization of the 'precentral knob' with computed tomography imaging. *Stereotact Funct Neurosurg, 85*(4), 158-161. doi:10.1159/000099074
Pascual-Leone, A., Gates, J.R., & Dhuna, A. (1991). Induction of speech arrest and counting errors with rapid-rate transcranial magnetic stimulation. *Neurology, 41*(5), 697-702.
Pascual-Leone, A., Nguyet, D., Cohen, L.G., Brasil-Neto, J.P., Cammarota, A., & Hallett, M. (1995). Modulation of muscle responses evoked by transcranial magnetic stimulation during the acquisition of new fine motor skills. *J Neurophysiol, 74*(3), 1037-1045. doi:10.1152/jn.1995.74.3.1037
Pascual-Leone, A., Bartres-Faz, D., & Keenan, J.P. (1999). Transcranial magnetic stimulation: studying the brain-behaviour relationship by induction of 'virtual lesions'. *Philos Trans R Soc Lond B Biol Sci, 354*(1387), 1229-1238. doi:10.1098/rstb.1999.0476
Pascual-Leone, A., Walsh, V., & Rothwell, J. (2000). Transcranial magnetic stimulation in cognitive neuroscience--virtual lesion, chronometry, and functional connectivity. *Curr Opin Neurobiol, 10*(2), 232-237.
Pascual-Leone, A., Davey, N.J., Rothwell, J., Wassermann, E., & Puri, B.K. (2002). Handbook of Transcranial Magnetic Stimulation. . *MIT Press.*
Paulsen, P.D.F., & Waschke, P.D.J. (2010). *Sobotta: Atlas der Anatomie des Menschen - Kopf, Hals und Neuroanatomie* (23 ed.). München: ELSEVIER Urban & Fischer.
Paus, T., Jech, R., Thompson, C.J., Comeau, R., Peters, T., & Evans, A.C. (1997). Transcranial magnetic stimulation during positron emission tomography: a new method for studying connectivity of the human cerebral cortex. *J Neurosci, 17*(9), 3178-3184.
Peelen, M.V., & Caramazza, A. (2012). Conceptual object representations in human anterior temporal cortex. *J Neurosci, 32*(45), 15728-15736. doi:10.1523/JNEUROSCI.1953-12.2012
Penfield, W., & Rasmussen, T. (1950). *The cerebral cortex of man: a clinical study of localization of function*. New York: The Macmillan Company.
Penfield, W., & Jasper, H.H. (1954). *Epilepsy and the functional anatomy of the human brain*. Boston: Little, Brown.
Petersen, S.E., Fox, P.T., Posner, M.I., Mintun, M., & Raichle, M.E. (1988). Positron emission tomographic studies of the cortical anatomy of single-word processing. *Nature, 331*(6157), 585-589. doi:10.1038/331585a0
Petrovich Brennan, N.M., Whalen, S., de Morales Branco, D., O'Shea J, P., Norton, I.H., & Golby, A.J. (2007). Object naming is a more sensitive measure of speech localization than number counting: Converging evidence from direct cortical stimulation and fMRI. *Neuroimage, 37 Suppl 1*, S100-108. doi:10.1016/j.neuroimage.2007.04.052
Picht, D.m.T. (2015). *Die navigierte transkranielle Magnetstimulation zur Planung neurochirurgischer Eingriffe im Bereich motorisch eloquenter Hirnareale.* (Habilitation), Charité-Universitätsmedizin Berlin.
Picht, T., Kombos, T., Gramm, H.J., Brock, M., & Suess, O. (2006). Multimodal protocol for awake craniotomy in language cortex tumour surgery. *Acta Neurochir (Wien), 148*(2), 127-137; discussion 137-128. doi:10.1007/s00701-005-0706-0
Picht, T., Mularski, S., Kuehn, B., Vajkoczy, P., Kombos, T., & Suess, O. (2009). Navigated transcranial magnetic stimulation for preoperative functional diagnostics in brain tumor surgery. *Neurosurgery, 65*(6 Suppl), 93-98; discussion 98-99. doi:10.1227/01.NEU.0000348009.22750.59
Picht, T., Schmidt, S., Brandt, S., Frey, D., Hannula, H., Neuvonen, T., Karhu, J., Vajkoczy, P., & Suess, O. (2011). Preoperative functional mapping for rolandic brain tumor surgery: comparison of navigated transcranial magnetic stimulation to direct cortical stimulation. *Neurosurgery, 69*(3), 581-588; discussion 588. doi:10.1227/NEU.0b013e3182181b89
Picht, T., Krieg, S.M., Sollmann, N., Rosler, J., Niraula, B., Neuvonen, T., Savolainen, P., Lioumis, P., Makela, J.P., Deletis, V., Meyer, B., Vajkoczy, P., & Ringel, F. (2013). A comparison of language mapping by preoperative navigated transcranial magnetic stimulation and direct cortical stimulation during awake surgery. *Neurosurgery, 72*(5), 808-819. doi:10.1227/NEU.0b013e3182889e01

Pierpaoli, C., & Basser, P.J. (1996). Toward a quantitative assessment of diffusion anisotropy. *Magn Reson Med, 36*(6), 893-906.
Pinto, M. (2012). *BASICS Neurologie* (Fischer, E.U. Ed. 3 ed.). Munich.
Poeppel, D. (1996). A critical review of PET studies of phonological processing. *Brain Lang, 55*(3), 317-351; discussion 352-385. doi:10.1006/brln.1996.0108
Poldrack, R.A., Wagner, A.D., Prull, M.W., Desmond, J.E., Glover, G.H., & Gabrieli, J.D. (1999). Functional specialization for semantic and phonological processing in the left inferior prefrontal cortex. *Neuroimage, 10*(1), 15-35. doi:10.1006/nimg.1999.0441
Potgieser, A.R., Wagemakers, M., van Hulzen, A.L., de Jong, B.M., Hoving, E.W., & Groen, R.J. (2014). The role of diffusion tensor imaging in brain tumor surgery: a review of the literature. *Clin Neurol Neurosurg, 124*, 51-58. doi:10.1016/j.clineuro.2014.06.009
Pouratian, N., & Bookheimer, S.Y. (2010). The reliability of neuroanatomy as a predictor of eloquence: a review. *Neurosurg Focus, 28*(2), E3. doi:10.3171/2009.11.FOCUS09239
Price, C.J., Devlin, J.T., Moore, C.J., Morton, C., & Laird, A.R. (2005). Meta-analyses of object naming: effect of baseline. *Hum Brain Mapp, 25*(1), 70-82. doi:10.1002/hbm.20132
Price, C.J., Crinion, J.T., & Macsweeney, M. (2011). A Generative Model of Speech Production in Broca's and Wernicke's Areas. *Front Psychol, 2*, 237. doi:10.3389/fpsyg.2011.00237
Price, C.J. (2012). A review and synthesis of the first 20 years of PET and fMRI studies of heard speech, spoken language and reading. *Neuroimage, 62*(2), 816-847. doi:10.1016/j.neuroimage.2012.04.062
Pujol, J., Deus, J., Losilla, J.M., & Capdevila, A. (1999). Cerebral lateralization of language in normal left-handed people studied by functional MRI. *Neurology, 52*(5), 1038-1043. doi:10.1212/wnl.52.5.1038
Rassow, J. (2012). *Biochemie* (Thieme Ed. 3 ed.). Stuttgart.
Rauschecker, J.P. (2012). Ventral and dorsal streams in the evolution of speech and language. *Front Evol Neurosci, 4*, 7. doi:10.3389/fnevo.2012.00007
Ravazzani, P., Ruohonen, J., Grandori, F., & Tognola, G. (1996). Magnetic stimulation of the nervous system: induced electric field in unbounded, semi-infinite, spherical, and cylindrical media. *Ann Biomed Eng, 24*(5), 606-616.
Ravazzani, P., Ruohonen, J., Tognola, G., Anfosso, F., Ollikainen, M., Ilmoniemi, R.J., & Grandori, F. (2002). Frequency-related effects in the optimization of coils for the magnetic stimulation of the nervous system. *IEEE Trans Biomed Eng, 49*(5), 463-471. doi:10.1109/10.995685
Robles, S.G., Gatignol, P., Lehericy, S., & Duffau, H. (2008). Long-term brain plasticity allowing a multistage surgical approach to World Health Organization Grade II gliomas in eloquent areas. *J Neurosurg, 109*(4), 615-624. doi:10.3171/JNS/2008/109/10/0615
Rocha-Filho, P.A. (2015). Post-craniotomy headache: a clinical view with a focus on the persistent form. *Headache, 55*(5), 733-738. doi:10.1111/head.12563
Rogic, M., Deletis, V., & Fernandez-Conejero, I. (2014). Inducing transient language disruptions by mapping of Broca's area with modified patterned repetitive transcranial magnetic stimulation protocol. *J Neurosurg, 120*(5), 1033-1041. doi:10.3171/2013.11.JNS13952
Rolheiser, T., Stamatakis, E.A., & Tyler, L.K. (2011). Dynamic processing in the human language system: synergy between the arcuate fascicle and extreme capsule. *J Neurosci, 31*(47), 16949-16957. doi:10.1523/JNEUROSCI.2725-11.2011
Rosler, J., Niraula, B., Strack, V., Zdunczyk, A., Schilt, S., Savolainen, P., Lioumis, P., Makela, J., Vajkoczy, P., Frey, D., & Picht, T. (2014). Language mapping in healthy volunteers and brain tumor patients with a novel navigated TMS system: evidence of tumor-induced plasticity. *Clin Neurophysiol, 125*(3), 526-536. doi:10.1016/j.clinph.2013.08.015
Rossi, S., Hallett, M., Rossini, P.M., Pascual-Leone, A., & Safety of, T.M.S.C.G. (2009). Safety, ethical considerations, and application guidelines for the use of transcranial magnetic stimulation in clinical practice and research. *Clin Neurophysiol, 120*(12), 2008-2039. doi:10.1016/j.clinph.2009.08.016
Rossini, P.M., Barker, A.T., Berardelli, A., Caramia, M.D., Caruso, G., Cracco, R.Q., Dimitrijevic, M.R., Hallett, M., Katayama, Y., Lucking, C.H., & et al. (1994). Non-invasive electrical and magnetic stimulation of the brain, spinal cord and roots: basic principles and

procedures for routine clinical application. Report of an IFCN committee. *Electroencephalogr Clin Neurophysiol, 91*(2), 79-92.
Rossini, P.M., Burke, D., Chen, R., Cohen, L.G., Daskalakis, Z., Di Iorio, R., Di Lazzaro, V., Ferreri, F., Fitzgerald, P.B., George, M.S., Hallett, M., Lefaucheur, J.P., Langguth, B., Matsumoto, H., Miniussi, C., Nitsche, M.A., Pascual-Leone, A., Paulus, W., Rossi, S., Rothwell, J.C., Siebner, H.R., Ugawa, Y., Walsh, V., & Ziemann, U. (2015). Non-invasive electrical and magnetic stimulation of the brain, spinal cord, roots and peripheral nerves: Basic principles and procedures for routine clinical and research application. An updated report from an I.F.C.N. Committee. *Clin Neurophysiol, 126*(6), 1071-1107. doi:10.1016/j.clinph.2015.02.001
Rotenberg, A., Harrington, M.G., Birnbaum, D.S., Madsen, J.R., Glass, I.E., Jensen, F.E., & Pascual-Leone, A. (2007). Minimal heating of titanium skull plates during 1Hz repetitive transcranial magnetic stimulation. *Clin Neurophysiol, 118*(11), 2536-2538. doi:10.1016/j.clinph.2007.08.003
Roth, B.J., Saypol, J.M., Hallett, M., & Cohen, L.G. (1991). A theoretical calculation of the electric field induced in the cortex during magnetic stimulation. *Electroencephalogr Clin Neurophysiol, 81*(1), 47-56.
Roth, B.J., Pascual-Leone, A., Cohen, L.G., & Hallett, M. (1992). The heating of metal electrodes during rapid-rate magnetic stimulation: a possible safety hazard. *Electroencephalogr Clin Neurophysiol, 85*(2), 116-123.
Roth, Y., Zangen, A., & Hallett, M. (2002). A coil design for transcranial magnetic stimulation of deep brain regions. *J Clin Neurophysiol, 19*(4), 361-370.
Roth, Y., Amir, A., Levkovitz, Y., & Zangen, A. (2007). Three-dimensional distribution of the electric field induced in the brain by transcranial magnetic stimulation using figure-8 and deep H-coils. *J Clin Neurophysiol, 24*(1), 31-38. doi:10.1097/WNP.0b013e31802fa393
Rothwell, J.C., Thompson, P.D., Day, B.L., Boyd, S., & Marsden, C.D. (1991). Stimulation of the human motor cortex through the scalp. *Exp Physiol, 76*(2), 159-200.
Roux, F.E., Lubrano, V., Lauwers-Cances, V., Tremoulet, M., Mascott, C.R., & Demonet, J.F. (2004). Intra-operative mapping of cortical areas involved in reading in mono- and bilingual patients. *Brain, 127*(Pt 8), 1796-1810. doi:10.1093/brain/awh204
Rubinov, M., & Sporns, O. (2010). Complex network measures of brain connectivity: uses and interpretations. *Neuroimage, 52*(3), 1059-1069. doi:10.1016/j.neuroimage.2009.10.003
Ruohonen, J., & Ilmoniemi, R.J. (1999). Modeling of the stimulating field generation in TMS. *Electroencephalogr Clin Neurophysiol Suppl, 51*, 30-40.
Ruohonen, J., & Karhu, J. (2010). Navigated transcranial magnetic stimulation. *Neurophysiol Clin, 40*(1), 7-17. doi:10.1016/j.neucli.2010.01.006
Rutherford, M.A., Cowan, F.M., Manzur, A.Y., Dubowitz, L.M., Pennock, J.M., Hajnal, J.V., Young, I.R., & Bydder, G.M. (1991). MR imaging of anisotropically restricted diffusion in the brain of neonates and infants. *J Comput Assist Tomogr, 15*(2), 188-198.
Rutten, G.J., & Ramsey, N.F. (2010). The role of functional magnetic resonance imaging in brain surgery. *Neurosurg Focus, 28*(2), E4. doi:10.3171/2009.12.FOCUS09251
Sacco, P., Turner, D., Rothwell, J., & Thickbroom, G. (2009). Corticomotor responses to triple-pulse transcranial magnetic stimulation: Effects of interstimulus interval and stimulus intensity. *Brain Stimul, 2*(1), 36-40. doi:10.1016/j.brs.2008.06.255
Saito, T., Tamura, M., Chernov, M.F., Ikuta, S., Muragaki, Y., & Maruyama, T. (2018). Neurophysiological Monitoring and Awake Craniotomy for Resection of Intracranial Gliomas. *Prog Neurol Surg, 30*, 117-158. doi:10.1159/000464387
Sakai, K., Ugawa, Y., Terao, Y., Hanajima, R., Furubayashi, T., & Kanazawa, I. (1997). Preferential activation of different I waves by transcranial magnetic stimulation with a figure-of-eight-shaped coil. *Exp Brain Res, 113*(1), 24-32.
Salinas, F.S., Lancaster, J.L., & Fox, P.T. (2007). Detailed 3D models of the induced electric field of transcranial magnetic stimulation coils. *Phys Med Biol, 52*(10), 2879-2892. doi:10.1088/0031-9155/52/10/016
Salinas, F.S., Lancaster, J.L., & Fox, P.T. (2009). 3D modeling of the total electric field induced by transcranial magnetic stimulation using the boundary element method. *Phys Med Biol, 54*(12), 3631-3647. doi:10.1088/0031-9155/54/12/002

Sanai, N., & Berger, M.S. (2008a). Mapping the horizon: techniques to optimize tumor resection before and during surgery. *Clin Neurosurg, 55*, 14-19.
Sanai, N., & Berger, M.S. (2008b). Glioma extent of resection and its impact on patient outcome. *Neurosurgery, 62*(4), 753-764; discussion 264-756. doi:10.1227/01.neu.0000318159.21731.cf
Sanai, N., Mirzadeh, Z., & Berger, M.S. (2008c). Functional outcome after language mapping for glioma resection. *N Engl J Med, 358*(1), 18-27. doi:10.1056/NEJMoa067819
Santiago-Rodriguez, E., Cardenas-Morales, L., Harmony, T., Fernandez-Bouzas, A., Porras-Kattz, E., & Hernandez, A. (2008). Repetitive transcranial magnetic stimulation decreases the number of seizures in patients with focal neocortical epilepsy. *Seizure, 17*(8), 677-683. doi:10.1016/j.seizure.2008.04.005
Sarubbo, S., Le Bars, E., Moritz-Gasser, S., & Duffau, H. (2012). Complete recovery after surgical resection of left Wernicke's area in awake patient: a brain stimulation and functional MRI study. *Neurosurg Rev, 35*(2), 287-292; discussion 292. doi:10.1007/s10143-011-0351-4
Sarwar, T., Ramamohanarao, K., & Zalesky, A. (2019). Mapping connectomes with diffusion MRI: deterministic or probabilistic tractography? *Magn Reson Med, 81*(2), 1368-1384. doi:10.1002/mrm.27471
Sastry, R., Bi, W.L., Pieper, S., Frisken, S., Kapur, T., Wells, W., 3rd, & Golby, A.J. (2017). Applications of Ultrasound in the Resection of Brain Tumors. *J Neuroimaging, 27*(1), 5-15. doi:10.1111/jon.12382
Saur, D., Kreher, B.W., Schnell, S., Kummerer, D., Kellmeyer, P., Vry, M.S., Umarova, R., Musso, M., Glauche, V., Abel, S., Huber, W., Rijntjes, M., Hennig, J., & Weiller, C. (2008). Ventral and dorsal pathways for language. *Proc Natl Acad Sci U S A, 105*(46), 18035-18040. doi:10.1073/pnas.0805234105
Schisterman, E.F., Perkins, N.J., Liu, A., & Bondell, H. (2005). Optimal cut-point and its corresponding Youden Index to discriminate individuals using pooled blood samples. *Epidemiology, 16*(1), 73-81.
Schonberg, T., Pianka, P., Hendler, T., Pasternak, O., & Assaf, Y. (2006). Characterization of displaced white matter by brain tumors using combined DTI and fMRI. *Neuroimage, 30*(4), 1100-1111. doi:10.1016/j.neuroimage.2005.11.015
Schrader, L.M., Stern, J.M., Koski, L., Nuwer, M.R., & Engel, J., Jr. (2004). Seizure incidence during single- and paired-pulse transcranial magnetic stimulation (TMS) in individuals with epilepsy. *Clin Neurophysiol, 115*(12), 2728-2737. doi:10.1016/j.clinph.2004.06.018
Schuhmann, T., Schiller, N.O., Goebel, R., & Sack, A.T. (2012). Speaking of which: dissecting the neurocognitive network of language production in picture naming. *Cereb Cortex, 22*(3), 701-709. doi:10.1093/cercor/bhr155
Schwarz-Friesel, M. (2008). *Einführung in die kognitive Linguistik* (3., vollst. überarb. und erw. Aufl. ed.). Tübingen: Francke.
Scott, S.K., Leff, A.P., & Wise, R.J. (2003). Going beyond the information given: a neural system supporting semantic interpretation. *Neuroimage, 19*(3), 870-876.
Seghier, M.L., Fagan, E., & Price, C.J. (2010). Functional subdivisions in the left angular gyrus where the semantic system meets and diverges from the default network. *J Neurosci, 30*(50), 16809-16817. doi:10.1523/JNEUROSCI.3377-10.2010
Seidel, K., Beck, J., Stieglitz, L., Schucht, P., & Raabe, A. (2013). The warning-sign hierarchy between quantitative subcortical motor mapping and continuous motor evoked potential monitoring during resection of supratentorial brain tumors. *J Neurosurg, 118*(2), 287-296. doi:10.3171/2012.10.JNS12895
Shahar, T., Rozovski, U., Marko, N.F., Tummala, S., Ziu, M., Weinberg, J.S., Rao, G., Kumar, V.A., Sawaya, R., & Prabhu, S.S. (2014). Preoperative imaging to predict intraoperative changes in tumor-to-corticospinal tract distance: an analysis of 45 cases using high-field intraoperative magnetic resonance imaging. *Neurosurgery, 75*(1), 23-30. doi:10.1227/NEU.0000000000000338
Siebner, H.R., & Rothwell, J. (2003). Transcranial magnetic stimulation: new insights into representational cortical plasticity. *Exp Brain Res, 148*(1), 1-16. doi:10.1007/s00221-002-1234-2

Simos, P.G., Breier, J.I., Fletcher, J.M., Foorman, B.R., Castillo, E.M., & Papanicolaou, A.C. (2002). Brain mechanisms for reading words and pseudowords: an integrated approach. *Cereb Cortex, 12*(3), 297-305. doi:10.1093/cercor/12.3.297

Siri, S., Tettamanti, M., Cappa, S.F., Della Rosa, P., Saccuman, C., Scifo, P., & Vigliocco, G. (2008). The neural substrate of naming events: effects of processing demands but not of grammatical class. *Cereb Cortex, 18*(1), 171-177. doi:10.1093/cercor/bhm043

Skare, S., & Andersson, J.L. (2001). On the effects of gating in diffusion imaging of the brain using single shot EPI. *Magn Reson Imaging, 19*(8), 1125-1128.

Sliwinska, M.W., Khadilkar, M., Campbell-Ratcliffe, J., Quevenco, F., & Devlin, J.T. (2012). Early and sustained supramarginal gyrus contributions to phonological processing. *Front Psychol, 3*, 161. doi:10.3389/fpsyg.2012.00161

Snodgrass, J.G., & Vanderwart, M. (1980). A standardized set of 260 pictures: norms for name agreement, image agreement, familiarity, and visual complexity. *J Exp Psychol Hum Learn, 6*(2), 174-215.

Sollmann, N., Hauck, T., Hapfelmeier, A., Meyer, B., Ringel, F., & Krieg, S.M. (2013a). Intra- and interobserver variability of language mapping by navigated transcranial magnetic brain stimulation. *BMC Neurosci, 14*, 150. doi:10.1186/1471-2202-14-150

Sollmann, N., Hauck, T., Obermuller, T., Hapfelmeier, A., Meyer, B., Ringel, F., & Krieg, S.M. (2013b). Inter- and intraobserver variability in motor mapping of the hotspot for the abductor policis brevis muscle. *BMC Neurosci, 14*, 94. doi:10.1186/1471-2202-14-94

Sollmann, N., Picht, T., Makela, J.P., Meyer, B., Ringel, F., & Krieg, S.M. (2013c). Navigated transcranial magnetic stimulation for preoperative language mapping in a patient with a left frontoopercular glioblastoma. *J Neurosurg, 118*(1), 175-179. doi:10.3171/2012.9.JNS121053

Sollmann, N., Tanigawa, N., Ringel, F., Zimmer, C., Meyer, B., & Krieg, S.M. (2014). Language and its right-hemispheric distribution in healthy brains: an investigation by repetitive transcranial magnetic stimulation. *Neuroimage, 102 Pt 2*, 776-788. doi:10.1016/j.neuroimage.2014.09.002

Sollmann, N. (2015). *Kartierung der menschlichen Sprache im Gehirn mittels navigierter transkranieller Magnetstimulation.* (Dissertation), Technische Universität München

Sollmann, N., Giglhuber, K., Tussis, L., Meyer, B., Ringel, F., & Krieg, S.M. (2015a). nTMS-based DTI fiber tracking for language pathways correlates with language function and aphasia - A case report. *Clin Neurol Neurosurg, 136*, 25-28. doi:10.1016/j.clineuro.2015.05.023

Sollmann, N., Ille, S., Hauck, T., Maurer, S., Negwer, C., Zimmer, C., Ringel, F., Meyer, B., & Krieg, S.M. (2015b). The impact of preoperative language mapping by repetitive navigated transcranial magnetic stimulation on the clinical course of brain tumor patients. *BMC Cancer, 15*, 261. doi:10.1186/s12885-015-1299-5

Sollmann, N., Ille, S., Obermueller, T., Negwer, C., Ringel, F., Meyer, B., & Krieg, S.M. (2015c). The impact of repetitive navigated transcranial magnetic stimulation coil positioning and stimulation parameters on human language function. *Eur J Med Res, 20*, 47. doi:10.1186/s40001-015-0138-0

Sollmann, N., Goblirsch-Kolb, M.F., Ille, S., Butenschoen, V.M., Boeckh-Behrens, T., Meyer, B., Ringel, F., & Krieg, S.M. (2016a). Comparison between electric-field-navigated and line-navigated TMS for cortical motor mapping in patients with brain tumors. *Acta Neurochir (Wien), 158*(12), 2277-2289. doi:10.1007/s00701-016-2970-6

Sollmann, N., Kubitscheck, A., Maurer, S., Ille, S., Hauck, T., Kirschke, J.S., Ringel, F., Meyer, B., & Krieg, S.M. (2016b). Preoperative language mapping by repetitive navigated transcranial magnetic stimulation and diffusion tensor imaging fiber tracking and their comparison to intraoperative stimulation. *Neuroradiology, 58*(8), 807-818. doi:10.1007/s00234-016-1685-y

Sollmann, N., Ille, S., Negwer, C., Boeckh-Behrens, T., Ringel, F., Meyer, B., & Krieg, S.M. (2017a). Cortical time course of object naming investigated by repetitive navigated transcranial magnetic stimulation. *Brain Imaging Behav, 11*(4), 1192-1206. doi:10.1007/s11682-016-9574-x

Sollmann, N., Tanigawa, N., Bulubas, L., Sabih, J., Zimmer, C., Ringel, F., Meyer, B., & Krieg, S.M. (2017b). Clinical Factors Underlying the Inter-individual Variability of the Resting Motor

Threshold in Navigated Transcranial Magnetic Stimulation Motor Mapping. *Brain Topogr, 30*(1), 98-121. doi:10.1007/s10548-016-0536-9
Soros, P., Cornelissen, K., Laine, M., & Salmelin, R. (2003). Naming actions and objects: cortical dynamics in healthy adults and in an anomic patient with a dissociation in action/object naming. *Neuroimage, 19*(4), 1787-1801.
Southwell, D.G., Hervey-Jumper, S.L., Perry, D.W., & Berger, M.S. (2016). Intraoperative mapping during repeat awake craniotomy reveals the functional plasticity of adult cortex. *J Neurosurg, 124*(5), 1460-1469. doi:10.3171/2015.5.JNS142833
Sparing, R., Mottaghy, F.M., Hungs, M., Brugmann, M., Foltys, H., Huber, W., & Topper, R. (2001). Repetitive transcranial magnetic stimulation effects on language function depend on the stimulation parameters. *J Clin Neurophysiol, 18*(4), 326-330.
Speckmann, E.-J., Hescheler, J., Köhling, R., Alzheimer, C., & Speckmann-Hescheler-Köhling. (2009). *Physiologie* (Fischer, E.U. Ed. 5 ed.). Munich.
Spena, G., Nava, A., Cassini, F., Pepoli, A., Bruno, M., D'Agata, F., Cauda, F., Sacco, K., Duca, S., Barletta, L., & Versari, P. (2010). Preoperative and intraoperative brain mapping for the resection of eloquent-area tumors. A prospective analysis of methodology, correlation, and usefulness based on clinical outcomes. *Acta Neurochir (Wien), 152*(11), 1835-1846. doi:10.1007/s00701-010-0764-9
Spena, G., Schucht, P., Seidel, K., Rutten, G.J., Freyschlag, C.F., D'Agata, F., Costi, E., Zappa, F., Fontanella, M., Fontaine, D., Almairac, F., Cavallo, M., De Bonis, P., Conesa, G., Foroglou, N., Gil-Robles, S., Mandonnet, E., Martino, J., Picht, T., Viegas, C., Wager, M., & Pallud, J. (2017). Brain tumors in eloquent areas: A European multicenter survey of intraoperative mapping techniques, intraoperative seizures occurrence, and antiepileptic drug prophylaxis. *Neurosurg Rev, 40*(2), 287-298. doi:10.1007/s10143-016-0771-2
Sporns, O. (2013). Structure and function of complex brain networks. *Dialogues Clin Neurosci, 15*(3), 247-262.
Staempfli, P., Jaermann, T., Crelier, G.R., Kollias, S., Valavanis, A., & Boesiger, P. (2006). Resolving fiber crossing using advanced fast marching tractography based on diffusion tensor imaging. *Neuroimage, 30*(1), 110-120. doi:10.1016/j.neuroimage.2005.09.027
Steinmetz, H., Furst, G., & Freund, H.J. (1990). Variation of perisylvian and calcarine anatomic landmarks within stereotaxic proportional coordinates. *AJNR Am J Neuroradiol, 11*(6), 1123-1130.
Steinmetz, H., Jancke, L., Kleinschmidt, A., Schlaug, G., Volkmann, J., & Huang, Y. (1992). Sex but no hand difference in the isthmus of the corpus callosum. *Neurology, 42*(4), 749-752. doi:10.1212/wnl.42.4.749
Stejskal, E., & Tanner, J. (1965). Spin diffusion measurements: spin echoes in the presence of a time-dependent field gradient. *J Chem Phys*.
Studholme, C., Hill, D.L., & Hawkes, D.J. (1996). Automated 3-D registration of MR and CT images of the head. *Med Image Anal, 1*(2), 163-175. doi:10.1016/s1361-8415(96)80011-9
Stummer, W., Pichlmeier, U., Meinel, T., Wiestler, O.D., Zanella, F., Reulen, H.J., & Group, A.L.-G.S. (2006). Fluorescence-guided surgery with 5-aminolevulinic acid for resection of malignant glioma: a randomised controlled multicentre phase III trial. *Lancet Oncol, 7*(5), 392-401. doi:10.1016/S1470-2045(06)70665-9
Stummer, W. (2014). The fear of 5-ALA--is it warranted? *World Neurosurg, 81*(5-6), e30-31. doi:10.1016/j.wneu.2013.09.048
Suess, O., Kombos, T., Suess, S., Stendel, R., Pietilae, T., & Brock, M. (2001). The influence of intra-operative brain shift on continuous cortical stimulation during surgery in the motor cortex--an illustrative case report. *Acta Neurochir (Wien), 143*(6), 621-623.
Suess, O., Suess, S., Mularski, S., Kuhn, B., Picht, T., Schonherr, S., & Kombos, T. (2007). [Evaluation of a DC pulsed magnetic tracking system in neurosurgical navigation: technique, accuracies, and influencing factors]. *Biomed Tech (Berl), 52*(3), 223-233. doi:10.1515/BMT.2007.040
Szaflarski, J.P., Binder, J.R., Possing, E.T., McKiernan, K.A., Ward, B.D., & Hammeke, T.A. (2002). Language lateralization in left-handed and ambidextrous people: fMRI data. *Neurology, 59*(2), 238-244. doi:10.1212/wnl.59.2.238

Szekely, A., Jacobsen, T., D'Amico, S., Devescovi, A., Andonova, E., Herron, D., Lu, C.C., Pechmann, T., Pleh, C., Wicha, N., Federmeier, K., Gerdjikova, I., Gutierrez, G., Hung, D., Hsu, J., Iyer, G., Kohnert, K., Mehotcheva, T., Orozco-Figueroa, A., Tzeng, A., Tzeng, O., Arevalo, A., Vargha, A., Butler, A.C., Buffington, R., & Bates, E. (2004). A new on-line resource for psycholinguistic studies. *J Mem Lang, 51*(2), 247-250. doi:10.1016/j.jml.2004.03.002

Szelenyi, A., Bello, L., Duffau, H., Fava, E., Feigl, G.C., Galanda, M., Neuloh, G., Signorelli, F., Sala, F., & Workgroup for Intraoperative Management in Low-Grade Glioma Surgery within the European Low-Grade Glioma, N. (2010). Intraoperative electrical stimulation in awake craniotomy: methodological aspects of current practice. *Neurosurg Focus, 28*(2), E7. doi:10.3171/2009.12.FOCUS09237

Tamura, Y., Ogawa, H., Kapeller, C., Prueckl, R., Takeuchi, F., Anei, R., Ritaccio, A., Guger, C., & Kamada, K. (2016). Passive language mapping combining real-time oscillation analysis with cortico-cortical evoked potentials for awake craniotomy. *J Neurosurg, 125*(6), 1580-1588. doi:10.3171/2015.4.JNS15193

Tarapore, P.E., Tate, M.C., Findlay, A.M., Honma, S.M., Mizuiri, D., Berger, M.S., & Nagarajan, S.S. (2012). Preoperative multimodal motor mapping: a comparison of magnetoencephalography imaging, navigated transcranial magnetic stimulation, and direct cortical stimulation. *J Neurosurg, 117*(2), 354-362. doi:10.3171/2012.5.JNS112124

Tarapore, P.E., Findlay, A.M., Honma, S.M., Mizuiri, D., Houde, J.F., Berger, M.S., & Nagarajan, S.S. (2013). Language mapping with navigated repetitive TMS: proof of technique and validation. *Neuroimage, 82*, 260-272. doi:10.1016/j.neuroimage.2013.05.018

Tarkiainen, A., Liljestrom, M., Seppa, M., & Salmelin, R. (2003). The 3D topography of MEG source localization accuracy: effects of conductor model and noise. *Clin Neurophysiol, 114*(10), 1977-1992.

Tassinari, C.A., Cincotta, M., Zaccara, G., & Michelucci, R. (2003). Transcranial magnetic stimulation and epilepsy. *Clin Neurophysiol, 114*(5), 777-798.

Taylor, J.S., Rastle, K., & Davis, M.H. (2013). Can cognitive models explain brain activation during word and pseudoword reading? A meta-analysis of 36 neuroimaging studies. *Psychol Bull, 139*(4), 766-791. doi:10.1037/a0030266

Theodore, W.H., Hunter, K., Chen, R., Vega-Bermudez, F., Boroojerdi, B., Reeves-Tyer, P., Werhahn, K., Kelley, K.R., & Cohen, L. (2002). Transcranial magnetic stimulation for the treatment of seizures: a controlled study. *Neurology, 59*(4), 560-562.

Thevenaz, P., Ruttimann, U.E., & Unser, M. (1998). A pyramid approach to subpixel registration based on intensity. *IEEE Trans Image Process, 7*(1), 27-41. doi:10.1109/83.650848

Thiebaut de Schotten, M., Ffytche, D.H., Bizzi, A., Dell'Acqua, F., Allin, M., Walshe, M., Murray, R., Williams, S.C., Murphy, D.G., & Catani, M. (2011). Atlasing location, asymmetry and inter-subject variability of white matter tracts in the human brain with MR diffusion tractography. *Neuroimage, 54*(1), 49-59. doi:10.1016/j.neuroimage.2010.07.055

Thiel, A., Herholz, K., von Stockhausen, H.M., van Leyen-Pilgram, K., Pietrzyk, U., Kessler, J., Wienhard, K., Klug, N., & Heiss, W.D. (1998). Localization of language-related cortex with 15O-labeled water PET in patients with gliomas. *Neuroimage, 7*(4 Pt 1), 284-295. doi:10.1006/nimg.1998.0334

Thielscher, A., Opitz, A., & Windhoff, M. (2011). Impact of the gyral geometry on the electric field induced by transcranial magnetic stimulation. *Neuroimage, 54*(1), 234-243. doi:10.1016/j.neuroimage.2010.07.061

Thompson-Schill, S.L., Swick, D., Farah, M.J., D'Esposito, M., Kan, I.P., & Knight, R.T. (1998). Verb generation in patients with focal frontal lesions: a neuropsychological test of neuroimaging findings. *Proc Natl Acad Sci U S A, 95*(26), 15855-15860.

Thurling, M., Kuper, M., Stefanescu, R., Maderwald, S., Gizewski, E.R., Ladd, M.E., & Timmann, D. (2011). Activation of the dentate nucleus in a verb generation task: A 7T MRI study. *Neuroimage, 57*(3), 1184-1191. doi:10.1016/j.neuroimage.2011.05.045

Todd, G., Flavel, S.C., & Ridding, M.C. (2009). Priming theta-burst repetitive transcranial magnetic stimulation with low- and high-frequency stimulation. *Exp Brain Res, 195*(2), 307-315. doi:10.1007/s00221-009-1791-8

Toft, P.B., Leth, H., Peitersen, B., Lou, H.C., & Thomsen, C. (1996). The apparent diffusion coefficient of water in gray and white matter of the infant brain. *J Comput Assist Tomogr, 20*(6), 1006-1011.

Tonn, J.C., & Stummer, W. (2008). Fluorescence-guided resection of malignant gliomas using 5-aminolevulinic acid: practical use, risks, and pitfalls. *Clin Neurosurg, 55*, 20-26.

Tournier, J.D., Calamante, F., King, M.D., Gadian, D.G., & Connelly, A. (2002). Limitations and requirements of diffusion tensor fiber tracking: an assessment using simulations. *Magn Reson Med, 47*(4), 701-708.

Trepel, P.D.m.M. (2017). *Neuroanatomie: Struktur und Funktion* (Fischer, E.U. Ed. 7 ed.).

Trinh, V.T., Fahim, D.K., Shah, K., Tummala, S., McCutcheon, I.E., Sawaya, R., Suki, D., & Prabhu, S.S. (2013). Subcortical injury is an independent predictor of worsening neurological deficits following awake craniotomy procedures. *Neurosurgery, 72*(2), 160-169. doi:10.1227/NEU.0b013e31827b9a11

Tussis, L., Sollmann, N., Boeckh-Behrens, T., Meyer, B., & Krieg, S.M. (2016). Language function distribution in left-handers: A navigated transcranial magnetic stimulation study. *Neuropsychologia, 82*, 65-73. doi:10.1016/j.neuropsychologia.2016.01.010

Ueno, T., & Lambon Ralph, M.A. (2013). The roles of the "ventral" semantic and "dorsal" pathways in conduite d'approche: a neuroanatomically-constrained computational modeling investigation. *Front Hum Neurosci, 7*, 422. doi:10.3389/fnhum.2013.00422

Ungerleider, L.G., Doyon, J., & Karni, A. (2002). Imaging brain plasticity during motor skill learning. *Neurobiol Learn Mem, 78*(3), 553-564. doi:10.1006/nlme.2002.4091

Valero-Cabre, A., & Pascual-Leone, A. (2005). Impact of TMS on the primary motor cortex and associated spinal systems. *IEEE Eng Med Biol Mag, 24*(1), 29-35.

Vassal, F., Schneider, F., & Nuti, C. (2013). Intraoperative use of diffusion tensor imaging-based tractography for resection of gliomas located near the pyramidal tract: comparison with subcortical stimulation mapping and contribution to surgical outcomes. *Br J Neurosurg, 27*(5), 668-675. doi:10.3109/02688697.2013.771730

Verhoeven, J.S., Sage, C.A., Leemans, A., Van Hecke, W., Callaert, D., Peeters, R., De Cock, P., Lagae, L., & Sunaert, S. (2010). Construction of a stereotaxic DTI atlas with full diffusion tensor information for studying white matter maturation from childhood to adolescence using tractography-based segmentations. *Hum Brain Mapp, 31*(3), 470-486. doi:10.1002/hbm.20880

Vorisek, I., & Sykova, E. (1997). Evolution of anisotropic diffusion in the developing rat corpus callosum. *J Neurophysiol, 78*(2), 912-919. doi:10.1152/jn.1997.78.2.912

Wagner, T., Valero-Cabre, A., & Pascual-Leone, A. (2007). Noninvasive human brain stimulation. *Annu Rev Biomed Eng, 9*, 527-565. doi:10.1146/annurev.bioeng.9.061206.133100

Wakana, S., Jiang, H., Nagae-Poetscher, L.M., van Zijl, P.C., & Mori, S. (2004). Fiber tract-based atlas of human white matter anatomy. *Radiology, 230*(1), 77-87. doi:10.1148/radiol.2301021640

Wakana, S., Caprihan, A., Panzenboeck, M.M., Fallon, J.H., Perry, M., Gollub, R.L., Hua, K., Zhang, J., Jiang, H., Dubey, P., Blitz, A., van Zijl, P., & Mori, S. (2007). Reproducibility of quantitative tractography methods applied to cerebral white matter. *Neuroimage, 36*(3), 630-644. doi:10.1016/j.neuroimage.2007.02.049

Wassermann, E.M. (1998). Risk and safety of repetitive transcranial magnetic stimulation: report and suggested guidelines from the International Workshop on the Safety of Repetitive Transcranial Magnetic Stimulation, June 5-7, 1996. *Electroencephalogr Clin Neurophysiol, 108*(1), 1-16.

Wassermann, E.M., Blaxton, T.A., Hoffman, E.A., Berry, C.D., Oletsky, H., Pascual-Leone, A., & Theodore, W.H. (1999). Repetitive transcranial magnetic stimulation of the dominant hemisphere can disrupt visual naming in temporal lobe epilepsy patients. *Neuropsychologia, 37*(5), 537-544.

Weiss, C., Tursunova, I., Neuschmelting, V., Lockau, H., Nettekoven, C., Oros-Peusquens, A.M., Stoffels, G., Rehme, A.K., Faymonville, A.M., Shah, N.J., Langen, K.J., Goldbrunner, R., & Grefkes, C. (2015). Improved nTMS- and DTI-derived CST tractography through

anatomical ROI seeding on anterior pontine level compared to internal capsule. *Neuroimage Clin, 7*, 424-437. doi:10.1016/j.nicl.2015.01.006
Wen, P.Y., & Kesari, S. (2008). Malignant gliomas in adults. *N Engl J Med, 359*(5), 492-507. doi:10.1056/NEJMra0708126
Werhahn, K.J., Kunesch, E., Noachtar, S., Benecke, R., & Classen, J. (1999). Differential effects on motorcortical inhibition induced by blockade of GABA uptake in humans. *J Physiol, 517 (Pt 2)*, 591-597.
Wernicke, C. (1874). Der aphasische Symptomenkomplex. Eine psychologische Studie auf anatomischer Basis. In Weigert, M.C. (Ed.). Breslau.
Wheat, K.L., Cornelissen, P.L., Sack, A.T., Schuhmann, T., Goebel, R., & Blomert, L. (2013). Charting the functional relevance of Broca's area for visual word recognition and picture naming in Dutch using fMRI-guided TMS. *Brain Lang, 125*(2), 223-230. doi:10.1016/j.bandl.2012.04.016
Willems, P.W., Taphoorn, M.J., Burger, H., Berkelbach van der Sprenkel, J.W., & Tulleken, C.A. (2006). Effectiveness of neuronavigation in resecting solitary intracerebral contrast-enhancing tumors: a randomized controlled trial. *J Neurosurg, 104*(3), 360-368. doi:10.3171/jns.2006.104.3.360
Williamson, J.B., Heilman, K.M., Porges, E.C., Lamb, D.G., & Porges, S.W. (2013). A possible mechanism for PTSD symptoms in patients with traumatic brain injury: central autonomic network disruption. *Front Neuroeng, 6*, 13. doi:10.3389/fneng.2013.00013
Witelson, S.F. (1989). Hand and sex differences in the isthmus and genu of the human corpus callosum. A postmortem morphological study. *Brain, 112 (Pt 3)*, 799-835. doi:10.1093/brain/112.3.799
Witwer, B.P., Moftakhar, R., Hasan, K.M., Deshmukh, P., Haughton, V., Field, A., Arfanakis, K., Noyes, J., Moritz, C.H., Meyerand, M.E., Rowley, H.A., Alexander, A.L., & Badie, B. (2002). Diffusion-tensor imaging of white matter tracts in patients with cerebral neoplasm. *J Neurosurg, 97*(3), 568-575. doi:10.3171/jns.2002.97.3.0568
Youden, W.J. (1950). Index for rating diagnostic tests. *Cancer, 3*(1), 32-35.
Yousry, T.A., Schmid, U.D., Alkadhi, H., Schmidt, D., Peraud, A., Buettner, A., & Winkler, P. (1997). Localization of the motor hand area to a knob on the precentral gyrus. A new landmark. *Brain, 120 (Pt 1)*, 141-157.
Zhu, F.P., Wu, J.S., Song, Y.Y., Yao, C.J., Zhuang, D.X., Xu, G., Tang, W.J., Qin, Z.Y., Mao, Y., & Zhou, L.F. (2012). Clinical application of motor pathway mapping using diffusion tensor imaging tractography and intraoperative direct subcortical stimulation in cerebral glioma surgery: a prospective cohort study. *Neurosurgery, 71*(6), 1170-1183; discussion 1183-1174. doi:10.1227/NEU.0b013e318271bc61
Zou, K.H., Tuncali, K., & Silverman, S.G. (2003). Correlation and simple linear regression. *Radiology, 227*(3), 617-622. doi:10.1148/radiol.2273011499
Zweig, M.H., & Campbell, G. (1993). Receiver-operating characteristic (ROC) plots: a fundamental evaluation tool in clinical medicine. *Clin Chem, 39*(4), 561-577.

8. ABBREVIATIONS

8.1. Not referring to the cortical parcellation system

3D	Three-dimensional
AC	Analysis combination
AE	All errors
AEWH	All errors without hesitation
AF	Arcuate fasciculus
allR	All regions
antR	Anterior regions
APB	Abductor pollicis brevis
AVM	Arteriovenous malformation
BBI	Best balance index
BI	Balance index
BIS	Bispectral index
BOLD	Blood oxygen level dependent
CPS	Cortical parcellation system
CrS	CPS region subdivision
CSF	Cerebrospinal fluid
DCS	Direct cortical stimulation
DICOM	Digital imaging and communications in medicine
DTI FT	Diffusion tensor imaging fiber tracking
DTI	Diffusion tensor imaging
DWI	Diffusion-weighted imaging
EC	Error category
ECoG	Electrocorticography
e-field	Electric field
EmC	Extreme capsule
EMG	Electromyography
En-TMS	Electric-field-navigated TMS
EOR	Extent of resection
ExC	External capsule
FA	Fractional anisotropy
FACT	Fiber assignment by a continuous tracking
FAT	Fractional anisotropy threshold
FLAIR	Fluid-attenuated-inversion-recovery
fMRI	Functional magnetic resonance imaging
FN	False negative
FP	False positive
HE	Hesitation errors
i.a.	Inter alia
IEMAS	Intraoperative examination monitor for awake surgery
IFOF	Inferior fronto-occipital fasciculus
ILF	Inferior longitudinal fasciculus
iMRI	Intraoperative magnetic resonance imaging
IPI	Interpicture interval
ISM	Intraoperative stimulation mapping
Ln-TMS	Line-navigated TMS
MAX	Maximum value
MdLF	Middle longitudinal fasciculus
MEDIAN	Median value
MEG	Magnetoencephalographic imaging

MEP	Motor evoked potential
MFL	Minimum fiber length
MIN	Minimum value
MRI	Magnetic resonance imaging
MV	Mean value
NBS	Navigated brain stimulation
NoF	Number of fibers
NPV	Negative predictive value
NRE	No response errors
nTMS	Navigated transcranial magnetic stimulation
OSHA	Occupational Safety and Health Administration
PACS	Picture archiving and communication system
PE	Performance errors
PET	Positron emission tomography
PEV	Principal eigenvector
postR	Posterior regions
PPT	Picture presentation time
PPV	Positive predictive value
PT	Phosphene threshold
PTI	Picture-to-trigger interval
r	Pearson's correlation coefficient
RMT	Resting motor threshold
ROC	Receiver operating characteristic
ROI	Region of interest
rTMS	Repetitive transcranial magnetic stimulation
SCS	Subcortical stimulation
SD	Standard deviation
SLF	Superior longitudinal fasciculus
TC	Threshold category
TE	Echo time
TN	True negative
TP	True positive
TR	Repetition time
UF	Uncinate fasciculus
VAS	Visual analogue scale
WHO	World Health Organisation
YI	Youden's index

8.2. Cortical parcellation system

aITG	Anterior inferior temporal gyrus
aMFG	Anterior middle frontal gyrus
aMTG	Anterior middle temporal gyrus
anG	Angular gyrus
aSFG	Anterior superior frontal gyrus
aSMG	Anterior supramarginal gyrus
aSTG	Anterior superior temporal gyrus
dLOG	Dorsal lateral occipital gyrus
dPoG	Dorsal post-central gyrus
dPrG	Dorsal pre-central gyrus
mITG	Middle inferior temporal gyrus
mMFG	Middle middle frontal gyrus
mMTG	Middle middle temporal gyrus
mPoG	Middle post-central gyrus
mPrG	Middle pre-central gyrus
mSFG	Middle superior frontal gyrus

mSTG	Middle superior temporal gyrus
opIFG	Opercular inferior frontal gyrus
orIFG	Orbital part of the inferior frontal gyrus
pITG	Posterior inferior temporal gyrus
pMFG	Posterior middle frontal gyrus
pMTG	Posterior middle temporal gyrus
polIFG	Polar inferior frontal gyrus
polITG	Polar inferior temporal gyrus
polLOG	Polar lateral occipital gyrus
polMFG	Polar middle frontal gyrus
polMTG	Polar middle temporal gyrus
polSFG	Polar superior frontal gyrus
polSTG	Polar superior temporal gyrus
PrG	Pre-central gyrus
pSFG	Posterior superior frontal gyrus
pSMG	Posterior supramarginal gyrus
pSTG	Posterior superior temporal gyrus
SPL	Superior parietal lobe
trIFG	Triangular inferior frontal gyrus
vLOG	Ventral lateral occipital gyrus
vPoG	Ventral post-central gyrus
vPrG	Ventral pre-central gyrus

9. ACKNOWLEDGEMENTS

For a scientific work to succeed, many different people make their respective important contributions. All deserve my gratitude and acknowledgement.

First of all, I would like to thank the head of the neurosurgical Clinic Univ.-Prof. Dr. med. Bernhard Meyer and his entire team, who provided the organisational framework and thus the basis for this dissertation.

Special thanks go to my doctoral supervisor, Prof. Dr. med. Sandro Krieg, and my mentor, Dr. med. Nico Sollmann. Many thanks for the always competent advice, the familiarization with the topic, the enabling of a publication and the necessary patience and perseverance until the work was finished. I would especially like to thank Nico Sollmann again for the uncomplicated and amicable cooperation as well as the many joint lunches.

Furthermore, I would like to thank the team of the working group for the humorous, cooperative and helpful collaboration. Especially to mention is my friend and team colleague, Moritz Klug, who was the connecting link to this working group and hence gave me the opportunity to begin with this doctoral thesis. Moreover, I could always count on his help and support. Further to mention are Lucia Bulubas, Dr. Vicki Butenschön, Neal Conway, Katharina Drummer, Sophia Fuss, Katrin Giglhuber, Theresa Hauck, Dr. med. Sebastian Ille, Anna Kelm, Tobias Laub, Stefanie Maurer, Dr. med. Chiara Negwer, Axel Schröder, Maximilian Schwendner and Noemie Wildschutz.

Finally, my thanks go to my loved family and friends, who mentally accompanied me on the long way and supported me tirelessly, in particular my parents, my brother and the blubbl-group. I dedicate this doctoral thesis to my two strongest motivators: my daughter Emilia and my husband Claudio - the carrot and the stick of necessity.

10. CURRICULUM VITAE

11. PUBLICATIONS

Original papers

Nico Sollmann, **Antonia Kubitscheck**, Stefanie Maurer, Sebastian Ille, Theresa Hauck, Jan S. Kirschke, Florian Ringel, Bernhard Meyer, et al.
Preoperative language mapping by repetitive navigated transcranial magnetic stimulation and diffusion tensor imaging fiber tracking and their comparison to intraoperative stimulation
Neuroradiology, DOI 10.1007/s00234-016-1685-y

Oral presentations

Comparison of language mapping by preoperative rTMS, rTMS-based fiber tracking and intraoperative stimulation.
Sektionstagung Neurophysiologie der Deutschen Gesellschaft für Neurochirurgie (DGNC), Munich
23. - 24.10.2015

Comparison of language mapping by preoperative rTMS, rTMS-based fiber tracking and intraoperative stimulation.
7th International Symposium - Navigated Brain Stimulation: Neurosurgery and Neuromodulation, Berlin
11. - 12.10.2015

Posters

Comparison of language mapping by preoperative rTMS, rTMS-based fiber tracking and intraoperative stimulation.
7th International Symposium - Navigated Brain Stimulation: Neurosurgery and Neuromodulation, Berlin
11. - 12.10.2015